Catchment Scale Downscaling of Hydroclimatic Variables from General Circulation Model Outputs

By

Sachindra Dhanapala Arachchige, (BSc, MSc)

Thesis submitted in fulfilment of the requirement for the degree of

Doctor of Philosophy

College of Engineering and Science, Victoria University, Australia

June 2014

ABSTRACT

Climate change influences events such as droughts, floods, extreme temperatures and sea level changes and hence affects the global food production, energy generation, and water resources adversely. Rising greenhouse gas (GHG) concentrations in the atmosphere are considered the dominant cause of climate change. General Circulation Models (GCMs) are used for the projection of climate into future, accounting for the GHG concentrations. However, the coarse spatial resolution of GCM outputs does not permit their direct use in catchment scale studies. Therefore either dynamic or statistical downscaling techniques are used for linking GCM outputs to catchment scale hydroclimatic variables.

The following issues associated with statistical downscaling were addressed in this study; (1) non-homogeneity in inputs used in the development and future projection phases of statistical downscaling models (SDMs), (2) propagation of GCM bias to outputs of SDMs, (3) varying nature of climate projections produced by SDMs depending on the GCM used for providing inputs, (4) complexity of multi-station and multi-station multivariate SDMs, and (5) performance comparison of linear regression techniques with non-linear regression techniques.

It is the common practice to develop (calibrate and validate) SDMs with reanalysis outputs and then use GCM outputs for the subsequent projections of catchment scale climate into future. Since these inputs used in the development and future projection phases of SDMs originate from two different sources, the inputs are not homogeneous. In this study, as a potential solution to the issue of non-homogeneity in inputs, a SDM at a point was developed with GCM outputs, in view of using it with the outputs of the same GCM for the projection of catchment scale precipitation into future. Despite the use of homogeneous sets of inputs to this SDM, it showed limited performance in the

development phase, in comparison to another SDM developed with reanalysis outputs according to the common practice.

Owing to the assumptions and approximations employed in the GCMs, their outputs contain bias, and this bias propagates to the outputs of SDMs. In this study, performances of different bias-correction techniques on their application to the outputs of a SDM were investigated. Performances of (1) equidistant quantile mapping, (2) nested bias-correction, and (3) monthly bias-correction in reducing the bias in the precipitation outputs of a SDM were also investigated. It was found that equidistant quantile mapping outperformed the other two techniques.

Since the assumptions and approximations used in GCMs differ from one GCM to another, they tend to produce different projections of climate into future. Projections of a predictand produced into future can vary depending on the GCM used for providing inputs to the SDM. As a solution to this issue, a SDM was developed (calibrated and validated) and precipitation projections into future were produced, using multi-model ensemble (MME) outputs. To generate MME outputs for the development of the SDM, the outputs of a set of different GCMs pertaining to the past climate were regressed against the corresponding reanalysis outputs. Then the multi-linear regression (MLR) equations between the outputs of these GCMs and reanalysis outputs were determined. The same MLR equations between the outputs of these GCMs and reanalysis outputs were used for deriving the MME outputs pertaining to future climate. A SDM was developed and precipitation projections into future were produced using these homogeneous sets of MME outputs generated for past and future. This procedure enabled producing a single projection of precipitation using the outputs of multiple GCMs.

The majority of the current multi-station downscaling techniques capable of maintaining the spatial coherence of a predictand among the stations are complex. In this study, a relatively simple yet effective multi-station downscaling technique was investigated. For this purpose, stations which showed high correlations with the other stations in the study area were identified for a predictand of interest, and SDMs were

developed (calibrated and validated) and projection of the predictand were produced into the future only at those stations. Then the linear regression relationships between the stations at which the SDMs were developed and other stations were determined for the predictand of interest, using the observations. Thereafter by using the outputs of the SDMs on the above linear regression relationships between the stations at which the SDMs were developed and other stations, the values of the predictand at other stations were determined for the past and the future climate. It was proven that this multi-station downscaling approach was capable of preserving the correlation structure of a predictand of interest among the stations. This multi-station downscaling approach was further extended to downscale multiple predictands at multiple stations concurrently. It was proven that the multi-station multivariate downscaling approaches developed in this study was capable of preserving the correlation structures among the stations for each predictand of interest while maintaining the correlation structures among different predictands at individual stations.

In statistical downscaling, both linear and non-linear regression techniques are widely used. In this study, a comparison of performances of two SDMs developed using least square support vector machine (LS-SVM – non-linear regression) and MLR for downscaling reanalysis outputs to monthly streamflows was investigated. It was found that LS-SVM is marginally better than MLR.

DECLARATION

"I, Sachindra Dhanapala Arachchige, declare that the PhD thesis entitled 'Catchment level downscaling of hydroclimatic variables from general circulation model outputs' is no more than 100,000 words in length including quotes and exclusive of tables, figures, appendices, bibliography, references and footnotes. This thesis contains no material that has been submitted previously, in whole or in part, for the award of any other academic degree or diploma. Except where otherwise indicated, this thesis is my own work".

Signature: 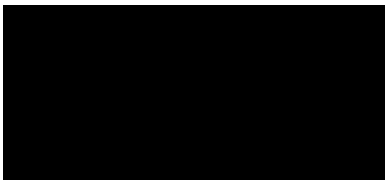

Date: 08/07/2014

ACKNOWLEDGMENTS

I would like to extend my sincere thanks to my principal supervisor Prof. Chris Perera for providing me with the necessary guidance throughout my PhD research. The valuable comments and suggestions provided by him were immensely helpful to me in successfully writing the journal and conference paper on which this thesis is based. The first associate supervisor of mine, Dr. Andrew Barton is praised for providing me with the data need for this study and his efforts in conveying the findings of this research to the industry. The second associate supervisor of mine, Dr. Fuchun Huang is appreciated for his vital comments on the use of statistics in this research.

I would also like to thank the Australian Research Council and the Grampians Wimmera Mallee Water Corporation for the financial assistance provided for this research project. I could not have pursued my PhD research in Australia if not for the scholarship funded by the above organisations. Finally, I would like to thank my family members, friends (especially Vipulkumar Patel) and other staff members of the Victoria University, Footscray park campus who helped me in many different ways during my PhD.

LIST OF PUBLICATIONS

Journal Articles

1. **Sachindra DA**, Huang F, Barton AF, Perera BJC. 2014a. Statistical downscaling of general circulation model outputs to precipitation Part 1: Calibration and validation. *International Journal of Climatology*. (Article in press, published online). DOI**:** 10.1002/joc.3914.

2. **Sachindra DA**, Huang F, Barton AF, Perera BJC. 2014b. Statistical downscaling of general circulation model outputs to precipitation Part 2: Bias-correction and future projections. *International Journal of Climatology*. (Article in press, published online). DOI: 10.1002/joc.3915.

3. **Sachindra DA**, Huang F, Barton AF, Perera BJC. 2013a. Least square support vector and multi-linear regression for statistically downscaling general circulation model outputs to catchment streamflows. *International Journal of Climatology* **33:** 1087-1106. DOI: 10.1002/joc.3493.

4. **Sachindra DA**, Huang F, Barton AF, Perera BJC. 2013b. Multi-model ensemble approach for statistically downscaling general circulation model outputs to precipitation. *Quarterly Journal of the Royal Meteorological Society*. (Article in press, published online). DOI**:** 10.1002/qj.2205.

5. **Sachindra DA**, Huang F, Barton AF, Perera BJC. 2013c. Statistical downscaling of general circulation model outputs to catchment scale

hydroclimatic variables: Issues, challenges and potential solutions. *Journal of Water and Climate Change*. (Article in press).

6. **Sachindra DA**, Huang F, Barton AF, Perera BJC. 2013d. Statistical downscaling of general circulation model outputs to precipitation, evaporation and temperature using a key-station approach. *Global and Planetary Change*. (Under review).

7. **Sachindra DA**, Huang F, Barton AF, Perera BJC. 2013e. Statistical downscaling of general circulation model outputs to evaporation, minimum temperature and maximum temperature using a key-predictand and key-station approach. *Journal of Water and Climate Change*. (Under review).

Refereed Conference Papers

8. **Sachindra DA**, Huang F, Barton AF, Perera BJC. 2011a. Statistical downscaling of general circulation model outputs to catchment streamflows. *Proceedings of MODSIM 2011 19th International Congress on Modelling and Simulation*, Perth, Australia, 12-16 December 2011, (CD) pp 2810-2816.

9. Perera BJC, **Sachindra DA,** Godoy W, Barton AF, Huang F. 2011b. Multi-objective planning and operation of water supply systems subject to climate change. *World Academy of Science, Engineering and Technology*, 60, (CD) pp 571-580.

10. **Sachindra DA**, Huang F, Barton AF, Perera BJC. 2012a. Issues associated with statistical downscaling of general circulation model outputs: A discussion. *Proceedings of the 2nd Practical Responses to Climate Change Conference*, Canberra, Australia, 1-3 May 2012, (CD) pp 98-105.

11. **Sachindra DA**, Huang F, Barton AF, Perera BJC. 2012b. Statistical downscaling of general circulation model outputs to precipitation, *Proceedings of the 34th Hydrology and Water Resources Symposium 2012*, Sydney, Australia, 20-22 November 2012, (CD) pp 595-602.

PART A:

DETAILS OF INCLUDED PAPERS: THESIS BY PUBLICATION

Chapter No.	Paper Title	Publication Status	Publication Title and Details
2	Statistical downscaling of general circulation model outputs to catchment scale hydroclimatic variables: Issues, challenges and potential solutions	Article in press	Journal of Water and Climate, Accepted for publication in November 2013, ERA Rank : N/A, Impact Factor : 1.000
3	Statistical downscaling of general circulation model outputs to precipitation Part 1: Calibration and validation	Article in press, published online	International Journal of Climatology, Accepted for publication in December 2013, ERA Rank : A, Impact Factor : 2.886
	Statistical downscaling of general circulation model outputs to precipitation Part 2: Bias-correction and future projections	Article in press, published online	International Journal of Climatology, Accepted for publication in December 2013, ERA Rank : A, Impact Factor : 2.886
4	Multi-model ensemble approach for statistically downscaling general circulation model outputs to precipitation	Article in press, published online	Quarterly Journal of the Royal Meteorological Society, Accepted for publication in May 2013, ERA Rank : A, Impact Factor : 3.327
5	Statistical downscaling of general circulation model outputs to precipitation, evaporation and temperature using a key-station approach	Under review	Global and Planetary Change, Submitted in May 2014, ERA Rank : A, Impact Factor : 3.155
	Statistical downscaling of general circulation model outputs to evaporation, minimum temperature and maximum temperature using a key-predictand and key-station approach	Under review	Journal of Water and Climate, Submitted in December 2013, ERA Rank : N/A, Impact Factor : 1.000
6	Least square support vector and multi-linear regression for statistically downscaling general circulation model outputs to catchment streamflows.	Published	International Journal of Climatology, 2013, ERA Rank : A, Impact Factor : 2.886

Declared by: Sachindra Dhanapala Arachchige

Signature: [redacted]

Date: [redacted] 08/07/2014

CONTENTS

CHAPTER 1

INTRODUCTION

1.1 Impacts of climate change on water resources

Water is an essential substance for the existence of life on the Earth. For humans, it is used for drinking, agriculture, sanitation, industries and required for protecting the environment. The majority of the human water uses need freshwater which is quite limited. Water resources in the word are unevenly distributed with respect to their quantity and also their quality (Vörösmarty et al., 2010). The ever rising global population demands more water and hence the per capita freshwater availability has shown a reducing trend (http://data.worldbank.org/indicator/). The variations in the distribution of surface and groundwater resources are governed by the changes in the climatic variables such as precipitation, temperature and evaporation (Chiew, 2007). In more elaborated terms, precipitation received by a catchment contributes to its water budget, and climatic variables such as evaporation, temperature, wind speed, atmospheric water vapour content determine some of the water losses from the catchment. The rise in temperature of water can change the rate of chemical reactions and hence influence the quality of water. Furthermore, intense precipitation events can increase the sediment loads entrained by the rivers and hence affect the quality of water (Kundzewicz et al., 2008).

The rising greenhouse gas (GHG) concentrations in the earth's atmosphere lead to global warming and as a result the hydrologic cycle is accelerated (Kunkel et al., 2013).

This causes changes in the global climate. As stated in Bates et al. (2008), global warming has influenced the hydrologic cycle causing; changes in the spatiotemporal patterns of precipitation, changes in the intensity and the extremes of climate variables, unusually high levels of melting of snow and ice, rise in the atmospheric water vapour content, increase in evaporation and changes in the runoff patterns. Since the climate is highly influential on the water resources within a catchment in many different ways as described earlier, knowledge of changing climate into the future is crucial for the effective management of water resources in a catchment.

Australia is one of the many countries affected by the climate change. The annual mean surface air temperature over Australia has shown a rising trend of 0.16˚C per decade since 1950 (Commonwealth Scientific and Industrial Research Organisation, 2007). Also an increase in the number of days with maximum temperature exceeding 35˚C (hot days) and a decrease in the number of days with maximum temperature below 15˚C (cold days) have been observed over Australia (Nicholls and Collins, 2006). Since 1950, the north-western region of Australia has shown a clear rise in the annual mean precipitation, and eastern Australia has experienced a decline in the annual mean precipitation (Commonwealth Scientific and Industrial Research Organisation, 2007). Since late 1960s, south-western Australia has experienced a significant decline in precipitation (Smith et al., 2000). The decrease in precipitation in south-western Australia is showing a continuing trend and it has caused an increasing and far greater decline in the inflows to the water supply reservoirs located in that region. Cai and Cowan (2008) found that a 1˚C rise in the average global temperature would lead to a 15% reduction in flows in the Murray-Darling Basin which contains the largest river system of Australia. The average of the annual precipitation over the southern region of south-eastern Australia declined by about 11% from the long-term average during the period 1997-2008, causing a much larger decline of 35% in runoff (Chiew et al., 2010).

The Millennium drought which prevailed during the period 1997-2010 over the Australian state of Victoria is considered to be the worst drought ever recorded in the history of the state (Timbal, 2009). In the period 1998-2007, the annual average

precipitation in Victoria declined by about 13% from the long-term average (Victorian Government Department of Sustainability and Environment, 2008). During this period, many water supply systems in Victoria experienced a large decline in inflows. As examples, the inflows to Melbourne's main water supply reservoirs declined by about 38% from the long-term average of the period 1913-1996 (Wallis et al., 2009) and the inflows to the reservoirs in the Grampians water supply system located in north-western Victoria declined by about 75% from the long-term average of the period 1903-1996 (Water in Drylands Collaborative Research Program, 2009).

General Circulation Models (GCMs) are used to simulate the effect of the rising GHG concentrations on the global climate. The simulations produced by GCMs are often in the order of a few hundred kilometres and hence cannot explain the local scale variability of climate which is more important in terms of water resources in a catchment (Tripathi et al., 2006). In other words, though the spatial resolution of GCM outputs are sufficient for a reasonably good representation of climate at the global and the continental scales, the catchment scale climate which is highly influenced by the topography and land use is not simulated adequately (Sachindra et al., 2014a). Therefore the direct use of GCM simulations in catchment scale studies such as hydrologic modelling and climate impact assessments is not possible (Jeong et al., 2013). Hence there is a need for translating the coarse scale information in the GCM simulations to catchment scale hydroclimatic variables such as precipitation, evaporation, temperature and streamflow. For this purpose, either dynamic or statistical downscaling techniques are used.

In Figure 1, the concept of downscaling using statistical and dynamic techniques is graphically illustrated. As shown in Figure 1, in statistical downscaling, statistical relationships are formulated between the coarse resolution GCM outputs and the hydroclimatic variables at the points of interest in the catchment. On the other hand, in dynamic downscaling, the relationships between the coarse resolution GCM outputs and the fine resolution grid of the Regional Climate Model (RCM) are developed

considering the physics of the atmosphere. More details on downscaling techniques are provided in Chapter 2.

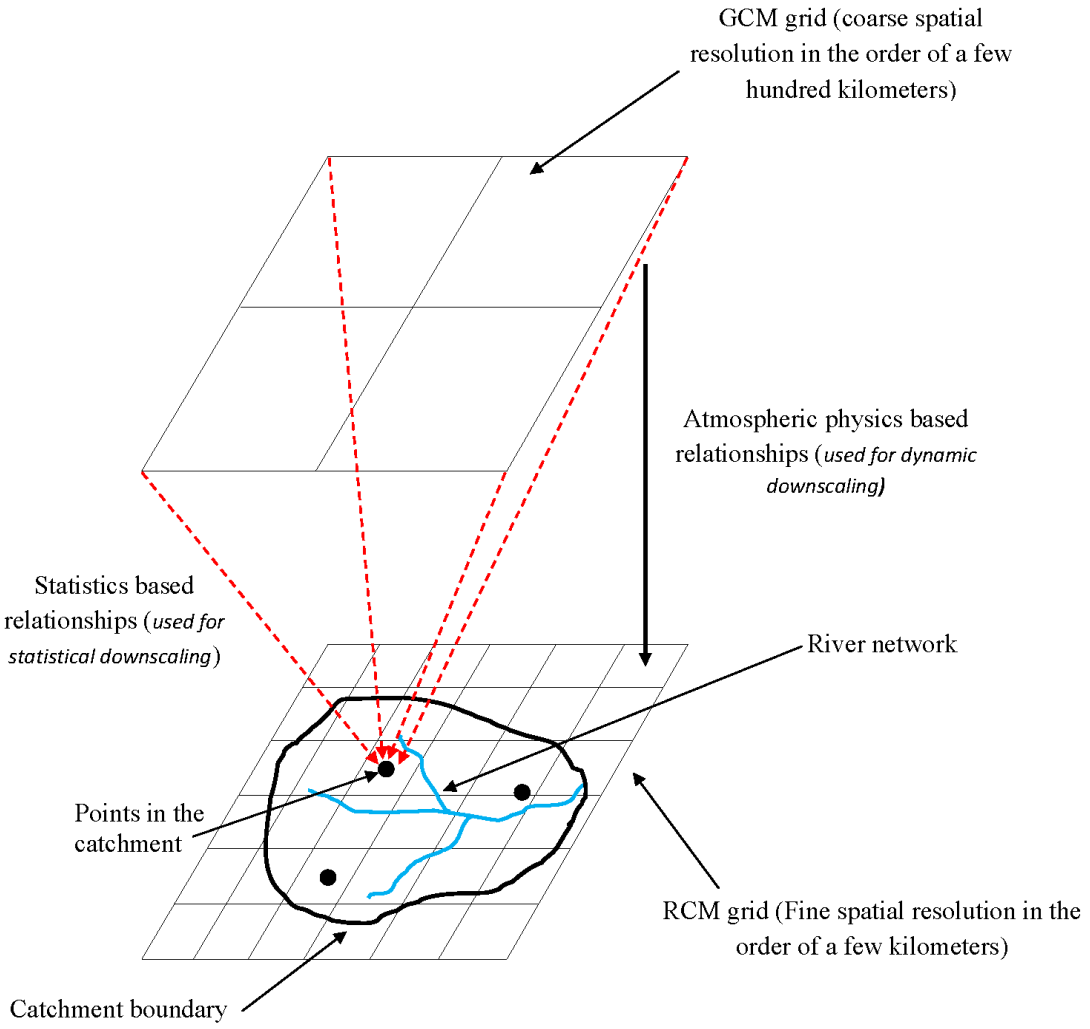

Figure 1 Statistical and dynamic downscaling

1.2 Aims of the study

The main aim of this study was to develop statistical models for downscaling monthly GCM outputs to catchment scale monthly precipitation, evaporation, minimum temperature, maximum temperature and streamflows at several stations located in the north-western region of Victoria, Australia. These stations are located in the operational

area of the Grampians Wimmera Mallee Water Corporation (GWMWater). Downscaling monthly GCM outputs to climatic variables at monthly temporal scale does not permit capturing the variations of them within a month (e.g. wet and dry days, extremes of temperature and precipitation). However, still monthly climatic projections produced using downscaling models can aid in the management of water resources which include operations such as water allocation for crops, domestic and industrial needs, and also environmental flows, especially in the planning stage of a water resources project. The following specific aims were considered under the main aim of the project.

- Analysis of the potential of using outputs of a GCM for the development (calibration and validation) of a downscaling model, in view of using the outputs of the same GCM for producing projections of catchment scale climate into the future.

- Assessment of different bias-correction techniques in post-processing the outputs of downscaling models.

- Use of a multi-model ensemble approach for generating a set of homogeneous inputs from the outputs of multiple GCMs for the development and the projection phases of a downscaling model.

- Development of a relatively simple methodology for downscaling GCM outputs to a predictand at multiple stations simultaneously while maintaining the spatial coherence.

- Development of a relatively simple methodology for downscaling GCM outputs to multiple predictands at multiple stations simultaneously while maintaining the coherence among the predictands and over space.

- Assessment of linear and non-liner regression techniques in statistical downscaling.

1.3 Study area

The aims of this study stated under Section 1.2 were demonstrated through a case study in the operational area of the Grampians Wimmera Mallee Water Corporation (GWMWater) in north-western Victoria, Australia. The location of the study area is shown in Figure 2. The operational area of GWMWater (about 62,000 km^2) contains a system of large-scale reservoirs which supplies water for domestic, industrial, agricultural and environmental requirements (Grampians Wimmera Mallee Water Corporation, 2011a). During the period 1997–2008, due to the Millennium drought, the inflows to the reservoirs of GWMWater declined by about 75% from the long-term average of the period 1903-1996 (Water in Drylands Collaborative Research Program, 2009). It was realised that the projection of climate into future over the operational area of GWMWater will enable the assessment of future availability of water resources in the system and enhance the management of its water resources. Therefore, this study was focussed on projecting the hydroclimatology of the operational area of GWMWater into future accounting for possible climate change.

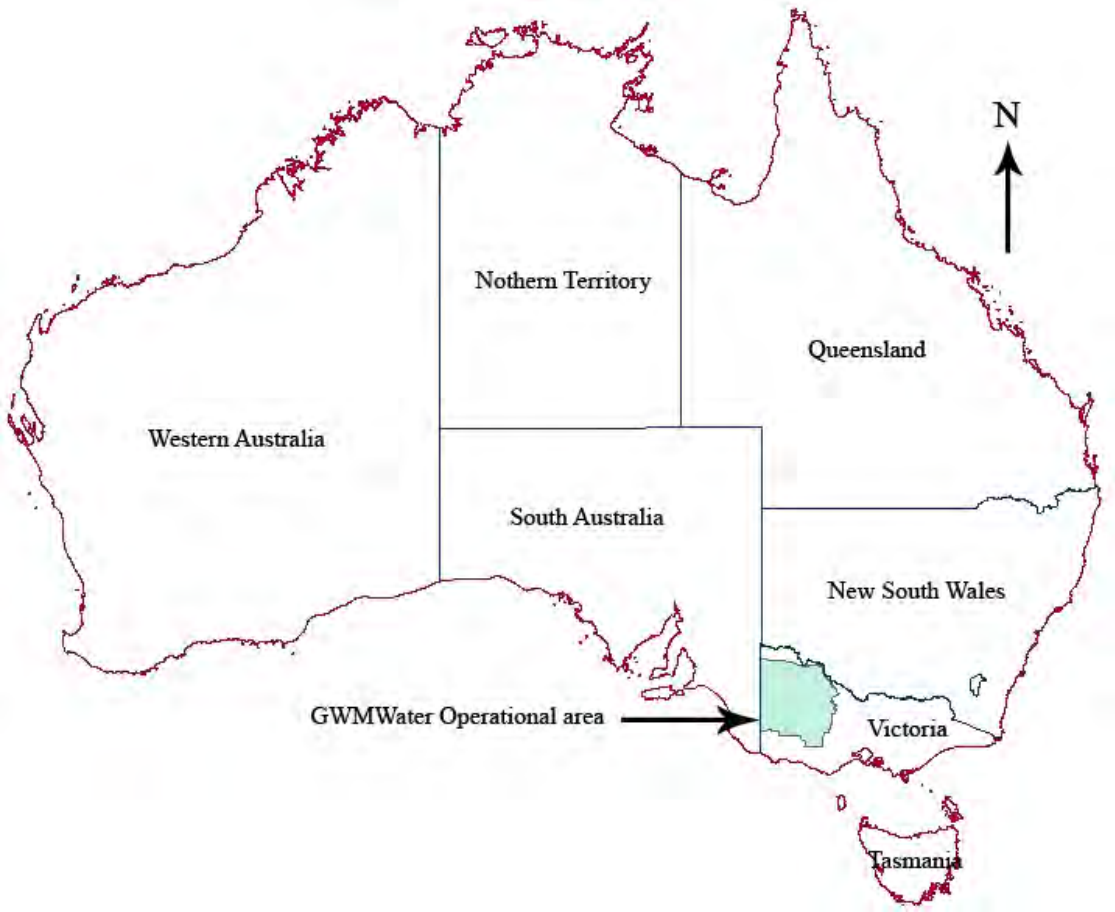

Figure 2 Operational area of the Grampians Wimmera Mallee Water Corporation

1.3.1 Topography

This study area can be subdivided into two zones based on the topography and hydroclimatology; (1) the northern region, and (2) the southern region. Figure 3 shows the topographic map of the study area. The elevation over the study area varies from about 25 m to 1200 m (above mean sea level) from north to south. As shown in Figure 3, the northern region of the study area is relatively flatter and the southern region is relatively mountainous. In the southern region, sand dunes and ridges are a distinct feature of the landscape (White et al., 2003).

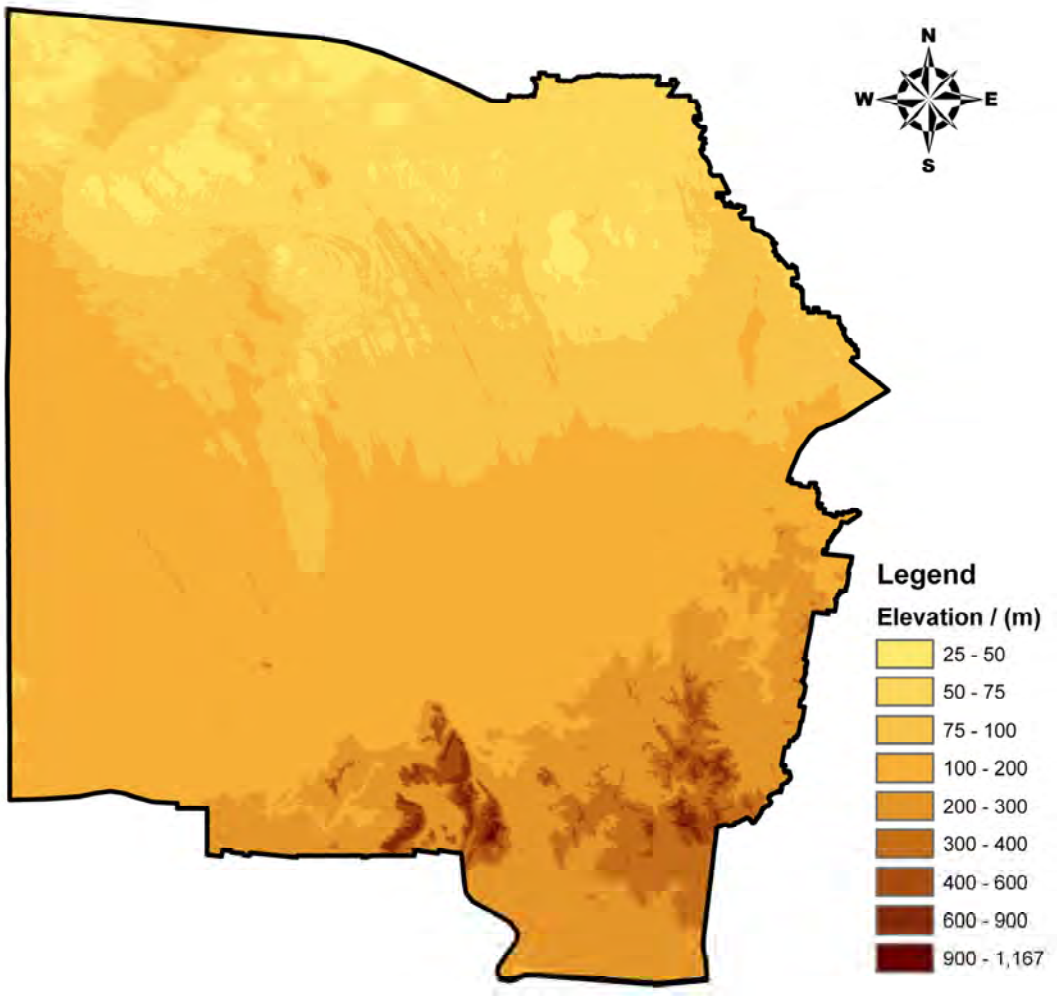

Figure 3 Topography of the study area

1.3.2 Land use and agriculture

The northern region of the study area is largely under the Mallee Catchment Management Authority (Mallee CMA), which covers the largest catchment area in Victoria (Mallee Catchment Management Authority, 2012). This region contains large number of wetlands and some of them are considered to be nationally significant. Also it contains a number of national parks such as: the Murray-Sunset national park, the Wyperfeld national park, the Hattah-Kulkyne national park and the Murray-Kulkyne regional park. In this region cereal crops, citrus, avocados, olives and vegetables are cultivated on a large scale.

The southern region of the study area is largely under the Wimmera Catchment Management Authority (Wimmera CMA) (Murray-Darling Basin Authority, 2010). Cereal cultivations, pasture productions for livestock are considered as the main agricultural activities. This area also contains large numbers of wetlands including the nationally important; Bitter swamp, Heards Lake and White Lake (Department of Planning and Community Development, 2012). The Grampians national park, the Little desert national park, and the St Arnaud range national park are among the national parks located in the region. The land use map of the entire study area is shown in Figure 4. The land use data used in Figure 4 were obtained from the website of Australian Department of Agriculture, Fisheries and Forestry at http://www.daff.gov.au/. In Figure 4, it was seen that, the majority of the study area is covered with cropping lands, grazing lands and national parks (nature conservations).

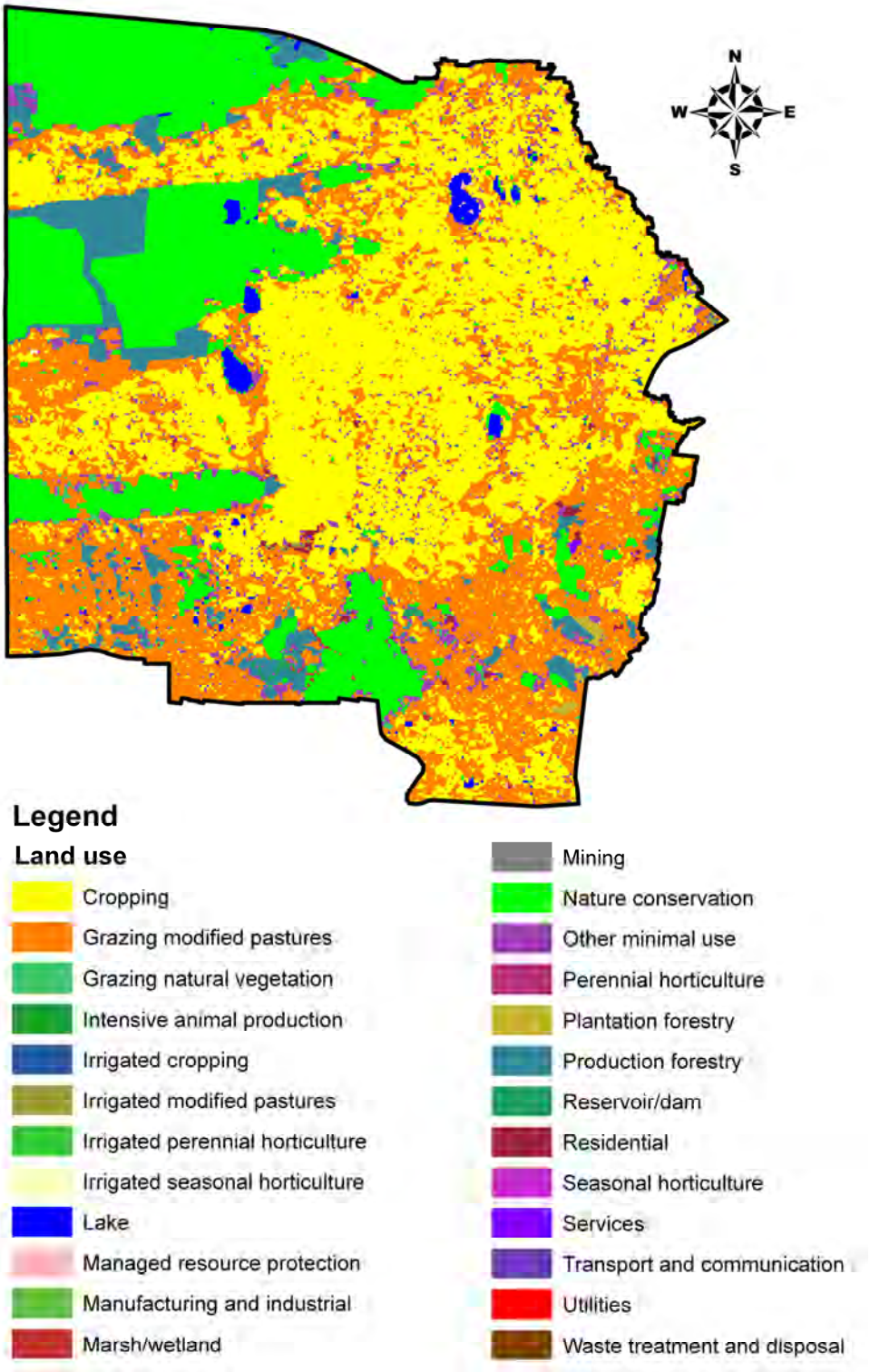

Figure 4 Land use of the study area

1.3.3 Soil

The northern region of the study area contains surface materials of aeolian origin (carried and produced by the action of winds) ranging from sands to clays, and in certain areas at greater depths marine deposits are also found along with limestone which contains freshwater (Rowan and Downes, 1963). Among the soil types; texture contrast soils (Sodosols), cracking clay soils (Vertosols), sandy soils (Rudosols and Tenosols), wet soils (Hydrosols) and calcareous soils (Calcarosols) are dominant (Department of Environment and Primary Industries, 2013a) in this region. The soil in this region is susceptible to erosion caused by winds and also farming practices (McRobert and Larsen, 2011).

The main types of soils in the southern region of the study area are; texture contrast soils (Sodosols, Kurosols, Chromosols), soils that lack strong texture contrast (Calcarosols), cracking clay soils (Vertosols) and sandy soils (Rudosols and Tenosols) (Department of Environment and Primary Industries, 2013b). The soil type map of the entire study area is provided in Figure 5. The soil type data used in Figure 5 were obtained from the website of the Australian Soil Resource Information System (ASRIS) at http://www.asris.csiro.au. Note that this soil classification is in accordance with the Australian Soil Classification defined in Isbell (2002).

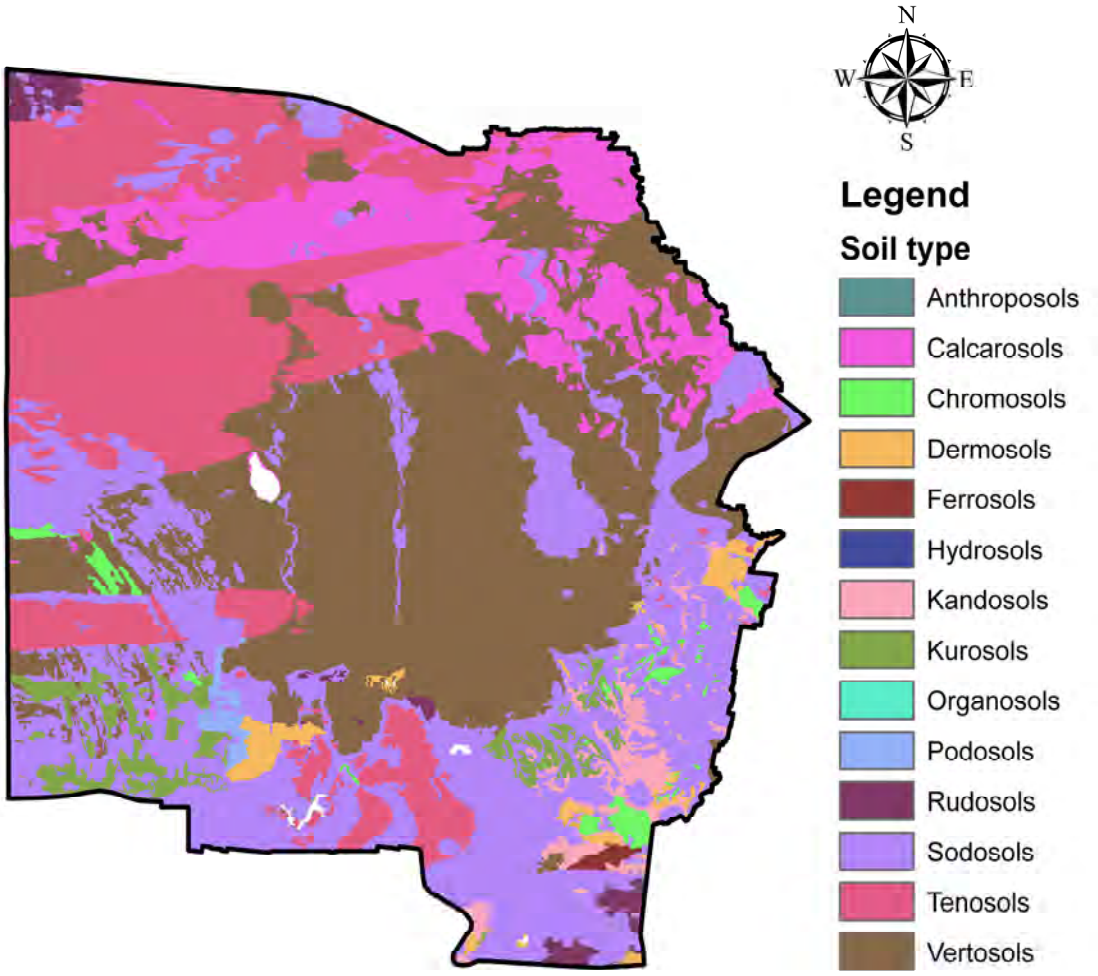

Figure 5 Soil types of the study area

1.3.4 Climate

The climate over south-eastern Australia which includes the present study area is influenced by north-west cloud bands, sub-tropical ridge, cut-off lows, El Nino Southern Oscillation, Indian Ocean Dipole (IOD) and the Southern Annular Mode (SAM) (Bureau of Meteorology Australia, 2010). The climate of the northern region of the study area is persistently dry and warm, while, the southern region is relatively wetter (Bureau of Meteorology Australia, 2013). Therefore the gradient of temperature and evaporation prevails in the north-south direction over the whole study area. The

gradient of precipitation exists in the south-north direction. However, the variations of climate within the northern and southern regions are minimal (White et al., 2003).

In this study, 17 climate observation stations located in the study area were considered for the projection of monthly precipitation, evaporation, minimum temperature and maximum temperature into future. Note that the observation station at Hamilton Airport is located slightly outside the study area. The relative spatial locations of the observation stations are shown in Figure 6, and their coordinates are provided in Table 1.

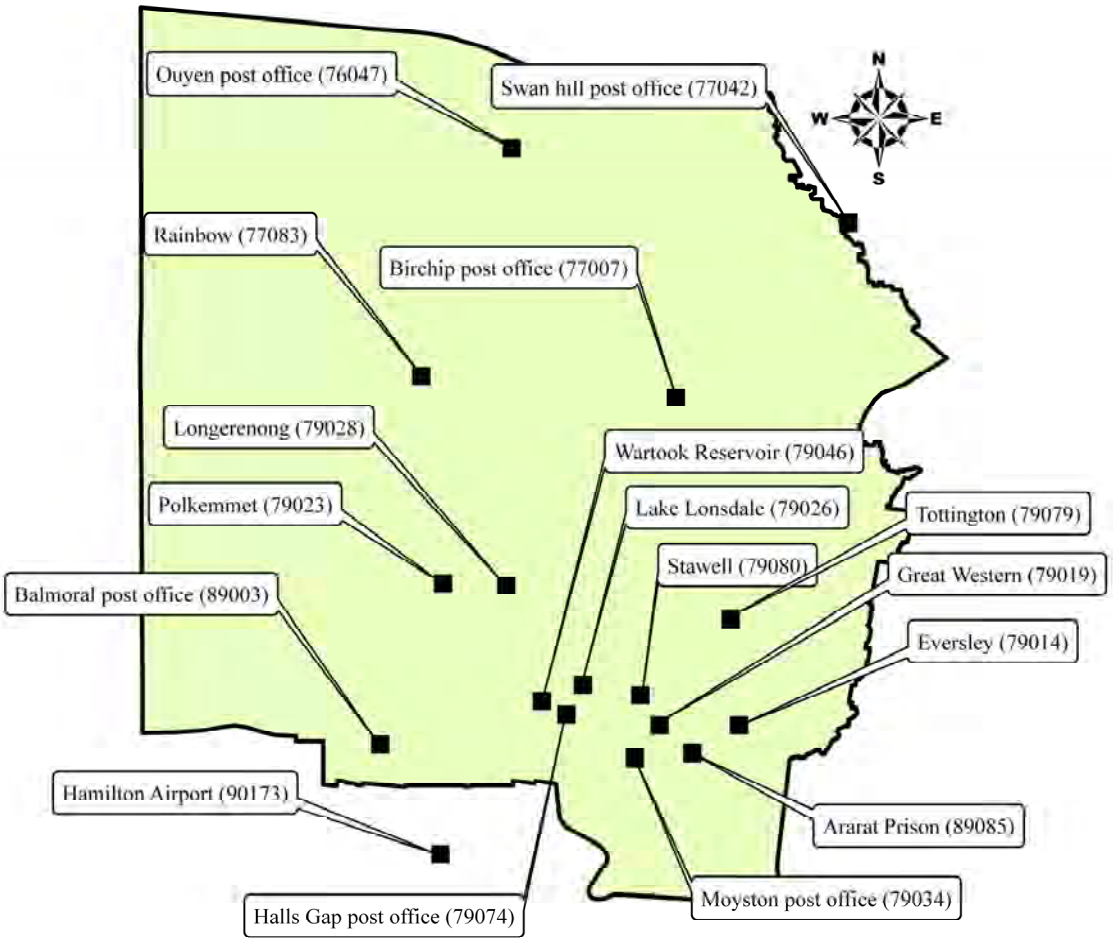

Figure 6 Climate observation stations considered in the study

Table 1 Locations of observation stations considered in the study

Name of the station	Station ID	Latitude	Longitude
Eversley	79014	-37.18	143.15
Ouyen post office	76047	-35.07	142.32
Birchip post office	77007	-35.98	142.92
Swan Hill post office	77042	-35.34	143.55
Rainbow	77083	-35.90	141.99
Great Western	79019	-37.18	142.86
Polkemmet	79023	-36.66	142.07
Lake Lonsdale	79026	-37.03	142.58
Longerenong	79028	-36.67	142.30
Moyston post office	79034	-37.30	142.77
Wartook reservoir	79046	-37.09	142.43
Hamilton airport	90173	-37.65	142.06
Halls Gap post office	79074	-37.14	142.52
Tottington	79079	-36.79	143.12
Stawell	79080	-37.07	142.79
Balmoral post office	89003	-37.25	141.84
Ararat prison	89085	-37.28	142.98

Station ID is as defined by the Bureau of Meteorology Australia at http://www.bom.gov.au/climate/data/stations/

The observation stations located at the Ouyen post office and the Halls Gap post office were considered as representative stations of the climate in the northern and southern regions of the study area respectively. The averages of precipitation over the period 1950-2010 at the Ouyen post office (located in the northern region) and the Halls Gap post office (located in the southern region) are compared for each calendar month in Figure 7. As shown in Figure 7, it was clear that the southern region receives more precipitation than the northern region in each calendar month. The annual averages of precipitation at the Ouyen post office and the Halls Gap post office are about 340 and 950 mm respectively for the period 1950-2010. The majority of precipitation over the southern region occurs in the period May to October which includes winter (June-August) and the lowest amount of precipitation occurs in the period December to March which includes summer (December-February). However, it was seen that the northern region remains persistently dry throughout the year.

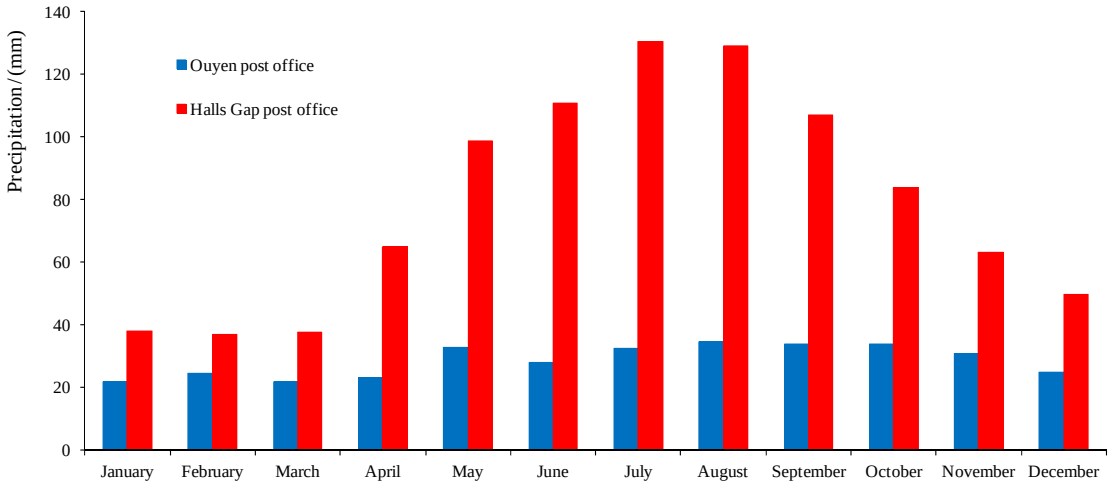

Figure 7 Average of precipitation over the period 1950-2010 at Ouyen post office and Halls Gap post office

In Figure 8, the averages of evaporation over the period 1950-2010 at the Ouyen post office and the Halls Gap post office in the study area are presented. It was seen that throughout the year, the northern region of the study area has relatively higher evaporation compared to that of southern region. The annual averages of evaporation over the period 1950-2010 at the Ouyen post office and the Halls Gap post office are about 1760 and 1320 mm respectively. Over the entire study area, the lowest amount of evaporation occurs in winter and the highest amount of evaporation occurs in summer.

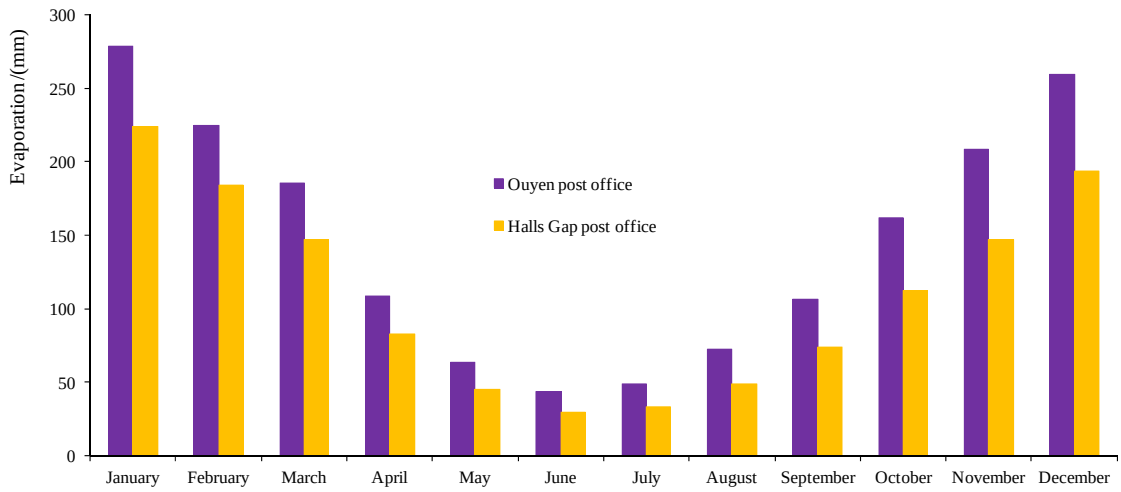

Figure 8 Average of evaporation over the period 1950-2010 at Ouyen post office and Halls Gap post office

In Figure 9, the averages of the maximum temperature at the Ouyen post office and the Halls Gap post office are presented for each calendar month for the period 1950-2010. In Figure 10, the averages of the minimum temperature at the two stations are shown for each calendar month for the period 1950-2010. It was observed that both the maximum and the minimum temperatures at the Ouyen post office are consistently higher than those at the Halls Gap post office. This indicated that the northern region of the study area is consistently warmer than the southern region. In fact, this aspect of the spatial variation of the temperature is responsible for the variations of evaporation across the study area discussed earlier.

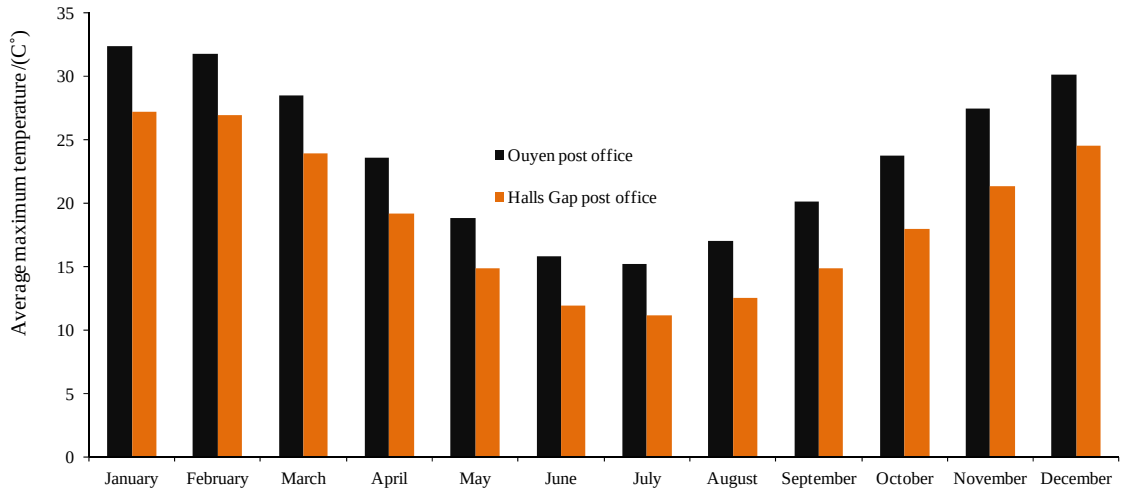

Figure 9 Average of maximum temperature over the period 1950-2010 at Ouyen post office and Halls Gap post office

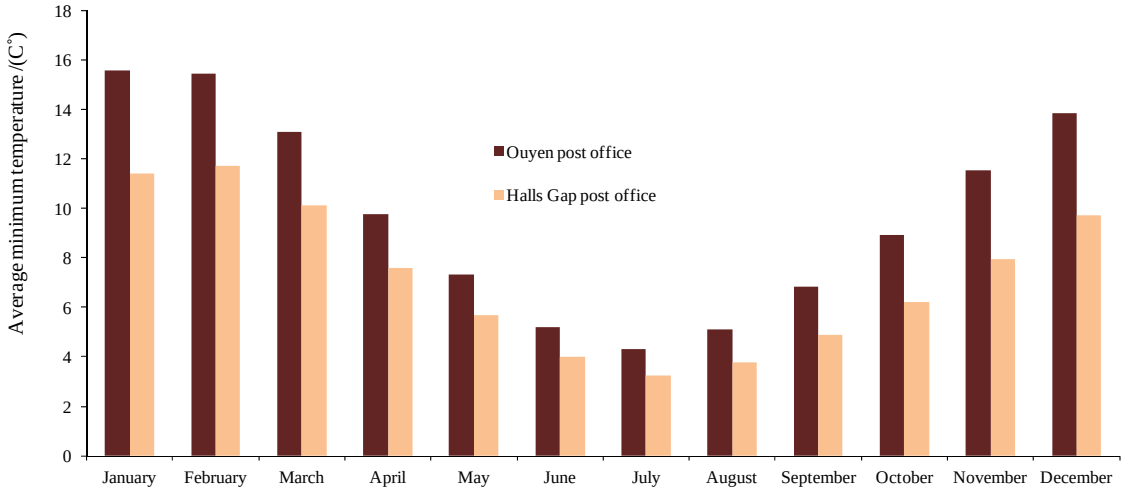

Figure 10 Average of minimum temperature over the period 1950-2010 at Ouyen post office and Halls Gap post office

1.3.5 Headworks system and water resources

The southern region of the study area contains most of the headworks systems of GWMWater as shown in Figure 11 (Figure obtained from Mala-Jetmarova et al., 2013).

The development of the Grampians based headworks system of GWMWater started with the construction of Lake Wartook (capacity = 29.5 GL) in 1887 and completed with the construction of Lake Bellfield (78.5 GL) in 1966 (Grampians Wimmera Mallee Water Corporation, 2011b). Lake Wartook on the MacKenzie River provides water to towns of Horsham and Natimuk and also to the environment. This reservoir is considered as a place with high recreational value (e.g. fishing). Lake Bellfield is located on Fyans creek and it provides water to towns of Halls Gap and Pomonal and also the Wimmera-Mallee pipeline system. This reservoir is known for its excellent water quality and low evaporative losses due to its relatively small surface area. The current headworks system is quite complex and highly interconnected. The other reservoirs included in this system are; Fyans (18.5 GL), Lonsdale (65.5 GL), Moora Moora (6.3 GL), Rocklands (348.3 GL), Toolondo (92.4 GL) and Taylors (27 GL). Lake Fyans is a relatively small reservoir which supplies water to towns of Ararat, Stawell, and Great Western. Lake Lonsdale is a large reservoir fed by the Mount William Creek and it is also regarded as an important provider of water to the environment. Owing to the relatively large surface area compared to volume held, both Lake Lonsdale and Lake Moora Moora experience high evaporative losses. Rocklands reservoir located on the Glenelg River is the largest reservoir in the Grampians headworks system of GWMWater. Taylors Lake supplies water to Wimmera-Mallee pipeline and also to the environment. Similar to Lake Wartook, this reservoir also has a high recreational value.

Until the recent past, the headworks system of GWMWater was utilising a network of earthen open channels (extending to over 18,000 km in length) for the conveyance of water. However this earthen open channel network was replaced at great cost with a network of pressurised pipelines (about 9,000km in length) known as the Wimmera-Mallee pipeline in 2010 (www.gwmwater.org.au). This pipeline reduced the evaporation and infiltration losses of the system significantly and aided in increasing the overall efficiency of the system. Modifications to GWMWater's water supply system with the Wimmera-Mallee pipeline was intended to provide increased resilience to drought and changes in the future climate. For the management of water resources in

this system in future, a set of the operating rules which accounts for the likely future climate change is needed. This study provides the hydroclimatic information pertaining to the future accounting for the likely future climate change needed for the management of this water supply system.

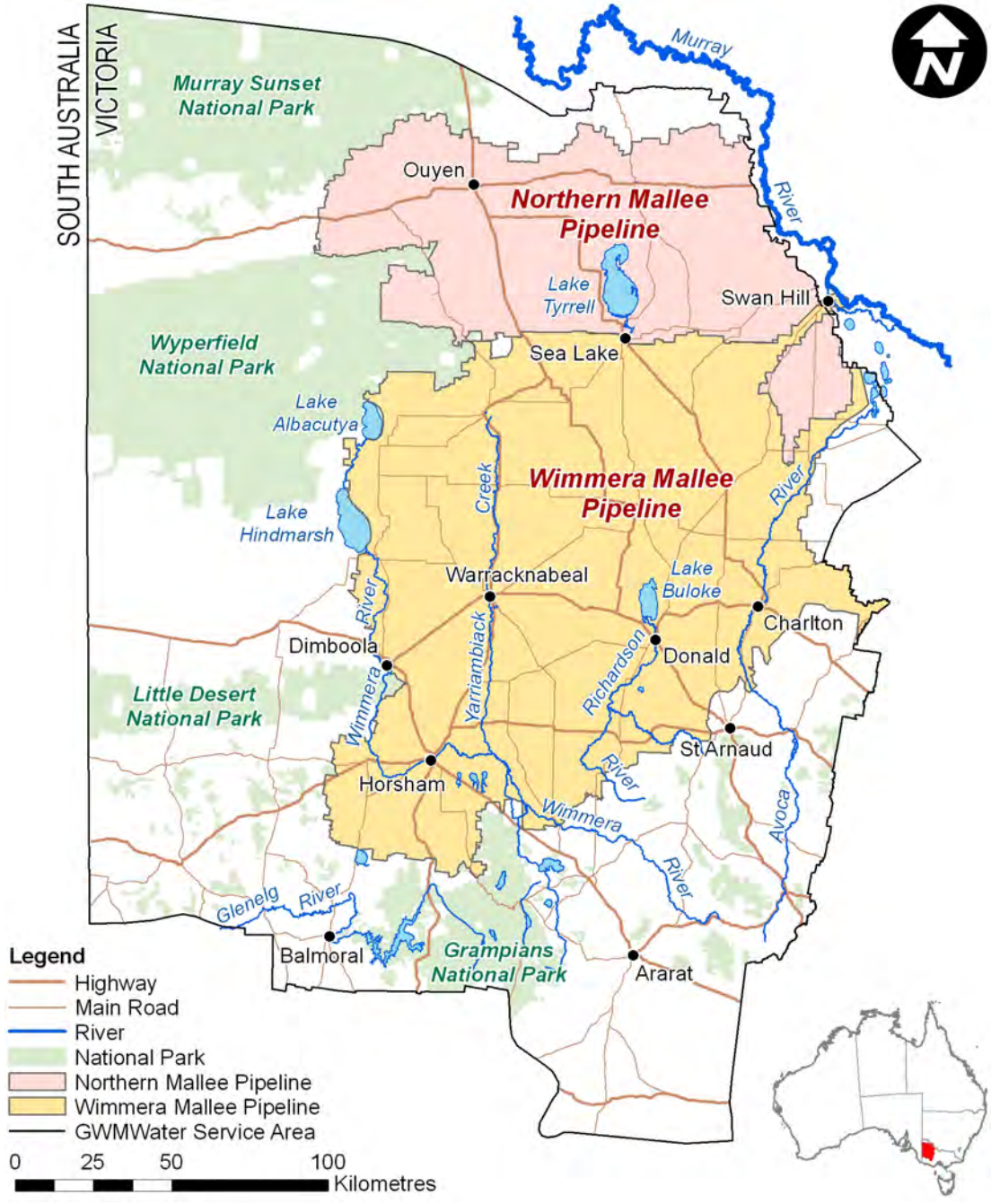

Figure 11 Headworks system of GWMWater

1.4 Research significance

Climate change influences the availability of water resources in a catchment. The recent droughts (e.g. Millennium drought 1997-2010), most likely caused or influenced by climate change, led to a large drop in inflows to many of the water supply reservoirs in Australia. Melbourne's water supply reservoirs, reservoirs of the Grampian Wimmera Mallee Water Corporation (GWMWater) in north-western Victoria, and reservoirs which serve Perth in south-west of Western Australia are good examples of reservoir systems affected. Projection of climate into the future accounting for likely climate change allows for water resource managers to better consider the planning and operation of these reservoirs in the future. As an example, the knowledge of the extreme precipitation is useful in the effective management of floods and droughts which involves design and construction of dams, reservoirs and flood levees. Furthermore, precipitation projections produced into the future aids in the determination of future availability of water in a catchment. Hence it is useful in determining the sustainable allocation of water and sharing resources for various purposes such as consumptive use, recreation and waterway health. Furthermore, the hydroclimatic projections produced in this study accounting for climate change, will feed into a parallel study which is focused on the development of a set of new operating rules for the management of water resources in the water supply systems of GWMWater.

In a conventional downscaling model, calibration and validation (development) are performed using some form of reanalysis outputs as inputs to the model. Then the projections of catchment scale climate into future are produced by using the outputs of a different GCM on the above developed downscaling model. The reanalysis data used in the development phase of the downscaling model are outputs of a GCM quality controlled and corrected against observations. The outputs of the GCM used for the projection of climate into future are not corrected or quality controlled as they refer to the future climate. Therefore there is a difference in quality of the inputs used to the downscaling model in its development and future projection phases. In such case, since the inputs to the downscaling model are obtained from two different sources with

different degrees of accuracy, these inputs are not homogeneous. In this study, two potential solutions for the above issue were investigated. As the first potential solution to the issue of non-homogeneity in inputs to a downscaling model, a statistical downscaling model was developed using the outputs of a GCM in view of using the outputs of the same GCM pertaining to future for producing projections of catchment scale climate into future. According to the knowledge of the author, there are no records in the published literature on the development of a downscaling model using GCM outputs as inputs prior to this study, possibly owing to the limited performances of such downscaling model. As the second potential solution, another statistical downscaling model was developed and the projections of catchment scale climate into future were produced using multi-model ensemble outputs derived from the outputs of a set of different GCMs as inputs to the model.

Furthermore, owing to differences in the structure, different GCMs tend to simulate the climate of the future differently. This phenomenon also influences the downscaling models, causing them to produce catchment scale projections of climate which vary with the GCM used in providing inputs to the downscaling model. As a solution to this issue, multi-model ensemble techniques are used in combining the outputs of different GCMs into a single projection. In this study, a downscaling model (the latter model described previously) was developed with multi-model ensemble outputs derived from the outputs of a set of different GCMs. The projections of catchment scale climate into the future were produced by introducing the multi-model ensemble outputs generated from the outputs of the same set of GCMs pertaining to the future. Hence this approach allows using the outputs of different GCM on a downscaling model for producing a single prediction at the point of interest in the catchment.

In a statistical downscaling study which involves downscaling at multiple stations, it is important to preserve the cross-correlation structure among the stations in the study area for a certain predictand and also among different predictands. However, the majority of the techniques currently used in multi-station and multi-station multivariate downscaling exercises are quite complex. As a solution to the above issue, in the current

study relatively simple yet effective approaches for multi-station and multi-station multivariate downscaling were developed. Furthermore, in this study downscaling GCM outputs directly to streamflows was investigated. This investigation was performed as downscaling GCM outputs directly to streamflows enables the making of a quick estimate of streamflows and avoids the need of a hydrologic model. Also, this study is the first in Australia to use statistical downscaling for the prediction of catchment streamflows, and is one of the very few studies across the world.

1.5 Outline of the thesis

This thesis consists of 7 chapters. The second chapter provides details on the literature on downscaling techniques in use and their applications. Also in the second chapter, the uncertainties in statistical downscaling arising from different sources such as; GHG emission scenarios, GCMs, observations against which downscaling models are calibrated, downscaling technique used, method of selection of predictors and how predictors are pre-processed are discussed along with some possible solutions such as bias-correction, multi-model ensemble techniques and GCM selection techniques. In chapters 3, 4, 5 and 6 investigations on the development of improved statistical downscaling methodologies for producing catchment scale projections of climate into future are presented.

The third chapter details the development (calibration and validation) of two statistical downscaling models for monthly precipitation; the first with reanalysis outputs and the second with GCM outputs. The first downscaling model was developed in the conventional manner using reanalysis outputs and is intended to be used with the outputs of another GCM for the projection of precipitation into future. Since inputs to this downscaling model during its development and future projection phases are obtained from two different sources with different degrees of accuracy, they are not homogeneous. As a solution to this issue, the second downscaling model was developed with the outputs of a GCM (same GCM used in the first downscaling model) and

intended to be used with the outputs of the same GCM for the projection of precipitation into future. A performance comparison of the above two downscaling models is provided in this chapter. The bias in GCM simulations and its propagation to the outputs of downscaling models is also discussed in this chapter. Furthermore this chapter details the investigation of the effectiveness of three different bias-corrections techniques in reducing the bias in the precipitation outputs of a downscaling model. The precipitation projections produced into future are also presented in the same chapter.

In chapter four, use of a multi-model ensemble approach in statistical downscaling is presented. Owing to the structural differences in GCMs, they tend to produce different projections of climate into the future. This causes the catchment scale projections produced by the downscaling model to vary with the GCM used for providing inputs to it. As a solution to this issue, this chapter describes the development of a downscaling model for monthly precipitation where projections into the future were produced using a set of homogeneous multi-model ensemble outputs derived from the outputs of multiple GCMs. In deriving multi-model ensemble outputs for the development (calibration and validation) phase of the downscaling model, outputs of several GCM were linked to the corresponding reanalysis outputs using multi-linear regression equations. The outputs of these multi-linear regression equations (multi-model ensemble outputs) were used for the development of the downscaling model. The inputs to the downscaling model corresponding to the future climate were generated by introducing the outputs of the set of GCMs pertaining to the future to the above multi-linear regression equations. The performance of this downscaling model during its calibration and validation phases are detailed along with the projection of precipitation produced into future.

In the fifth chapter the introduction of a relatively simple yet effective multi-station and multi-station multivariate statistical downscaling approaches are presented. In the multi-station downscaling approach, for a certain predictand, stations which showed high correlations with the other stations in the study area were identified, and downscaling models were developed (calibrated and validated) only at those stations. Then, linear regression equations were developed between the stations at which the downscaling

models were developed and the other stations which showed high correlations with them, using the observations. Thereafter, by applying the outputs of the above downscaling models on the aforementioned linear regression relationships, the values of the predictand at other stations were determined. This multi-station downscaling approach was further improved to a multi-station multivariate downscaling approach which is capable of downscaling GCM outputs to multiple predictands at multiple stations simultaneously. In this chapter, the performances of these multi-station and multi-station multivariate downscaling approaches were detailed along with the projections produced into future.

In chapter six of this thesis, development of a downscaling model for directly downscaling GCM outputs to catchment streamflows is detailed. In this chapter, the use of multi-linear regression (a linear regression technique) and least square support vector machine regression (non-linear regression technique) in downscaling are investigated. The impacts of the use of principal component analysis in pre-processing the inputs to downscaling models are also detailed in the same chapter.

Finally, in chapter seven a summary and the conclusions drawn from the study are presented along with some recommendations for future work. Figure 12 shows the interconnection between the work described in the papers included in the thesis.

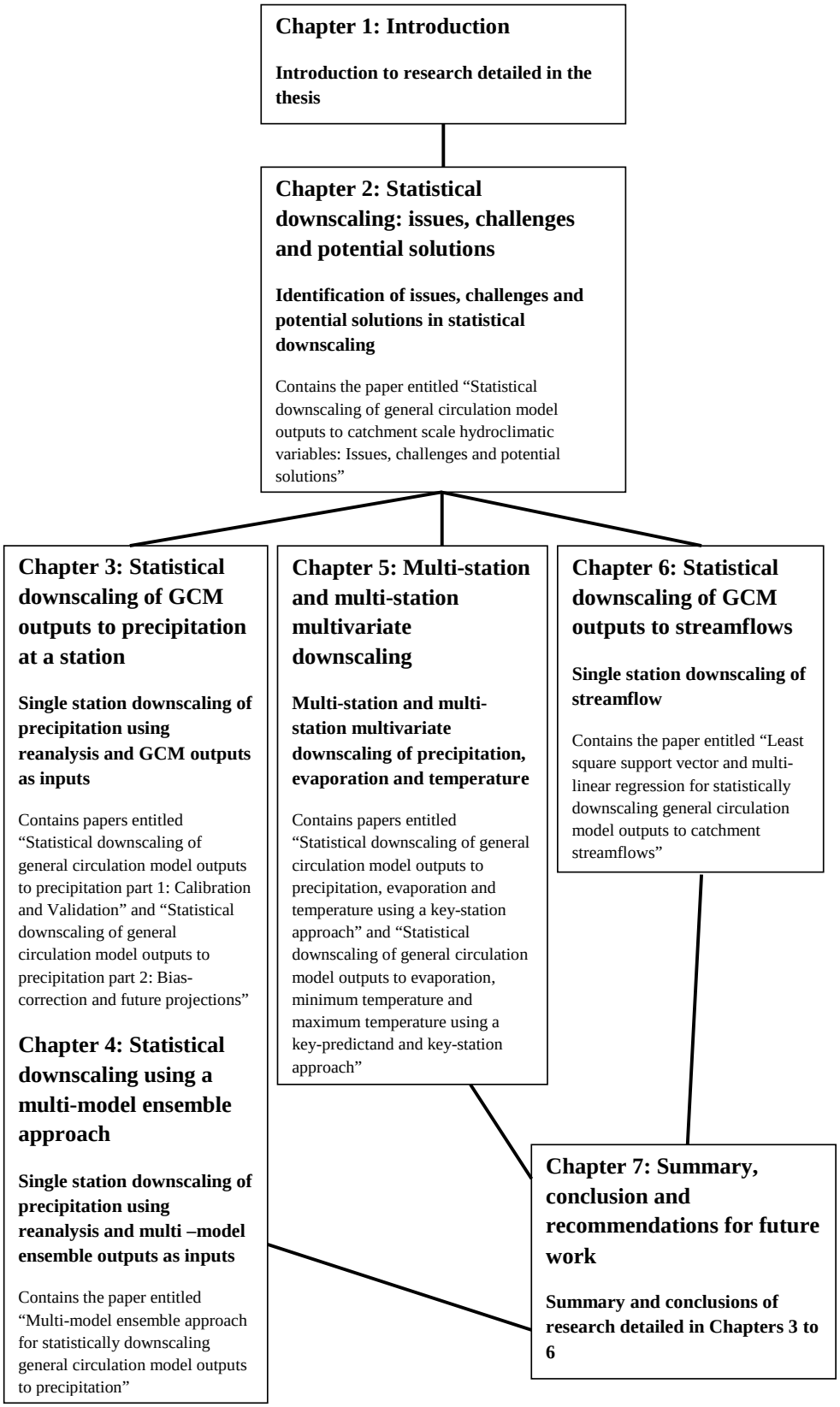

Figure 12 Interconnection between work described in the thesis

CHAPTER 2

STATISTICAL DOWNSCALING: ISSUES, CHALLENGES AND POTENTIAL SOLUTIONS

2.1 Introduction

Changes in the global climate since the 20th century were mostly due to the anthropogenic greenhouse gas (GHG) emissions than the natural variability of the climate (Crowley, 2000). During the 800,000 year period leading to the industrial revolution (1750-1850), the concentration of the atmospheric carbon dioxide which is the most dominant GHG, varied between 180 to 280 parts per million (ppm) (Tripati et al., 2009). Since then, due to the intense consumption of fossil fuels, the average global carbon dioxide concentration in the atmosphere has risen from 280 ppm to 397 ppm by May 2013 (Earth System Research Laboratory, 2013). The GHGs in the atmosphere absorb some of the radiation reflected by the earth's surface received from the sun, and this natural phenomenon is called "the greenhouse effect". The greenhouse effect aids the maintenance of the global temperature at a suitable level for the existence of the life. The rising GHG concentrations in the atmosphere intensify the natural greenhouse effect and cause an imbalance in earth's radiative energy budget (Trenberth et al., 2009) leading to human induced climate change (Hughes, 2003). Increase in the global temperature, sea level rise due to melting glaciers, changes in the precipitation patterns which cause floods and droughts are some of the impacts of the climate change (Intergovernmental Panel on Climate Change, 2000).

General Circulation Models (GCMs), based on the laws of physics are regarded as the most credible tools available for the projection of global climate hundreds of years into future considering the atmospheric GHG concentrations (Maraun et al., 2010). First in 1904, Bjerknes (1904) stated that, the condition of the atmosphere at a certain time and the laws of physics according to which one weather condition develops from another should be known, with sufficient accuracy for meteorological predictions. Bjerknes formulated a system of equations for seven basic variables of the atmosphere (pressure, temperature, density, humidity and the three components of velocity) based on the Newton's laws of motion, mass continuity, ideal gas law, and laws of thermodynamics to describe the atmospheric motions and energy flows (Tribbia and Anthes, 1987). However, Bjerknes was unable to solve these equations numerically despite his attempts of graphical solutions (Lynch, 2008). Richardson (1922) attempted a manual numerical solution to these equations for the first time. With the invention of computers in the latter half of the 20th century, numerical weather predictions became a reality. Philips (1956) performed the first long-range weather forecast up to one month. Since then, the increasing knowledge of the atmospheric processes and advances in computer technology aided the rapid evolvement of GCMs over time.

Though GCMs are regarded as the best tools available for the projection of the global climate hundreds of years into future (Anandhi et al., 2008), their outputs are at coarse spatial resolutions in the order of a few hundred kilometers (Tripathi et al., 2006). In other words, GCMs are unable to resolve sub-grid scale features such as topography, clouds and land use which influence much of the variance of climate at the catchment scale (Tisseuil et al., 2010). Therefore the outputs of GCMs cannot be directly used in catchment scale climate impact studies, which in general need hydroclimatic data at fine spatial resolutions (Willems and Vrac, 2011). As a solution to the mismatch between the coarse scale climate presented in GCM outputs and the catchment scale climate, downscaling techniques have been developed (Chen et al., 2010). There are two broad classes of downscaling techniques; (1) dynamic downscaling techniques and (2) statistical downscaling techniques. Sections 2.2 and 2.3 provide an overview on

dynamic and statistical downscaling respectively. These two sections contain some of the literature that is not discussed in detail in Section 2.5 on the two classes of downscaling. In Section 2.5, the issues and challenges associated with statistical downscaling approaches are presented along with some potential solutions.

2.2 Dynamic downscaling

In dynamic downscaling, an atmospheric physics based model called a Regional Climate Model (RCM) is nested in a GCM for the simulation of regional climate (Murphy, 1998). In this process, the initial and lateral boundary conditions to the RCM are provided by the GCM at multiple vertical and horizontal levels (Wilby and Fowler, 2011). This information is fed into the RCM through a lateral buffer zone (also known as the relaxation zone) in which the coarse GCM grid resolution is gradually converted into finer grid resolution in the RCM. In the RCM, this information is processed using the physics and the dynamics of the atmosphere, and the regional patterns of the climate variables are generated (Rummukainen, 2010). In certain cases, the spatial resolution gap between the GCM and the RCM can be quite large. As an example, when nesting a RCM with a spatial resolution of 10 km in a GCM which has a spatial resolution of 250 km, the resolution difference between the GCM and the RCM is in the order of 25. In such case, multiple nesting which involves downscaling starting from a larger domain with coarser spatial resolution and progressively migrating to smaller domains with finer spatial resolution (until the desired spatial resolution is attained) is performed (Rojas, 2006).

RCMs are widely used in the field of weather prediction, palaeoclimate studies, study of effect of land use changes on climate, simulation of plausible future climatic conditions in a selected region etc (Mearns et al., 2003). Dynamic downscaling techniques are capable of simulating the catchment scale climate at spatial resolution of about 5 - 50 kilometres (Yang et al., 2012). They produce spatially continuous fields of climate variables preserving spatial correlations and physics underlying the climatic processes

(Vasiliades et al., 2009). Another advantage of dynamic downscaling is that these approaches are capable of simulating the regional climate according to the changes in the regional land use. Since RCMs are operated at higher spatial resolutions, the improved representation of topographic features such as mountains, water bodies and other land features aid in the simulation of local climate more accurately (Rummukainen, 2010).

However, the high computational cost associated with the implementation of dynamic downscaling is considered to be a major drawback (Haas and Pinto, 2012). The selection of the domain size and the grid resolution are regarded as important choices in a regional climate simulation performed using a RCM. According to Jones et al. (1995) the optimal domain size and the grid resolution may vary depending on the region over which the RCM is run. The domain size and the grid resolution are directly related with the computational cost of a regional climate simulation (Qian and Lareef, 2010). Although the RCMs are operated at relatively finer spatial resolutions, some of the topography may be coarsely represented. As an example, even a spatial resolution of 5 kms may not be sufficient for the proper representation of a rapidly changing topography. This causes the RCM to incorrectly simulate the location and intensity of precipitation events that are highly influenced by the local topography (Malby et al., 2007). Also they cannot produce climate simulations at point scale (e.g. at weather stations) (Rummukainen, 2010) and the extremes simulated by them may dampen compared to those observed at weather stations (Haylock et al., 2008).

Furthermore, the dynamic downscaling techniques are quite sensitive to the initial conditions provided by the GCM. Also RCM may take some time called the spin up time in order to establish a stable relationship with the GCM (to attain climate equilibrium) (Panitz et al., 2013) and the simulations produced by the RCM during this period are not considered as credible predictions. Hence the RCM simulations produced during the spin up time are disregarded. The spin up time of a dynamic downscaling exercise may be in the order of a few months or a few years (Denis et al., 2002). The accuracy of RCM simulations depends on both the GCM outputs used as inputs to the

RCM and the parameterisation schemes employed in the RCM (Yhang and Hong, 2008). The bias in GCM boundary conditions propagates into the regional climate simulation produced by the RCM leading to erroneous projections of climate (Piani et al., 2010). Also the dynamic downscaling techniques are based on the assumption that the parameterisation schemes used in the RCMs for the simulation of the past climate are equally applicable for the changing climate in future (Sachindra et al., 2014a).

2.3 Statistical downscaling

Statistical downscaling techniques attempt to develop empirical relationships between the GCM outputs (e.g. mean sea level pressure, geopotential heights) and the catchment scale hydroclimatic variables (e.g. precipitation, evaporation and streamflows). The following advantages of the statistical downscaling techniques have been documented in Wilby and Wigly (1997). Statistical downscaling techniques are relatively simple and associated with low computational costs in comparison to their counterpart dynamic downscaling techniques. Unlike dynamic downscaling, statistical downscaling can provide projections at specific points in a catchment (e.g. observation station). Furthermore, statistical downscaling methods are capable of downscaling GCM outputs to variables such as streamflows, leaf wetness etc that are not simulated by GCMs. Statistical downscaling techniques can be easily applied to different regions. Also for the development of a statistical downscaling model, a profound knowledge in atmospheric physics is not essential (Sachindra et al., 2013a).

Although statistical downscaling techniques posses the above advantages, they are associated with the following disadvantages. All statistical downscaling techniques are based on the assumption that the relationships determined between the large scale atmospheric variables (e.g. GCM or reanalysis outputs) and observations of the predictand for the past climate are also valid for the changing climate in future (von Storch et al., 2000). Under changing climate this assumption may be less reliable. This assumption is similar to that made on the applicability of parameterisation schemes

in dynamic downscaling for the future climate. Statistical downscaling techniques in general need a long set of observations for the reliable calibration and validation of downscaling models (Charles et al., 2004; Sachindra et al., 2014a). Therefore in data scarce regions, successful implementation of statistical downscaling models is a challenge. Also statistical downscaling models are considerably dependent on the predictors that are used as inputs to these models (Fowler et al., 2007). The simulations produced by a statistical downscaling model are sensitive to the atmospheric domain for which the inputs are extracted (Wilby and Wigly, 2000). The under-estimation of extreme events is also documented as a limitation of statistical downscaling techniques (D'onofrio et al., 2010).

Statistical downscaling techniques are classified under three categories (1) regression based methods, (2) weather classification techniques, and (3) weather generation techniques (Wilby et al., 2004).

2.3.1 Regression based methods

In regression based statistical downscaling methods, empirical relationships between the large scale atmospheric variables (e.g. reanalysis outputs, GCM outputs) and the observations of catchment scale hydroclimatic variables are developed for the past climate using either linear or non-linear regression techniques (Chen et al., 2010). These relationships are used with the large scale atmospheric variables simulated by GCMs pertaining to future for the projection of catchment scale hydroclimate into future. According to Nasseri et al. (2013), regression based methods are considered the most widely used statistical downscaling techniques. This is mainly because regression based downscaling methods are easy to implement and also several ready to use software packages/toolboxes such as SDSM (Statistical DownScaling Model) (Wilby and Dawson, 2012), ASD (Automated Statistical Downscaling) (Hessami et al., 2008), GeneXproTools (Ferreira, 2006), LS-SVMlab toolbox (De Brabanter et al., 2010) etc are available. However, the regression based downscaling methods in general tend to poorly simulate the variance in the observations of the predictand of interest. Also the

extreme events are under-predicted often by them (Tripathi et al., 2006; Sachindra et al., 2013a). Furthermore, the linearity assumption of predictor-predictand relationships and the assumption of normality of inputs to the downscaling model in linear regression techniques may not be true for certain data sets (Wilby and Fowler, 2011).

Joshi et al. (2013) compared the performances of two statistical downscaling models developed using the Relevance Vector Machine (RVM – a non-linear regression technique) and Multiple Linear Regression (MLR) for downscaling GCM outputs directly to low flow indices pertaining to three rivers in eastern Canada. It was found that RVM based downscaling model outperforms the MLR based downscaling model in the simulation of low flow indices. Furthermore, it was commented that the complexity of the RVM technique may have a negative impact on the computation time, particularly when the input sample size is considerably large. Sachindra et al. (2013a) used Least Square Support Vector Machine (LS-SVM – a non-linear regression technique) and MLR for downscaling reanalysis outputs to monthly streamflows at a station located in north-western Victoria, Australia. It was found that LS-SVM was marginally better than MLR in the simulation of streamflows. Meenu et al. (2013) employed MLR and LS-SVM techniques for downscaling GCM outputs to daily precipitation and temperature over a catchment in the state of Karnataka, India. The downscaled precipitation and temperature were introduced into a hydrologic model for simulating streamflows. It was commented that the downscaling models developed using the MLR technique were able to simulate the variance of the minimum and the maximum temperature much better than that of precipitation, and the LS-SVM based downscaling model was able to better capture the precipitation in comparison to the models based on MLR. Goyal and Ojha (2012) used Artificial Neural Networks (ANN – a non-linear regression technique) and MLR for downscaling GCM outputs to monthly mean minimum and maximum temperature at a station located in Rajasthan, India. It was concluded that the ANN based downscaling model was much effective in comparison to its counterpart model based on MLR in downscaling large scale atmospheric variables into monthly mean minimum and maximum temperature at the station of interest. In a study conducted by Ghosh and Katkar (2012), which employed

MLR, ANN and SVM for downscaling GCM outputs to monthly precipitation, it was found that all techniques yield similar performances in the calibration phase of the downscaling model. However, the SVM based model was able to simulate the high precipitation values better in comparison to the other two models based on ANN and MLR techniques. Furthermore, it was stated that the ANN based model was better at simulating low and intermediate precipitation values. The ANN and LS-SVM techniques were employed by Tripathi et al. (2006) for downscaling GCM outputs to monthly precipitation over India. It was stated that both these techniques fail to correctly capture the extreme precipitation events seen among the observations.

2.3.2 Weather classification techniques

Weather classification techniques (weather typing) in statistical downscaling aim at classifying the large scale weather conditions into number of discrete states (weather types) based on their synoptic similarities, and links them with the observations of predictands. Then corresponding to the future states of the large scale weather characterised by the climate models, the catchment scale weather pertaining to future is derived. In other words, weather classification methods link the occurrences of large scale weather patterns with local scale climate. The following advantages and disadvantages of weather classification techniques were documented in Huth et al. (2008). The main benefit of weather classification techniques is that they are capable of downscaling highly non-linear relationships between the predictors and the predictand of interest. However, these techniques are dependent on the assumption that a certain large scale weather pattern seen in the past will lead to the same local scale weather condition in future. Another issue associated with weather classification techniques is that if a weather type characterised by the GCM for the future is not found among the past weather types, the determination of the local weather becomes chaotic.

In literature, weather classification techniques are grouped into several categories based on different attributes. Kalkstein et al. (1996) classified the weather classification techniques based on the scale of application (point, regional and continental) and the

climatological phenomena (pressure patterns based weather type and thermal and moisture properties of air mass). Yarnal (1993) subdivided the weather classification techniques into two main categories; (1) manual and (2) automated. Whereas Huth et al. (2008) classified weather classification techniques into three types; (1) subjective, (2) objective, and (3) mixed (hybrid). The manual and automated methods stated in Yarnel (1993) are the same defined in Huth et al. (2008) as subjective and objective weather classification techniques respectively. The subjective methods of weather classification are also called manual classification techniques and the classification is mainly based on the expert knowledge of the physical attributes of the circulations (e.g. visual analysis of synoptic charts). Sheridan (2002) documented the following disadvantages of subjective weather classification techniques. The classification choices are arbitrary to a large degree and also the classification process is time consuming. Another disadvantage is that a weather classification scheme defined over a certain region cannot be applied to another region. The Lamb weather types (Lamb, 1972) defined over the British Isles is one of the early subjective weather classification schemes based on the attributes of the air flow direction and the level of cyclonicity. The Hess–Brezowsky weather classification by Hess and Brezowsky (1977) is also another subjective weather classification scheme based on the circulation patterns (surface pressure) over the Europe and the North-East Atlantic region.

The objective weather classification techniques are dependent on various numerical methodologies. They are also known as automated techniques as these techniques need the use of a computer owing to their complexity. Some of the numerical methodologies used in the automated weather classification techniques are; correlation coefficients for the determination of similarity between weather patterns (Lund, 1963), clustering algorithms (Kalkstein et al., 1987; D'onofrio et al., 2010), principal component analysis (Huth et al., 2008), self-organizing maps (Cassano et al., 2006), classification and regression trees (Cannon et al., 2002), hidden Markov models (Hughes and Guttorp, 1994), linear discriminant function analysis (Kalkstein et al., 1996), cumulative logistic regression and nonlinear regression (Cheng et al., 2011) etc. The objective weather classification techniques are easy to apply and computationally effective than the

subjective techniques. However, these techniques are applicable to a single station or a region at a time (Sheridan et al., 2002).

The mixed weather classification techniques possess some subjective and objective attributes (e.g. James (2007)). Frakes and Yarnal (1997) used a mixed weather classification technique in which the sea-level pressure charts over the eastern USA were manually classified into several groups and then a correlation coefficient based procedure was used for the assignment of local scale weather to each weather group. They stated that this hybrid scheme is more reliable than a subjective or an objective weather classification technique.

2.3.3 Weather generation techniques

In weather generation techniques, the weather pertaining to future is generated by adjusting the parameters of the weather generator according the changes in the GCM outputs pertaining to future (Kou et al., 2007; Wilks, 2010). They are parametric stochastic models which generate time series of weather data while preserving the statistics of observations such as averages, variances and covariances, frequencies, extremes etc (Wilks and Wilby, 1999). The simplest weather generator for daily precipitation may have two parameters; (1) the probability of occurrence of a wet day, and (2) the amount of precipitation.

In the application of the above weather generator, the values of the two parameters from the GCM outputs for the future climate and also for the past climate pertaining to the baseline period (simulated by the same GCM) are determined. Then the percentage changes of the two parameters in the GCM outputs for the future with respect to those simulated for the baseline period are determined. Thereafter the values of the two parameters pertaining to the observed precipitation of the baseline period are scaled either up or down, corresponding to the above determined changes. These scaled parameters are used in the generation of occurrences of wet days and precipitation amounts at the station of interest. The most important advantage of weather generators

is that they can be used to generate time series of weather data of unlimited length and number (Kreienkamp et al., 2013). These synthetic time series of weather data provide a way for the assessment of risk involved in the design of water resources systems (Mehrotra et al., 2006). However the majority of the weather generators are not capable of preserving the spatial correlation structure seen among the observations at multiple stations located in the same study area (Baigorria and Jones, 2010). Furthermore, the multi-station weather generation techniques capable of preserving the spatial coherence among stations are complex and the number of parameters in a multi-station weather generator may increase largely with the number of stations (Mehrotra et al., 2006).

Richardson (1981) used a weather generation technique based on the first order Markov chains and an exponential distribution for the simulation of daily precipitation and a multivariate (multiple variables simulated concurrently) auto-regression model for the simulation of daily maximum temperature, minimum temperature and solar radiation. It was stated that the simulation of the maximum temperature, the minimum temperature and the solar radiation is much effective than that of precipitation, as the observations of these climatic variables contain less zeros and their distributions are much less skewed. This weather generation techniques proposed in Richardson (1981) is regarded as the most popular daily weather generation technique (Wilks and Wilby, 1999). Wilks (1992) used the weather generation techniques specified by Richardson (1981) for the simulation of catchment scale daily precipitation, maximum temperature, minimum temperature and solar radiation using the GCM outputs. Wilks (1998) extended the precipitation generation mechanism specified in Richardson (1981) for the generation of daily precipitation at multiple stations. Wilks (1999) further extended the weather generation models defined in Richardson (1981) for the concurrent simulation of precipitation, maximum temperature, minimum temperature and solar radiation at multiple stations. Also in the studies by Khalili et al. (2007), Srikanthan and Pegram (2009), Jeong et al. (2013), models for the generation of daily precipitation at multiple stations are detailed.

VICTORIA UNIVERSITY
MELBOURNE AUSTRALIA

2.4

PART B:

DECLARATION OF CO-AUTHORSHIP AND CO-CONTRIBUTION: PAPERS INCORPORATED IN THESIS BY PUBLICATION

This declaration is to be completed for each conjointly authored publication and placed at the beginning of the thesis chapter in which the publication appears.

Declaration by [candidate name]: Sachindra Dhanapala Arachchige

Signature:

Date: 08/07/2014

Paper Title:
Statistical downscaling of general circulation model outputs to catchment scale hydroclimatic variables: Issues, challenges and potential solutions.

In the case of the above publication, the following authors contributed to the work as follows:

Name	Contribution %	Nature of Contribution
Sachindra Dhanapala Arachchige	85	Conceptual ideas, analysis, paper writing
Fuchun Huang	5	Critical comments, help with statistics
Andrew Barton	5	Critical comments, industry inputs
Chris Perera	5	Critical comments, discussion of conceptual ideas

VICTORIA UNIVERSITY
MELBOURNE AUSTRALIA

DECLARATION BY CO-AUTHORS

The undersigned certify that:

1. They meet criteria for authorship in that they have participated in the conception, execution or interpretation of at least that part of the publication in their field of expertise;
2. They take public responsibility for their part of the publication, except for the responsible author who accepts overall responsibility for the publication;
3. There are no other authors of the publication according to these criteria;
4. Potential conflicts of interest have been disclosed to **a)** granting bodies, **b)** the editor or publisher of journals or other publications, and **c)** the head of the responsible academic unit; and
5. The original data is stored at the following location(s):

Location(s):
College of Engineering and Science,Victoria University,Melbourne,Australia

and will be held for at least five years from the date indicated below:

		Date
Signature 1	[redacted]	29/07/2013
Signature 2	[redacted]	29/07/2013
Signature 3	[redacted]	16/8/2013
Signature 4	[redacted]	26/07/13

2.5 Statistical downscaling: issues, challenges and potential solutions

As stated earlier in Section 2.3, statistical downscaling techniques possess number of advantages such as the simplicity in structure, low computational cost, ability to simulate hydroclimatic variables that are not even simulated by GCMs, point scale projections etc. However, these techniques are subjected to a cascade of uncertainties originating from different sources such as GHG emission scenarios, GCMs, observations against which downscaling models are calibrated, downscaling technique used, method of selection of predictors, how predictors are pre-processed etc. Therefore in decision making, the catchment scale hydroclimatic projections produced by any downscaling model should be used cautiously with an understanding of the uncertainties lying beneath the projections. Some of the issues in a downscaling study can also be remedied in several ways such as application of a bias-correction, use of long records of observations for model calibration, uncertainty analysis of projections using several GHG emission scenarios, ensemble approaches for the combination of several predictions into one single prediction etc.

In this section the issues and the challenges associated with statistical downscaling of GCM outputs to catchment scale hydroclimatic variables are discussed along with some of the potential remedies.

This section contains the following journal paper;

1. **Sachindra DA**, Huang F, Barton AF, Perera BJC. 2013c. Statistical downscaling of general circulation model outputs to catchment scale hydroclimatic variables: Issues, challenges and potential solutions. *Journal of Water and Climate*. (Article in press). (SCImago journal rank indicator = Q2; Impact Factor: 1.000).

Manuscript Accepted for publication in Journal of Water and Climate Change

Statistical Downscaling of General Circulation Model Outputs to Catchment Scale Hydroclimatic Variables: Issues, Challenges and Potential Solutions

D.A. Sachindra[a]*, F. Huang[a], A. Barton[a,b], and B.J.C. Perera[a]

[a]*Victoria University, P.O. Box 14428, Melbourne, Victoria 8001, Australia.*

[b]*Federation University, PO Box 663, Ballarat, Victoria 3353, Australia.*

*Correspondence to: D. A. Sachindra, College of Engineering and Science, Footscray Park Campus, Victoria University, P.O. Box 14428, Melbourne, Victoria 8001, Australia. E-mail: sachindra.dhanapalaarachchige@live.vu.edu.au. Telephone: +61 03 9919 4907.

Published as: Dhanapala Arachchige, Sachindra, Huang, Fuchun, Barton, Andrew and Perera, B. J. C (2014) Statistical downscaling of general circulation model outputs to catchment scale hydroclimatic variables: issues, challenges and possible solutions. Journal of Water and Climate Change, 5 (4). pp. 496-525

Available from: https://doi.org/10.2166/wcc.2014.056

Abstract

The aim of this paper is to discuss the issues and challenges associated with statistical downscaling of GCM outputs to hydroclimatic variables at catchment scale and also to discuss potential solutions to address these issues and challenges. Outputs of GCMs (predictors of statistical downscaling models) suffer a considerable degree of uncertainty, mainly due to the lack of theoretical robustness caused by the limited understanding of various physical processes of the atmosphere and the incomplete mathematical representation of those processes in GCMs. The presence of number of future GHG emission scenarios with equal likelihood of occurrence leads to scenario uncertainty. Outputs of a downscaling study are dependent on the quality and the length of the record of field observations, as statistical downscaling models are calibrated and validated against these observations of the hydroclimatic variables (predictands of statistical downscaling models). The downscaled results vary from one statistical downscaling technique to another due to different representations of the predictor-predictand relationships. Also different techniques used in selecting the predictors for statistical downscaling models influence the model outputs. Although statistical downscaling faces the above issues, still it is considered as a potential method of predicting the catchment scale hydroclimatology from GCM outputs.

Keywords*: Statistical downscaling, General Circulation Model, Greenhouse Gas Emission.*

INTRODUCTION

Anthropogenic climate change caused by the increasing Greenhouse Gases (GHGs) in the Earth's atmosphere is a well-accepted phenomenon (Wilks 2010), alongside the natural variability of climate. With the accumulation of the GHGs, the global climate is expected to change throughout the 21st century (IPCC 2000; Dessai et al., 2005). In the modern world, influences of climate change on water resources have received increasing attention (Chen et al., 2010), as water is one of the essential resources for the existence of humans, animals and plants.

General Circulation Models (GCMs), based on the laws of physics are regarded as the most credible tools available for the projection of global climate, hundreds of years into future, considering the possible future atmospheric GHG concentrations defined by GHG emission scenarios (Prudhomme et al., 2003). However, GCMs produce their outputs at coarse grid resolutions and therefore unable to represent sub-grid scale climate properly (Anandhi et al., 2008). Hydroclimatic data at finer resolutions are needed for hydrologic studies at the catchment scale (Prudhomme et al., 2003). This scale mismatch, between the GCM outputs and the hydroclimatic data needed at the catchment level, is addressed by employing downscaling techniques (Fowler et al., 2007).

Downscaling techniques are grouped under two broad classes; dynamic downscaling and statistical downscaling. In dynamic downscaling, a higher resolution Regional Climate Model (RCM) is nested in a coarse resolution GCM, and boundary conditions are fed into the RCM from the GCM. RCMs simulate physical processes of the atmosphere at the catchment scale unlike the GCMs (Fistikoglu & Okkan 2011). These RCMs exhibit reasonable potential in capturing the extremes of climate variables (such as precipitation) at the catchment scale (Huntingford et al., 2003). Dynamic downscaling generates spatially continuous fields of climate variables preserving spatial correlations and physics underlying the climatic processes (Vasiliades et al., 2009). The major disadvantages of dynamic downscaling techniques are that, they are

computationally expensive and are highly dependent on the boundary conditions provided by the GCM (Chu et al., 2010).

Statistical downscaling relies on the empirical relationships derived between the GCM outputs (predictors of statistical downscaling models) and catchment scale variables (predictands of statistical downscaling models) such as precipitation, streamflow, surface air temperature etc (Hay & Clark 2003). Wilby et al. (2004) classified statistical downscaling techniques under three categories; regression methods, weather classification methods and weather generators. In regression methods, linear or non-linear mathematical relationships between GCM outputs and catchment level variables are derived. In weather classification techniques, predictands are estimated by matching the present state of the weather with a past similar state (of the weather) in record (Wilby et al., 2004). Weather generators produce weather data for the future by scaling their parameters either up or down by the equivalent changes observed in GCM outputs for future. They produce synthetic weather sequences, which capture the essential features of the observed weather (Kou et al., 2007). This enables the generation of catchment scale time series of climate variables, which resembles the larger-scale changes in the GCM outputs. Statistical downscaling techniques are simpler and computationally less expensive in comparison with dynamic downscaling techniques and could be used without profound knowledge of the physical processes of the hydrologic cycle. Therefore often GCM outputs are statistically downscaled for the assessment of possible impacts of climate change at the catchment scale. All statistical downscaling techniques are dependent on the assumptions that, (1) the empirically derived predictor-predictand relationships are valid under the changing climate in future, (2) predictors (of the statistical downscaling models) used are realistically simulated by GCMs, and (3) predictors clearly depict the climate change signal (von Storch et al., 2000).

Multiple Linear Regression (MLR) (Chen et al., 2010), Artificial Neural Networks (ANN) (Tripathi et al., 2006), Support Vector Machine (SVM) (Anandhi et al., 2008), Relevance Vector Machine (RVM) (Ghosh & Mujumdar 2008), and Gene Expression

Programming (GEP) (Hashmi et al., 2009a; Coulibaly 2004) are some of the widely used regression based statistical downscaling techniques. Method of meteorological analogues (Timbal et al., 2009), recursive partitioning (Schnur & Lettenmaier 1998) and nonhomogenous hidden Markov models (Mehrotra et al., 2004) are examples of weather classification techniques. Combination of Markov chains and two parameter Gamma distribution is an example of a typical weather generator in use (Richardson 1981).

Although statistical downscaling approaches possess number of advantages, they are susceptible to a cascade of uncertainties and errors introduced at various stages of the process. Therefore statistical downscaling is associated with many issues and the process faces number of challenges in delivering a reliable output at the catchment scale, minimising the cascade of uncertainties. According to Hashmi et al. (2009a), there are four major types of issues associated with the projection of catchment scale climate into future, which are the uncertainties in; (1) GHG emission scenarios, (2) GCMs, (3) observations, and (4) downscaling techniques. Dessai et al. (2005) stated that the uncertainties embedded in regional scale climate projections are mainly due to the uncertainties in projections of GHG emissions produced into future, the presence of different GCMs which employ different internal structures, and the numerous downscaling techniques in use.

This paper presents a discussion on some of the issues and challenges associated with statistical downscaling of hydroclimatic variables to catchment scale, and also potential solutions to these issues and challenges. For better readability, these issues and possible solutions are detailed under several sub topics; uncertainties in GCM predictions, uncertainties in GHG emission scenarios, issues with observations of hydroclimatic variables, issues with statistical downscaling techniques, and issues with the predictors of downscaling models.

UNCERTAINTIES IN GCM PREDICTIONS

GCMs consider the surface of the Earth, oceans and atmosphere in three dimensional grid boxes, in solving the physics based mathematical equations, which are used to describe the complex atmospheric motions. On these equations of atmospheric motion, different assumptions and approximations are employed by different GCMs. The assumptions and approximations, horizontal and vertical grid resolutions and the process explicitly modelled in a GCM, could vary from one GCM to another, causing differences in their outputs. In other words, due to a variety of model structures based on various assumptions and approximations, employed to simplify the complex nature of the atmosphere, different GCMs produce different predictions (Yu et al., 2002). As an example, GCMs project different rises in global mean surface air temperatures by the end of the 21st century in the range of 1.5˚ - 4.5˚ C, when the carbon dioxide concentration in the atmosphere is doubled (Covey et al., 2003).

Smith & Chandler (2009) assessed 22 GCMs involved in the Coupled Model Intercomparison Project phase 3 (CMIP3), and commented that ECHAM5, GFDL2.0, GFDL2.1, MIROC3.2 (high-resolution) and HadCM3 could better represent the Australian rainfall and the ENSO phenomena, than the other models. In that study, the agreement between the precipitation outputs of GCMs and the observed precipitation was assessed using root mean square error (RMSE) and correlation coefficients. Hewitson & Crane (2006) assessed the agreement of daily precipitation predictions of ECHAM4.5, HadCM3 and CSIRO Mk2 over South Africa, and found that there are large differences in predictions among these models. Perkins et al. (2007) used the overlap between the Probability Density Functions (PDF) of several GCM outputs and the corresponding observations as a measure of prediction skills of 14 GCMs over Australia. There, it was realised that BCCR2.0, ECHAM5 and ECHO-G could better reproduce the observed precipitation over Australia. Furthermore, it was realised that MIROC3.2 (high resolution), MIROC3.2 (medium resolution) and ECHO-G better reproduced the maximum temperature, while the minimum temperatures were better predicted by GFDL2.1, CSIRO Mk3 and CGCM1. Lambert & Boer (2001) proved that

different GCMs could simulate different variables with various levels of accuracies. Gleckler et al. (2008) assessed the ability of 21 CMIP3 GCMs in reproducing 22 different variables under the IPCC 20th century climate experiment, across the entire globe, and found that the accuracy of GCMs vary over space and the variable considered. According to the above examples, it is clear that different GCMs show different levels of sensitivities to the climate over a certain geographic region, and the same GCM could better predict some variables than others.

Owing to computational limitations, GCMs are operated at relatively coarse spatial resolutions (Ward & Sun 2006). When the spatial resolution of a GCM is halved (e.g. when 5.0˚ x 5.0˚ is halved it becomes 2.5˚ x 2.5˚), approximately the model becomes ten times slower due to the increased computational load (Tebaldi & Knutti 2010). The coarse spatial resolution of GCMs is a major challenge in using their outputs directly at the catchment level. At this coarse scale, GCMs fail to correctly represent sub-grid scale features such as land use, the development of cold and warm fronts (i.e. convective cloud processes), and hurricanes (Parry et al., 2004). With the advancements in atmospheric and computer sciences, more GCM outputs at relatively finer spatial resolutions are available under Coupled Model Intercomparison Project phase 5 (CMIP5). The median of the spatial resolution of the CMIP5 GCMs is finer than that of CMIP3 GCMs, but the finest resolution of CMIP5 remains the same as that of CMIP3 (Teng et al., 2012). However, still the spatial resolutions of GCMs are too coarse for the direct application of their outputs at the catchment scale. The outputs of 23 CMIP3 and over 50 CMIP5 GCMs, produced at different spatiotemporal resolutions are currently available to public on the website of Program for Climate Model Diagnosis and Inter-comparison (PCMDI) at http://www.pcmdi.llnl.gov/.

Most of the catchment level studies need not only data at fine spatial resolutions but also data at fine temporal resolutions, preferably at sub-daily scales. As an example, in developing Intensity - Frequency - Duration (IFD) curves accounting for possible climate change at a certain location, rainfall data at very fine temporal resolutions (at the resolution of few minutes) are needed (Nguyen et al., 2008). However, currently

very limited GCM outputs (also valid for CMIP5 GCMs) are available to the public on web archives at fine temporal resolutions, even at 3 hour level. Furthermore, GCM data are available to public on the web archives (e.g. http://www-pcmdi.llnl.gov/, http://www.ipcc-data.org/), only for a limited number of variables at the daily and especially at the sub-daily time scales, unlike the monthly time scale. This is because, though GCMs are run at fine temporal scales, it will take large amount of computer storage space to save the projections corresponding to all time steps. Due to this issue, most of the GCM data are aggregated to coarse time steps (e.g. monthly time step) and archived on the web.

According to Prudhomme et al. (2002), daily rainfall predictions of GCMs are associated with considerable uncertainties, implying that sub-daily scale outputs have more uncertainties compared to daily and monthly GCM outputs. Wilby et al. (1998) stated that, the use of GCM outputs at catchment scale is not only restricted by their coarse spatial resolution but also by the high unreliability at temporal scales finer than months. As an example, when the daily precipitation outputs of a GCM are summed to obtain monthly precipitation, monthly precipitation amounts could become more reliable, since under or over estimations of daily precipitation totals could compensate each other in summing. Hence, monthly GCM outputs could have a better reliability over daily or sub-daily outputs. During the aggregation of GCM data from finer temporal resolutions to coarser temporal resolutions, the amounts might be well estimated at the coarser temporal resolution. However, the aggregation of data, results in a loss of information on events, which take place at fine temporal scales such as the occurrences of daily maximum and minimum temperatures and variations in precipitation during a day. Though there is considerable uncertainty in daily and sub-daily GCM outputs, number of the downscaling exercises have been performed at the daily time scale, since the majority of catchment scale investigations (e.g. hydrologic modelling) require hydroclimatic inputs at finer temporal resolutions. However, it should be noted that finer the temporal resolution of the GCM outputs less reliable they are. If a certain downscaling study uses daily or sub-daily GCM outputs (even monthly outputs), therefore it is advisable to perform a bias-correction on them. Some of the

bias-correction measures applied to GCM outputs stated in the past literature, have been summarised below. It is clear that, with the advancement of knowledge on various atmospheric processes, the GCM uncertainty is further reduced. Therefore in the future more reliable GCM outputs at finer time scales could be expected.

The bias is a quantitative representation of the uncertainty in GCM outputs. Simply, the GCM bias is explained as the difference between the GCM outputs and the corresponding observations (Salvi et al., 2011). Sharma et al. (2007) stated that, GCM outputs often contain bias which hinders their direct use at the catchment level, along with the coarse spatial resolution. Ojha et al. (2012) stated that, the bias in GCM outputs should be corrected prior to any use. According to Li et al. (2010), GCM bias is due to the limited knowledge of the physical processes of the atmosphere and the simplification of the naturally complex climate system in the mathematical equations used in GCMs. The correction of bias can be done in two ways; (1) application of bias-correction to raw GCM outputs, and (2) the correction of bias in the outputs of the downscaling models which were run with the GCM outputs (Sachindra et al., 2014). There are different bias-correction techniques available. The widely used bias correction methods are monthly bias-correction (Johnson & Sharma 2012), nested bias-correction (Johnson & Sharma 2012), quantile mapping technique (Panofsky & Brier 1968), equidistant quantile mapping technique (Li et al., 2010), linear scaling, local intensity scaling, power transformation, variance scaling, and delta-change approach (Teutschbein & Seibert 2012). These methods can be applied either to the raw GCM/RCM outputs or to the outputs of a downscaling model.

The monthly bias-correction is one of the simplest bias-correction techniques in use. In this method, for the correction of bias in the hydroclimatic variable (output of a GCM/RCM or a downscaling model) for the past climate, the average and the standard deviation of the time series of the hydroclimatic variable are replaced with those of reference data (e.g. observations or reanalysis outputs) (Johnson & Sharma 2012). The correction of bias of the hydroclimatic variable in future climate is based on the assumption that, the bias in the variable during the past is the same in the future. Unlike

the monthly bias-correction, the nested bias-correction (Johnson & Sharma 2012) is capable of correcting the average, the standard deviation and also the lag 1 autocorrelations of a hydroclimatic variable, simultaneously at monthly and annual time scales. It also assumes that, the bias in the variable (to be bias-corrected) for the past climate will remain the same in the future (Johnson & Sharma 2012). The monthly and the nested bias-corrections were used by Ojha et al. (2012) and Johnson & Sharma (2012) for correcting the bias in the monthly precipitation outputs of GCMs, over India and Australia respectively.

Another technique used in the bias-correction of hydroclimatic variables is the quantile mapping technique (Panofsky & Brier 1968). In this technique, all statistical moments of the hydroclimatic variables to be corrected (e.g. outputs of a GCM or a downscaling model) are matched with those of a reference set of data (e.g. observations or reanalysis outputs) for the past climate. This is achieved by mapping the Cumulative Distribution Functions (CDF) of the hydroclimatic variables onto that of reference data. For bias-correcting the projections produced into future, first, corresponding to the values of the hydroclimatic variable for the future projections, the CDF values are extracted from the CDF which was derived from the model predictions for the past climate. Then pertaining to these CDF values, the bias-corrected values of the hydroclimatic variable for the future climate are extracted from the CDF of the reference data set. The quantile mapping technique was used by Wood et al. (2004) for correcting the bias in the precipitation and temperature outputs of a GCM. Ghosh & Mujumdar (2008) used quantile mapping for the bias correction of streamflow downscaled from GCM outputs.

The equidistant quantile mapping technique (Li et al., 2010) is a variant of quantile mapping. Similar to quantile mapping, in equidistant quantile mapping, for the bias-correction of a hydroclimatic variable pertaining to the past climate, its CDF is mapped onto the CDF of the reference data set. In the application of the equidistant quantile mapping technique for the future climate, the difference between the CDF of the hydroclimatic variable and the CDF of the reference data set, of the past climate, is subtracted from the CDF of the hydroclimatic variable pertaining to future climate. Li et

al. (2010) successfully bias-corrected the precipitation and temperature produced by a GCM with equidistance quantile mapping.

A gamma distribution based quantile mapping technique was used by Piani et al. (2010) for bias-correction of daily precipitation downscaled using a RCM over Europe. They commented that this bias-correction is capable of correcting the statistical moments and also the other statistical properties (e.g. intensity, extremes) of daily precipitation with good accuracy. According to Lafon et al. (2013), linear scaling, nonlinear scaling, gamma distribution based quantile mapping and empirical distribution based quantile mapping were able to correct the average and the standard deviation of the variable of interest with a good degree of accuracy, but the accuracy of higher order statistical moments (i.e. skewness and kurtosis) were found to be sensitive to the correction technique and its calibration period. They concluded that empirical distribution based quantile mapping performs better than the other bias-correction techniques. Similarly, Gudmundsson et al. (2012) analysed the effectiveness of distribution-derived quantile mapping, parametric quantile mapping and nonparametric quantile mapping. They also commented that empirical (nonparametric) distribution based quantile mapping performed better than the other bias-correction techniques used in the study. In empirical distribution based quantile mapping, the CDFs of the variable of interest are derived from the observations and model simulations, whereas in parametric quantile mapping (e.g. based on the gamma distribution) a theoretical distribution is fitted to the observations and model simulations. The advantage of using empirical distribution based quantile mapping is that, since the CDFs of the variable of interest are derived from the observations and the model simulations, the errors associated with fitting a theoretical distribution to these data can be avoided (Sachindra et al., 2014). However, in using empirical distribution based quantile mapping, frequent interpolation and extrapolation of the CDFs may introduce errors to the bias-correction (Li et al., 2010).

Sachindra et al (2014) used equidistant quantile mapping, monthly and nested bias-corrections on monthly precipitation outputs of a downscaling model. In that study, it was found that, when the scatter of the variable is large, the reduction of scatter using

any of these techniques is of limited success. Furthermore, Sachindra et al. (2013c) found that when the scatter of the climate variable of interest against observations is small, monthly bias-correction can reduce the scatter and improve its mean, standard deviation and also the time series. It should be noted that in that study only monthly bias-correction techniques was used. Both quantile mapping and equidistant quantile mapping, attempt to correct the statistical moments of the prediction, as in these techniques the correction is applied to the CDFs. On the other hand, monthly and nested bias-corrections are focused on correcting some of the statistics of the variable, and no explicit measure is taken to correct the CDF.

Ensemble techniques are helpful in combining multiple predictions (e.g. of GCMs or downscaling models) into a single prediction. This aids in reducing the uncertainty associated with the use of multiple predictions. There are two types of ensembles; (1) ensemble of predictions obtained from the same model, and (2) ensemble of predictions obtained from a set of different models (Kharin & Zwiers 2002). In ensemble modelling, the GCMs which have proven to perform well over the study area should be selected as the ensemble members, since this helps in reducing the noise in the ensemble prediction (Knutti et al., 2010). Several methods are used in deriving the ensemble predictions. These methods are applicable to the outputs of the GCMs, RCMs and also to the outputs of downscaling models. Averaging is the simplest method of deriving an ensemble prediction (Maqsood et al., 2004). In this technique, the set of predictions is added together and the average prediction is calculated. Knutti et al. (2010) and Warner et al. (2010) stated that multi-model ensemble average is superior to the predictions produced by any single model in the ensemble. In averaging, equal weights are assigned to each member of the ensemble. This assumes that, all members of the ensemble perform with equal accuracy. However, this assumption is not correct, as ensemble members (e.g. different GCMs) perform with different degrees of accuracy (Maqsood et al., 2004).

The technique of assigning weights to each member of the ensemble based on their individual performances and hence obtaining the weighted average is a better approach,

than simply obtaining the average of predictions by assigning equal weights to each ensemble member (Zhang & Huang 2013). Ingol-Blanco (2011) determined the weights for the members in an ensemble of 5 GCMs by considering their ability in simulating the streamflows using a hydrologic model, which was run with the precipitation and temperature data downscaled from these GCMs. The ratio between the root mean square error of a GCM in reproducing streamflow and the sum of root mean square errors of all GCMs in the ensemble in reproducing streamflow, was used in the determination of weights for each GCM, in each calendar month. Zhang & Huang (2013) considered multiple factors for the assessment of the performances of an ensemble of 4 RCMs, in assigning weights to them. The factors considered in that study, included the ability of the RCMs to reproduce the inter-annual and seasonal circulation patterns of precipitation and temperature, extremes of daily precipitation and temperature, precipitation occurrence etc. Then, for each of the factors considered, skill scores were derived, and those scores were combined to a single weight value for each RCM. However, the determination of weights is dependent on the factors considered in the study and how the skill scores of these factors are combined to a single weight. Therefore Christensen et al. (2010) stated that the method of assigning weights for models, based on their performances is subjective to a certain extent. Min & Hense (2006) used Bayesian model averaging and simple arithmetic averaging for ensemble predictions of global mean surface temperature from a set of GCMs. In that study, for Bayesian model averaging, the Bayes factors (defined in Kass & Raftery 1995) were used as the weights for each individual GCM, and in simple arithmetic averaging, equal weights were assigned to each GCM. They concluded that a better agreement was seen between the observations and the ensemble prediction produced using the Bayesian model averaging technique. It was argued that the better performance of the multi-model ensemble prediction based on the Bayesian model averaging technique was possibly due to the fact that Bayes factors assign relatively larger weights to better models and smaller weights to models that perform poorly.

Krishnamurti et al. (1999) regressed the outputs of 8 climate models, against the corresponding observations, using multi-linear regression (MLR) to obtain ensemble

predictions over the entire globe. It was commented by them that, the ensemble predictions produced in the above manner are more accurate than the ensemble mean and also better than any of the predictions of the individual GCMs which formed the ensemble. Kharin & Zwiers (2002) found that in general the forecast produced by regressing the mean forecast of an ensemble of models against the observations (using simple linear regression relationships) is more skilful than the forecasts produced by regressing the forecast of each individual model against observations (using multi-linear regression relationships). Furthermore, they found that when the size of the ensemble increases (e.g. number of GCMs), the skill of the ensemble forecast produced by the former technique levels off and degrades with the latter technique. Sachindra et al. (2013b) used multi-linear regression technique to regress the 20th century climate experiment outputs of HadCM3, ECHAM5 and GFDL2.0 with NCEP/NCAR reanalysis data for producing a set of multi-model ensemble outputs. These multi-model ensemble outputs were subsequently used in the calibration and validation of a statistical downscaling model. The outputs of HadCM3, ECHAM5 and GFDL2.0 pertaining to future climate were then introduced to the above multi-linear regression equations to generate multi-model ensemble outputs as inputs to the downscaling model, for projecting catchment scale climate into future. This way, the quality mismatches (bias) which exist between the NCEP/NCAR reanalysis outputs and GCM outputs are minimised, and the model calibration, validation and future projections are performed with a relatively homogeneous set of inputs, composed of outputs of multiple GCMs.

Sensible selection of a sub-set of GCMs from the large pool of existing GCMs is a possible way of narrowing the uncertainty range in a statistical downscaling exercise. For the selection of a sub-set of GCMs, a pool of GCMs should be assessed. Giorgi & Mearns (2002) stated that, models can be assessed based on their performances and also based on the convergence of their outputs. The model performance refers to how well models can reproduce the past climate (e.g. climate of the 20th century) over the area of interest. The model convergence refers to the degree of agreement among the models, of the climate projections produced by them into future. A subset of GCMs can be selected based on their performances in the past and considering the convergence of their

projections produced into future. Dessai et al. (2005) assessed the model performance and model convergence for monthly precipitation and monthly temperature outputs of 9 GCMs, using skill scores. Finally the performance and convergence skills scores were combined together to obtain a single skill score for each GCM. Johnson & Sharma (2009) used the variable convergence scores to measure how well the projections of models produced into future, converge with each other, over Australia. The variable convergence scores used by them were based on the coefficient of variation of eight climatic variables simulated by nine GCMs. They commented that the highest agreement between the GCMs was seen for pressure and temperature and the least agreement was observed for precipitation. Gleckler et al. (2008) assessed the performances of 21 GCMs using the root mean square error computed between the 20th century climate experiment outputs of the GCMs and corresponding reanalysis outputs. Anandhi et al. (2011) used a skill score measure proposed by Perkins et al. (2007) which was based on the overlap between then PDF of the model output and the PDF of the observations. In many studies, owing to time and resource limitations, only limited number of GCMs is employed (Johnson & Sharma 2009). However, prior any statistical downscaling study, if the available resources permit, it is advisable to assess multiple GCMs and identify the most suitable GCM or GCMs for the study area and the catchment scale predictand considered in the study.

UNCERTAINTIES IN GHG EMISSION SCENARIOS

GHG emission scenarios are the pictures of plausible future atmospheric GHG concentrations based on literature and assumptions (IPCC 2000). According to Moss et al. (2010), emission scenarios describe possible future releases of GHGs and substances such as aerosols which influence the radiation balance of the earth, leading to changes in climatic conditions. It should be noted that, the GHG emission scenarios are not predictions but projections developed with expert judgements on possible conditions of the future world. Climate change scenarios obtained by forcing the GCMs with different GHG emission scenarios enable the researchers to study the possible future changes in the climate system influenced by human activities.

In 1990, Intergovernmental Panel on Climate Change (IPCC) formulated four GHG emission scenarios and these were followed by a set of six IS92 emission scenarios, introduced in 1992. In year 2000, with the release of the Special Report on Emission Scenarios (SRES), the IPCC introduced a newer set of GHG emission scenarios replacing the IS92 emission scenarios (IPCC 2000). IPCC SRES emission scenarios were based on the possible demographic, socio-economic and technological developments of the future world. SRES emission scenarios were used in CMIP3, to force the 23 GCMs involved in that project.

In the SRES, the IPCC defined several GHG emission scenarios (40 in number) under four storylines (or scenario families). The four storylines (A1, A2, B1, and B2) described the evolution of the forces driving the global GHG emissions. In brief, the A1 storyline refers to a world with rapid economic and technological growth; A2 describes a world with regional economic development; B1 depicts a world with more cleaner and resource efficient technologies; and B2 explains a world oriented to protect the environment and the social equity.

Though there are 40 GHG emission scenarios defined by the IPCC, most GCMs have produced their outputs under a limited number of scenarios defined as marker scenarios. A marker scenario is a scenario in a certain scenario family, illustrative of the storyline to which it belongs (IPCC 2000). However, marker scenarios are equally likely to occur as the other scenarios. The presence of IPCC SRES marker scenarios reduces the large number of scenarios to a manageable number, making the use of GHG emission scenarios feasible in climate impact assessments. Details of IPCC SERS marker scenarios are provided in Table 1.

Table 1 IPCC SRES marker scenarios defined in IPCC (2000)

Scenario	CO_2 concentration by 2100 in ppm	Key features of scenario
A2	850	World with high population growth, high energy use, medium to high changes in land use, limited availability of resources, slow invention of new efficient technology.
A1B	720	World with low population growth, very high energy use, limited changes in land use, medium availability of resources, rapid invention of new efficient technology.
B2	620	World with low population growth, intermediate level of economic growth, use of less fossil fuels and increase in the use of cleaner forms of energy.
B1	550	World with low population growth, low energy use, high changes in land use, limited availability of resources, medium level of invention of new efficient technology.

According to van Vuuren et al. (2011a), there exists a requirement of new GHG emission scenarios, for executing the latest GCMs (e.g. CMIP5 GCMs) which need more input information than the GCMs developed in the past. Further, there is a rising interest among the research community on the scenarios which incorporate climate policies which have not been considered in the IPCC SRES.

Representative Concentration Pathways (RCPs) are the latest set of GHG emission scenarios used in forcing the 50 (or more) GCMs involved in the CMIP5. RCPs are not purely a new set of emission scenarios, but they have been developed considering the emission scenarios found in the existing literature (representative of the existing GHG emission scenarios in literature). Four RCPs namely; RCP2.6, RCP4.5, RCP6.0 and RCP8.5 have been developed by the research community consisting of modellers of climate, ecosystem, integrated assessment and emission inventory experts (van Vuuren et al., 2011a). RCP2.6, RCP4.5, RCP6.0 and RCP8.5 refer to possible radiative forcing levels of 2.6, 4.5, 6.0 and 8.5 W/m^2 respectively, at the end of the 21^{st} century. Both IS92 and SRES emission scenarios did not incorporate any possible climate change mitigation policies in the future world (no-climate-policy scenarios). However, some of the RCPs include climate policies, enabling the investigation of there impacts on the

future global climate. RCPs in general, project GHG emission levels up to year 2100 and their extensions called Extended Concentration Pathways (ECP) project up to year 2300. These ECP could aid in the study of relatively slow processes such as sea level rise (van Vuuren et al., 2011c). Details of RCPs are provided in Table 2.

Table 2 Details of representative concentrative pathways (RCPs)

Scenario	**CO_2 concentration by 2100 in ppm**	**Key features of scenario**	**Reference**
RCP2.6	421	Associated with a stringent climate policy, resulting relatively low levels of radiative forcing caused by very low levels of GHG emissions. Radiative forces rise to about 3 W/m^2 by the mid 21st century and declines to about 2.6 W/m^2 by the end of the century. Refer to a global mean temperature rise of about 2˚C by the end of this century.	van Vuuren et al. (2011b)
RCP4.5	538	Stabilization of radiative forcing at 4.5 W/m^2 by year 2100, through the implementation of climate policies.	Thomson et al. (2011)
RCP6.0	670	Stabilization of radiative forcing at 4.5 and 6.0 W/m^2 by year 2100, through the implementation of climate policies. Intervention of climate policies is much less compared to that of RCP2.6 and RCP4.5.	Masui et al. (2011)
RCP8.5	936	A scenario which describes a world with high population, medium rate of technological development, and high energy demand leading to higher GHG emissions. Unlike the other three RCPs, RCP8.5 does not incorporate any climate policies.	Riahi et al. (2011)

The actual future evolution of the GHG concentrations is largely uncertain due to the highly varying nature of the world (van Vuuren & O'Neill 2006). The largest uncertainties to a statistical downscaling study are introduced by the GHG emission scenarios, and these uncertainties could hardly be eliminated (Giorgi 2010). Since the GHG emission scenarios have equal likelihood of occurrence, which scenario will better represent the future world is a challenging question. One of the causes of scenario uncertainty is the different global population projections employed in different scenarios which are based on different assumptions on fertility and mortality (Arnell, 2004). According to Tebaldi & Knutti (2010), scenario uncertainty is more related to decision making, whereas the GCM uncertainty is linked with the limited

understanding of the atmospheric processes and their incomplete representation in mathematical equations in the GCMs. Though cannot be eliminated, in certain recent studies GHG scenario uncertainty has been handled in innovative manners as discussed in the next paragraph.

Prudhomme et al. (2010) proposed a GHG emission "scenario neutral approach" for climate change impact studies as an alternative to the widely practised GHG emission scenario-led approach. In the conventional emission scenario-led approach, GCM outputs pertaining to different GHG scenarios are downscaled to catchment scale and then applied to an impact model (e.g. flood simulation model) for quantification of the impacts of likely climate change on the environment. However, due to the presence of a multitude of emission scenarios, climate impact models produce number of plausible realizations of likely impacts on water resources in a catchment. Making decisions on the future water resources in a catchment using this large number of plausible realizations of likely future impacts becomes a challenge. The scenario neutral approach is seen as a potential solution to this issue. According to the scenario neutral approach, outputs of GCMs pertaining to multiple GHG emission scenarios are downscaled to catchment scale climatic variables such as precipitation and temperature. Then the downscaled climate information pertaining to future is used as input to an impact model. This process produces an ensemble of plausible simulations on the likely impacts of climate change on the environment. Then these simulations are analysed to see whether the changes in the future climate can affect any predefined safety margins in the catchment (e.g. certain flood level). Application of the scenario neutral approach is also found in Bastola et al. (2011). The application of a method similar to the scenario neutral approach called "decision scaling technique" is found in Brown et al. (2012).

In the past, researchers have mainly used the GCM outputs under IPCC SRES marker scenarios in the statistical downscaling models, for the projection of catchment scale hydroclimatology into future (refer to Table 3). Examples are: A1B, A2, B1 and COMMIT (Anandhi et al., 2008; 2009), A2, A1B and B1 (Mehrotra & Sharma 2010), A2 and B1 (Lavaysse et al., 2012), A2 and B2 (Yang et al., 2012; Chen et al., 2010;

Chu et al., 2010; Wetterhall et al., 2009), A2 (Hashmi et al., 2009a; Hewitson & Crane, 2006), and B2 (Ghosh & Mujumdar 2008). According to the above examples, it was understood that many of the statistical downscaling studies have considered the A2 scenario for the future projection of catchment level hydroclimatology into future, due to its pessimistic nature. This allows the identification of the worst possible impacts of rising GHG emissions, on the future catchment level hydroclimatology. However, it is not advisable to use a single GHG emission scenario to produce the catchment level projections, owing to the uncertain nature of the future behaviour of the world, which governs the amounts of GHG emissions (e.g. IPCC (2000) recommended the use of a variety of SRES GHG scenarios in any study). Sachindra et al. (2014) statistically downscaled outputs of HadCM3 pertaining to A2 and B1 GHG emission scenarios to monthly precipitation at a station located in Victoria, Australia. It was found that the differences of long term seasonal means and standard deviations of precipitation pertaining to A2 and B1 scenarios were negligible. However under the A2 GHG scenario maximum precipitation was clearly higher than that under B1 GHG scenario. Hence it was realised that the use of different GHG scenarios can provide a way for the quantification of uncertainty on the extremes of climate. On the other hand, the use of multiple GHG emission scenarios is a computationally costly process.

ISSUES WITH OBSERVATIONS OF HYDROCLIMATIC VARIABLES

Statistical downscaling studies need long records of observations of the predictands (e.g. hydroclimatic variables such as precipitation, streamflow, temperature, evaporation and humidity) for model calibration and validation (Wilby & Wigley, 1997). A longer record of observations is highly preferred (Sachindra et al., 2013a) as it exposes the downscaling model to a larger range of observations, including extreme values of the predictand. In the calibration of a downscaling model, the model parameters are adjusted until the model predictions become as close as possible to the observations of the predictand. The validation involves the evaluation of the model predictions against the observations of the predictand, for a period independent of calibration in which the best parameters yielded in calibration are remained fixed. Therefore, the reliability of

outputs of a statistical downscaling model is also dependent on the quality of the field observations. In many areas of the world, long records of observations of hydroclimatic variables are scarce (Feddersen & Andersen, 2005). This issue limits the length of the calibration and validation periods causing the model predictions to be less reliable, since the model is exposed to a limited data range of the predictand. The unavailability of observations at finer temporal resolutions (e.g. sub-daily) and poor spatial coverage of observations are also issues encountered in many regions (Hijmans et al., 2005).

Errors in observations of hydroclimatic variables exist due to; technical faults in measuring instrument (Domeneghetti et al., 2012), human errors in obtaining the observations, poor recording practices caused by negligence, various missing data infilling techniques, extrapolation of streamflow rating curves out of their design range (Herschy, 2009) etc. Various hydroclimatic variables are measured using instrument ranging from simple gauges to complex automatic recording gauges. The instrument can have systematic or random errors due to poor maintenance, poor calibration or factory faults. The proper maintenance of measuring equipment is quite important since this allows keeping the instrument uniform throughout its life span. The instrument should be calibrated against an accurate device at regular intervals.

Human observation errors are more likely to take place when the reader is unskilled or negligent. When the instrument is a non-recording gauge, a reader has to manually obtain the reading from the gauge. In this process, due to incorrect observation practices such as not maintaining a horizontal line of sight while obtaining the temperature readings from a mercury column thermometer or obtaining the atmospheric pressure readings from the incorrect scale of an analogue barometer, observations may become erroneous. Due to human negligence, records of hydroclimatic data could also contain errors such as decimal dot placed at an incorrect place of the record.

Due to incomplete records of hydroclimatic variables, various missing data infilling techniques are practised. Averaging, normal ratio method (Chow et al., 1988), interpolation (e.g. inverse distance weighting method used by Simanton & Osborn,

1980), and regression techniques (e.g. multi-linear regression used by Terzi, 2012) are some of the techniques used in filling the missing data in a record of observations. All these infilling techniques introduce uncertainty to the record as these are approximations of the actual observations.

When the length of the observed record of the streamflow is limited at a certain station, there is a possibility of expanding it with the streamflow record at a neighbouring station. This is achievable when the flow data at that station (station with limited records) display a high correlation with those at a neighbouring station. In such situations, a linear regression relationship could be developed between the nearby station and the station with limited records of flow data. This way the limited data set could be expanded (Gupta 2008). Anandhi et al. (2009) successfully used this technique for extending short records of monthly minimum/maximum temperatures, which were subsequently used in the calibration and validation of a statistical downscaling model. Hubbard & You (2005) stated that the missing records of hydroclimatic variables could be estimated with the data from neighbouring sites using spatial regression test and inverse distance weighing methods. Unlike the inverse distance weighing method which assigns the largest weight to the nearest station, the spatial regression test assigns the largest weight to the station which displays the lowest RMSE with the data of the station of interest.

The rating curve is an approximation of the actual discharge-stage (water level of the stream with respect to a certain datum) relationship of a stream at a selected location. Therefore, there is a certain degree of uncertainty even when the discharge readings are obtained within the design range of the rating curve. Errors to streamflow data are introduced particularly when the rating curve is extrapolated to obtain, either abnormally high or low flows from the observed stage readings (Pelletier 1988). According to Herschy (2009) when the upper part of the rating curve is extrapolated to predict peak streamflow, logarithmic extrapolation, stage-velocity-area method and Manning equation method can be used for the extension of the rating curve. Regular

updating of the rating curve and expansion of its range are solutions applicable at the field level, for improving the reliability of streamflow records.

Prior to using a record of hydroclimatic observations in the calibration and validation phases of a statistical downscaling model, the possible outliers (implausible values) of these observations should be identified and eliminated, as these could lead to erroneous models. Outliers in a record of hydroclimatic variables (e.g. precipitation, streamflow) are difficult to be differentiated from the hydroclimatic extremes such as peak streamflows, at a glance. In such instances, it is advisable to compare the extreme value which is suspected to be an outlier at a certain observation station, with the corresponding values at the nearby stations. If similar extreme or comparably high values are found in the records of the nearby stations, it could be argued that the extreme value at the station of interest is more a real extreme rather than an outlier. Some outliers in a record of observations can be identified relatively easily due to the physically impossible nature they possess; e.g. negative precipitation data, and improbable zero precipitation values at a certain station while there are records of significant levels of precipitation at the neighbouring stations (Einfalt & Michaelides 2008).

Feng et al. (2004) presented a comprehensive systematic approach for detection and correction of errors in observed daily climatic data including precipitation, minimum/maximum temperatures, sunshine duration, wind speed, relative humidity and evaporation. In this approach, initially the climatic data were checked against possible high and low extremes, by comparing them with various possible climatic extremes predefined in literature. The climatic data which satisfy the above test were then checked for the internal consistency by identifying errors such as the presence of a maximum daily temperature which was lower than the minimum daily temperatures. Next, the time series of data at the station was subjected to a temporal outlier check, in which implausible values of the climatic variable with respect to its values on the previous day and the next day were identified. This was followed by a spatial outlier check in which the data at the station of interest were compared with those at

neighbouring stations to find implausible entries. The missing data and the erroneous data identified with the above checks were estimated using the method specified in Hubbard (2001), where linear regression equations between the station with missing values and its neighbouring stations were used to estimate the missing values.

Effect of the wind (usually leads to an underestimation of precipitation), wetting of the funnel which guides rain into the rain gauge, evaporation losses, partial or full clogging and poor maintenance are some of the common causes of systematic errors associated with precipitation gauges (Sciuto et al., 2009). Corrections to these errors have been discussed in Sevruk & Klemm (1989) & Zhang et al. (2004).

ISSUES WITH STATISTICAL DOWNSCALING TECHNIQUES

There exists a multitude of different statistical downscaling techniques starting from relatively simple ones such as the method of meteorological analogues, proceeding up to highly complex non-linear regression techniques like Artificial Neural Networks (ANN), Support Vector Machine (SVM), Relevance Vector Machine (RVM) and Gene Expression Programming (GEP). These statistical downscaling techniques approximate the actual predictor-predictand relationship. The uncertainties associated with different statistical downscaling techniques (e.g. linear, non-linear, weather generation etc.) are mainly due to different representations of the relationships between the GCM outputs and catchment level hydroclimatic variables. Table 3 contain the GCMs, GHG emission scenarios and downscaling techniques used in some of the past studies along with the major conclusions drawn on the downscaling techniques.

Table 3 GCMs, GHG scenarios and downscaling techniques used in past studies

GCMs	GHG emission scenario	Predictands	Downscaling techniques	Major conclusions on techniques	Reference
BCM2.0, CNRM-CM3,CNRM-CM4; MIROC3.2, CGCM2.3.2	A1B, A2 and B1	Monthly precipitation	MLR, ANN and SVM	ANN better captured low and medium precipitation values. SVM better captured high precipitation values.	Ghosh & Katkar (2012)
CGCM2	IS92	Monthly precipitation	LS-SVM, ANN	LS-SVM performed slightly better than ANN. Both techniques failed to correctly reproduce the extremes of observed precipitation. ANN can trap at a locally optimum solution, but SVM is free of this issue.	Tripathi et al. (2006)
HadCM3	A2, B2	Daily precipitation	MARS, MT, KNN, GA-SVM, MLR	Performances of downscaling models were sensitive to the techniques used in modelling the occurrences and the amounts of precipitation.	Nasseri et al. (2013)
POAMA	N/A	Daily precipitation	Metrological analogues	Analog downscaling method reduced the bias in the statistics of seasonal precipitation and the number of wet days in the precipitation output of the GCM.	Charles et al. (2013)
CGCM3.1	COMMIT, A1B, A2 and B1	Daily precipitation	Nonparametric kernel regression, KNN, CRF method, weather generator by Wilks (1999)	Temporal variability and extremes of precipitation were better captured by nonparametric kernel regression.	Kannan & Ghosh (2013)
CGCM3, ECHAM5	A1B, A2 and B1	Daily precipitation	MLR, GLM, NHMM	NHMM based model was more capable in preserving the spatial correlation structure among stations.	Hu et al. (2013)

MLR = multi-linear regression, ANN = artificial neural network, SVM = support vector machine, LS-SVM = least square support vector machine, GA-SVM = genetic algorithm-optimized support vector machine, MARS = multivariate adaptive regression splines, MT = model tree, KNN = k-nearest neighbor, CRF = conditional random field, GLM = generalised linear model, NHMM = non-homogeneous hidden Markov model.

Table 3 Continued

GCMs	GHG emission scenario	Predictands	Downscaling techniques	Major conclusions on techniques	Reference
NCEP/NCAR	N/A	Daily precipitation	MLR, CCA, SCA	Differences of performances between the three techniques when used with the same set of predictors are small. However when each individual technique is used with different sets of predictors greater differences of performances seen.	Lutz et al. (2012)
NCEP/NCAR	N/A	Daily precipitation	MLR, GEP	GEP showed better performances than MLR in both calibration and validation periods.	Hashmi et al. (2011)
HadCM3	A2	Daily precipitation	MLR, a stochastic weather generator (LARS-WG), GEP	When the precipitation outputs of the three downscaling models were combined using a Bayesian approach (Tebaldi et al. 2005) to obtain a weighted multi-model ensemble prediction (WMME), it was found that WMME was superior to all individual techniques.	Hashmi et al. (2009)
CGCM1	IS92a	Daily precipitation and daily minimum/maximum temperatures	MLR, a stochastic weather generator (LARS-WG), ANN	In the simulation of average daily precipitation, LARS-WG produced the least error. Both MLR and LARS-WG reproduced the variance of precipitation far better than that by ANN. It was concluded that LARS-WG was the best technique in downscaling all three predictands and ANN was the worst.	Khan et al. (2006)

SCA = simulated annealing and diversified randomization cluster analysis, CCA = canonical correlation analysis, GEP = gene expression programming, LARS-WG = Long Ashton research station weather generator.

Table 3 Continued

GCMs	GHG emission scenario	Predictands	Downscaling techniques	Major conclusions on techniques	Reference
NCEP/NCAR	N/A	Daily precipitation and daily minimum/maximum temperatures	MLR, a stochastic weather generator (LARS-WG)	Weather generator displayed a much higher skill in reproducing the monthly mean wet and dry spell lengths in comparison with those produced by MLR. Both techniques reproduced the means of precipitation and minimum/maximum temperature with good accuracy.	Dibike & Coulibaly (2005)
NCEP/NCAR	N/A	Daily precipitation	NHMM, KNN	KNN technique could better preserve the spatial correlations of precipitation occurrences. NHMM could reproduce the total number of wet days per season with a better accuracy. Neither of the techniques adequately reproduced the solitary wet days per season.	Mehrotra et al. (2004)
NCEP/NCAR	N/A	Daily and monthly precipitation	Analogue, CCA, CART, ANN	Relatively simple analogue method produced better results than CCA, CART and far better results than the complex ANN technique.	Zorita & von Storch (1999)

CART = classification and regression trees

Table 3 Continued

GCMs	GHG emission scenario	Predictands	Downscaling techniques	Major conclusions on techniques	Reference
NCEP/NCAR	N/A	Monthly streamflows	LS-SVM, MLR	Very comparable performances for both LS-SVM and MLR. However, LS-SVM showed slightly better capabilities in downscaling streamflows. Both techniques failed to properly capture the high streamflows in calibration and validation.	Sachindra et al. (2013a)
CCSR	B2	Monthly streamflows	SVM, RVM	RVM outperformed SVM. Even RVM cannot properly capture the extreme values of streamflows. SVM is prone to severe overfitting.	Ghosh & Mujumdar (2008)
CGCM3	COMMIT, A1B, A2 and B1	Monthly maximum/minimum temperature and evaporation	PLS, ANN	Very comparable performances for both ANN and PLS seen. However, ANN showed marginally better performances in calibration.	Goyal & Ojha (2011)
ECHAM5	A2	Monthly maximum/minimum temperature and evaporation	MLR	High degree of accuracy was seen in simulating the statistics and the time series of the three predictands.	Sachindra et al. (2013c)
CGCM3.1	A1B, A2 and B1	Daily minimum and maximum temperature	Single conjunctive rule learner, Decision table, MT, and REPTree	MT showed superior performances compared to those of other three techniques for both predictands.	Goyal et al. (2012)

RVM = relevance vector machine, PLS = Partial least square regression, REPTree = decision/regression tree algorithm.

In the Statistical and Regional Dynamical Downscaling of Extremes for European regions (STARDEX) project, it was concluded that the skills of statistical downscaling techniques vary non-systematically from station to station, season to season, predictand to predictand and also method to method (STARDEX, 2005). It was also commented that, the means of climatic variables were better reproduced than the extremes. Furthermore, compared to the intensity of the precipitation extremes, their occurrences

and persistence were better captured by statistical downscaling techniques. Also, according to the findings of the STARDEX project, statistical downscaling techniques displayed better skills in downscaling GCM outputs to temperature than downscaling GCM outputs to precipitation. Under the STARDEX project, 10 indices of extreme precipitation and temperature were defined, which could be used in evaluating the skill of downscaling models, in reproducing the extreme climatic events. Wang et al. (2012) successfully used these indices for the assessment of the outputs of several statistical downscaling models.

An inherent issue with statistical downscaling is its failure of properly capturing the peaks of the hydroclimatic variables. This is due to the inability of statistical downscaling techniques in explaining the entire range of variance of a certain hydroclimatic variable (Tripathi et al., 2006). Sachindra et al. (2013a) reported that high streamflows in time series are not properly reproduced even by a complex non-linear statistical downscaling technique such as LS-SVM or by relatively simple MLR technique. Ghosh & Mujumdar (2008) discovered that RVM (complex non-linear downscaling technique) was also not able to capture the peaks successfully in a time series of streamflow.

Weather generators have been widely used in the simulation of weather sequences from observations (e.g. Richardson, (1981)) and also in downscaling large scale atmospheric variables to catchment scale predictands (e.g. Wilks, (1999)). Weather generators can produce any number of sequences of any desired length for a climate variable. Also weather generators are capable of downscaling GCM outputs to catchment scale predictands, while preserving the changes in the statistics characterised in the GCM outputs (Fowler et al., 2007). In the past studies, the capability of weather generators in downscaling large scale atmospheric variables to daily climatic variables at the catchment scale has been detailed. Some of those studies are discussed below.

Min et al. (2011) used the combination of first order two state Markov chains (for the simulation of occurrences) and skewed normal distribution (for the simulation of

amounts) in generating daily precipitation time series at 8 stations in Korea. They found that this weather generation technique reproduces the higher quartiles and the maximum of daily precipitation with good accuracy. However it was realised that rare extreme precipitation events with return periods in the order of few hundreds of years were not properly captured by this weather generator. Chen et al. (2011) also reported that weather generator based downscaling methods are suitable for the simulation of extremes of temperature. In a study by Hashmi et al. (2009b) which used LARS-WG weather generator (uses a semi-empirical distribution for precipitation amounts), it was commented that annual maximum series of daily precipitation simulated by the weather generator and corresponding observations are of the same order. However, the agreement between each individual observed and model simulated annual maximum daily precipitation was small. Chen et al. (2006) employed a weather generator based on the first order two state Markov chains and gamma distribution for downscaling daily precipitation at 17 stations in China. They used 32 years of observations to determine the parameters of the weather generator for each station, which were then used in the weather generator to generate multiple series of precipitation. It was found that there is a close agreement between the observed and generated time series of precipitation at the daily and monthly time scales.

Downscaling at several observation stations can be performed either at individual stations separately (e.g. Anandhi et al. (2008)) or at multiple stations concurrently (e.g. Jeong et al. (2012a)). When downscaling is performed at individual stations in a study area, no explicit measure is taken for the preservation of the cross-correlation structure among the stations for the predictand of interest, unlike when downscaling is performed at multiple stations concurrently which enables the plausible representation of spatial variations of the predictand of interest over space. While maintaining the cross-correlation structure among the stations for each predictand, the preservation of cross-correlation structures between different predictands is also considered to be an important task. This enables the plausible representation of relationships between different predictands at individual stations and among different stations (e.g. Khalili et al. (2011)).

The multivariate multi-linear regression (MMLR) technique was used by Jeong et al. (2012b) for downscaling GCM simulations to daily maximum and minimum temperature concurrently at 9 observation stations. First they used MMLR for downscaling GCM outputs to deterministic time series of daily maximum and minimum temperature. Then the spatially correlated random noise (generated from the multivariate normal distribution) between the two predictands and the stations was added to the deterministic time series. It was concluded that the addition of spatially correlated random noise to the deterministic time series of the predictands improved the reproduction of cross-correlation structures between the predictands at individual stations and the cross-correlation structures between stations for each individual predictand.

Khalili et al. (2011) used a multi-station multivariate downscaling strategy for downscaling reanalysis outputs to daily minimum and maximum temperature at 10 stations in Canada. In that study, for each predictand and each station, separate multi-linear regression relationships between reanalysis outputs and the predictands of interest were developed. Then the residuals of the multi-linear regression relationships pertaining to the minimum temperature and the maximum temperature were determined using a multivariate spatial moving average process. It was concluded that this downscaling approach was able to accurately simulate the spatiotemporal variations of daily minimum and maximum temperature.

Srinivas et al. (2013) used the least square support vector machine (LS-SVM) regression for simultaneous downscaling of GCM outputs to daily maximum and minimum temperature at 4 stations in India. In that study, the stations were separated into clusters based on the cross-correlation structures of each individual predictand. For each cluster, a representative station which showed high correlations with other stations was identified for each individual predictand, and LS-SVM based inter-station relationships between the representative station and the other stations were developed

using observations. Then LS-SVM based downscaling models were developed for each predictand at the representative stations using observations. Finally the outputs of the downscaling models developed at the representative stations were introduced to the inter-station relationships to determine daily maximum and minimum temperature at other stations. It was stated that this multi-station statistical downscaling methodology produced better performances than the multi-station multivariate downscaling approaches used by Khalili et al. (2011) and Jeong et al. (2012b). However, it should be noted that in the approach used by Srinivas et al. (2013), no explicit measure was taken to preserve the cross-correlation structure between different predictands.

Sachindra et al. (2013c) proposed a multi-station multivariate downscaling methodology for simultaneous downscaling of GCM outputs using a key-predictand and key-station approach. In this approach, first the predictands which showed high correlations with other predictands at each individual station were identified (these predictands were called key-predictands). Then for each key-predictand, the stations which showed high correlations with all predictands at other stations were identified (these stations were called the key-stations). The MLR based relationships were developed between key-predictands and other predictands at key-stations (called intra-station regression relationships) and also between the key-predictands at key-stations and all predictands at other stations (called inter-station regression relationships). Downscaling models using the MLR technique were built at the key-stations for key-predictands. Using the outputs of these downscaling models on the intra and inter-station regression relationships, values of all predictands at all stations were determined. The effectiveness of this key-predictand and key-station approach was demonstrated by its application to evaporation, minimum temperature and maximum temperature at 4 stations in Victoria, Australia.

Ghosh & Katkar (2012) found that ANN is more capable of simulating low and medium values of precipitation, whereas SVM is better in capturing high precipitation values. Tripathi et al. (2006) commented that LS-SVM is slightly more capable than ANN in

downscaling GCM outputs to precipitation. However, both techniques failed to correctly capture the extreme values of precipitation. Similarly, Ghosh & Mujumdar (2008) commented that both RVM and SVM fail to reproduce the extremes of monthly streamflows, and unlike RVM, the SVM technique was subject to severe over-fitting. According to the above findings, it was realised that it is impossible to identify a certain technique as the best or the worst in downscaling. However, it could be recommended to use a relatively simple downscaling technique such as MLR or method of analogue and analyse its ability in reproducing the observations of the predictand, and if the results are not satisfactory, then a more complex downscaling technique could be experimented. The development of downscaling models for each calendar month separately, can aid in better capturing the seasonal variations of the predictand (Sachindra et al., 2013b).

The major assumption involved in statistical downscaling is that the relationships which existed between the large scale atmospheric variables and catchment scale hydroclimatic variables in the past are valid for the changing climate in future. In other words, the predictor-predictand relationships are stationary over time. However, under changing climate this assumption may not be valid.

Hewitson & Crane (2006) stated that the proper selection of large scale atmospheric variables which reliably describe the climate of the past could increase the confidence of the predictor-predictand stationarity assumption. Sachindra et al. (2013a) used a technique for the selection of predictors that are consistently correlated with the predictand over time (for details refer to “issues with the selection of predictors”). The use of consistently correlated predictors in a downscaling model allows developing consistent relationships between the predictors and predictand over time hence supports the predictor-predictand stationarity assumption.

Duan et al. (2012) used a relatively simple approach for the analysis of uncertainty in the predictor-predictand relationship under changing climate. In that study, MLR based

models were used to downscale 150 years of observations of atmospheric variables to monthly precipitation. For each 30 year time slice, a separate downscaling model was calibrated. The regression coefficients of MLR equations were plotted considering a 30 year running window, for visualisation of the variation of the coefficients. Furthermore, the five 30 year time slices were used to determine whether the changes in the regression coefficients form one time slice to another was statistically significant. It was found that the coefficients and the constants of the MLR relationships show statistically significant variations over time indicating that predictor-predictand relationships are not stationary. Projections of precipitation were produced using the outputs of five GCMs on each of the five downscaling models. This process enabled the quantification of uncertainty introduced by the non-stationarity of the predictor-predictand relationships and also by different GCMs.

Change in the frequency of occurrence of modes of natural climate variability (atmospheric circulation regimes) is considered as a result of climate change (Corti et al., 1999). Considering this feature, Raje & Mujumdar (2010) proposed a methodology for accounting the non-stationarity in the predictor-predictand relationship. They used PCA and k - mean clustering for identification of modes of natural climate variability in GCM simulated 500hpa geopotential heights. Then pertaining to each mode of natural variability, a separate streamflow downscaling model was developed using the conditional random field (CDF) technique (different predictor-predictand relationship for each mode of natural climate variability). Thereafter using the outputs of GCMs corresponding to each mode of natural climate variability (identified previously), on the downscaling models, streamflow was projected into future. The streamflow projected into future by each downscaling model for each GHG emission scenario and GCM was converted to standardised streamflow indices and combined together.

ISSUES ASSOCIATED WITH PREDICTORS

Issues associated with the predictors of statistical downscaling techniques can be subdivided into two categories; (a) issues with the method of selection of predictors, and (b) issues with processing the selected predictors, prior to their application in the downscaling model. In the next two sub-sections, these two categories are described.

Issues with the selection of predictors

One possible cause of uncertainty associated with statistical downscaling is the method of selection of predictor variables. In general, probable variables for any statistical downscaling study are selected based on the past literature and physics related to the processes underlying the hydrologic cycle (Sachindra et al., 2013a). The selection of potential variables from the pool of probable variables is performed in many different ways.

Dibike & Coulibaly (2005) used Pearson correlation coefficients and scatter plots between probable predictor data (NCEP/NCAR reanalysis outputs) and observations of daily precipitation and daily minimum/maximum temperatures (predictands), for identification of potential predictors in a statistical downscaling exercise. It was found that, the correlations between the predictors and daily precipitation were quite low compared to those for daily minimum/maximum temperatures. It was further realised that, the strength of the correlations between a certain predictor and a predictand varied from one calendar month to another.

Anandhi et al. (2008) also used Pearson, Spearman and Kendall's Tau correlation coefficients and scatter plots for selecting potential predictors from a pool of probable predictors. In that investigation, considering the seasonal variations of the predictor-predictand relationships, potential predictors were selected for dry and wet seasons separately. They stated that, the selection of too few potential predictors by imposing a stringent threshold on the correlation between predictors and predictand, could lead to

poor characterisation of the atmospheric processes in the downscaling model. On the other hand, the selection of too many potential predictors by imposing a very low threshold on the predictor-predictand correlations could introduce noise to the downscaling model.

In downscaling NCEP/NCAR reanalysis outputs to monthly catchment streamflows, Sachindra et al. (2013a) used the Pearson correlation coefficients to identify potential predictors for each calendar month from a pool of probable variables. Unlike in the previous studies (e.g. Anandhi et al., 2008; 2009) which considered correlations between the predictors and predictand for the whole period of the study, in the study performed by Sachindra et al. (2013a), the correlations between the monthly streamflows and the probable predictors were calculated for three 20 year time slices (covering the whole period of the study) and the whole period of the study. The predictors which displayed good statistically significant ($p \leq 0.05$) correlations consistently with streamflows in the three 20 year time slices and the whole period were selected for calibration and validation of the downscaling model. These predictors were ranked according to the strength of the correlations they maintained with the predictand, over the whole period of the study. Initially, the predictors with ranks 1, 2 and 3 (predictors which have the strongest correlations with the predictand) were introduced to the downscaling model and the model performance in validation was measured with the Nash-Sutcliffe Efficiency (NSE) (Nash & Sutcliffe 1970). Then the next predictors with ranks 4, 5, 6 etc were introduced to the model one at a time, until the model performance in terms of NSE is maximised. The set of predictors which maximised the downscaling model performance in validation were retained as the final set of predictors for each calendar month. With each of these 12 sets of predictors, 12 (one for each calendar month) statistical downscaling models were developed.

It should be noted that the correlation coefficient analysis is only capable in identifying the linear relationships between the predictors and predictands (Sharma 2000). However, the use of scatter plots along with correlation coefficients is a more effective way of identifying the dependence structures (e.g. linear or non-linear) of predictands

on predictors. This is because the scatter plots provide a graphical representation of the predictor-predictand relationships which is useful in recognising a non-linear relationship which is not captured correctly by the correlation coefficients. Tripathi et al. (2006) stated that Classification and Regression Trees (CART) and graphical sensitivity analysis (Cannon & Mckendry 2002) are more capable techniques in determining non-linear relationships, existing between GCM predictors and catchment level predictands. To select potential predictors from a pool of NCEP/NCAR probable variables, in downscaling 6h surface wind fields, Faucher et al. (1999) applied CART. They stated that it is important to have physically meaningful relationships between probable predictors and predictands for successful implementation of the CART technique.

Partial Mutual Information (PMI) criterion is another technique that had been used in identifying the potential predictors for a hydroclimatic prediction model. Sharma (2000) stated that the process of using PMI for the selection of potential predictors is successful in identifying potential predictors that either have linear or non-linear dependence structures with the predictand considered. In that approach, the probable predictor which showed the highest PMI score with the predictand was identified first. Then the PMI scores were recalculated by randomly rearranging (boot strapping) the values of the above selected predictor, and the predictand. The 95^{th} percentile of the PMI scores, calculated from the randomly rearranged samples of the predictor variable, were compared with the PMI score calculated earlier. If the PMI score of the selected predictor was higher than the 95^{th} percentile of the PMI scores calculated from randomly rearranged samples, then this predictor was selected as a potential predictor and it was removed from the pool of probable variables. The above steps were repeated until all potential predictors were identified.

In statistical downscaling, a variety of predictors are used for predicting number of predictands. In general, GCMs simulate a large number of climatic variables (predictors of downscaling models). The combinations of predictors used in statistical downscaling models vary depending on the predictand, geographic region and also the season.

Among the variety of predictands, precipitation could be regarded as the most widely predicted climatic variable in downscaling (e.g. Hewitson & Crane 2006; Anandhi et al., 2008). Minimum/mean/maximum temperatures, evaporation, humidity, streamflow etc have also been predicted with statistical downscaling techniques. Tables 4, 5, 6 and 7 provide some of the predictor-predictand combinations used in the previous statistical downscaling studies, in different geographic regions of the world. It should be understood that the sets of predictors shown in Tables 4, 5, 6 and 7 should be treated as probable predictors. Therefore it is advisable to use a suitable technique to identify the potential predictors before using them as inputs to a statistical downscaling model. A good predictor should (a) have a physically meaningful association with the predictand, which should be stable and stationary over time, (b) be able to explain low frequency variability and trends (e.g. year to year or multi year), and (c) be at an appropriate spatial scale and reliably simulated by the GCMs (STARDEX 2005).

Table 4 Predictors used in the previous studies for downscaling precipitation

Predictors used in the downscaling study	Region	Time step	Reference
Specific humidity at 850hPa and 925hPa pressure levels, Air temperatures at 200hPa, 500hPa, 700hPa and 925hPa pressure levels, Geopotential heights at 200hPa and 925hPa pressure levels, Zonal wind speeds at 200hPa and 925hPa pressure levels, Precipitable water content	India	Monthly	Anandhi et al.(2008)
Specific humidity near earth surface, Surface skin and near surface air temperatures, Air temperatures at 200hPa, 500hPa and 850hPa pressure levels, Geopotential heights at 500hPa and 850hPa pressure levels, Zonal wind speeds near earth surface and 850hPa pressure level, Meridional wind speeds near earth surface, 200hPa, 500hPa and 850hPa pressure levels, Downwelling shortwave flux near earth surface, Total precipitation, Convective precipitation, Snow area fraction, Snow depth, Mean sea level pressure, Total soil moisture content	USA	Monthly	Najafi et al. (2011)
Relative humidity near earth surface, 500hPa and 850hPa pressure levels, Surface air temperature, Geopotential height at 500hPa pressure level, Zonal wind speed at 500hPa pressure level, Vorticity at 500hPa pressure level, Mean sea level pressure	China	Daily	Yang et al. (2012)
Specific humidity at 850hpa pressure level, Maximum air temperatures at 2m height and at 850hPa pressure level, Zonal wind speed at 850hPa pressure level, Meridional wind speed at 850hPa pressure level, Mean sea level pressure, Total precipitation	Australia	Daily	Timbal et al. (2009)
Geopotential heights at 500hPa and 700hPa pressure levels, 500-1000hPa Geopotential height thickness, Mean sea level pressure, Vertical pressure velocity at 500hPa	Turkey	Monthly	Tatli et al. (2004)
Specific humidity near earth surface and 700hPa pressure level, Relative humidity near earth surface and 700hPa pressure level, Surface air temperature, Zonal and meridional wind speeds near earth surface and 700hPa pressure levels	South Africa	Daily	Hewitson and Crane (2006)

Table 5 Predictors used in the previous studies for downscaling minimum/maximum temperature

Predictors used in the downscaling study	Region	Time step	Reference
Air temperature at 925hPa pressure level, Zonal and meridional wind speeds at 925hPa pressure level, Shortwave radiation, Longwave radiation, Sensible heat net flux at earth surface	India	Monthly	Anandhi et al.(2009)
Specific humidity near earth surface, at 500hPa and 850hPa pressure levels, Geopotential heights at 500hPa and 850hPa pressure levels, Mean air temperature, Mean sea level pressure, Zonal wind speed at 850hPa pressure level, Meridional wind speeds near earth surface and at 500hPa pressure level, Divergence near earth surface and at 850hPa pressure level, Near surface vorticity	Canada	Daily	Coulibaly et al.(2005)
Specific humidity at 500hPa, 850hPa and 1000hPa pressure levels, Mean air temperature at 2m height, Mean sea level pressure, Zonal and meridional wind speeds near earth surface, at 500hPa and 850hPa pressure levels, Sensible heat flux, Latent heat flux	Chile	Daily	Souvignet and Heinrich (2011)
Specific humidity at 850hPa pressure level, Maximum air temperature at 2m height, Air temperature at 850hPa pressure level, Zonal and meridional wind speeds at 850hPa pressure level, Mean sea level pressure	Australia	Daily	Timbal et al. (2009)
Geopotential heights at 500hPa and 850hPa pressure levels, Zonal wind speed at 500hPa pressure level, Mean air temperature at 2m height, Mean sea level pressure	China	Daily	Wang et al. (2012)

Table 6 Predictors used in the previous studies for downscaling evaporation

Predictors used in the downscaling study	Region	Time step	Reference
Relative humidity at 850hPa and 925hPa pressure levels, Maximum air temperature at 2m height, Air temperature at 850hPa pressure level, Mean sea level pressure	Australia	Daily	Timbal et al. (2009)
Relative and specific humidity near earth surface, Zonal wind speed near earth surface, Geopotential height at 500hPa pressure level, Surface air temperature, Mean sea level pressure	China	Daily	Yang et al. (2012)
Zonal and meridional wind speeds at 925hPa pressure level, Geopotential heights at 200hPa and 500hPa pressure levels, Air temperature at 200hPa, 500hPa and 925hPa pressure levels	India	Monthly	Goyal and Ojha (2011)

Table 7 Predictors used in the previous studies for downscaling streamflow

Predictors used in the downscaling study	Region	Time step	Reference
Relative humidity at 750hPa pressure level, Geopotential heights at 200hPa, 500hPa, 700hPa and 850hPa pressure levels, 500hPa-200hPa and 850hPa-500hPa Geopotential height thicknesses	South Africa	Monthly	Landman et al. (2001)
Specific humidity at 850hPa pressure level, Geopotential height at 500hPa pressure level, 1000hPa-500hPa Geopotential height thickness, Mean sea level pressure	Canada	5 day average	Cannon and Whitfield (2002)
Specific humidity near earth surface, Geopotential height at 500hPa pressure level, Air temperature at 2m height, Mean sea level pressure	India	Monthly	Ghosh and Mujumdar (2008)
Specific humidity and Relative humidity at 500hPa, 850hPa and 1000hPa pressure levels, Geopotential heights at 500hPa, 850hPa and 1000hPa pressure levels, Land skin temperature, Air temperature at 500hPa, 850hPa and 1000hPa pressure levels, Convective precipitation rate at surface, Precipitation rate at surface, Mean sea level pressure, Surface pressure, Sensible heat net flux at surface, Latent heat net flux at surface, Clear sky downward longwave flux at surface, Clear sky downward solar flux at surface, Clear sky upward solar flux at surface, Downward longwave radiation flux at surface, Downward solar radiation flux at surface, Upward longwave radiation flux at surface, Upward solar radiation flux at surface, Total cloud cover	France	Daily	Tisseuil et al. (2010)
Specific humidity at 850hPa pressure level, Relative humidity at 700hPa, 850hPa and 1000hPa pressure levels, Geopotential heights at 500hPa, 700hPa and 850hPa pressure levels, Volumetric soil moisture contents in 0 to 10 cm and 10 to 200 cm soil layers	Australia	Monthly	Sachindra et al. (2013a)

According to the previous statistical downscaling studies considered in Table 4, for downscaling GCM outputs to precipitation, GCM outputs of; humidity, wind speed, air temperatures and geopotential height, at various levels of the atmosphere have been used, irrespective of the geographic region. In downscaling minimum/maximum temperature, GCM outputs of; wind speed and air temperature have been widely employed along with other variables such as heat fluxes. Anandhi et al. (2009) stated

that the inclusion of surface heat fluxes along with other variables in the downscaling model could improve the predictions of monthly maximum temperature. Furthermore, Timbal et al. (2009) commented that the thermal predictors play an important role in the prediction of minimum/maximum temperatures. There is a clear similarity between the predictors used in downscaling precipitation and those used in downscaling streamflows. This is because the precipitation is the main driver of streamflow. Hence, it could be concluded that in a study where GCM outputs are downscaled to streamflow, the probable predictors could be selected from a pool of predictors used in downscaling GCM outputs to precipitation. However, predictors which are specifically related to the generation of streamflows such as soil moisture content could also be considered depending on how influential they are on the generation of streamflows (Sachindra et al., 2013a). As shown in Table 6, for downscaling GCM outputs to evaporation, the predictors similar to those used for downscaling precipitation have been used in the past studies. It was realised that, although there are some differences between the sets of predictors used in downscaling GCM outputs to precipitation, temperature, streamflow and evaporation, there are many common predictors among these pools of predictors. This is due to the inter-relationships of the hydroclimatic processes of these predictands. It could be concluded that in a statistical downscaling study, the pool of probable predictors could be selected based on past literature and relevant hydroclimatology, however the influences of each predictor on a predictand should be thoroughly analysed before including them in the downscaling model. According to Wetterhall et al. (2005), any variable is usable as a predictor in statistical downscaling, as long as there is a plausible relationship between that variable and the predictand considered in the investigation. Downscaling GCM outputs to precipitation with higher accuracies is more difficult than achieving the same for minimum/maximum temperatures, evaporation and dew point (Timbal et al., 2009). Since streamflow is related to precipitation and other variables such as evaporation, wind speed, soil moisture etc, it could be deduced that, downscaling GCM outputs to streamflows with higher accuracy is more difficult than downscaling GCM outputs to precipitation.

Due to the seasonal variations of the atmospheric circulations, the selection of predictors for each season (e.g. summer, autumn, winter, spring; wet, dry; calendar months) is advisable. This process is referred to as seasonal stratification (Anandhi et al., 2008). It enables developing separate downscaling model for each season. Seasonal stratification is performed in two distinct ways; fixed seasons and floating seasons (Anandhi et al., 2008). In fixed seasons, the beginning and the end of a season is fixed, but in floating seasons the beginning and the end of a season could vary over time. Anandhi et al. (2008) successfully applied the floating method to identify the wet and dry seasons using the K-mean clustering technique (MacQueen 1967). Under changing climate, it is difficult to assume that conventional seasons will have their fixed beginning and end in the future, therefore the concept of floating seasons is seen as a solution to address this issue.

In calibration and validation of a statistical downscaling model, predictor data are obtained from a reanalysis data source. Table 8 provides the details of some of the reanalysis data in use.

Table 8 Reanalysis data sets

Reanalysis data set	Availability of data		Horizontal spatial resolution	Reference
	Temporal	Spatial		
NCEP/NCAR	1948 - present	Global	2.5˚ x 2.5˚	Kalnay et al. (1996)
NCEP/DOE-2	1979 - present	Global	2.5˚ x 2.5˚	Kanamitsu et al. (2002)
ERA-15	1979 - 1993	Global	2.5˚ x 2.5˚	Gibson et al. (1997)
ERA-40	1957 - 2002	Global	2.5˚ x 2.5˚	Uppala et al. (2005)
ERA-Interim	1979 - present	Global	1.5˚ x 1.5˚	Dee et al. (2011)
JRA-25	1979 - 2004	Global	1.25˚ x 1.25˚	Onogi et al. (2007)
20CR	1871 - 2010	Global	2.0˚ x 2.0˚	Compo et al. (2011)
NARR	1979 - present	North American continent	0.3˚ x 0.3˚	Mesinger et al. (2006)

ERA = European Centre for Medium - Range Weather Forecasts reanalysis, JRA-25 = Japanese 25-year reanalysis, 20CR = Twentieth century reanalysis, NARR = North American regional reanalysis

According to Kistler et al. (2001), there are three distinct phases in reanalysis data; (1) early period from 1940 to 1957 when the first upper air observations were obtained, (2) employment of the modern rawinsonde network during the period 1958-1978, and (3) satellite era from 1979 to present. The availability of observations for the reanalysis

largely increased from 1950s to 1990s (Compo et al., 2011). Owing to the abundance of better quality observations, in the modern satellite era (post 1979 period) the reliability of reanalysis data became relatively higher (Bromwich & Fogt, 2004). In a study performed by Mooney et al. (2011) over Ireland (11 stations) considering the period 1989-2001, it was commented that ERA-Interim, ERA-40 and NCEP/NCAR reanalysis reproduced the observed monthly mean 2 m air temperatures in summer with good accuracy. However, they found that all three reanalysis data sets significantly over-estimated the monthly mean 2 m air temperatures in winter. In a comparison performed by Bromwich & Fogt (2004) between ERA-40 and NCEP/NCAR reanalysis data, over the high and mid-latitudes of the southern hemisphere, it was found that, prior to the modern satellite era both reanalysis data sets showed significant deviations from the observations. It was also found that, in the modern satellite era ERA-40 reanalysis data performed better than NCEP/NCAR reanalysis data in this region (Bromwich & Fogt 2004). Simmons et al. (2004) found that ERA-40 data showed a better agreement with the global surface air temperature anomalies than with NCEP/NCAR reanalysis data during the period 1958-2001. Furthermore, they found that the agreement between ERA-40 global surface air temperature anomalies and observations was stronger in the period 1979-2001 than that over the period 1958-1978, owing to the inclusion of satellite data in reanalysis in the post 1979 period. According to the above findings it is seen that, the quality of reanalysis data prior to the satellite era is relatively low and also the quality of the reanalysis data may vary from one set of data to another.

The selection of a certain reanalysis data set for providing the inputs for calibration and validation of a statistical downscaling model is mainly dependant on the length of the calibration and validation periods of the downscaling model and the availability of a certain reanalysis data set over that period. Also the past performances of the reanalysis data sets over the study area of interest may be considered in the selection of a reanalysis data set for the development of a downscaling model.

Issues with predictor pre-processing

The Principal Component Analysis (PCA) is widely used in statistical downscaling (e.g. Tripathi et al., 2006; Ghosh & Mujumdar 2008; Anandhi et al., 2009) as a way of extracting the variance in a large set of GCM outputs to a manageable number of variables called Principal Components (PC). PCA approach is helpful in removing the redundant information included in a set of GCM outputs, before they are introduced to a statistical downscaling model. This process makes the statistical downscaling model more stable and efficient (Anandhi et al., 2008). The exact way of using PCA in the preparation of inputs to a statistical downscaling model for its calibration, validation and projections into future was not explicitly documented in the past studies, for example Tripathi et al., 2006; Ghosh & Mujumdar 2008; Anandhi et al., 2009. In an analysis performed by Sachindra et al. (2013a), the coefficients of PCs extracted for the calibration phase of the downscaling model, were used to obtain the PCs for the validation phase. This was performed since the coefficients of the PCs obtained for the model calibration should become fixed components of the downscaling model for validation and projection into future. When the coefficients of the PCs extracted for calibration were applied on the validation data, in certain instances it caused the PCs of the validation phase to be significantly correlated with each other (Sachindra et al., 2013a). This process caused the model to overfit during calibration and underfit in validation, thus introducing a large uncertainty to the hydroclimatic projections produced into future. Therefore PCA should be used with extra caution in statistical downscaling exercises, where model calibration, validation and projections into future are performed.

It is the common practice to use some reanalysis data as inputs to the downscaling model in its calibration and validation. However, the hydroclimatic projections into future are produced by introducing the outputs of a GCM to the downscaling model. The accuracy of reanalysis data is much higher than those of GCM outputs, since reanalysis data are quality controlled and corrected against observations (e.g. NCEP/NCAR reanalysis data – Kalnay et al., 1996). The GCM outputs used in the

downscaling model in producing the catchment scale projections into future, are less reliable in comparison to the reanalysis outputs used in calibration and validation of the model. In other words, the model development and projection of catchment scale climate into future are done with input data originated from two different sources with different levels of accuracies. Therefore these data used in the model as inputs are not homogeneous in quality. This could cause the statistical downscaling model to perform better in model calibration and validation, and produce less reliable projections into future with GCM outputs. Sachindra et al. (2013b) addressed the issue of non-homogeneity in input data used in the development and projection of a downscaling model. They regressed the 20^{th} century climate experiment outputs of HadCM3, ECHAM5 and GFDL2.0 against the NCEP/NCAR reanalysis outputs and using these regression relationships homogeneous sets of input for the downscaling model for its calibration, validation and future projections were generated.

Another problem associated with the reanalysis data and the GCM outputs, is the mismatch between the spatial resolutions of these two data sources. As an example, the most widely used NCEP/NCAR reanalysis data are available at the spatial resolution of 2.5˚ along longitude and latitude (some NCEP/NCAR outputs are also available approximately at 1.9˚ resolution), but the resolution of different GCMs vary from this (e.g. HadCM3 has a resolution of 2.75˚ x 3.75˚). As a solution to this spatial resolution mismatch between reanalysis outputs and GCM outputs, GCM outputs are interpolated to the reanalysis grid (e.g. Tripathi et al., 2006; Ghosh & Mujumdar 2008; Anandhi et al., 2009). The interpolation of GCM data from their original grid to the reanalysis grid can introduce errors into the input to the statistical downscaling model, as interpolation yields approximate values. The use of GCM data of fine spatial scales could be regarded as a possible solution to reduce the impacts of the spatial mismatch between reanalysis and GCM outputs. GCM data at finer spatial resolution refer to denser grids, hence the interpolation becomes more reliable.

SUMMARY AND CONCLUSIONS

Whatever the statistical downscaling technique employed in a downscaling study, it is faced with a cascade of issues and challenges, as described in this paper. These issues are mainly emerging from uncertainties in general circulation models (GCMs), uncertainties in greenhouse gas (GHG) emission scenarios, issues with observations of hydroclimatic variables, issues with different statistical downscaling techniques and issues with predictor selection and prepossessing criteria. The GCM uncertainty is mainly due to the lack of perfect understanding of variety of atmospheric processes and their incomplete mathematical representation (owing to the assumptions and approximations) in GCMs. However, with the advancement of science, the GCM uncertainty will reduce. The GHG emission scenario uncertainty is a result of the uncertainties associated with the technological, demographic and socio-economic developments of the future world. The uncertainties linked with the future GHG emission scenarios are difficult to be eliminated. Issues associated with observations of various catchment scale hydroclimatic variables (precipitation, streamflow, temperature, pan evaporation, humidity etc) are due to; errors in measuring instrument, observations and recording errors caused by human negligence, missing data infilling techniques, extrapolation of streamflow rating curves out of their design range etc. The issues linked with the statistical downscaling techniques are mainly due to different representations of predictor-predictand relationships (e.g. linear, non-linear) by different statistical downscaling techniques. Issues with predictors are related with the different predictor selection criteria such as linear or non-linear methods.

The selection of a better performing subset of GCMs from the large pool of GCMs is a possible way of reducing the uncertainty introduced to the downscaling exercise by the relatively poor performing GCMs. Better performing GCMs can be identified based on the model performance (spatiotemporal agreement with past observations – for example see; Harvey & Wigley, (2003)) and convergence of outputs (agreement of different GCMs on simulations produced into future – for example see; Johnson & Sharma

(2009)). Use of various bias-correction techniques may aid in reducing the mismatch between the GCM outputs and observations (or reanalysis data).

In a statistical downscaling study, it is advisable to consider at least two future GHG emission scenarios which represent the plausible high and low GHG concentrations. This enables the identification of the possible higher and lower impacts of GHG emissions on catchment hydroclimatology. The latest set of GHG emission scenarios referred to as Representative Concentration Pathways (RCPs), contain a few scenarios which incorporate the influences of climate policies on future GHG emissions, unlike the past GHG emission scenarios (e.g. SRES scenarios). RCPs could be regarded as more plausible realisations of future GHG concentrations as many countries in the world have already implemented of climate policies in view of minimising the GHG emissions.

There could be outliers, in the records of observations which are used for the statistical downscaling model calibration and validation. Careful analysis of observations, prior to using them in a downscaling study will help in the identification and elimination of the outliers from the record and lead to a more dependable data set and a model. When the record of hydroclimatic observations is too short at a certain station, the short record could be extended through mathematical relationships (e.g. linear regression equations) with a longer record available at a neighbouring station.

The uncertainties introduced to the outputs of a statistical downscaling study, due to the use of different statistical downscaling techniques, are much less in comparison to the uncertainties arising from GCMs and greenhouse gas emission scenarios. It is advisable to use a relatively simple statistical downscaling technique (e.g. linear regression) at the beginning of a statistical downscaling study. If this simple downscaling method does not adequately reproduce the observations of the predictand, then a more complex downscaling technique could be experimented. Furthermore, it should be noted that there is no single superior statistical downscaling technique.

Any potential predictor used in a statistical downscaling study should have a plausible relationship with the predictand considered. If correlation coefficients were used for the selection of potential predictors, it is encouraged to analyse the consistency of the correlation between predictors and predictands over time. The use of scatter plots in predictor selection aids in visually identifying the nature of the predictor-predictand relationship. Unlike correlation coefficients, Partial Mutual Information criterion (PMI) is capable in identifying both linear and non-linear predictor-predictand dependence structures.

Statistical downscaling of GCM outputs to catchment scale hydroclimatic variables is part of an ever evolving science. Although there are some issues associated with statistical downscaling, still it is regarded as a potential technique for predicting the catchment scale hydroclimatology, under changing climate. Outputs of a statistical downscaling study should only be used as indications of future catchment hydroclimatology, than exact predictions.

ACKNOWLEDGEMENTS

The authors acknowledge the financial assistance provided by the Australian Research Council Linkage Grant Scheme and Grampians Wimmera Mallee Water Corporation for this project.

REFERENCE

Anandhi, A., Srinivas, V.V., Nanjundiah, R.S. & Nagesh Kumar, D. 2008 Downscaling precipitation to river basin in India for IPCC SRES scenarios using support vector machine. *Int. J. Climatol.* **28,** 401-420.

Anandhi, A., Srinivas, V.V., Nanjundiah, R.S. & Nagesh Kumar, D. 2009 Role of predictors in downscaling surface temperature to river basin in India for IPCC SRES scenarios using support vector machine. *Int. J. Climatol.* **29**, 583–603.

Anandhi, A., Frei, A., Pradhanang, S.M., Zion, M.S., Pierson, D.C. & Schneiderman, E.M. 2011 AR4 climate model performance in simulating snow water equivalent over Catskill mountain watersheds, New York, USA. *Hydrol. Process.* **25,** 3302–3311.

Arnell, N.W. 2004 Climate change and global water resources: SRES emissions and socio-economic scenarios. *Global Environ. Chang.* **14,** 31-52.

Bastola, S., Murphy, C. & Sweeney, J. 2011 The sensitivity of fluvial flood risk in Irish catchments to the range of IPCC AR4 climate change scenarios. *Sci. Total Environ.* **409,** 5403-5415.

Bromwich, D.H. & Fogt, R.L. 2004 Strong trends in the skill of the ERA40 and NCEP-NCAR reanalyses in the high and mid-latitudes of the southern hemisphere, 1958–2001. *J. Climate.* **17,** 4603–4620.

Brown, C., Ghile, Y, Laverty, M. & Li, K. 2012 Decision scaling: Linking bottom-up vulnerability analysis with climate projections in the water sector. *Water Resour. Res*. **48,** W09537

Cannon, A.J. & McKendry, I.G. 2002 A graphical sensitivity analysis for statistical climate models: Application to Indian monsoon rainfall prediction by artificial neural networks and multiple linear regression models. *Int. J. Climatol.* **22,** 1687-1708.

Cannon, A.J. & Whitfield, P.H. 2002 Downscaling recent streamflow conditions in British Columbia, Canada using ensemble neural network models. *J. Hydrol.* **259,** 136-151.

Charles, A., Timbal, B., Fernandez, E. & Hendon, H. 2013 Analog downscaling of seasonal rainfall forecasts in the Murray darling basin. *Mon. Weather Rev.* **141,** 1099-1117.

Chen, J., Brissette, F.P. & Leconte, R. 2011 Uncertainty of downscaling method in quantifying the impact of climate change on hydrology. *J. Hydrol.* **401,** 190-202.

Chen, J., Brissette, F.P. & Leconte, R. 2012 Coupling statistical and dynamical methods for spatial downscaling of precipitation. *Climatic Change* **114,** 509-526.

Chen, T.S., Yu, P.S. & Tang, Y.H. 2010 Statistical downscaling of daily precipitation using support vector machines and multivariate analysis. *J. Hydrol.* **385**, 13–22.

Chen, Y. D., Chen, X., Xu, C.Y. & Shao, Q. 2006 Downscaling of daily precipitation with a stochastic weather generator for the subtropical region in South China. *Hydrol. Earth Syst. Sci. Discuss.* **3,** 1145-1183.

Chow, V.T., Maidment, D.R. & Mays, L.W. 1988 *Applied Hydrology*. McGraw Hill Book Company.

Christensen, J.H., Kjellström, E., Giorgi, F., Lenderink, G. & Rummukainen, M. 2010 Weight assignment in regional climate models. *Climate Res.* **44,** 179-194.

Chu, J.T., Xia, J., Xu, C.Y. & Singh, V.P. 2010 Statistical downscaling of daily mean temperature, pan evaporation and precipitation for climate change scenarios in Haihe River, China. *Theor. Appl. Climatol.* **99**, 149–161.

Compo, G.P., Whitaker, J.S., Sardeshmukh, P.D., Matsui, N., Allan, R.J., Yin, X., Gleason, B.E., Vose, R.S., Rutledge, G., Bessemoulin, P., Brönnimann, S., Brunet, M., Crouthamel, R.I., Grant, A.N., Groisman, P.Y., Jones, P.D., Kruk, M.C., Kruger, A.C., Marshall, G.J., Maugeri, M., Mok, H.Y., Nordli, Ø., Ross, T.F., Trigo, R.M., Wang, X.L., Woodruff, S.D. & Worley, S.J. 2011 The twentieth century reanalysis project. *Q. J. Roy. Meteor. Soc.* **137,** 1–28.

Corti, S., Molteni, F. & Palmer, T.N. 1999 Signature of recent climate change in frequencies of natural atmospheric circulation regimes. *Nature*. 398, 799-802.

Coulibaly, P. 2004 Downscaling daily extreme temperatures with genetic programming. *Geophys. Res. Lett*. 31, 1-4.

Coulibaly, P., Dibike, Y.B. & Anctil, F. 2005 Downscaling precipitation and temperature with temporal neural networks. *J. Hydrometeor.* **6,** 483-496.

Covey, C., AchutaRao, K.M., Cubasch, U., Jones, P., Lambert, S.J., Mann, M.E., Phillips, T.J. & Taylor, K.E. 2003 An overview of results from the coupled model intercomparison project. *Global Planet. Change.* **37,** 103-133.

Dee, D.P., Uppala, S.M., Simmons, A.J., Berrisford, P., Poli, P., Kobayashi, S., Andrae, U., Balmaseda, M.A., Balsamo, G., Bauer, P., Bechtold, P., Beljaars, A.C.M., van de Berg, L., Bidlot, J., Bormann, N., Delsol, C., Dragani, R., Fuentes, M., Geer, A.J., Haimberger, L., Healy, S.B., Hersbach, H., Hólm, E.V., Isaksen, L., Kållberg, P., Köhler, M., Matricardi, M., McNally, A.P., Monge-Sanz, B.M., Morcrette, J.J., Park, B.K., Peubey, C., de Rosnay, P., Tavolato, C., Thépaut, J.N. & Vitart, F. 2011 The ERA-Interim reanalysis: configuration and performance of the data assimilation system. *Q. J. Roy. Meteor. Soc.* **137,** 553-597.

Dessai, S., Lu, X. & Hulme, M. 2005 Limited sensitivity analysis of regional climate change probabilities for the 21st century. *J. Geophys. Res-Atmos.* **110,** 1-17.

Dibike, Y.B. & Coulibaly, P. 2005 Hydrologic impact of climate change in the Saguenay watershed: comparison of downscaling methods and hydrologic models. *J. Hydrol.* **307,** 145-163.

Domeneghetti, A., Castellarin, A. & Brath, A. 2012 Assessing rating-curve uncertainty and its effects on hydraulic model calibration. *Hydrol. Earth Syst. Sci.* **16,** 1191–1202.

Duan, J., McIntyre, N. & Onof, C. 2012 Resolving non-stationarity in statistical downscaling of precipitation under climate change scenarios. *British Hydrological Society Eleventh National Symposium, Hydrology for a changing world, Dundee, UK*.

Einfalt, T. & Michaelides, S. 2008 Quality control of precipitation data. In: *Precipitation: Advances in measurement, estimation and prediction* (S. Michaelides, ed.). Springer, Dordrecht, Netherlands. pp. 101-126.

Faucher, M., Burrows, W.R. & Pandolfo, L. 1999 Empirical-statistical reconstruction of surface marine winds along the western coast of Canada. *Climate Res.* **11,** 173-190.

Feddersen, H. & Andersen, U. 2005 A method for statistical downscaling of seasonal ensemble predictions. *Tellus A*. **57,** 398-408.

Feng, S., Hu, Q. & Qian, W. 2004 Quality control of daily meteorological data in China, 1951-2000: A new dataset. *Int. J. Climatol.* **24,** 853-870.

Fistikoglu, O. & Okkan, U. 2011 Statistical downscaling of monthly precipitation using NCEP/NCAR reanalysis data for tahtali river basin in Turkey. *J.Hydr. Eng. ASCE.* **16,** 157-164.

Fowler, H.J., Blenkinsop, S. & Tebaldi, C. 2007 Linking climate change modelling to impacts studies: recent advances in downscaling techniques for hydrological modelling. *Int. J. Climatol.* **27**, 1547–1578.

Ghosh, S. & Katkar S. 2012 Modeling uncertainty resulting from multiple downscaling methods in assessing hydrological impacts of climate change. *Water Resour. Manag*. **26,** 3559-3579.

Ghosh, S. & Mujumdar, P.P. 2008 Statistical downscaling of GCM simulations to streamflow using relevance vector machine. *Adv. Water Resour.* **31,** 132-146.

Gibson, J.K., Kallberg, P., Uppala, S., Nomura, A., Hernandez, A. & Serrano, E. 1997 *ERA Description*. Online report available at http://www.ecmwf.int/research/era/ERA-15/Report_Series/index.html. 3-62.

Giorgi, F. & Mearns, L.O. 2002 Calculation of average, uncertainty range, and reliability of regional climate changes from AOGCM simulations via the "reliability ensemble averaging" (REA) method. *J. Climate.* **15,** 1141-1158.

Giorgi, F. 2010 Uncertainties in climate change projections, from the global to the regional scale. *EPJ Web of Conferences* **9,** 115-129.

Gleckler, P.J., Taylor, K.E. & Doutriaux, C. 2008 Performance metrics for climate models. *J. Geophys. Res-Atmos.* **113,** 1-20.

Goyal, M.K. & Ojha, C.S.P. 2011 PLS regression-based pan evaporation and minimum-maximum temperature projections for an arid lake basin in India. *Theor. Appl. Climatol.* **105,** 403-415.

Goyal, M.K., Burn, D.H. & Ojha, C.S.P. 2012 Evaluation of machine learning tools as a statistical downscaling tool: Temperatures projections for multi-stations for Thames River Basin, Canada. *Theor. Appl. Climatol.* **108,** 519-534.

Gudmundsson, L., Bremnes, J.B., Haugen, J.E. & Skaugen, T.E. 2012 Technical note: Downscaling RCM precipitation to the station scale using quantile mapping – a comparison of methods. *Hydrol. Earth Syst. Sci.* **9,** 6185-6201.

Gupta, R.S. 2008 *Hydrology and Hydraulic Systems*. Waveland Press, Illinois.

Harvey, L.D.D. & Wigley, T.M.L. 2003 Charactering and comparing control-run variability of eight coupled AOGCMs and of observations part 1: Temperature. *Clim. Dynam.* **21,** 619–646.

Hashmi, M.Z., Shamseldin, A.Y. & Melville, B.W. 2009a Statistical downscaling of precipitation: state-of-the-art and application of Bayesian multi-model approach for uncertainty assessment. *Hydrol. Earth Syst. Sci.* **6,** 6535-6579.

Hashmi, M.Z., Shamseldin, A.Y. & Melville, B.W. 2009b Downscaling of future rainfall extreme events: A weather generator based approach. *Proceedings of 18th World IMACS congress and MODSIM09 international congress on modelling and simulation*, pp 3928-3934.

Hashmi, M.Z., Shamseldin, A.Y. & Melville, B.W. 2011 Statistical downscaling of watershed precipitation using Gene Expression Programming (GEP). *Environ. Modell. Softw.* **26,** 1639-1646.

Hay, L.E. & Clark, M.P. 2003 Use of statistically and dynamically downscaled atmospheric model output for hydrologic simulations in three mountainous basins in the western United States. *J. Hydrol.* **282,** 56-75.

Herschy, R.W. 2009 *Streamflow measurement*. 3rd edition. Routledge, Taylor and Francis group. London.

Hewitson, B.C. & Crane, R.G. 2006 Consensus between GCM climate change projections with empirical downscaling: precipitation downscaling over South Africa. *Int. J. Climatol.* **26,** 1315-1337.

Hijmans, R.J., Cameron, S.E., Parra, J.L., Jones, P.G. & Jarvis, A. 2005 Very high resolution interpolated climate surfaces for global land areas. *Int. J. Climatol.* **25,** 1965-1978.

Hu, Y., Maskey, S. & Uhlenbrook, S. 2013 Downscaling daily precipitation over the Yellow River source region in China: A comparison of three statistical downscaling methods. *Theor. Appl. Climatol.* **112,** 447-460.

Hubbard, K.G. & You, J. 2005 Sensitivity analysis of quality assurance using the spatial regression approach - A case study of the maximum/minimum air temperature. *J. Atmos. Ocean. Tech.* **22,** 1520-1530.

Hubbard, K.G. 2001 Multiple station quality control procedures. In: *Proceedings of automated weather stations for applications in agriculture and water resources management: current use and future perspectives* (K.G. Hubbard & M.V.K. Sivakumar, ed), 6-10 March 2000. Lincoln, Nebraska, USA, pp. 133-136.

Huntingford, C., Jones, R.G., Prudhomme, C., Lamb, R., Gash, J.H.C. & Jones, D.A. 2003 Regional climate-model predictions of extreme rainfall for a changing climate. *Q. J. Roy. Meteor. Soc.* **129,** 1607-1621.

Ingol-Blanco, E.M. 2011 Modeling climate change impacts on hydrology and water resources: case study Rio Conchos basin. *PhD Thesis*. The University of Texas, Austin, USA, pp. 61-63.

IPCC, 2000 IPCC special report on emissions scenarios - Summary for policymakers. Online report available at http://www.ipcc.ch/pdf/special-reports/spm/sres-en.pdf. 4-8.

Jeong, D.I., St-Hilaire, A., Ouarda, T.B.M.J. & Gachon, P. 2012a Multisite statistical downscaling model for daily precipitation combined by multivariate multiple linear regression and stochastic weather generator. *Climatic Change* **114,** 567-591.

Jeong, D.I., St-Hilaire, A., Ouarda, T.B.M.J. & Gachon, P. 2012b A multivariate multi-site statistical downscaling model for daily maximum and minimum temperatures. *Climate Res.* **54,** 129-148.

Johnson, F. & Sharma, A. 2009 Measurement of GCM skill in predicting variables relevant for hydroclimatological assessments. *J. Climate.* **22,** 4373-4382.

Johnson, F. & Sharma, A. 2012 A nesting model for bias correction of variability at multiple time scales in general circulation model precipitation simulations. *Water Resour. Res.* **48,** 1-16.

Kalnay, E., Kanamitsu, M., Kistler, R., Collins, W., Deaven, D., Gandin, L., Iredell, M., Saha, S., White, G., Woollen, J., Zhu, Y., Chelliah, M., Ebisuzaki, W., Higgins, W., Janowiak, J., Mo, K.C., Ropelewski, C., Wang, J., Leetmaa, A., Reynolds, R., Jenne, R. & Joseph, D. 1996 The NCEP/NCAR reanalysis project. *B. Am. Meteorol. Soc.* **77,** 437-471.

Kanamitsu, M., Ebisuzaki, W., Woollen, J., Yang, S.K., Hnilo, J.J., Fiorino, M. & Potter, G.L. 2002 NCEP-DOE AMIP-II Reanalysis (R-2). *B. Am. Meteorol. Soc.* **83,** 1631–1643.

Kannan, S. & Ghosh, S. 2013 A nonparametric kernel regression model for downscaling multisite daily precipitation in the Mahanadi basin. *Water Resour. Res.* **49,** 1360-1385.

Kass, R.E. & Raftery A. E. 1995 Bayes factors. *J. Am. Stat. Assoc.* **90,** 773 - 795.

Khalili, M., Brissette, F. & Leconte R. 2011 Effectiveness of multi-site weather generator for hydrological modelling. *J. Am. Water Resour. As.* **47,** 303-314.

Khan, M.S., Coulibaly, P. & Dibike, Y. 2006 Uncertainty analysis of statistical downscaling methods using Canadian global climate model predictors. *Hydrol. Process.* **20,** 3085-3104.

Kharin, V.V. & Zwiers, F.W. 2002 Climate predictions with multimodel ensembles. *J. Climate.* **15,** 793-799.

Kistler, R., Kalnay, E., Collins, W., Saha, S., White, G., Woollen, J., Chellian, M., Edisuzaki, W., Kanamitso, M., Kousky, V., Van Den Dool, H., Jenne, R. & Fiorino, M. 2001 The NCEP-NCAR 50-Year Reanalysis: monthly means CD-ROM and documentation. *B. Am. Meteorol. Soc.* **82,** 247–267.

Knutti, R., Furrer, R., Tebaldi, C., Cermak, J. & Meehl, GA. 2010 Challenges in combining projections from multiple climate models. *J. Climate.* **23,** 2739–2758.

Kou, X., Ge, J., Wang, Y. & Zhang, C. 2007 Validation of the weather generator CLIGEN with daily precipitation data from the Loess Plateau, China. *J. Hydrol.* **347,** 347-357.

Krishnamurti, T.N., Kishtawal, C.M., LaRow, T.E., Bachiochi, D.R., Zhang, Z., Williford, C.E., Gadgil, S. & Surendran, S. 1999 Improved weather and seasonal climate forecasts from multimodel superensemble. *Science* **285,** 1548-1550.

Lafon, T., Dadson, S., Buys, G. & Prudhomme, C. 2013 Bias correction of daily precipitation simulated by a regional climate model: A comparison of methods. *Int. J. Climatol.* **33,** 1367-1381.

Lambert, S.J. & Boer, G.J. 2001 CMIP1 evaluation and intercomparison of coupled climate models. *Clim. Dynam.* **17,** 83-106.

Landman, W.A., Mason, S.J., Tyson, P.D. & Tennant, W.J. 2001 Statistical downscaling of GCM simulations to streamflow. *J. Hydrol.* **252**, 221–236.

Lavaysse, C., Vrac, M., Drobinski, P., Lengaigne, M. & Vischel, T. 2012 Statistical downscaling of the French Mediterranean climate: Assessment for present and projection in an anthropogenic scenario. *Nat. Hazard Earth Sys.* **12,** 651-670.

Li, H., Sheffield, J. & Wood, E.F. 2010 Bias correction of monthly precipitation and temperature fields from intergovernmental panel on climate change AR4 models using equidistant quantile matching. *J. Geophys. Res-Atmos.* **115,** 1-20.

Lutz, K., Jacobeit, J., Philipp, A., Seubert, S., Kunstmann, H. & Laux, P. 2012 Comparison and evaluation of statistical downscaling techniques for station-based precipitation in the Middle East. *Int. J. Climatol*. **32,** 1579-1595.

MacQueen, J. 1967 Some methods for classification and analysis of multivariate observation. In: *Proceedings of the Fifth Berkeley Symposium on Mathematical Statistics and Probability*. *Vol. 1* (L.M. Le Cam & J. Neyman, ed.). University of California Press, Berkeley, USA, pp. 281–297.

Maqsood, I., Khan, M.R. & Abraham, A. 2004 An ensemble of neural networks for weather forecasting. *Neural Computing and Applications* **13,** 112-122.

Masui, T., Matsumoto, K., Hijioka, Y., Kinoshita, T., Nozawa, T., Ishiwatari, S., Kato, E., Shukla, P.R., Yamagata, Y. & Kainuma, M. 2011 An emission pathway for stabilization at 6 W/m^2 radiative forcing. *Climatic Change* **109,** 59-76.

Mehrotra, R. & Sharma, A. 2010 Development and application of a multisite rainfall stochastic downscaling framework for climate change impact assessment. *Water Resour. Res.* **46,** 1-17.

Mehrotra, R., Sharma, A. & Cordery, I. 2004 Comparison of two approaches for downscaling synoptic atmospheric patterns to multisite precipitation occurrence. *J. Geophys. Res-Atmos.* **109,** 1-15.

Mesinger, F., Dimego, G., Kalnay, E., Mitchell, K., Shafran, P.C., Ebisuzaki, W., Jovic, D., Woollen, J., Rogers, E., Berbery, E.H., Ek, M.B., Fan, Y., Grumbine, R., Higgins, W., Li, H., Lin, Y., Manikin, G., Parrish, D. & Shi, W. 2006 North American regional reanalysis: a long-term, consistent, high-resolution climate dataset for the North American domain, as a major improvement upon the earlier global reanalysis datasets in both resolution and accuracy. *B. Am. Meteorol. Soc.* **87,** 343–360.

Min, S.K. & Hense, A. 2006 A Bayesian approach to climate model evaluation and multi-model averaging with an application to global mean surface temperatures from IPCC AR4 coupled climate models. *Geophys. Res. Lett*. **33,** L08708

Min, Y.M., Kryjov, V.N., An, K.H., Hameed, S.N., Sohn, S.J., Lee, W.J. & Oh, J.H. 2011 Evaluation of the weather generator CLIGEN with daily precipitation characteristics in Korea. *Asia-Pac. J. Atmos. Sci.* **47,** 255-263.

Mooney, P.A., Mulligan, F.J. & Fealy, R. 2011 Comparison of ERA-40, ERA-Interim and NCEP/NCAR reanalysis data with observed surface air temperatures over Ireland. *Int. J. Climatol.* **31,** 545–557.

Moss, R.H., Edmonds, J.A., Hibbard, K.A., Manning, M.R., Rose, S.K., van Vuuren, D.P., Carter, T.R., Emori, S., Kainuma, M., Kram, T., Meehl, G.A., Mitchell, J.F.B., Nakicenovic, N., Riahi, K., Smith, S.J., Stouffer, R.J., Thomson, A.M., Weyant, J.P. & Wilbanks, T.J. 2010 The next generation of scenarios for climate change research and assessment. *Nature* **463,** 747-756.

Najafi, M., Moradkhani, H. & Wherry, S. 2011 Statistical downscaling of precipitation using machine learning with optimal predictor selection. *J.Hydr. Eng. ASCE.* **16,** 650-664.

Nash, J.E. & Sutcliffe, J.V. 1970 River flow forecasting through conceptual models, part 1 - A discussion of principles. *J. Hydrol.* **10,** 282-290.

Nasseri, M., Tavakol-Davani, H. & Zahraie, B. 2013 Performance assessment of different data mining methods in statistical downscaling of daily precipitation. *J. Hydrol.* **492,** 1-14.

Nguyen, V.T.V., Desramaut, N. & Nguyen, T.D. 2008 Estimation of design storms in consideration of climate variability and change. *Proceedings of 11th International Conference on Urban Drainage.* August 31-September 5 2008. Edinburgh, Scotland, pp. 1-11.

Ojha, R., Kumar, D.N., Sharma, A. & Mehrotra, R. 2012 Assessing severe drought and wet events over India in a future climate using a nested bias correction approach. *J.Hydr. Eng. ASCE.* Article in press.

Onogi, K., Tsutsui, J., Koide, H., Sakamoto, M., Kobayashi, S., Hatsushika, H., Matsumoto, T., Yamazaki, N., Kamahori, H., Takahashi, K., Kadokura, S., Wada, K., Kato, K., Oyama, R., Ose, T., Mannoji, N. & Taira, R. 2007 The JRA-25 reanalysis. *J. Meteorol. Soc. Jpn.* **85,** 369-432.

Panofsky, H.A. & Brier, G.W. 1968 *Some Applications of Statistics to Meteorology*. Pennsylvania State University, Pennsylvania.

Parry, M.L., Rosenzweig, C., Iglesias, A., Livermore, M. & Fischer, G. 2004 Effects of climate change on global food production under SRES emissions and socio-economic scenarios. *Global Environ. Chang.* **14,** 53-67.

Pelletier, P.M. 1988 Uncertainties in the single determination of river discharge: a literature review. *Can. J. Civ. Eng.* **15,** 834-850.

Perkins, S.E., Pitman, A.J., Holbrook, N.J. & McAneney, J. 2007 Evaluation of the AR4 climate models' simulated daily maximum temperature, minimum temperature, and precipitation over Australia using probability density functions. *J. Climate.* **20,** 4356-4376.

Piani, C., Haerter, J.O. & Coppola, E. 2010 Statistical bias correction for daily precipitation in regional climate models over Europe. *Theor. Appl. Climatol.* **99,** 187-192.

Prudhomme, C., Reynard, N. & Crooks, S. 2002 Downscaling of global climate models for flood frequency analysis: Where are we now? *Hydrol. Process.* **16,** 1137-1150.

Prudhomme, C., Jakob, D. & Svensson, C. 2003 Uncertainty and climate change impact on the flood regime of small UK catchments. *J. Hydrol.* **277,** 1-23.

Prudhomme, C., Wilby, R.L., Crooks, S., Kay, A.L. & Reynard, N.S. 2010 Scenario-neutral approach to climate change impact studies: application to food risk. *J. Hydrol.* **390,** 198–209.

Raje, D. & Mujumdar, P.P. 2010 Constraining uncertainty in regional hydrologic impacts of climate change: nonstationarity in downscaling. *Water Resour. Res.* **46,** W07543

Riahi, K., Rao, S., Krey, V., Cho, C., Chirkov, V., Fischer, G., Kindermann, G., Nakicenovic, N. & Rafaj, P. 2011 RCP 8.5 - A scenario of comparatively high greenhouse gas emissions. *Climatic Change* **109,** 33-57.

Richardson, C.W. 1981 Stochastic simulation of daily precipitation, temperature, and solar radiation. *Water Resour. Res.* **17,** 182-190.

Sachindra, D.A., Huang, F., Barton, A.F. & Perera, B.J.C. 2014 Statistical downscaling of general circulation model outputs to precipitation Part 2: bias-correction and future projections. *Int. J. Climatol.* (Article in press), doi: 10.1002/joc.3915.

Sachindra, D.A., Huang, F., Barton, A.F. & Perera, B.J.C. 2013a Least square support vector and multi-linear regression for statistically downscaling general circulation model outputs to catchment streamflows. *Int. J. Climatol.* **33,** 1087-1106

Sachindra, D.A., Huang, F., Barton, A.F. & Perera, B.J.C. 2013b. Multi-model ensemble approach for statistically downscaling general circulation model outputs to precipitation. *Q. J. Roy. Meteor. Soc.* (Article in press), doi: 10.1002/qj.2205.

Sachindra, D.A., Huang, F., Barton, A.F. & Perera, B.J.C. 2013c Statistical Downscaling of General Circulation Model Outputs to Evaporation, Minimum Temperature and Maximum Temperature Using a Key-Predictand and Key-Station Approach. *Journal of Water and Climate Change*. (Under review).

Salvi, K., Kannan, S. & Ghosh, S. 2011 Statistical downscaling and bias-correction for projections of Indian rainfall and temperature in climate change studies. *Proceedings of 4th International Conference on Environmental and Computer Science*. 16 - 18 September 2011, Singapore, pp.7-11.

Schnur, R. & Lettenmaier, D.P. 1998 A case study of statistical downscaling in Australia using weather classification by recursive partitioning. *J. Hydrol.* **213,** 362-379.

Sciuto, G., Bonaccorso, B., Cancelliere, A. & Rossi, G. 2009 Quality control of daily rainfall data with neural networks. *J. Hydrol.* **364,** 13-22.

Sevruk, B. & Klemm, S. 1989 *Catalogue of national standard precipitation gauges. Instruments and Observing Methods, Report No.39*. Geneva, Switzerland.

Sharma, A. 2000 Seasonal to interannual rainfall probabilistic forecasts for improved water supply management : Part 1-A strategy for system predictor identification. *J. Hydrol.* **239,** 232-239.

Sharma, D., Gupta, A.D. & Babel, M.S. 2007 Spatial disaggregation of bias-corrected GCM precipitation for improved hydrologic simulation: Ping River Basin, Thailand. *Hydrol. Earth Syst. Sci.* **11,** 1373-1390.

Simanton, J.R. & Osborn, H.B. 1980. Reciprocal-distance estimation of point rainfall. *J. Hydraul. Eng. Div.* **106,** 1242-1246.

Simmons, A.J., Jones, P.D., da Costa Bechtold, V., Beljaars, A.C.M., Kollberg, P.W., Saarinen, S., Uppala, S.M., Viterbo, P. & Weldi, N. 2004 Comparison of trends and low-frequency variability in CRU, ERA-40, and NCEP/NCAR analyses of surface air temperature. *J. Geophys. Res-Atmos.* **109,** D24115.

Smith, I. & Chandler, E. 2009 Refining rainfall projections for the Murray Darling basin of south-east Australia-the effect of sampling model results based on performance. *Climatic Change* **102,** 377-393.

Souvignet, M. & Heinrich, J. 2011 Statistical downscaling in the arid central Andes: Uncertainty analysis of multi-model simulated temperature and precipitation. *Theor. Appl. Climatol.* **106,** 229-244.

Srinivas, V.V., Basu, B., Nagesh Kumar, D. & Jain, S.K. 2013 Multi-site downscaling of maximum and minimum daily temperature using support vector machine. *Int. J. Climatol.* (Article in press).

STARDEX, 2005 *STARDEX downscaling climate extremes*. Available online at http://www.cru.uea.ac.uk/projects/stardex/reports/STARDEX_FINAL_REPORT.pdf. 3-18

Tatli, H., Dalfes, H.N. & Mentes, S.S. 2004 A statistical downscaling method for monthly total precipitation over Turkey. *Int. J. Climatol.* **24,** 161–180.

Tebaldi, C. & Knutti, R. 2010 Climate models and their projections of future changes. In: *Climate Change and Food Security: Adapting Agriculture to a Warmer World* (D. Lobell & M. Burke, ed.). Springer, Dordrecht, Netherlands, pp. 31-56.

Tebaldi, C., Smith, R., Nychka, D. & Mearns, L. 2005 Quantifying uncertainty in projections of regional climate change: a Bayesian approach to the analysis of multi-model ensembles. *J. Clim.* **18,** 1524–1540.

Teng, J., Chiew, F.H. & Vaze, J. 2012 Will CMIP5 GCMs reduce or increase uncertainty in future runoff projections. *American Geophysical Union - Fall Meeting*, 3-7 December 2012. San Francisco, USA.

Terzi, O. 2012 Monthly rainfall estimation using data-mining process. *Applied Computational Intelligence and Soft Computing*. 1-6.

Teutschbein, C. & Seibert J. 2012 Bias correction of regional climate model simulations for hydrological climate-change impact studies: Review and evaluation of different methods. *J. Hydrol.* **456-457,** 12-29.

Thomson, A., Calvin, K., Smith, S., Kyle, P., Volke, A., Patel, P., Delgado-Arias, S., Bond-Lamberty, B., Wise, M., Clarke, L. & Edmonds, J. 2011 RCP4.5: a pathway for stabilization of radiative forcing by 2100. *Climatic Change* **109,** 77-94.

Timbal, B., Fernandez, E. & Li, Z. 2009 Generalization of a statistical downscaling model to provide local climate change projections for Australia. *Environ. Modell. Softw.* **24,** 341-358.

Tisseuil, C., Vrac, M., Lek, S. & Wade, A.J. 2010 Statistical downscaling of river flows. *J. Hydrol.* **385**, 279–291.

Tripathi, S., Srinivas, V.V. & Nanjundiah, R.S. 2006 Downscaling of precipitation for climate change scenarios: a support vector machine approach. *J. Hydrol.* **330,** 621-640.

Uppala, S.M., KÅllberg, P.W., Simmons, A.J., Andrae, U., Bechtold, V.D.C., Fiorino, M., Gibson, J.K., Haseler, J., Hernandez, A., Kelly, G.A., Li, X., Onogi, K., Saarinen, S., Sokka, N., Allan, R.P., Andersson, E., Arpe, K., Balmaseda, M.A., Beljaars, A.C.M., Berg, L.V.D., Bidlot, J., Bormann, N., Caires, S., Chevallier, F., Dethof, A., Dragosavac, M., Fisher, M., Fuentes, M., Hagemann, S., Hólm, E., Hoskins, B.J., Isaksen, L., Janssen, P.A.E.M., Jenne, R,. Mcnally, A., Mahfouf, J.F., Morcrette, J.J., Rayner, N.A., Saunders, R.W., Simon, P., Sterl, A., Trenberth, K.E., Untch, A., Vasiljevic., D., Viterbo, P. & Woollen, J. 2005 The ERA-40 re-analysis. *Q. J. Roy. Meteor. Soc.* **131,** 2961–3012.

van Vuuren, D.P. & O'Neill, B.C. 2006 The consistency of IPCC's SRES scenarios to 1990-2000: Trends and recent projections. *Climatic Change* **75,** 9-46.

van Vuuren, D.P., Stehfest, E., den Elzen, M.G.J., Kram, T., van Vliet, J., Deetman, S., Isaac, M., Goldewijk, K.K., Hof, A., Beltran, A.M., Oostenrijk, R. & van Ruijven, B. 2011b RCP2.6: Exploring the possibility to keep global mean temperature increase below 2°C. *Climatic Change* **109,** 95-116.

van Vuuren, P.D., Edmonds, J.A., Kainuma, M., Riahi, K. & Weyant, J. 2011c A special issue on the RCPs. *Climatic Change* **109,** 1-4.

van Vuuren, P.D., Edmonds, J.A., Kainuma, M., Riahi, K., Thomson, A.M., Hibbard, K., Hurtt, G.C., Kram, T., Krey, V., Lamarque, J.F., Masui, T., Meinshausen, M., Nakicenovic, N., Smith, S.J. & Rose, S. 2011a The representative concentration pathways: An overview. *Climatic Change* **109,** 5-31.

Vasiliades, L., Loukas, A. & Patsonas, G. 2009 Evaluation of a statistical downscaling procedure for the estimation of climate change impacts on droughts. *Nat. Hazard Earth Sys.* **9,** 879-894.

von Storch, H., Hewitson, B. & Mearns, L. 2000 Review of empirical downscaling techniques. *Proceedings of RegClim spring meeting*, 8 - 9 May 2000, Jevnaker, Norway. Available online at http://regclim.met.no/rapport_4/Default.htm. (Accessed on 1st October 2012).

Wang, X., Yang, T., Shao, Q., Acharya, K., Wang, W. & Yu, Z. 2012 Statistical downscaling of extremes of precipitation and temperature and construction of their future scenarios in an elevated and cold zone. *Stoch. Env. Res. Risk A.* **26,** 405-418.

Ward, L. & Sun, M.N. 2006 Climate Downscaling: Assessment of the added values using regional climate models. In: *Climate Prediction and Agriculture Advances and Challenges* (M.V.K. Sivakumar & Hansen. J. ed.). Springer-Verlag, Berlin, Germany, pp 15-29.

Warner, T.T. 2011 *Numerical Weather and Climate Prediction*. Cambridge University Press, Cambridge.

Wetterhall, F., Bárdossy, A., Chen, D., Halldin, S. & Xu, C.Y. 2009 Statistical downscaling of daily precipitation over Sweden using GCM output. *Theor. Appl. Climatol.* **96,** 95-103.

Wetterhall, F., Halldin, S. & Xu, C.Y. 2005 Statistical precipitation downscaling in central Sweden with the analogue method. *J. Hydrol.* **306,** 136-174.

Wilby, R.L. & Dawson, C.W. 2012 The Statistical DownScaling Model: insights from one decade of application. *Int. J. Climatol.* Article in Press.

Wilby, R.L. & Wigley, T.M.L. 1997 Downscaling general circulation model output: a review of methods and limitations. *Prog. Phys. Geog.* **21,** 530-548.

Wilby, R.L., Charles, S.P., Zorita, E., Timbal, B., Whetton, P. & Mearns, L.O. 2004 *Guidelines for use of climate scenarios developed from statistical downscaling methods, supporting material to the IPCC.* Available online at http://www.ipcc-data.org/. 3-21.

Wilby, R.L., Wigley, T.M.L., Conway, D., Jones, P.D., Hewitson, B.C., Main, J. & Wilks, D.S. 1998 Statistical downscaling of general circulation model output: A comparison of methods. *Water Resour. Res.* **34,** 2995-3008.

Wilks, D.S. 1999 Multi-site downscaling of daily precipitation with a stochastic weather generator. *Climate Res.* **11,** 125-136.

Wilks, D.S. 2010 Use of stochastic weather generators for precipitation downscaling. Wiley Interdisciplinary Reviews. *Climate Change* **1,** 898-907.

Wood, A.W., Leung, L.R., Sridhar, V. & Lettenmaier, D.P. 2004 Hydrologic implications of dynamical and statistical approaches to downscaling climate model outputs. *Climatic Change* **62,** 189-216.

Yang, T., Li, H., Wang, W., Xu, C.Y. & Yu, Z. 2012 Statistical downscaling of extreme daily precipitation, evaporation, and temperature and construction of future scenarios. *Hydrol. Process.* **26,** 3510–3523.

Yu, P.S., Yang, T.C. & Wu, C.K. 2002 Impact of climate change on water resources in southern Taiwan. *J. Hydrol.* **260,** 161-175.

Zhang, H. & Huang, G.H. 2013 Development of climate change projections for small watersheds using multi-model ensemble simulation and stochastic weather generation. *Clim. Dynam.* Article in press.

Zhang, Y., Ohata, T., Yang, D. & Davaa, G. 2004 Bias correction of daily precipitation measurements for Mongolia. *Hydrol. Process.* **18,** 2991-3005.

Zorita, E. & Von Storch, H. 1999 The analog method as a simple statistical downscaling technique: comparison with more complicated methods. *J. Climate.* **12,** 2474-2489.

CHAPTER 3

STATISTICAL DOWNSCALING OF GCM OUTPUTS TO PRECIPITATION AT A STATION

3.1 Introduction

In this chapter, statistical downscaling of GCM outputs to monthly precipitation at a single station in the study area is presented. In statistical downscaling, it is the common practice to use some form of reanalysis outputs for the calibration and validation (development) of the downscaling model, and then use the corresponding outputs of a GCM on the downscaling model for the projection of climate at the catchment scale into future. The major issue associated with this conventional approach is that the outputs of two different sources with different degrees of accuracy are used as inputs to the downscaling model in its development and future projection phases. In other words, the inputs to the downscaling model are not homogeneous.

When the conventional approach is used in developing statistical downscaling models, owing to non-homogeneity in inputs, it can yield downscaling models which perform well with reanalysis outputs but fail to perform well with corresponding GCM outputs. This is because unlike GCM outputs, reanalysis outputs are quality controlled and corrected against observations. In other words, reanalysis outputs are of better quality compared to corresponding GCM outputs. A downscaling model should not only perform well with reanalysis outputs, but also it should perform adequately with GCM

outputs. This is because, though the downscaling model is calibrated and validated using reanalysis outputs as inputs, projections of catchment scale climate into future are produced using the outputs of GCMs as inputs to the downscaling model. The use of GCM outputs pertaining to the past climate as inputs to a downscaling model in its calibration phase allows the determination of parameters of the downscaling model specifically suitable for that GCM. This enables producing more reliable projections of catchment scale climate into the future. Therefore, the use of GCM outputs for the calibration, validation and future projection phases as inputs to a statistical downscaling model is seen as a potential solution to the issue of non-homogeneity in inputs.

In this chapter, calibration and validation of two statistical downscaling models; the first with NCEP/NCAR reanalysis outputs and the second with HadCM3 outputs are described. Following the common practice in the first downscaling model, the calibration and the validation were performed using NCEP/NCAR reanalysis outputs as inputs to the model in view of using the outputs of HadCM3 for the projection of precipitation into future. The second downscaling model was calibrated and validated using the 20th century climate experiment outputs of HadCM3 in view of using HadCM3 outputs for the projection of precipitation into future. In the first downscaling model which was developed according to the common practise (conventional manner), the input data to the model are obtained from two different sources with different degrees of accuracy. Hence the input data to this downscaling model are not homogeneous in its development and projection phases. However, the second downscaling model was developed and intended to be used with a homogeneous set of inputs derived from the same GCM. In the above manner, the issue of using inputs obtained from different sources for the calibration, validation and future projections in a conventional downscaling model was attempted to be resolved. The performances of the above two statistical downscaling models were compared graphically and numerically for the calibration and the validation phases.

The bias in the outputs of HadCM3 was identified and the effect of that bias in the outputs of the downscaling model seen over the historical period was corrected using

three bias-correction methods; (1) the equidistant quantile mapping, (2) the nested bias-correction and (3) the monthly bias-correction. A comparison of performances of the above three bias-correction techniques is also included in this chapter along with the precipitation projections produced into future at the station of interest.

Some of the inputs to the downscaling models developed in this study were correlated with each other. According to Tabachnick & Fidell (2007), issues due to multi-collinearity (e.g. unstable coefficients in MLR equations) can occur when the correlation between any two predictor variables is extremely high (greater than 0.90). However, the correlations between the inputs to the downscaling models developed in this study were not extremely high, so that the multi-collinearity in the inputs to downscaling model did not make the coefficients in the MLR equations unstable.

Furthermore, it should be noted that depending on the set of inputs (e.g. obtained from different GCMs or from same GCM but different sets of predictors) to the downscaling model, the projections/predictions of the predictand of interest produced by the downscaling model and its parameters can vary. As a solution to the above issue, ensemble techniques can be used to combine the outputs of downscaling models produced using different inputs obtained from the pool outputs of the same GCM or using a common set of inputs obtained from the pools of outputs of different GCMs. More information on the use of ensemble techniques in statistical downscaling is provided in Chapter 4 of the thesis.

This chapter contains the following two journal papers. The first paper discusses the development of the two statistical downscaling models and the second paper details the application of the bias-correction and the precipitation projections produced into future.

1. **Sachindra DA**, Huang F, Barton AF, Perera BJC. 2014a. Statistical downscaling of general circulation model outputs to precipitation Part 1: Calibration and validation. *International Journal of Climatology*. (Article in

press, published online). DOI**:** 10.1002/joc.3914. (SCImago journal rank indicator = Q1; ERA Rank = A; Impact Factor = 2.886)

2. **Sachindra DA**, Huang F, Barton AF, Perera BJC. 2014b. Statistical downscaling of general circulation model outputs to precipitation Part 2: Bias-correction and future projections. *International Journal of Climatology*. (Article in press, published online). DOI: 10.1002/joc.3915. (SCImago journal rank indicator = Q1; ERA Rank = A; Impact Factor = 2.886)

VICTORIA UNIVERSITY
MELBOURNE AUSTRALIA

3.2

PART B:

DECLARATION OF CO-AUTHORSHIP AND CO-CONTRIBUTION: PAPERS INCORPORATED IN THESIS BY PUBLICATION

This declaration is to be completed for each conjointly authored publication and placed at the beginning of the thesis chapter in which the publication appears.

Declaration by [candidate name]: Sachindra Dhanapala Arachchige

Signature:

Date: 08/07/2014

Paper Title:
Statistical downscaling of general circulation model outputs to precipitation part 1: Calibration and validation.

In the case of the above publication, the following authors contributed to the work as follows:

Name	Contribution %	Nature of Contribution
Sachindra Dhanapala Arachchige	85	Conceptual ideas, analysis, paper writing
Fuchun Huang	5	Critical comments, help with statistics
Andrew Barton	5	Critical comments, industry inputs
Chris Perera	5	Critical comments, discussion of conceptual ideas

VICTORIA UNIVERSITY
MELBOURNE AUSTRALIA

DECLARATION BY CO-AUTHORS

The undersigned certify that:

1. They meet criteria for authorship in that they have participated in the conception, execution or interpretation of at least that part of the publication in their field of expertise;
2. They take public responsibility for their part of the publication, except for the responsible author who accepts overall responsibility for the publication;
3. There are no other authors of the publication according to these criteria;
4. Potential conflicts of interest have been disclosed to **a)** granting bodies, **b)** the editor or publisher of journals or other publications, and **c)** the head of the responsible academic unit; and
5. The original data is stored at the following location(s):

Location(s):
College of Engineering and Science,Victoria University,Melbourne,Australia

and will be held for at least five years from the date indicated below:

		Date
Signature 1	[redacted]	29/07/2013
Signature 2	[redacted]	29/07/2013
Signature 3	[redacted]	16/8/2013
Signature 4	[redacted]	26/07/13

VICTORIA UNIVERSITY
MELBOURNE AUSTRALIA

PART B:

DECLARATION OF CO-AUTHORSHIP AND CO-CONTRIBUTION: PAPERS INCORPORATED IN THESIS BY PUBLICATION

This declaration is to be completed for each conjointly authored publication and placed at the beginning of the thesis chapter in which the publication appears.

Declaration by [candidate name]: Signature: Date: 08/07/2014

Sachindra Dhanapala Arachchige

Paper Title:

Statistical downscaling of general circulation model outputs to precipitation part 2: Bias-correction and future projections.

In the case of the above publication, the following authors contributed to the work as follows:

Name	Contribution %	Nature of Contribution
Sachindra Dhanapala Arachchige	85	Conceptual ideas, analysis, paper writing
Fuchun Huang	5	Critical comments, help with statistics
Andrew Barton	5	Critical comments, industry inputs
Chris Perera	5	Critical comments, discussion of conceptual ideas

VICTORIA UNIVERSITY
MELBOURNE AUSTRALIA

DECLARATION BY CO-AUTHORS

The undersigned certify that:

1. They meet criteria for authorship in that they have participated in the conception, execution or interpretation of at least that part of the publication in their field of expertise;
2. They take public responsibility for their part of the publication, except for the responsible author who accepts overall responsibility for the publication;
3. There are no other authors of the publication according to these criteria;
4. Potential conflicts of interest have been disclosed to **a)** granting bodies, **b)** the editor or publisher of journals or other publications, and **c)** the head of the responsible academic unit; and
5. The original data is stored at the following location(s):

Location(s):
College of Engineering and Science,Victoria University,Melbourne,Australia

and will be held for at least five years from the date indicated below:

		Date
Signature 1	[redacted]	29/07/2013
Signature 2	[redacted]	29/07/2013
Signature 3	[redacted]	16/8/2013
Signature 4	[redacted]	26/07/13

INTERNATIONAL JOURNAL OF CLIMATOLOGY
Int. J. Climatol. (2014)
Published online in Wiley Online Library
(wileyonlinelibrary.com) DOI: 10.1002/joc.3914

RMetS
Royal Meteorological Society

3.3 Statistical downscaling of general circulation model outputs to precipitation – part 1: calibration and validation

D. A. Sachindra,[a]* F. Huang,[a] A. Barton[a,b] and B. J. C. Perera[a]

[a] *College of Engineering and Science, Footscray Park Campus, Victoria University, Melbourne, Australia*
[b] *School of Science, Information Technology and Engineering, University of Ballarat, Victoria, Australia*

ABSTRACT: This article is the first of two companion articles providing details of the development of two separate models for statistically downscaling monthly precipitation. The first model was developed with National Centers for Environmental Prediction/National Center for Atmospheric Research (NCEP/NCAR) reanalysis outputs and the second model was built using the outputs of Hadley Centre Coupled Model version 3 GCM (HadCM3). Both models were based on the multi-linear regression (MLR) technique and were built for a precipitation station located in Victoria, Australia. Probable predictors were selected based on the past literature and hydrology. Potential predictors were selected for each calendar month separately from the NCEP/NCAR reanalysis data, considering the correlations that they maintained with observed precipitation. Based on the strength of the correlations, these potential predictors were introduced to the downscaling model until its performance in validation, in terms of Nash–Sutcliffe Efficiency (NSE), was maximized. In this manner, for each calendar month, the final sets of potential predictors and the best downscaling models with NCEP/NCAR reanalysis data were identified. The HadCM3 20th century climate experiment data corresponding to these final sets of potential predictors were used to calibrate and validate the second model. In calibration and validation, the model developed with NCEP/NCAR reanalysis data displayed NSEs of 0.74 and 0.70, respectively. The model built with HadCM3 outputs showed NSEs of 0.44 and 0.17 during the calibration and validation periods, respectively. Both models tended to under-predict high precipitation values and over-predict near-zero precipitation values, during both calibration and validation. However, this prediction characteristic was more pronounced by the model developed with HadCM3 outputs. A graphical comparison of observed precipitation, the precipitation reproduced by the two downscaling models and the raw precipitation output of HadCM3, showed that there is large bias in the precipitation output of HadCM3. This indicated the need of a bias-correction, which is detailed in the second companion article.

KEY WORDS statistical downscaling; precipitation; general circulation model

Received 10 December 2012; Revised 19 July 2013; Accepted 5 December 2013

1. Introduction

Changes in the global climate since the 20th century (notably rises in the global temperature), were mostly attributed to anthropogenic greenhouse gas (GHG) emissions, rather than natural variability in climate (Crowley, 2000). Furthermore, as stated in IPCC (2007), the rise in global and continental temperatures during the 20th century can be credibly reproduced with climate models, only if both natural and anthropogenic forces were considered. Sea level rise, reduction of snow coverage, extreme precipitation events, heat waves and rise in the frequencies of hot events and tropical cyclones are considered to be some of the impacts of climate change (Alavian *et al.*, 2009).

Over the period 1997–2008, the average precipitation over the southern part of southeast Australia declined by about 11% from the long term average, leading to a reduction in runoff of approximately 35% (Chiew *et al.*, 2010). The Australian state of Victoria suffered a severe drought (referred to as 'the Millennium drought') from 1997, until the torrential rainfalls in late 2010 and early 2011. During 1998–2007, annual average precipitation in Victoria decreased by about 13% from the long term average and the highest decline in rainfall of 28%, occurred over the autumn months. The average rainfall in autumn and early winter dropped well below the long term average, while the rainfall in summer remained as it was (Timbal and Jones, 2008). This drought forced the introduction of severe water restrictions in many regions of Victoria. The region southwest of Western Australia is experiencing a drought which has been in effect since late 1960s (Smith *et al.*, 2000). Unlike the Millennium drought, which has now ended, the drought in southwest of Western Australia has not shown any signs of ending and is considered to have experienced a step change in climate (Government of Western Australia Department of Water, 2009). The changes in the climate described in the above examples are believed to be the possible impacts

* Correspondence to: D. A. Sachindra, College of Engineering and Science, Footscray Park Campus, Victoria University, Melbourne, Victoria 8001, Australia. E-mail: sachindra.dhanapalaarachchige@live.vu.edu.au

of anthropogenic climate change and natural variability of the climate.

Precipitation is regarded as the predominant factor in determining the availability of water resources in a catchment. The food supply of humans and animals, irrigation, hydropower generation and recreational purposes are just some of the major sectors directly under the influence of precipitation. Hence, it is understood that the reliable prediction of future precipitation, especially under a changing climate, is of great importance in assessing future water availability.

General circulation models (GCMs) are considered the most reliable tools in studying climate change (Maraun *et al.*, 2010). They have proven their potential in reproducing the past observed climatic changes, considering the GHG concentrations in the atmosphere (Goyal *et al.*, 2012). However, GCMs produce their projections at relatively coarse spatial scales and they are unable to resolve sub-grid scale features such as topography, clouds and land use. Since GCMs generate outputs at coarse grid scales in the order of a few hundred kilometres, their outputs cannot be directly used in catchment scale climate impact studies, which usually need hydroclimatic data at fine spatial resolutions. The scale mismatch between the GCM outputs and the hydroclimatic information needed at the catchment level is a major obstacle in climate impact assessment studies of hydrology and water resources (Willems and Vrac, 2011).

As a solution to the scale mismatch between the GCMs outputs and the hydroclimatic information required at catchment scale, downscaling techniques have been developed. Downscaling techniques are classified into two broad classes; dynamic downscaling and statistical downscaling. In dynamic downscaling, outputs of GCMs are fed into regional climate models (RCMs) as boundary conditions to enable the prediction of the regional climate at the spatial scale of 5–50 km (Yang *et al.*, 2012). This procedure is based on the complex physics of atmospheric processes and involves high computational costs. In dynamic downscaling techniques, it is assumed that the parameterisation schemes selected for the past climate are also valid for the climate in future. In addition, dynamic downscaling techniques are highly dependant on the boundary conditions provided by the GCMs. However, dynamic downscaling could produce spatially distributed hydroclimatic predictions over the catchment of interest (Maurer and Hidalgo, 2008).

Statistical downscaling relies on the empirical relationships derived between the GCM outputs (predictors of downscaling models) and the catchment scale hydroclimatic variables (predictands of downscaling models) such as precipitation, streamflow and evaporation (Hay and Clark, 2003). Unlike dynamic downscaling, statistical downscaling does not involve complex atmospheric physics and hence is computationally less expensive (Sachindra *et al.*, 2012). In statistical downscaling, for the establishment of relationships between the GCM outputs and the catchment scale hydroclimatic variables, preferably long records of observed hydroclimatic data are required (Sachindra *et al.*, 2013). This is because a long record of observations could possibly contain the full variability of the observed climate and hence allow the downscaling models to better model the changes in the climate. However, this can limit the effective use of statistical downscaling in data scarce regions. Statistical downscaling techniques are based on the major assumption that the relationships derived between the GCM outputs and the catchment scale hydroclimatic variables for the past observed climate are equally valid for the future, under changing climate (von Storch *et al.*, 2000). Also similar to dynamic downscaling, statistical downscaling techniques are highly dependent on the outputs of the GCMs which are used as inputs to the downscaling model.

Statistical downscaling techniques are grouped under three categories; weather classification, regression models and weather generators (Wilby *et al.*, 2004). In weather classification methods, large scale weather patterns are grouped under a finite number of discrete states (Anandhi, 2010). Then the links between the catchment scale weather at certain times and the large scale weather patterns are identified. Hence, by considering the large scale weather patterns at any given time, the corresponding catchment scale weather can be deduced. The method of meteorological analogs (Timbal *et al.*, 2009, Charles *et al.*, 2013; Shao and Li, 2013) and recursive partitioning (Schnur and Lettenmaier, 1998) are examples for the weather classification techniques. Regression techniques develop either linear or nonlinear regression equations between the GCM outputs and the catchment scale hydroclimatic variables. Regression based downscaling methods are regarded as the most widely used statistical downscaling techniques (Nasseri *et al.*, 2013). This is mainly due to their simplicity and effectiveness. Chu *et al.* (2010) used multi-linear regression (MLR) for downscaling GCM outputs to daily mean temperature, pan evaporation and precipitation. Tisseuil *et al.* (2010) used artificial neural networks (ANN), generalized additive models (GAM), generalized linear models (GLM) and aggregated boosted trees (ABT) for downscaling GCM outputs to daily streamflows. Gene expression programming (GEP) and MLR techniques were employed by Hashmi *et al.* (2011) for downscaling GCM outputs to daily precipitation. The least square support vector machine regression (LS-SVM-R) was used by Anandhi *et al.* (2012) and Sachindra *et al.* (2013) for downscaling GCM outputs to daily relative humidity and monthly streamflows, respectively. Model output statistics (MOS) is a statistical downscaling technique used in post-processing the outputs of climate or weather models (Maraun *et al.*, 2010), by relating them with catchment scale observation using a linear regression technique (Marzban *et al.* 2006). This enables the reduction of systematic bias in the predictions of the model. Weather generators produce weather data for the future by scaling their parameters according to the corresponding changes characterized in the GCM outputs for the future. These techniques possess the advantage of generating

series of climatic data of any desired length of time with similar statistical properties as observations used in the weather generator (Khalili *et al.*, 2009). The combination of Markov chains and two parameter Gamma distribution is an example of a weather generator (Richardson, 1981), in which Markov chains are used to predict the occurrences of a climatic variable and the Gamma distribution is used to determine the corresponding amounts. The applications of weather generators in statistical downscaling are found in the studies of Semenov and Stratonovitch (2010), Iizumi *et al.* (2012), Khazaei *et al.* (2013).

In general, any statistical downscaling model is calibrated and validated (developed) using the reanalysis outputs (e.g. NCEP/NCAR) and observations, corresponding to the past climate. For producing the future projections, outputs of a GCM pertaining to a certain GHG emission scenario are introduced to this downscaling model. This procedure does not provide a smooth transition from the model development phase (calibration and validation) to the future projection phase, as the former and latter steps are performed with the outputs of two different sources which have different levels of accuracy. In other words, the inputs used in the development phase and the future projection phase of a conventional downscaling model are not homogeneous. As a solution to this issue, a downscaling model calibrated and validated with GCM outputs can be used in producing future projections with the outputs of the same GCM, pertaining to a future GHG emission scenario. Since the outputs of the same GCM are used for the model development and future projections, there is homogeneity in the modelling process. However, in the published literature there was no evidence of past studies which attempted the use of a downscaling model developed with GCM outputs.

This article, which is the first of a series of two companion papers, discusses the calibration and validation of two statistical downscaling models based on MLR) technique. The two statistical downscaling models were developed separately, for downscaling monthly outputs of (1) National Centers for Environmental Prediction/National Center for Atmospheric Research (NCEP/NCAR) reanalysis and (2) Hadley Centre Coupled Model version 3 GCM (HadCM3), to monthly precipitation. As the case study, a precipitation station located within the Grampians water supply system in north-western Victoria in Australia was selected. A performance comparison between two downscaling models for the calibration and validation phases was also performed.

Downscaling GCM outputs to precipitation at monthly temporal scale does not permit capturing the variations of precipitation within a month (e.g. wet and dry days, precipitation intensity and extremes of precipitation). However, still monthly precipitation projections produced using downscaling models could aid in the management of water resources which include operations such as water allocation for crops, domestic and industrial needs and also environmental flows, especially in the planning stage of a water resources project.

The remainder of this article was structured as follows. The study area and the data used in the study were briefly described in Section 2, followed by the generic methodology in Section 3. Thereafter, in Section 4, the application of this methodology to the precipitation station considered was provided along with a discussion on the model results. A summary on the model development process and results, along with the conclusions drawn from the study were provided in Section 5. In the second article the bias-correction and future precipitation projections are detailed.

2. Study area and data

The Grampians water supply system in north-western Victoria is a large multi reservoir system owned and operated by the Grampians Wimmera Mallee Water (GWMWater) Cooperation (www.gwmwater.org.au). For this study, a precipitation station at Halls Gap post office (Lat. -37.14°, Lon. 142.52°, elevation from mean sea level about 236 m), located in the Grampians system was selected. At this station, the annual average precipitation over the period 1950–2010 was about 950 mm. In this region, winter and summer are the wettest and the driest seasons, respectively. Observed daily precipitation record from 1950 to 2010 was obtained from the SILO database (http://www.longpaddock.qld.gov.au/silo/) of Queensland Climate Change Centre of Excellence and aggregated to monthly precipitation, for the calibration and validation of downscaling models. In that observed daily precipitation record 31.2% of the data were missing and those missing data were filled by the Queensland Climate Change Centre of Excellence in the SILO database using the spatial interpolation method detailed in Jeffrey *et al.* (2001). In order to provide the inputs for the calibration and validation of the first downscaling model, NCEP/NCAR monthly reanalysis data for the period 1950–2010 were downloaded from http://www.esrl.noaa.gov/psd/. Monthly precipitation outputs produced by the HadCM 3 GCM for the 20th century climate experiment were extracted from the programme for climate model diagnosis and inter-comparison (PCMDI) (https://esgcet.llnl.gov:8443/index.jsp) for the period 1950–1999, for developing the second downscaling model.

3. Generic methodology

The first step of the downscaling exercise was to define an adequately large atmospheric domain above the precipitation station. It was considered that an adequately large atmospheric domain would enable sufficient atmospheric influence on the climate at the points of interest (e.g. a precipitation station) within the catchment.

A set of probable predictor variables was identified based on a review of past literature on downscaling GCM outputs to precipitation and hydrology. These probable variables are the most likely candidates to influence precipitation at the catchment scale. In selecting

predictors in the past studies (e.g. Anandhi *et al.*, 2008; Timbal *et al.*, 2009; Kannan and Ghosh, 2013), factors such as (1) availability in GCM and reanalysis data sets, (2) reliable simulation by GCMs (3) usage in similar studies, (4) fundamentals of hydrology, (4) correlations with the predictand, etc. were considered. Potential predictors are subsets of the set of probable predictor variables. These sets of potential predictors are the most influential variables on precipitation at the stations considered. The predictor-predictand relationships vary from season to season and also from (geographic) region to region, following the spatiotemporal variations of the atmospheric circulations (Karl *et al.*, 1990). Therefore the sets of potential predictors also vary spatiotemporally. In this study, in order to better model the precipitation, considering the seasonal variations of the atmospheric circulations, potential predictors were identified for each calendar month, and downscaling models were developed separately for each of the 12 calendar months. Sachindra *et al.* (2013) found that both Least Square SVM (a complex nonlinear downscaling technique) and MLR (a relatively simple linear downscaling technique) have comparable capabilities in directly downscaling GCM outputs to catchment scale streamflows. Hence, in this study MLR technique was used to downscale GCM outputs to catchment scale precipitation.

Following the methodology proposed by Sachindra *et al.* (2013), the probable predictors obtained from a reanalysis database were split into 20 year time slices, in the chronological order. The Pearson correlation coefficients (Pearson, 1895) between these probable predictors and the observed monthly precipitation were calculated for each 20 year time slice and the whole period, at all grid points in the atmospheric domain, for each calendar month. Thereafter, the probable variables which exhibited the best statistically significant correlations (at 95% confidence level, $p = 0.05$) with observed precipitation, over all 20 year time slices and the whole period consistently, were extracted as the potential predictors. The consistently correlated variables refer to the predictors which maintained correlations without any sign variations (e.g. positive to negative or vice versa) and large variation in magnitudes over the time slices and the whole period of the study. Once the selection of potential predictors was completed, two downscaling models were developed (calibrated/validated) separately, the first using the reanalysis outputs and the second with the corresponding 20th century climate experiment outputs of the GCM. The development of two separate downscaling models, one with reanalysis outputs and the other with GCM outputs, enabled the determination of how accurately the model developed with GCM outputs could reproduce the past precipitation observations, in comparison to its counterpart model. Furthermore, this process allows for understanding the potential of the downscaling model developed with GCM outputs, for its use in producing the precipitation projections into future. Reanalysis data are accepted to be more accurate than GCM outputs, owing to the rigorous quality control and corrective measures to which they are subjected to (e.g. NCEP/NCAR reanalysis – Kalnay *et al.*, 1996). Since the reanalysis outputs are more accurate than the GCM outputs, the downscaling model built with reanalysis outputs should better perform in the calibration and validation periods. If the downscaling model developed with GCM outputs was capable of reproducing the past precipitation observations adequately, it enables the use of this same model for the future projections of precipitation. In this case, a homogeneous set of data produced by the same GCM is used for the calibration, validation and future projection. Therefore, this can be regarded as a better option, than using the GCM outputs pertaining to future on the downscaling model developed with reanalysis outputs to project the precipitation at the station of interest into future.

For the calibration phase of the downscaling model developed with reanalysis data, the first two thirds of these reanalysis (corresponding to potential predictors) and observed precipitation data (predictand) were used, while the rest of the data were used for the model validation. The potential predictors for both calibration and validation were standardized with the means and the standard deviations of reanalysis data corresponding to the calibration phase (Sachindra *et al.*, 2013). In model calibration, initially, the three potential predictors which have shown the best correlations with precipitation over the whole period of the study were introduced to the downscaling model. The parameters (coefficients and constants in the MLR equations) of the downscaling model were optimized in calibration, by minimizing the sum of the squares of the errors. Then the model validation was performed with the calibrated model. The performance of the model during calibration and validation in reproducing the observed precipitation was assessed using the Nash–Sutcliffe efficiency (NSE; Nash and Sutcliffe, 1970). Thereafter, the next potential predictors which showed the best correlation with precipitation were introduced to the previously added predictors of the downscaling model, one at a time. This process of stepwise addition of potential predictors was practised until the model performance in terms of NSE in validation reaches a maximum. This process allowed finding the best set of potential predictors and the best downscaling model for a calendar month. The downscaling model calibration and validation were performed for each calendar month separately.

If the stepwise development was not employed in the development of the model based on the reanalysis outputs, all potential predictors could have been introduced into the downscaling model at once. This could have introduced data redundancy errors due to the inter-dependency or cross-correlations between the predictors leading, to over-fitting in calibration and under-fitting in validation. The stepwise model development and selection of the model which showed the best performance in validation guaranteed the avoidance of selection of models which showed over-fitting in calibration and under-fitting in validation.

As mentioned earlier in this article, the second downscaling model (with sub-models for each calendar month) was developed (calibrated/validated) with the GCM outputs corresponding to the climate of the 20th century. In the calibration and validation of this downscaling model, observed precipitation at the station of interest was used as the predictand. The same calibration period used for first model was also used for this model. The rest of the GCM data were used for the validation. Inputs for both the calibration and validation phases of this model were standardized with the means and the standard deviations of the GCM outputs pertaining to the calibration period. The best potential predictors identified in the calibration and validation processes of the downscaling model developed with reanalysis outputs were also used in the development of this model, assuming the validity of these potential predictors for both downscaling models. The calibration of the second model was performed for each calendar month by introducing the 20th century climate outputs of the GCM pertaining to the best potential predictors. The optimum parameters of the MLR based downscaling models were determined by minimizing the sum of the squared errors between the model predicted precipitation and the observed precipitation. These MLR models with the same parameters determined in the calibration phase were used in the validation. Unlike in the development of the model which was driven with reanalysis outputs, stepwise development process was not adopted in building the model driven with GCM outputs, as the best potential variables were already identified.

Graphical and numerical comparisons between the observed precipitation and precipitation outputs of the above described two statistical downscaling models were performed. Both graphical and numerical assessments were employed, as numerical assessments alone may not be robust enough in the evaluation of model performances. The graphical comparison of precipitation included the time series and scatter plots of the model reproduced precipitation against observations. The numerical assessment of the two downscaling models was done by statistical measures such as average, standard deviation, coefficient of variation, NSE, seasonally adjusted NSE (SANS) (Wang, 2006; Sachindra *et al.*, 2013) and the coefficient of determination (R^2). Note that all MLR based downscaling models discussed in this article were developed using the statistics toolbox in MATLAB (Version - R2008b).

4. Application

The generic methodology described in Section 3 was applied to the precipitation station at the Halls Gap post office in the operational area of GWMWater, Victoria, Australia.

4.1. Atmospheric domain for downscaling

There are no clear guidelines on the selection of the optimum size of the atmospheric domain for a statistical downscaling study. Najafi *et al.* (2011) successfully used an atmospheric domain with 7×4 grid points in the longitudinal and latitudinal directions, respectively at a spatial resolution of 2.5° in both directions, for the statistical downscaling of outputs of CGCM3 to monthly precipitation. Their study demonstrated that the atmospheric domain does not necessarily have to be a square in shape. However, if the atmospheric domain is too rectangular in shape, the influences of large scale atmospheric circulations on the point of interest in the catchment are more considered on the wider sides of the domain, and the influences coming from the narrower sides are less considered or neglected. Hence, such domain shape should be avoided in statistical downscaling. A larger atmospheric domain increases the computational cost and time involved in the investigation. However, a larger domain aids in identifying influences of large scale atmospheric circulations over a wider area. When the atmospheric domain is too small, it may not be able to adequately capture the atmospheric circulations responsible for the hydroclimatology in the catchment. Therefore, the atmospheric domain which is an important component of any statistical downscaling study should be of adequate size and of an appropriate shape. In general a domain size of 6×6 grid points at a spatial resolution of 2.5° in both longitudinal and latitudinal directions is a regarded as an adequate size (Tripathi *et al.*, 2006). An atmospheric domain with spatial dimensions of 7×6 grid points at a spatial resolution of 2.5° in both longitudinal and latitudinal directions was selected for the downscaling study described in this article. The size of this atmospheric domain was determined considering its ability to represent the large scale atmospheric phenomena which influence the precipitation at the point of interest and also the computational cost. The same atmospheric domain over the same study area was successfully used by Sachindra *et al.* (2013) for statistically downscaling GCM outputs to catchment streamflows. The spatial resolution of this atmospheric domain was maintained at 2.5° in both longitudinal and latitudinal directions, making it compliant with the spatial resolution of the NCEP/NCAR reanalysis outputs. The atmospheric domain used in this study is shown in Figure 1. The shaded region in Figure 1 depicts the operational area of GWMWater, and the precipitation station considered in this study is located in its south most region.

4.2. Selection of probable and potential predictors for downscaling

A pool of probable predictors was selected based on hydrology and past studies by Anandhi *et al.* (2008) and Timbal *et al.* (2009), on downscaling GCM outputs to precipitation. In the downscaling study by Timbal *et al.* (2009), predictor variables influential on the generation of precipitation, over the south and south eastern Australia (this includes the present study area) were identified. The probable predictor pool selected for the study described in this article consisted of geopotential heights at 200 hPa,

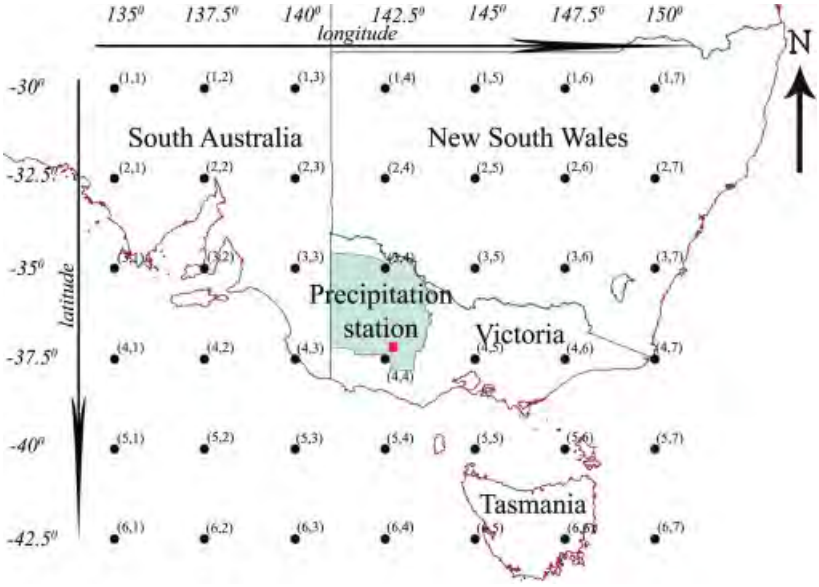

Figure 1. Atmospheric domain for downscaling.

500 hPa, 700 hPa, 850 hPa and 1000 hPa pressure levels; relative humidity at 500 hPa, 700 hPa, 850 hPa and 1000 hPa pressure levels; specific humidity at 2 m height, 500 hPa, 850 hPa and 1000 hPa pressure levels; air temperatures at 2 m height, 500 hPa, 850 hPa and 1000 hPa pressure levels; surface skin temperature, surface pressure, mean sea level pressure, surface precipitation rate and zonal and meridional wind speeds at 850hpa pressure level. These probable predictors were common for all calendar months. The monthly data for these 23 probable predictors for the 42 grid points shown in Figure 1 were extracted from the NCEP/NCAR reanalysis data archive at http://www.esrl.noaa.gov/psd/.

The probable predictors and the observed monthly precipitation totals from 1950 to 2010 were split into three 20 year time slices; 1950–1969, 1970–1989 and 1990–2010. The last time slice was 21 years in length. The Pearson correlation coefficients between the probable predictors and the observed monthly precipitation were calculated for all three time slices and the whole period (1950–2010), at each grid point in the atmospheric domain (see Figure 1). The probable predictors which showed good statistically significant correlations (at 95% confidence level, $p = 0.05$) consistently over the three time slices and the whole period were selected as the potential predictors (Sachindra *et al.*, 2013). This process was repeated for all 12 calendar months, yielding 12 sets of potential predictors.

The El Niño-Southern Oscillation (ENSO) and the Indian Ocean Dipole (IOD) are regarded as two large scale atmospheric phenomena influential on the climate of Victoria, Australia. A correlation analysis performed over the period 1950–2010 between the Southern Oscillation Index (SOI) which is representative of ENSO and observed precipitation at the Halls Gap post office indicated that these correlations vary between 0.03 (March) and 0.33 (October). Similarly, the correlations between the Dipole Mode Index (DMI) which is representative of IOD and observed precipitation ranged between −0.01 (February) and −0.46 (August) during the period 1958–2010. Hence, it was realized that the influences of these large scale atmospheric phenomena on the observed precipitation at the Halls Gap post office are weak in nature. Therefore it was understood that the inclusion of such indices in the inputs to the downscaling models will not lead to any improvement to the precipitation predictions. Furthermore, Chiew *et al.* (1998) detailed the influences of ENSO on the rainfall, drought and streamflows in Australia, using the SOI and sea surface temperature (SST), and concluded that, the correlations between these ENSO indicators and hydroclimatic variables are not sufficiently strong for a consistent prediction.

4.3. MLR downscaling model calibration and validation

4.3.1. Model calibration and validation with NCEP/NCAR data

The potential predictors selected from the probable pool were separated into two chronological groups; 1950 to 1989 and 1990 to 2010, the former for model calibration and the latter for model validation. The potential predictors were standardized for both calibration and validation periods using the means and the standard deviations pertaining to the period 1950 to 1989 (calibration period). The standardized potential variables were ranked based on the magnitude of their correlations with the observed monthly precipitation, over the whole period of the study (1950–2010). Then these potential variables were introduced to the MLR based downscaling model as described in Section 3. In the manner described in Section 3, for

each calendar month the best set of potential predictors and the best MLR based downscaling model were selected. Table 1 shows the final (or the best) set of potential predictors used in the downscaling model developed with NCEP/NCAR reanalysis outputs for the month of January. Also this table contains the correlations between the observed precipitation and the final set of potential predictors, during the three 20 year time slices and the whole period of the study.

Table 2 provides the final sets of potential predictors used in the downscaling models in each calendar month. The final sets of potential predictors used in the downscaling models consisted of: surface precipitation rate; specific humidity, relative humidity and geopotential heights at various pressure levels; mean sea level pressure; surface pressure and zonal and meridional wind speeds at 850 hPa pressure level. However, surface precipitation rate was identified as the most influential potential predictor on precipitation, appearing in the final sets of potential predictors for all calendar months except July. Surface precipitation rate produced by GCMs is a precipitation flux (precipitation per unit time across unit area at earth surface) which is analogous to precipitation at a point over a specific time period (e.g. daily or monthly precipitation). Therefore the strong influence of surface precipitation rate on monthly precipitation was justified. The highest correlations between the NCEP/NCAR precipitation rate and the observed precipitation over the period 1950–2010 within each calendar month were June (0.82), August (0.82), October (0.79), September (0.77), December (0.74), May (0.71), January (0.69), April (0.64), February (0.61), March (0.61) and November (0.48). Precipitation outputs of GCMs have been also used in the past downscaling studies. Timbal *et al.* (2009) used precipitation rate in downscaling daily precipitation and Tisseuil *et al.* (2010) used precipitation rate for downscaling daily streamflows. Maraun *et al.* (2013) stated that despite the errors, the precipitation output of a GCM can still contain useful information about the observed precipitation. Hence it was realized that precipitation output of a GCM can be used as an input to a downscaling model.

Specific humidity (mass of water vapour per unit mass of air), and relative humidity (ratio of actual water vapour pressure of the air to the saturation vapour pressure) at various pressure levels are indicators of the atmospheric water vapour content which leads to the formation of clouds (Peixoto and Oort, 1996). Humidity variables (relative or specific humidity) which are indictors of the atmospheric water vapour content were potential predictors in 7 (February, March, May, September, October, November and December) of the 12 calendar months. According to Nazemosadat and Cordery (1997), geopotential heights are influential on the generation of precipitation, as they are representative of large scale atmospheric pressure variations such as the El Niño Southern Oscillation (ENSO). Zonal and meridional wind fields are influential on the evaporation from open surface water bodies and they govern the movement of rain bearing clouds (Bureau of Meteorology, 2010), and hence it was suitable to include wind fields in the final sets of potential predictors. It is noteworthy to mention that, according to Table 2, except in August and November, grid point {4,4} found to be a dominant location for the final sets of potential predictors. The grid point {4,4} is the closest grid point to the precipitation station considered in this study.

In general, humidity variables and precipitation rate are more capable of explaining the precipitation process (refer to Table 2). However as shown in Table 2, in the month of July, the set of potential predictors used in the downscaling models contained only the wind speeds and the geopotential heights at 850 hPa. It was realized that these variables are still able to explain the precipitation process with a good degree of accuracy, as the downscaling model developed for July using the NCEP/NCAR reanalysis outputs displayed NSEs of 0.58 and 0.50 in the calibration and validation phases, respectively. Furthermore, as these potential variables are selected based on the magnitude and also the consistency of correlations with observed precipitation over time, it is argued that the final sets of potential predictors used in the downscaling models are able to characterize the changes in precipitation at the point of interest, also in the future.

In Table 2, it could be found that the majority of the potential predictors in the final sets were selected from the grid points surrounding the precipitation station of interest [(3,3), (3,4), (3,5), (4,3), (4,4), (4,5), (5,3), (5,4) and (5,5)]. However, some potential predictors in the final sets were selected from the distant grid points of the domain as the precipitation at the station of interest is not only influenced by the atmosphere in close proximity to the station but also by the atmospheric processes that occur far away. The best grid locations of the potential predictors provided in Table 2 were selected not only based on the strength of the correlation between the potential predictors and observed precipitation, but also considering the consistency of the correlation over three time slices and the whole period of the study. Therefore it was assumed that the best grid locations of the final sets of potential predictors used in this study will remain the same in future.

4.3.2. Model calibration and validation with HadCM3 20th century climate experiment data

The 20th century climate experiment data of HadCM3 GCM were obtained for the period 1950–1999, corresponding to the final sets of potential predictors shown in Table 2. HadCM3 model has been forced with both natural and anthropogenic forcings to reproduce the climate of the 20th century (Knight, 2003). As the natural forcings; SST and sea-ice anomalies, variations in the total solar irradiance and stratospheric volcanic aerosols, etc. have been used in HadCM3. As anthropogenic forcings; GHG concentrations in the atmosphere, changes in tropospheric and stratospheric ozone, the effects of atmospheric sulphate aerosols and

Table 1. Final set of potential predictors used in the January downscaling model and their correlations with observed precipitation in each time slice and whole period.

Rank of variable	Potential variables for January	Grid location	Time slice	Correlation with precipitation
1	Surface precipitation rate	4,4	1950–1969	0.910
			1970–1989	0.581
			1990–2010	0.651
			1950–2010	**0.693**
2	1000 hPa specific humidity	3,3	1950–1969	0.532
			1970–1989	0.532
			1990–2010	0.603
			1950–2010	**0.550**
3	850 hPa meridional wind	3,6	1950–1969	−0.466
			1970–1989	−0.698
			1990–2010	−0.468
			1950–2010	**−0.548**
4	850 hPa meridional wind	3,5	1950–1969	−0.400
			1970–1989	−0.724
			1990–2010	−0.522
			1950–2010	**−0.544**
5	1000 hPa specific humidity	3,4	1950–1969	0.487
			1970–1989	0.553
			1990–2010	0.516
			1950–2010	**0.515**
6	850 hPa meridional wind	2,6	1950–1969	−0.420
			1970–1989	−0.585
			1990–2010	−0.506
			1950–2010	**−0.513**
7	2 m specific humidity	3,3	1950–1969	0.430
			1970–1989	0.550
			1990–2010	0.540
			1950–2010	**0.510**
8	Surface precipitation rate	3,3	1950–1969	0.608
			1970–1989	0.413
			1990–2010	0.523
			1950–2010	**0.498**
9	1000 hPa specific humidity	4,4	1950–1969	0.595
			1970–1989	0.508
			1990–2010	0.412
			1950–2010	**0.494**
10	850 hPa relative humidity	1,2	1950–1969	0.438
			1970–1989	0.475
			1990–2010	0.596
			1950–2010	**0.483**
11	2 m specific humidity	3,4	1950–1969	0.448
			1970–1989	0.533
			1990–2010	0.482
			1950–2010	**0.482**

Bold values refer to calibration and validation periods of the study.

changes in land surface characteristics have been used in HadCM3. The 20th century climate experiment data of HadCM3 were split into two groups; (a) 1950–1989 for model calibration and (b) 1990–1999 for the model validation. HadCM3 data for both the calibration and validation phases were standardized with the means and the standard deviations of HadCM3 data corresponding to 1950–1989 period. In calibration, the standardized sets of data pertaining to the best potential predictors shown in Table 2 were introduced to the MLR based downscaling model. During calibration, the optimum values for the model parameters were determined by minimizing the sum of squared errors between the model predicted and observed precipitation values. In validation, the HadCM3 data for the 1990–1999 period were introduced to the calibrated MLR models. The same procedure was repeated for all calendar months. Unlike in the calibration and validation of the downscaling

Table 2. Final sets of potential predictors for each calendar month.

Month	Potential variables used in the model with grid locations
January	Surface precipitation rate {(3,3),(4,4)} 1000 hPa specific humidity {(3,3),(3,4),(4,4)} 850 hPa meridional wind {(2,6),(3,5),(3,6)} 850 hPa relative humidity {(1,2)} 2 m specific humidity {(3,3),(3,4)}
February	Surface precipitation rate {(3,4),(4,4),(4,5)}
March	Surface precipitation rate {(3,3),(3,4),(3,5),(4,3),(4,4),(4,5),(4,6)}
April	850 hPa relative humidity {(4,3),(4,4)} Surface precipitation rate {(4,3)}
May	Surface precipitation rate {(4,4),(5,5)} 850 hPa geopotential height {(4,3)}
June	Surface precipitation rate {(3,2),(3,3),(4,2),(4,3),(4,4),(4,5)} Mean sea level pressure {(4,3),(5,3)} 850 hPa zonal wind {(2,4)} Surface pressure{(4,3),(5,3),(5,4)}
July	850 hPa zonal wind {(1,3),(1,4)} 850 hPa geopotential height {(4,3),(4,4),(4,5)}
August	Surface precipitation rate {(4,3),(5,4),(5,5)}
September	Surface precipitation rate {(2,1),(2,2),(3,2),(3,3),(3,5),(4,2),(4,3),(4,4),(4,5)} 850 hPa relative humidity {(3,3)} 700 hPa relative humidity {(3,4)}
October	Surface precipitation rate {(3,2),(4,2),(4,3),(4,4)} 850 hPa relative humidity {(4,3)} 700 hPa geopotential height {(1,1)}
November	850 hPa relative humidity {(3,2),(3,3)} Surface precipitation rate {(4,3),(4,5)}
December	Surface precipitation rate {(2,1),(3,2),(4,3),(4,4),(5,5)} 850 hPa relative humidity {(3,2)}

hPa, atmospheric pressure in hectopascal; the locations are given within brackets (see Figure 1).

model which was developed with NCEP/NCAR reanalysis outputs, the stepwise development procedure was not adopted in these models. A correlation coefficient analysis performed between the 20th century climate experiment outputs of HadCM3 and NCEP/NCAR reanalysis outputs over the period 1950–1999, revealed that these correlations are quite weak (e.g. 0.2–0.4). Hence it was realized that HadCM3 outputs pertaining to the 20th century climate experiment contain large bias. Therefore it was understood that whether the final sets of potential predictors are selected using a stepwise procedure or not, they will not change the performance of the model developed with HadCM3 outputs. It was assumed that final sets of potential predictors identified in the development of the model driven with NCEP/NCAR outputs are also applicable for this model. The difference between the statistical downscaling models built with the HadCM3 20th century experiment data ($Model_{(HadCM3)}$) and the models built with the NCEP/NCAR reanalysis data ($Model_{(NCEP/NCAR)}$) was that these two models had different optimum values for their parameters (coefficients and constants in MLR equations).

4.3.3. Calibration and validation results of the downscaling models

Figure 2 shows the time series of monthly observed precipitation and monthly precipitation reproduced by the downscaling model developed with NCEP/NCAR data, for the period 1950–2010. According to Figure 2, the monthly precipitation reproduced by this downscaling model, was in close agreement with the observed precipitation during both calibration and validation periods. Although the model validation was performed in a relatively dry period which included the Millennium drought (1997–2010), this downscaling model has been able to capture the monthly precipitation pattern and the magnitude with good accuracy.

Figure 3 shows the scatter plots of monthly observed precipitation and precipitation reproduced by the downscaling model developed with NCEP/NCAR data, for the calibration (1950–1989) and validation (1990–2010) phases. As seen in Figure 3, during both the calibration and validation periods, near zero monthly precipitation values were over predicted and relatively large precipitation values were under-predicted. However, these scatter plots of the model predictions against the observations further confirmed that, the prediction capabilities of the model developed with NCEP/NCAR data in validation are very much comparable with those during calibration.

Figure 4 illustrates the time series of monthly observed precipitation and monthly precipitation reproduced by the downscaling model built with HadCM3 data, for the period 1950–1999. It was seen that this model was not able to satisfactorily reproduce the high precipitation values. Furthermore, the agreement between the observed and model reproduced precipitation was much less compared to that of the model developed with NCEP/NCAR reanalysis outputs. However, the model developed with HadCM3 outputs properly captured the pattern of the observed precipitation as shown in Figure 4. It should be noted that the validation phase of the model developed with HadCM3 data was confined to the period 1990–1999, due to the unavailability of data beyond year 1999, under the 20th century climate experiment.

Figure 5 represents the scatter plots for the calibration (1950–1989) and validation (1990–1999) phases of the downscaling model developed with HadCM3 data. It was seen that in the calibration and validation phases, high precipitation values were largely under-predicted. During both phases, the model displayed a clear trend of over-predicting the majority of low precipitation values. However, these characteristics were also seen in the predictions of the model developed with NCER/NCAR data, but with less intensity.

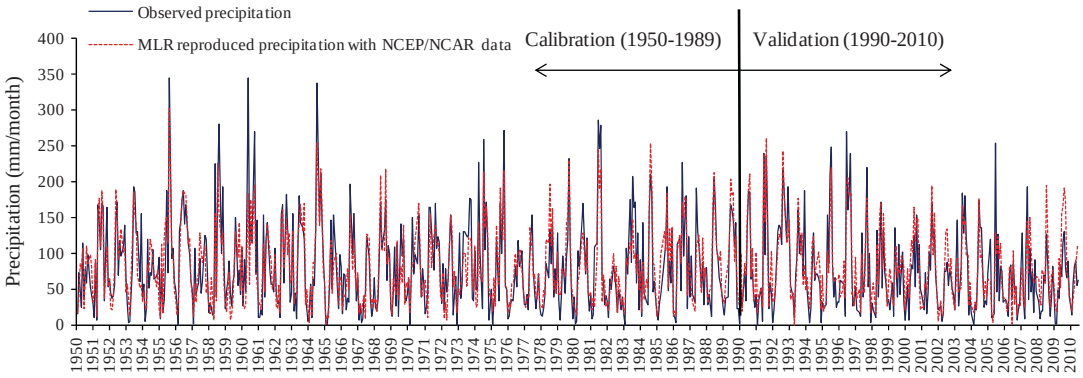

Figure 2. Observed and Model$_{(NCEP/NCAR)}$ reproduced monthly precipitation (1950 to 2010).

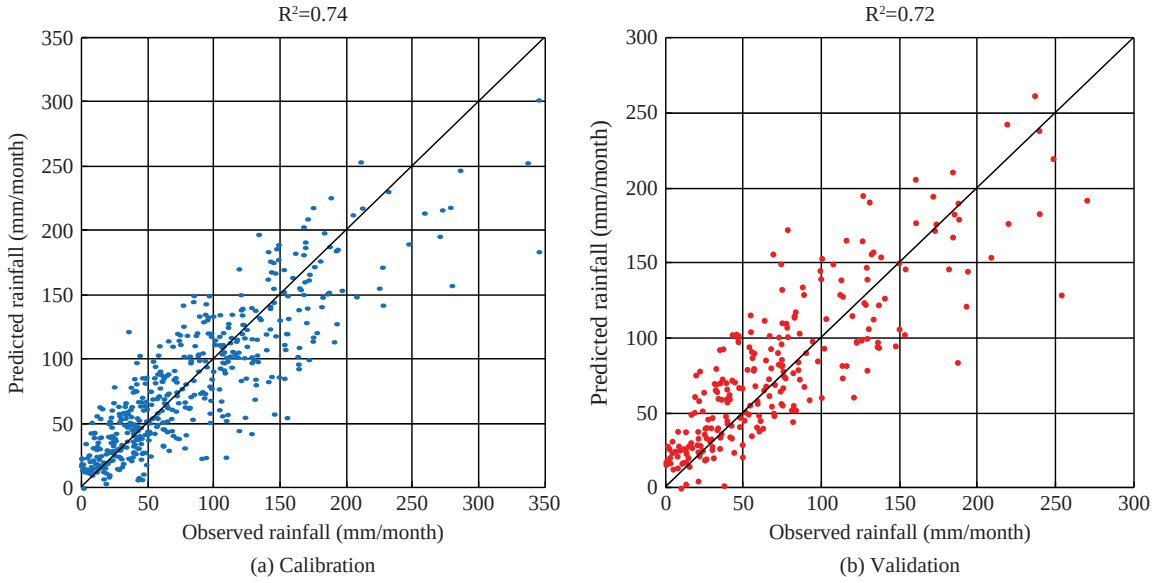

Figure 3. Scatter plots of observed and Model$_{(NCEP/NCAR)}$ reproduced monthly precipitation for calibration (1950–1989) and validation (1990–2010).

Statistical downscaling models in general fail to capture the full range of the variance of a predictand such as precipitation (Wilby *et al.*, 2004). This is because, in general the variance in the observations of precipitation is much greater than the variance in the large scale atmospheric variables obtained from the GCM or the reanalysis data. When the downscaling model is run with the GCM or the reanalysis data it tends to explain the mid range of the variance of the observed precipitation better than the low and high extremes. Therefore statistical downscaling models in general tend to reproduce the average of the precipitation better than the low and high extremes. In other words, this results in an under-estimation of large precipitation values and over-estimations of near zero precipitation values. Tripathi *et al.* (2006) also commented that even a downscaling model based on support vector machine technique (complex nonlinear regression technique) fails to properly reproduce the extremes of precipitation though it captures the average well.

The performances of the two downscaling models, during the calibration and validation phases were numerically assessed by comparing the mean, the standard deviation and the coefficient of variation of the model predictions with those of observations, and these results are shown in Table 3. It can be seen that both downscaling models developed with NCEP/NCAR and HadCM3 outputs reproduced the observed averages of the precipitation with good accuracy, in both calibration and validation phases. This finding was quite consistent with that of Sachindra *et al.* (2013), in which MLR and LS-SVM techniques were employed for downscaling NCEP/NCAR outputs to streamflows. However, in this study, neither of the two models properly captured the standard deviation and the coefficient of variation of the observed precipitation, during both the calibration and validation phases. This characteristic was more noticeable in the outputs of the downscaling model developed with HadCM3 data. It indicated that, in particular, the model developed with HadCM3 data could not reproduce the entire variance

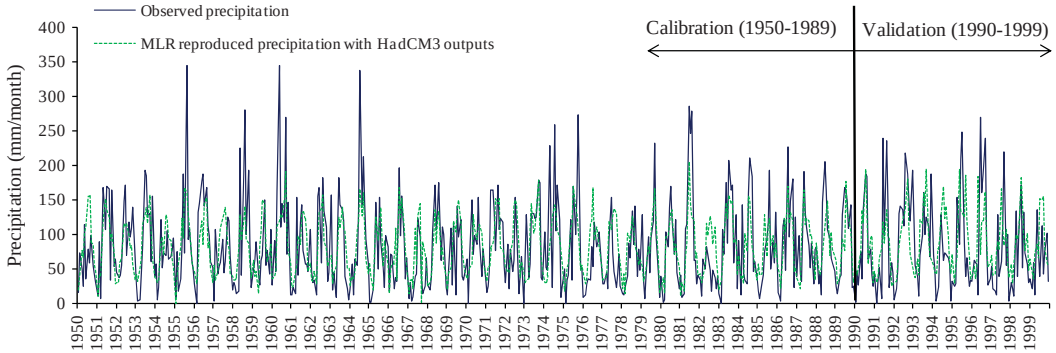

Figure 4. Observed and Model$_{(HadCM3)}$ reproduced monthly precipitation (1950 to 1999).

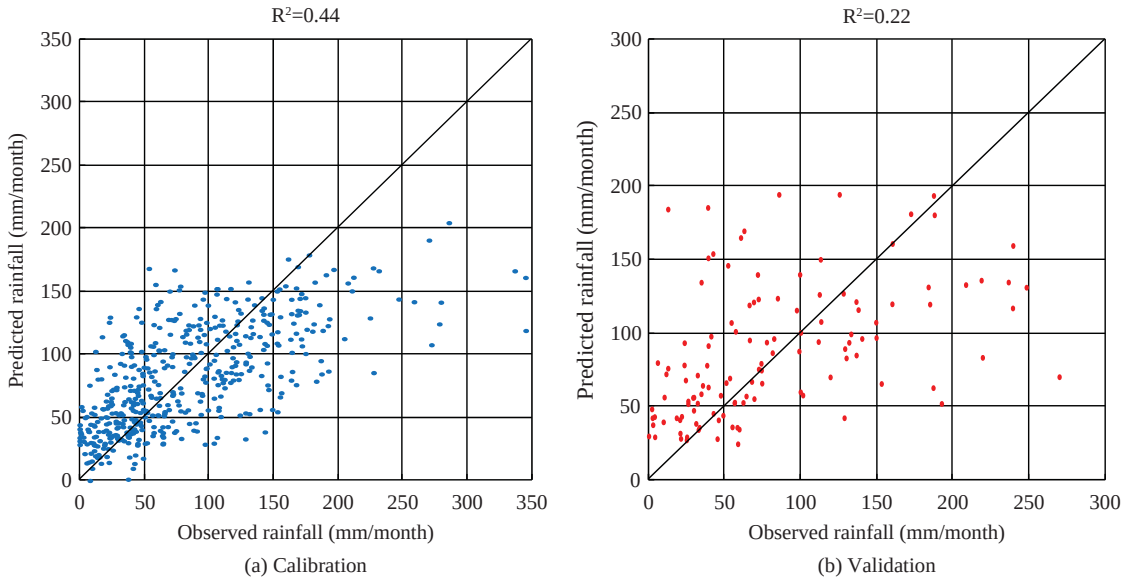

Figure 5. Scatter plots of observed and Model$_{(HadCM3)}$ reproduced monthly precipitation for calibration (1950–1989) and validation (1990–1999).

of the observed precipitation. In Figure 4, the same characteristic was seen in the time series plots. This characteristic was seen with less severity in the outputs of the model developed with NCEP/NCAR reanalysis data.

The model performances in calibration and validation were further quantified with the NSE, the SANS and the coefficient of determination (R^2). The SANS considers the seasonal means of precipitation in measuring the model performances, unlike the original NSE, which considers only the mean of precipitation for the whole period. During calibration, the statistical downscaling model developed with NCEP/NCAR reanalysis data displayed NSE, SANS and R^2 of 0.74, 0.66 and 0.74, respectively. However, for the same period, the downscaling model developed with HadCM3 outputs, produced NSE, SANS and R^2 of 0.44, 0.26 and 0.44, respectively. In the validation phase, the model developed with NCEP/NCAR outputs produced NSE, SANS and R^2 of 0.70, 0.61 and 0.72. During the validation period, the model developed with HadCM3 outputs, produced NSE, SANS and R^2 of 0.17, −0.20 and 0.22, respectively. These findings indicated that both downscaling models have performed relatively better during the calibration period than in the validation period. However, it was seen that the downscaling model developed with NCEP/NCAR data performed well in the calibration and validation phases, compared to its counterpart model which was built with HadCM3 outputs. This statement was further supported by the findings of scatter plots shown in Figures 3 and 5.

Figure 6 depicts the agreement between the precipitation reproduced by the model developed with NCEP/NCAR outputs and the observed precipitation, during the calibration (1950–1989) and validation (1990–2010) periods, on a seasonal basis. As shown in Figure 6, it was determined that this model demonstrates good capabilities in reproducing the observations in calibration and validation, in all four seasons, despite the tendencies of under-predicting high precipitation values and over-predicting near zero precipitation values which were evident in all four seasons. The four seasons are defined as summer (December–February), autumn (March–May), winter (June–August) and spring (September–November).

Table 3. Performances of downscaling models in calibration and validation.

Statistic	Calibration (1950–1989)			Validation (1990–2010)/*(1990–1999)*[a]			
	Observations	$\text{Model}_{(\text{NCEP/NCAR})}$	$\text{Model}_{(\text{HadCM3})}$	Observations		$\text{Model}_{(\text{NCEP/NCAR})}$	$\text{Model}_{(\text{HadCM3})}$
				1990–2010	1990–1999		
Avg	81.8	82.0	81.7	73.3	***81.8***	81.0	***87.6***
Std	61.7	53.2	41.1	56.9	***64.3***	51.9	***44.5***
C_v	0.75	0.65	0.50	0.78	***0.79***	0.64	***0.51***
NSE		0.74	0.44			0.70	***0.17***
SANS		0.66	0.26			0.61	***−0.20***
R^2		0.74	0.44			0.72	***0.22***

Avg, average of monthly precipitation in mm; C_v, coefficient of variation; NSE, Nash–Sutcliffe efficiency; R^2, coefficient of determination; Std, standard deviation of monthly precipitation in mm; SANS, Seasonally Adjusted Nash–Sutcliffe efficiency. [a]Bold italicized values in the table refer to period 1990–1999.

Figure 7 displays the seasonal scatter plots for the calibration (1950–1989) and validation (1990–1999) periods of the model developed with HadCM3 outputs. Large under-predictions of precipitation were seen in all four seasons during both the calibration and validation phases of this model. During all four seasons in the validation period, a relatively poor agreement between the observed and model reproduced precipitation was seen. This characteristic was more intense in autumn, winter and spring than in summer.

Table 4 shows the seasonal statistics of the observed precipitation and the precipitation reproduced by the models developed with NCEP/NCAR reanalysis and HadCM3 data, for the calibration and validation periods. In the calibration phase, during all four seasons, averages of the observed precipitation were near perfectly reproduced by both downscaling models. In the validation phase, although not as good as in calibration, both models were capable in reproducing the averages of observed precipitation in all four seasons with some under and over-predictions. During all four seasons in the validation period, both downscaling models tended to over-predict the average of the observed precipitation. This was due to the fact that the calibration was performed over a wetter period and the validation was done during a relatively dryer period. However, according to Figures 2 and 4 both downscaling models were able to adequately capture the precipitation pattern seen in the observations, throughout the calibration and validation periods. The underestimation of the standard deviation and the coefficient of variation was seen in all four seasons of both models, during the calibration and validation periods. This characteristic was more severe in the case of the model developed with HadCM3 outputs. Since there is a large scale gap between the GCM outputs and the catchment scale, not all the variance in observations of a predictand (at a point in the catchment) can be explained by the GCM. Therefore, regression based statistical downscaling techniques are capable of capturing only the part of the variance (deterministic component of the variance) of a predictand which is conditioned by the GCM (Hewitson *et al.*, 2013). The local scale random variance of the predictand (stochastic component of the variance) is not simulated by the regression based downscaling models, as it is not explicitly explained by the GCM. At the catchment scale, capturing the full variance of a predictand is important. This can be achieved by the application of a suitable bias-correction method for post-processing the outputs of the downscaling model (Maraun, 2013). Techniques such as randomization may also help in capturing the full variance of a predictand (von Storch, 1999).

In the model developed with NCEP/NCAR data, the best performances in calibration in terms of NSE and R^2 were seen during winter while the lowest performances were observed in summer. For this model, in validation, autumn produced the best performance. The model developed with HadCM3 outputs showed relatively low NSE and R^2 in all four seasons of the calibration period. The negative NSEs were seen in autumn, winter and spring during the validation period, which indicated the limited performances of this downscaling model.

As mentioned in Section 1, the largest drop in precipitation over Victoria during the Millennium drought was observed in autumn. The decline in the average of the observed precipitation in autumn, during the Millennium drought (1997–2010), at the station considered in this study, was 27.5%, from the long-term average (1950–1989). The downscaling model developed with NCEP/NCAR reanalysis outputs was able to successfully reproduce this large drop in the average as 22.4%.

According to the findings discussed previously, it was realized that the downscaling model developed with NCEP/NCAR reanalysis data has better potential in downscaling precipitation, in comparison with its counterpart model built with HadCM3 outputs. This was due to the better quality of NCEP/NCAR reanalysis outputs characterized by better synchronicity with observed precipitation, high precipitation simulation, etc. in comparison to those of HadCM3 outputs. Furthermore, it was seen that MLR has the potential for modelling the relationship between the predictors and the monthly precipitation adequately. As shown in Tables 3 and 4, and Figure 3 with the final sets of potential variables given in Table 2, the downscaling model developed with NCEP/NACR reanalysis outputs reproduced the observed precipitation with good degree of accuracy. Therefore it

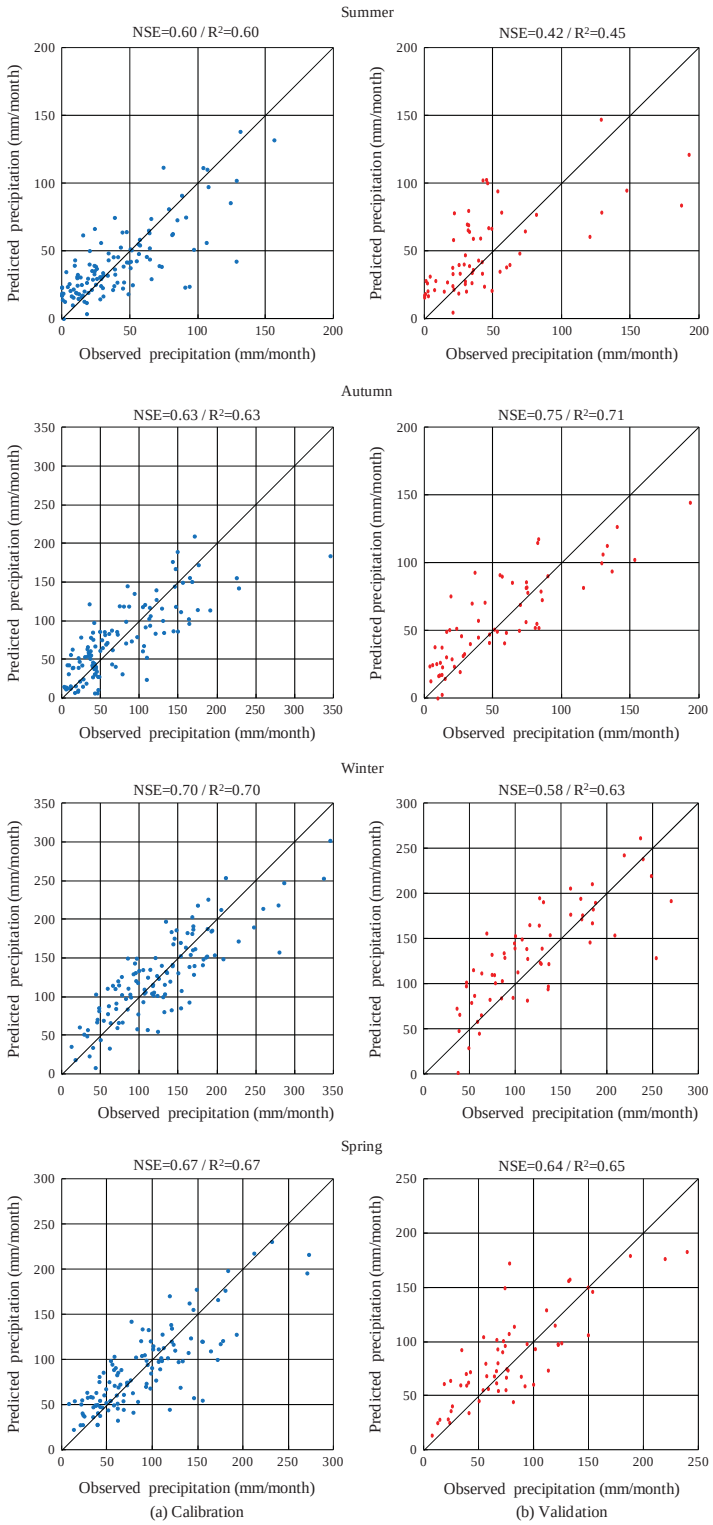

Figure 6. Seasonal scatter plots of observed and Model$_{(NCEP/NCAR)}$ reproduced monthly precipitation for calibration (1950–1989) and validation (1990–2010).

was realized that the final sets of potential variables used in the downscaling models are capable of capturing the precipitation process to a good degree.

Figure 8 shows the exceedance probability curve for the observed precipitation, precipitation reproduced by the downscaling models with NCEP/NCAR and HadCM3 outputs, and the raw precipitation output of HadCM3 model for the 20th century climate experiment at grid point {4,4} (see Figure 1 for location), over the period 1950–1999. Since point {4,4} is the closest grid point to the precipitation station, HadCM3 20th century climate experiment outputs at this point was considered to be

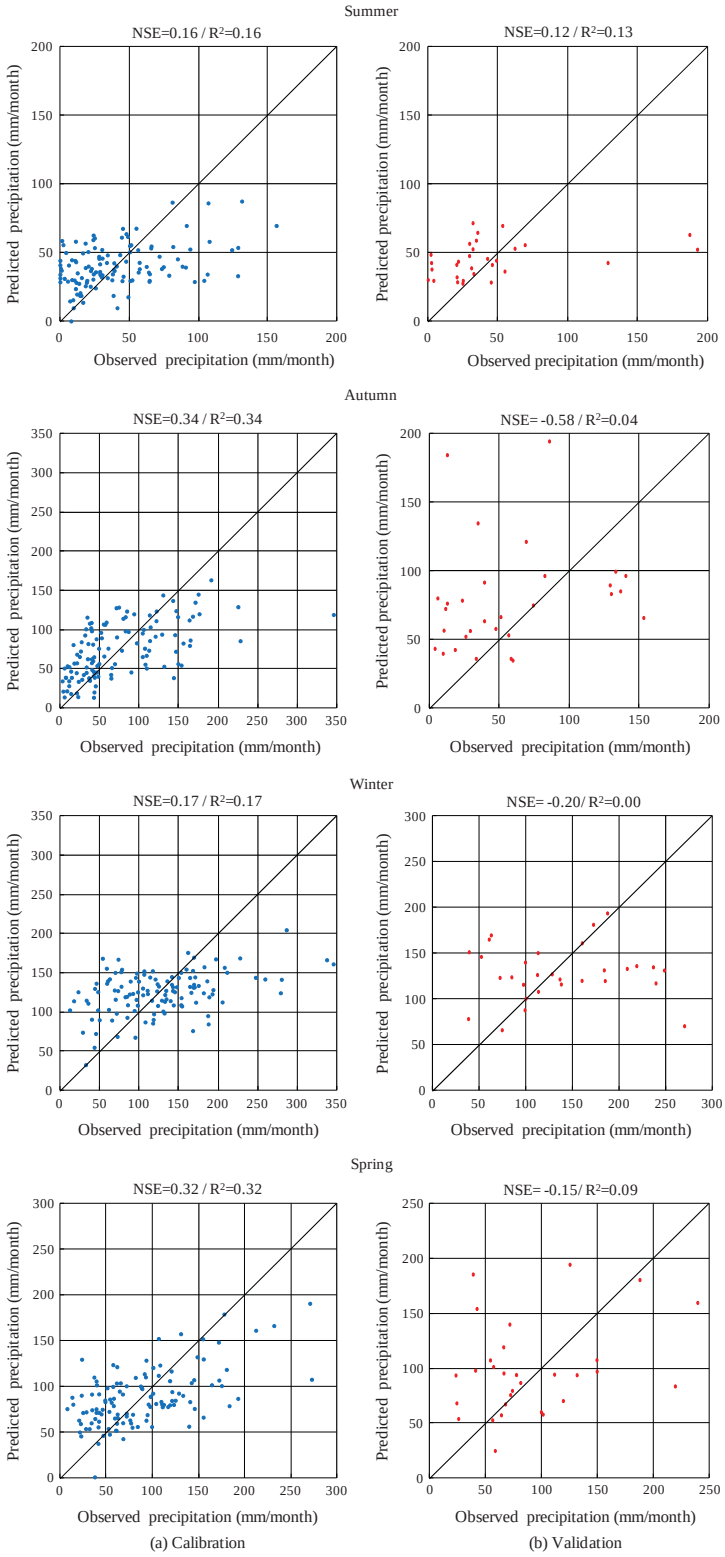

Figure 7. Seasonal scatter plots of observed and Model$_{(HadCM3)}$ reproduced monthly precipitation for calibration (1950–1989) and validation (1990–1999).

representative of the precipitation station considered in this study. Note that the precipitation rate (which was the observed precipitation equivalent output of HadCM3) was converted to monthly precipitation, for plotting the corresponding exceedance curve in Figure 8.

According to Figure 8, it was seen that there is a large mismatch between the raw precipitation output at grid point {4,4} of HadCM3 model and the observed precipitation, during the period 1950–1999. The large bias in the precipitation output of HadCM3 indicated that its

Table 4. Seasonal performances of downscaling models.

Model	Statistic	Calibration (1950–1989)				Validation (1990–2010)/*(1990–1999)*[a]			
		Season				Season			
		Summer	Autumn	Winter	Spring	Summer	Autumn	Winter	Spring
Observed	Avg	40.7	73.7	125.1	87.7	42.9/***(44.3)***	54.1/***(57.0)***	119.4/***(136.1)***	78.3/***(89.8)***
$Model_{(NCEP/NCAR)}$		40.7	73.7	125.1	87.7	49.2	57.8	132.5	85.1
$Model_{(HadCM3)}$		40.3	73.8	125.1	87.8	***(44.9)***	***(78.8)***	***(128.3)***	***(98.5)***
Observed	Std	33.7	58.8	64.5	53.5	41.0/***(46.8)***	43.1/***(46.5)***	61.2/***(66.3)***	48.4/***(55.1)***
$Model_{(NCEP/NCAR)}$		26.0	46.6	54.1	43.9	29.8	33.1	54.1	41.7
$Model_{(HadCM3)}$		15.6	34.4	26.7	30.5	***(12.7)***	***(39.0)***	***(30.0)***	***(42.0)***
Observed	C_v	0.83	0.80	0.52	0.61	0.96/***(1.06)***	0.80/***(0.82)***	0.51/***(0.49)***	0.62/***(0.61)***
$Model_{(NCEP/NCAR)}$		0.64	0.63	0.43	0.50	0.61	0.57	0.41	0.49
$Model_{(HadCM3)}$		0.39	0.47	0.21	0.35	***(0.28)***	***(0.49)***	***(0.23)***	***(0.43)***
$Model_{(NCEP/NCAR)}$	NSE	0.60	0.63	0.70	0.67	0.42	0.75	0.58	0.64
$Model_{(HadCM3)}$		0.16	0.34	0.17	0.33	***(0.12)***	***(−0.58)***	***(−0.20)***	***(−0.15)***
$Model_{(NCEP/NCAR)}$	R^2	0.60	0.63	0.70	0.67	0.45	0.71	0.63	0.65
$Model_{(HadCM3)}$		0.16	0.34	0.17	0.33	***(0.13)***	***(0.04)***	***(0.00)***	***(0.09)***

Avg, average of monthly precipitation in mm; C_v, coefficient of variation; NSE, Nash–Sutcliffe efficiency; R^2, coefficient of determination; Std, standard deviation of monthly precipitation in mm. [a]Bold italicized values in brackets in the table refer to period 1990–1999.

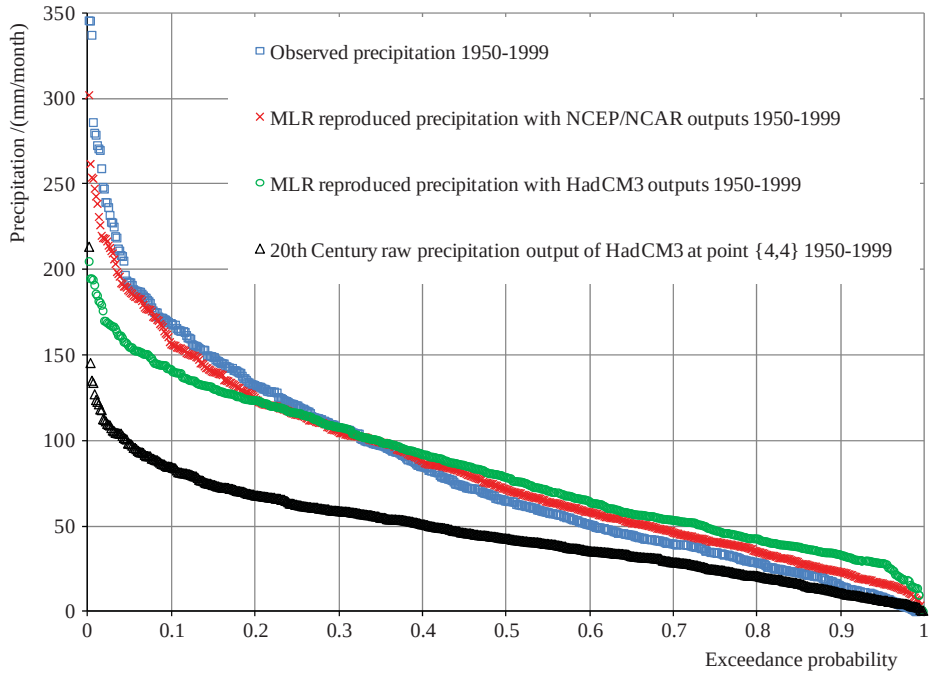

Figure 8. Precipitation probability exceedance curves (1950–1999).

regional precipitation simulation is less reliable. Larger differences between the observations and raw HadCM3 precipitation outputs were seen for precipitations with low probability of exceedance, such as extremely high precipitations. Furthermore, relatively small anomalies were seen for precipitation values with low magnitudes. For the majority of exceedance probabilities, this mismatch was seen as a large under-prediction in HadCM3 precipitation outputs. The mismatch between the observations and the raw HadCM3 precipitation output was mainly due to the bias present in HadCM3 outputs. As defined by Salvi *et al.* (2011), bias is the difference between the GCM outputs and the pertaining observations. GCM bias is a result of the limited knowledge of the atmospheric processes and the simplified representation of the complex climate system in GCMs (Li *et al.*, 2010). The other possible factor contributing to the poor agreement between observations and HadCM3 outputs is, that grid point {4,4} may not exactly represent the precipitation at the station considered in this study. Furthermore, in case of the precipitation gauge located at the Halls Gap

post office, topographical reasons also have possibly contributed to the bias in the GCM outputs, as Halls Gap is located in a valley surrounded by a mountain range.

It was noted that the mismatch between the observations and the precipitation downscaled with HadCM3 outputs was less in comparison with that between the observations and the raw precipitation outputs of HadCM3 at grid point {4,4}. This indicated that when the raw outputs of HadCM3 are statistically downscaled to monthly precipitation, the impact of bias in these raw HadCM3 outputs, on downscaled precipitation was less evident. However, this reduction in bias was not adequate as still there was considerable mismatch between the observed and downscaled precipitation (refer to Figure 8). Therefore, it could be argued that a correction to the bias that is present in HadCM3 outputs is needed in producing precipitation projections into future. It was seen that the precipitation exceedance curve of raw precipitation output of HadCM3 at grid point {4,4} had deviated largely from the precipitation exceedance curve of observations. However, the exceedance curves of precipitation reproduced by the downscaling models developed with NCEP/NCAR reanalysis outputs and HadCM3 outputs were in relatively better agreement with the precipitation exceedance curve of observed precipitation. This led to the conclusion that, the precipitation outputs of the downscaling models developed with NCEP/NCAR reanalysis outputs and HadCM3 outputs are much better than the raw precipitation output of HadCM3 at grid point {4,4}. Furthermore, considering the limited agreement seen between the precipitation downscaled with the NCEP/NACR and HadCM3 outputs, it was realized that there is a quality mismatch between the data of these two sources. The second article of this series of two companion articles, describes the bias correction and the precipitation projections produced into future in detail.

5. Summary and conclusions

This article, which is the first of a series of two companion articles, discussed the development (calibration and validation) of two precipitation downscaling models, employing the MLR technique. The first statistical downscaling model was developed with the NCEP/NCAR reanalysis outputs and the second downscaling model was developed with the HadCM3 outputs. The precipitation station at the Halls Gap post office which is located in the north western part of Victoria, Australia was selected for the demonstration of the development process of the two downscaling models.

It is the general practice to calibrate and validate the downscaling model with some form of reanalysis data (e.g. NCEP/NCAR) for the past climate, and use the outputs of a GCM pertaining to future on the same downscaling model for the projection of climate into future. The major disadvantage of this procedure is that, for the model development and future projections, data from two entirely different sources are used. This study investigated the potential of using a downscaling model calibrated and validated with GCM outputs, which does not have the above issue.

The selection of probable predictors for these downscaling models was based on the past statistical downscaling studies and hydrology. Potential predictors were extracted for each calendar month from the set of probable predictors considering the Pearson correlations between the probable predictors and observed precipitation, under three 20 year time slices (1950–1969, 1970–1989 and 1990–2010) and the entire period of the study (1950–2010). Potential predictors obtained from the NCEP/NCAR reanalysis outputs were introduced to the MLR based downscaling model, sequentially, based on the magnitude of the correlation between observed precipitation and predictors, over the whole period of the study. This process was continued until the model performances in validation in terms of NSE was maximized. In this manner, the final sets of potential predictors for each calendar month were identified, and downscaling models for each calendar month were developed separately. The HadCM3 outputs corresponding to the final sets of potential predictors identified previously were used for the development of the second downscaling model. It was assumed that these final sets of potential predictors are valid for both downscaling models, developed with NCEP/NCAR and HadCM3 outputs.

The MLR based downscaling model developed with NCEP/NCAR reanalysis outputs proved capable in reproducing the observed monthly precipitation during both calibration (1950–1989) and validation (1990–2010) phases. The performances of this model in calibration were slightly better than those in validation. This model was also able to capture the precipitation drop occurred during the Millennium drought (1997–2010) satisfactorily. However, it displayed tendencies of over-predicting low precipitation values and under-predicting high precipitation values during both the calibration and validation periods.

On the other hand, the MLR based downscaling model developed with HadCM3 outputs displayed limited performances with respect to the model developed with NCEP/NCAR reanalysis outputs during both calibration and validation stages. This model performed better during calibration (1950–1989) than in validation (1990–1999). Similar to the model developed with NCEP/NCAR reanalysis outputs, this downscaling model also displayed tendencies of over-predicting and under-predicting low and high precipitation values, respectively. However, the over and under-predictions associated with the model developed with HadCM3 outputs were much severe than those for its counterpart downscaling model. Due to the termination of HadCM3 outputs at 1999 for the 20th century climate experiment, the validation phase of this downscaling model was confined to 1990–1999. Therefore it was not possible to see how this downscaling

model will reproduce the precipitation during the Millennium drought.

The conclusions drawn from this study are:

1. The precipitation rate which is the precipitation equivalent output of a GCM was found as the most influential predictor on precipitation at the station of interest, over the entire year, except in July;
2. Humidity, geopotential heights, mean sea level and surface pressure, and wind speeds also showed good correlations with observed precipitation consistently over time;
3. The downscaling model developed with NCEP/NCAR reanalysis outputs performed well in both calibration and validation, while the performances of the model developed with HadCM3 outputs were limited;
4. There was a quality mismatch between the NCEP/NCAR reanalysis and HadCM3 outputs, over the period 1950–1999; and
5. A bias-correction should be applied in projecting the precipitation into future at the station of interest.

The application of the bias-correction and the projections of precipitation into future are presented in the second companion article of this series of articles.

Acknowledgements

The authors acknowledge the financial assistance provided by the Australian Research Council Linkage Grant scheme and the Grampians Wimmera Mallee Water Corporation for this project. The authors also wish to thank the editor and the two anonymous reviewers for their useful comments, which have improved the quality of this article.

References

Alavian V, Qaddumi HM, Dickson E, Diez SM, Danilenko AV, Hirji RF, Puz G, Pizarro C, Jacobsen M, Blankespoor B. 2009. Water and Climate Change: Understanding the Risks and Making Climate-smart Investment Decisions. The Worldbank: Washington, DC. http://documents.worldbank.org/curated/en/2009/11/11717870/water-climate-change-understanding-risks-making-climate-smart-investment-decisions (accessed on 19 July 2013).

Anandhi A. 2010. Assessing impact of climate change on season length in Karnataka for IPCC SRES scenarios. *J. Earth Syst. Sci.* **119**: 447–460, DOI: 10.1007/s12040-010-0034-5.

Anandhi A, Srinivas VV, Nanjundiah RS, Kumar DN. 2008. Downscaling precipitation to river basin in India for IPCC SRES scenarios using support vector machine. *Int. J. Climatol.* **28**: 401–420, DOI: 10.1002/joc.1529.

Anandhi A, Srinivas VV, Nanjundiah RS, Kumar DN. 2012. Daily relative humidity projections in an Indian river basin for IPCC SRES scenarios. *Theor. Appl. Climatol.* **108**: 85–104, DOI: 10.1007/s00704-011-0511-z.

Bureau of Meteorology. 2010. Australian Climate Influences. http://www.bom.gov.au/watl/about-weather-and-climate/australian-climate-influences.shtml (accessed 25 September 2012).

Charles A, Timbal B, Fernandez E, Hendon H. 2013. Analog downscaling of seasonal rainfall forecasts in the Murray darling basin. *Mon. Weather Rev.* **141**: 1099–1117, DOI: 10.1175/MWR-D-12-00098.1.

Chiew FHS, Piechota TC, Dracup JA, McMahon TA. 1998. El Nino/Southern Oscillation and Australian rainfall, streamflow and drought: Links and potential for forecasting. *J. Hydrol.* **204**: 138–149, DOI: 10.1016/S0022-1694(97)00121-2.

Chiew FHS, Young WJ, Cai W, Teng J. 2010. Current drought and future hydroclimate projections in southeast Australia and implications for water resources management. *Stoch. Environ. Res. Risk Assess.* **25**: 602–612, DOI: 10.1007/s00477-010-0424-x.

Chu JT, Xia J, Xu CY, Singh VP. 2010. Statistical downscaling of daily mean temperature, pan evaporation and precipitation for climate change scenarios in Haihe River, China. *Theor. Appl. Climatol.* **99**: 149–161, DOI: 10.1007/s00704-009-0129-6.

Crowley TJ. 2000. Causes of climate change over the past 1000 years. *Science* **289**: 270–277, DOI: 10.1126/science.289.5477.270.

Government of Western Australia Department of Water. 2009. Streamflow trends in south-west Western Australia. Surface water hydrology series. Report no. HY32. http://www.water.wa.gov.au/PublicationStore/first/87846.pdf (accessed 1 November 2012).

Goyal MK, Burn DH, Ojha CSP. 2012. Evaluation of machine learning tools as a statistical downscaling tool: temperatures projections for multi-stations for Thames river basin, Canada. *Theor. Appl. Climatol.* **108**: 519–534, DOI: 10.1007/s00704-011-0546-1.

Hashmi MZ, Shamseldin AY, Melville BW. 2011. Statistical downscaling of watershed precipitation using Gene Expression Programming (GEP). *Environ. Model. Softw.* **26**: 1639–1646, DOI: 10.1016/j.envsoft.2011.07.007.

Hay LE, Clark MP. 2003. Use of statistically and dynamically downscaled atmospheric model output for hydrologic simulations in three mountainous basins in the western United States. *J. Hydrol.* **282**: 56–75, DOI: 10.1016/S0022-1694(03)00252-X.

Hewitson B, Jack C, Coop L. 2013. Addressing deterministic and stochastic variance in statistical downscaling. In *European Geophysical Union General Assembly*. Vienna, Austria, 7–12 April, 2013.

Iizumi T, Takayabu I, Dairaku K, Kusaka H, Nishimori M, Sakurai G, Ishizak NN, Adachi SA, Semenov MA. 2012. Future change of daily precipitation indices in Japan: a stochastic weather generator-based bootstrap approach to provide probabilistic climate information. *J. Geophys. Res. D: Atmos.* **117**: D11114, DOI: 10.1029/2011JD017197.

IPCC. 2007. IPCC Fourth assessment: synthesis report – summary for policymakers, 6–9. http://www.ipcc.ch/pdf/assessment-report/ar4/syr/ar4_syr_spm.pdf (accessed on 8 November 2012).

Jeffrey SJ, Carter JO, Moodie KB, Beswick AR. 2001. Using spatial interpolation to construct a comprehensive archive of Australian climate data. *Environ. Model. Softw.* **16**: 309–330, DOI: 10.1016/S1364-8152(01)00008-1.

Kalnay E, Kanamitsu M, Kistler R, Collins W, Deaven D, Gandin L, Iredell M, Saha S, White G, Woollen J, Zhu Y, Chelliah M, Ebisuzaki W, Higgins W, Janowiak J, Mo KC, Ropelewski C, Wang J, Leetmaa A, Reynolds R, Jenne R, Joseph D. 1996. The NCEP/NCAR reanalysis project. *Bull. Am. Meteorol. Soc.* **77**: 437–471, DOI: 10.1175/1520-0477(1996)077<0437:TNYRP>2.0.CO;2.

Kannan S, Ghosh S. 2013. A nonparametric kernel regression model for downscaling multisite daily precipitation in the Mahanadi basin. *Water Resour. Res.* **49**: 1360–1385, DOI: 10.1002/wrcr.20118.

Karl TR, Wang WC, Schlesinger ME, Knight RW, Portman D. 1990. A method of relating general circulation model simulated climate to the observed local climate part I: seasonal statistics. *J. Clim.* **3**: 1053–1079, DOI: 10.1175/1520-0442(1990)003<1053:AMORGC>2.0.CO;2.

Khalili M, Brissette F, Leconte R. 2009. Stochastic multi-site generation of daily weather data. *Stoch. Environ. Res. Risk Assess.* **23**: 837–849, DOI: 10.1007/s00477-008-0275-x.

Khazaei MR, Ahmadi S, Saghafian B, Zahabiyoun B. 2013. A new daily weather generator to preserve extremes and low-frequency variability. *Clim. Change*, DOI: 10.1007/s10584-013-0740-5.

Knight J. 2003. Report on forcings for the C20C and EMULATE HadAM3 experiments. http://hadc20c.metoffice.com/forcings.pdf (accessed on 30 May 2013).

Li H, Sheffield J, Wood EF. 2010. Bias correction of monthly precipitation and temperature fields from Intergovernmental Panel on Climate Change AR4 models using equidistant quantile matching. *J. Geophys. Res. D: Atmos.* **115**: 1–20, DOI: 10.1029/2009JD012882.

Maraun D. 2013. Bias correction, quantile mapping, and downscaling: Revisiting the inflation issue. *J. Clim.* **26**: 2137–2143, DOI: 10.1175/JCLI-D-12-00821.1.

Maraun D, Wetterhall F, Ireson AM, Chandler RE, Kendon EJ, Widmann M, Brienen S, Rust HW, Sauter T, Themel M, Venema

VKC, Chun KP, Goodess CM, Jones RG, Onof C, Vrac M, Thiele-Eich I. 2010. Precipitation downscaling under climate change: Recent developments to bridge the gap between dynamical models and the end user. *Rev. Geophys.* **48**, DOI: 10.1029/2009RG000314.

Marzban C, Sandgathe S, Kalnay E. 2006. MOS, perfect prog, and reanalysis. *Mon. Weather Rev.* **134**: 657–663, DOI: 10.1175/MWR3088.1.

Maurer EP, Hidalgo HG. 2008. Utility of daily vs. monthly large-scale climate data: an intercomparison of two statistical downscaling methods. *Hydrol. Earth Syst. Sci.* **12**: 551–563, DOI: 10.5194/hess-12-551-2008.

Najafi M, Moradkhani H, Wherry S. 2011. Statistical downscaling of precipitation using machine learning with optimal predictor selection. *J. Hydrol. Eng.* **16**: 650–664, DOI: 10.1061/(ASCE) HE.1943-5584.0000355.

Nash JE, Sutcliffe JV. 1970. River flow forecasting through conceptual models, part 1 – a discussion of principles. *J. Hydrol.* **10**: 282–290, DOI: 10.1016/0022-1694(70)90255-6.

Nasseri M, Tavakol-Davani H, Zahraie B. 2013. Performance assessment of different data mining methods in statistical downscaling of daily precipitation. *J. Hydrol.* **492**: 1–14, DOI: 10.1016/j.jhydrol.2013.04.017.

Nazemosadat MJ, Cordery I. 1997. The influence of geopotential heights on New South Wales rainfall. *Meteorol. Atmos. Phys.* **63**: 179–193, DOI: 10.1007/BF01027384.

Pearson K. 1895. Mathematical contributions to the theory of evolution. iii. regression heredity and panmixia. *Philos. Trans. R. Soc. Lond. A* **187**: 253–318, DOI: 10.1098/rsta.1896.0007.

Peixoto JP, Oort AH. 1996. The climatology of relative humidity in the atmosphere. *J. Clim.* **9**: 3443–3463, DOI: 10.1175/1520-0442(1996)009<3443:TCORHI>2.0.CO;2.

Richardson CW. 1981. Stochastic simulation of daily precipitation, temperature, and solar radiation. *Water Resour. Res.* **17**: 182–190, DOI: 10.1029/WR017i001p00182.

Sachindra DA, Huang F, Barton AF, Perera BJC. 2012. Issues associated with statistical downscaling of general circulation model outputs: a discussion. In *Proceedings of Practical Responses to Climate Change National Conference*. Canberra, Australia, 1–3 May 2012.

Sachindra DA, Huang F, Barton AF, Perera BJC. 2013. Least square support vector and multi-linear regression for statistically downscaling general circulation model outputs to catchment streamflows. *Int. J. Climatol.* **33**: 1087–1106, DOI: 10.1002/joc.3493.

Salvi K, Kannan S, Ghosh S. 2011. Statistical downscaling and bias-correction for projections of Indian rainfall and temperature in climate change studies. In *4th International Conference on Environmental and Computer Science*. Singapore, 16–18 September, 7–11.

Schnur R, Lettenmaier DP. 1998. A case study of statistical downscaling in Australia using weather classification by recursive partitioning. *J. Hydrol.* **213**: 362–379, DOI: 10.1016/S0022-1694(98)00217-0.

Semenov MA, Stratonovitch P. 2010. Use of multi-model ensembles from global climate models for assessment of climate change impacts. *Clim. Res.* **41**: 1–14, DOI: 10.3354/cr00836.

Shao Q, Li M. 2013. An improved statistical analogue downscaling procedure for seasonal precipitation forecast. *Stoch. Environ. Res. Risk Assess.* **27**: 819–830, DOI: 10.1007/s00477-012-0610-0.

Smith IN, McIntosh P, Ansell TJ, Reason CJC, McInnes K. 2000. Southwest Western Australian winter rainfall and its association with Indian Ocean climate variability. *Int. J. Climatol.* **20**: 1913–1930, DOI: 10.1002/1097-0088(200012)20:15<1913::AID-JOC594>3.0.CO;2-J.

von Storch H. 1999. On the use of "inflation" in statistical downscaling. *J. Clim.* **12**: 3505–3506, DOI: 10.1175/1520-0442(1999)012<3505:OTUOII>2.0.CO;2.

von Storch H, Hewitson B, Mearns L. 2000. Review of empirical downscaling techniques. In *Proceedings of RegClim Spring Meeting*. Jevnaker, Norway, 8–9 May. http://regclim.met.no/rapport_4/Default.htm (accessed on 1 October 2012).

Timbal B, Jones DA. 2008. Future projections of winter rainfall in southeast Australia using a statistical downscaling technique. *Clim. Change* **86**: 165–187, DOI: 10.1007/s10584-007-9279-7.

Timbal B, Fernandez E, Li Z. 2009. Generalization of a statistical downscaling model to provide local climate change projections for Australia. *Environ. Model. Softw.* **24**: 341–358, DOI: 10.1016/j.envsoft.2008.07.007.

Tisseuil C, Vrac M, Lek S, Wade AJ. 2010. Statistical downscaling of river flows. *J. Hydrol.* **385**: 279–291, DOI: 10.1016/j.jhydrol.2010.02.030.

Tripathi S, Srinivas VV, Nanjundiah RS. 2006. Downscaling of precipitation for climate change scenarios: a support vector machine approach. *J. Hydrol.* **330**: 621–640, DOI: 10.1016/j.jhydrol.2006.04.030.

Wang W. 2006. *Stochasticity, Nonlinearity and Forecasting of Streamflow Processes*. Deft University Press: Amsterdam, the Netherlands; 72–73.

Wilby RL, Charles SP, Zorita E, Timbal B, Whetton P, Mearns LO. 2004. Guidelines for use of climate scenarios developed from statistical downscaling methods, supporting material to the IPCC, 3–21. http://www.ipcc-data.org/.

Willems P, Vrac M. 2011. Statistical precipitation downscaling for small-scale hydrological impact investigations of climate change. *J. Hydrol.* **402**: 193–205, DOI: 10.1016/j.jhydrol.2011.02.030.

Yang T, Li H, Wang W, Xu CY, Yu Z. 2012. Statistical downscaling of extreme daily precipitation, evaporation, and temperature and construction of future scenarios. *Hydrol. Process.* **26**: 3510–3523, DOI: 10.1002/hyp.8427.

INTERNATIONAL JOURNAL OF CLIMATOLOGY
Int. J. Climatol. (2014)
Published online in Wiley Online Library
(wileyonlinelibrary.com) DOI: 10.1002/joc.3915

RMetS
Royal Meteorological Society

3.4 Statistical downscaling of general circulation model outputs to precipitation – part 2: bias-correction and future projections

D. A. Sachindra,[a]* F. Huang,[a] A. Barton[a,b] and B. J. C. Perera[a]

[a] *College of Engineering and Science, Footscray Park Campus, Victoria University, Melbourne, Australia*
[b] *School of Science, Information Technology and Engineering, University of Ballarat, Victoria, Australia*

ABSTRACT: This article is the second of a series of two articles. In the first article, two models were developed with National Centers for Environmental Prediction/National Center for Atmospheric Research (NCEP/NCAR) reanalysis and HadCM3 outputs, for statistically downscaling these outputs to monthly precipitation at a site in north-western Victoria, Australia. In that study, it was seen that the downscaling model developed with NCEP/NCAR reanalysis outputs performs much better than the model developed with HadCM3 outputs. Furthermore, it was found that there is large bias in HadCM3 outputs which needs to be corrected. In this article, the downscaling model developed with NCEP/NCAR reanalysis outputs was used to downscale HadCM3 20th century climate experiment outputs to monthly precipitation over the period 1950–1999. In all four seasons, the precipitation downscaled with HadCM3 20th century outputs, displayed a large scatter and the majority of precipitation was overestimated. The precipitation downscaled with HadCM3 outputs was bias-corrected against the observed precipitation pertaining to the period 1950–1999, using three techniques: (1) equidistant quantile mapping (EDQM), (2) monthly bias-correction (MBC) and (3) nested bias-correction (NBC). Although all these bias-correction techniques were able to adequately correct the statistics of downscaled precipitation, the magnitude of the scatter of precipitation remained almost the same. Considering the performances and its ability to correct the cumulative distribution of precipitation, EDQM was selected for the bias-correction of future precipitation projections. HadCM3 outputs for the A2 and B1 greenhouse gas scenarios were introduced to the downscaling model and the downscaled precipitation for the period 2000–2099 was bias-corrected with the EDQM technique. Both A2 and B1 scenarios indicated a rise in the average of future precipitation in winter and a drop in it in summer and spring. These scenarios showed an increase in the maximum monthly precipitation in all seasons and an increase in percentage of months with zero precipitation in summer, autumn and spring.

KEY WORDS statistical downscaling; precipitation; general circulation model; bias

Received 10 December 2012; Revised 19 July 2013; Accepted 5 December 2013

1. Introduction

Over the 800 000-year period prior to the industrial revolution (1750–1850), the concentration of the atmospheric carbon dioxide [dominant greenhouse gas (GHG)] fluctuated approximately between 180 and 280 parts per million (ppm) (Tripati *et al.*, 2009). Since the industrial revolution, owing to the consumption of fossil fuels, the concentration of the global mean atmospheric carbon dioxide level rose from 280 to 397 ppm by April 2013 (Earth System Research Laboratory, 2013). The rising concentrations of GHGs (mainly carbon dioxide) have increased the greenhouse effect leading to human-induced climate change, which is no longer a hypothetical phenomenon (Hughes, 2003). As stated by Dessai *et al.* (2005), the global climate is expected to change throughout the 21st century. Climate change has shed its impacts, on humans as well as flora and fauna in many different ways. Impacts of climate change on health of humans (Thomas *et al.*, 2012), agricultural food production (Ziska *et al.*, 2012), floods (Prudhomme *et al.*, 2013) and water resources (Arnell and Gosling, 2013) are only some of the multitude of themes discussed in the literature.

General circulation models (GCMs) are the prime tools used in the projection of climate into the future (Fu *et al.*, 2012). GCMs are based on the theories of atmospheric physics. They are forced with plausible realizations on future GHG concentrations, in order to produce projections on global climate into future. The coarse resolution of GCM outputs hinders their direct use in catchment scale studies (Iizumi *et al.*, 2011). Downscaling techniques are used to link the coarse resolution GCM outputs with the catchment scale climatic variables. All downscaling techniques are based on the assumption that large-scale climate represented in GCM outputs is

* Correspondence to: D. A. Sachindra, College of Engineering and Science, Footscray Park Campus, Victoria University, P.O. Box 14428, Melbourne, Victoria 8001, Australia.
E-mail: sachindra.dhanapalaarachchige@live.vu.edu.au

influential on the catchment scale hydroclimatology (Maraun *et al.*, 2010). There are two broad classes of downscaling techniques, namely; dynamic downscaling and statistical downscaling. In order to obtain local-scale climatic information, dynamic downscaling approaches employ regional climate models (RCMs) nested in GCMs (Murphy, 1998). Dynamic downscaling techniques are associated with high computational costs (Sun and Chen, 2012) due to the complex physics-based structure of the RCMs. However, owing to the use of physics-based equations to relate the predictors (GCM outputs which are used as input to downscaling models) with predictands (outputs of downscaling models – e.g. precipitation), dynamic downscaling techniques are capable in producing more reliable climatic information at local scale. This is because it is reasonable to assume that the same physics which was valid for the climate in the past is also valid for the climate in the future. On the other hand, statistical downscaling techniques are dependent on the empirical relationships developed between the GCM outputs and local-scale hydroclimatic variables. Statistical downscaling methods are computationally more efficient, due to the simplicity in their structure. In statistical downscaling techniques, it is assumed that the relationships derived between the predictors and predictands for the past observed climate are also applicable for the possible future climate (Iizumi *et al.*, 2011). However, the validity of this assumption cannot be tested at present as the future climate has not yet occurred (Chu *et al.*, 2010).

Statistical downscaling techniques are grouped under three classes; regression methods, weather typing (classification) and weather generators (Wilby *et al.*, 2004). In regression-based downscaling methods either linear or nonlinear relationships between the predictors and the predictand of interest are developed. By far, the regression-based methods are regarded as the most widely used statistical downscaling techniques (Nasseri *et al.*, 2013). Meenu *et al.* (2013) used the multi-linear regression (MLR) technique for downscaling GCM outputs to daily precipitation and then the downscaled precipitation was used in a hydrologic model to simulate streamflows. Samadi *et al.* (2013) used the MLR technique and artificial neural networks (ANN; nonlinear regression method) for downscaling GCM outputs to daily precipitation and temperature. They commented that the MLR-based downscaling technique was more capable than the ANN-based downscaling method in reproducing the observations of precipitation and temperature. Ghosh and Katkar (2012) employed MLR, ANN and support vector machine (SVM; nonlinear regression method) for downscaling GCM outputs to monthly precipitation. In that study, it was found that though the three regression-based downscaling models displayed similar overall performances in the calibration phase, the ANN-based model was able to better capture the relatively low and medium precipitation values and the SVM-based model was better at simulating relatively high values of precipitation.

In weather classification methods, patterns of large-scale weather characterized by a global or a regional model are linked to a local-scale weather variable. Method of meteorological analogues is a widely used weather classification technique (Timbal *et al.*, 2009; Shao and Li, 2013). Also recursive partitioning is another classification type downscaling method (Schnur and Lettenmaier, 1998). Charles *et al.* (2013) used the method of meteorological analogues for downscaling GCM outputs to precipitation. It was found that this method was able to correct the bias in statistics of seasonal precipitation and also the number of wet days simulated by the GCM. In weather generation techniques, weather data for future are produced by scaling the parameters of the weather generator either up or down according to the changes in the GCM outputs pertaining to future. As an example the simplest weather generator for daily precipitation could have two parameters: (1) the probability of occurrence of a wet day and (2) the precipitation amount. In such case, the percentage changes in the parameters characterized by the GCM for the future climate with respect to those in the baseline period are determined. Then the values of the parameters pertaining to observed precipitation of the baseline period are scaled corresponding to the above determined changes. The new scaled parameters are used to generate time series of occurrence of wet days and precipitation amounts at the station of interest that reflects the large-scale changes in the precipitation simulated by the GCM. Applications of weather generation techniques are detailed in the studies of Chen *et al.* (2012) and Fatichi *et al.* (2011).

The classification of statistical downscaling techniques detailed by Maraun *et al.* (2010) separates the statistical downscaling techniques into three different categories: (1) perfect prognosis, (2) model output statistics (MOS) and (3) weather generators. Perfect prognosis methods involve establishing statistical relationships between the large-scale atmospheric variables and the catchment scale hydroclimatic variables, using regression techniques or weather classification approaches. In MOS methods, statistical relationships between the outputs of a RCM or a weather model and catchment scale observations of a predictand are used to improve the model outputs.

Although GCMs are regarded as the best tools available for projection of climate into the future, there are biases in GCM outputs. GCM bias is simply explained as the deviation of GCM outputs from the observations (Salvi *et al.*, 2011). However, in more elaborated terms, incorrect reproduction of extreme temperatures, prediction of excess number of wet days with low-intensity rainfalls, under or over-prediction of climatic variables, incorrect seasonal variations and so on are some of the forms of biases prevailing in GCM outputs (Teutschbein and Seibert, 2012). Chen *et al.* (2011) defined GCM bias as a time-independent component of the error in GCM outputs. According to Ojha *et al.* (2012), GCMs often incorrectly estimate the occurrences and intensities of precipitation. The limited understanding of the atmosphere and the simplified representation of the atmospheric processes in GCMs are regarded as the main causes of GCM bias (Li *et al.*, 2010). In general,

prognostic variables of a GCM contain relatively less bias than the diagnostic variables that are derived from the prognostic variables. Since prognostic variables do not always show good relationships with the predictands of interest, diagnostic variables are also used in developing the downscaling models despite their larger bias. The correction of bias is performed in two distinct ways: (1) the correction of bias in GCM outputs and (2) the correction of bias in the predictands (e.g. precipitation) which were downscaled from GCM outputs. However, neither of the above approaches is capable of correcting the inherent physics and thermodynamics of the GCM simulations, as bias-correction has no direct connection with the internal functions of the GCM. There are number of different bias-correction techniques in use, which are applicable to GCM outputs and also to the predictands downscaled from GCM outputs.

Ojha *et al.* (2012) reported that the bias seen in the GCM outputs should be corrected before their subsequent use. Johnson and Sharma (2012) used the nested bias-correction (NBC) for correcting the bias in monthly precipitation outputs of GCMs, over Australia. NBC corrects the bias in means, standard deviations and lag 1 autocorrelations of GCM outputs, simultaneously at both monthly and annual time scales. They commented that the NBC is successful when the bias in GCM outputs is not very large. Ojha *et al.* (2012) applied both NBC and monthly bias-correction (MBC) for removing the bias in precipitation outputs of number of GCMs, over India. Unlike the NBC described earlier, in the monthly bias-correction, only the means and standard deviations of the monthly GCM outputs are corrected with respect to those of the observations. In both nested and monthly bias-corrections, the statistics of the observed climatic data and the corresponding statistics of the past GCM outputs are used in the correction of the GCM outputs pertaining to future. These two methods assume that the biases in the model outputs for the past climate will remain same for the future climate (Johnson and Sharma, 2012).

Wood *et al.* (2004) employed the quantile mapping technique for bias-correcting the monthly precipitation and temperature outputs of a GCM. The quantile mapping (Panofsky and Brier, 1968) is a technique which can match all statistical moments of GCM outputs with those of observations, as in this technique cumulative distribution functions (CDFs) of GCM outputs for the past are mapped onto the CDF of the past observations. For the correction of bias in the GCM outputs pertaining to the future climate, first, corresponding to the values of the climatic variable for the future projections, the CDF values are obtained from the CDF which was derived from the past GCM simulations. Then pertaining to these CDF values, the bias-corrected values of the climatic variable for the future climate are extracted from the CDF of the observations of the past. Piani *et al.* (2010) used a gamma distribution-based quantile mapping technique for the bias-correction of daily precipitation downscaled by the RCM over Europe. It was concluded that this bias-correction is capable of correcting the average and the other statistical moments of precipitation and also the statistical properties such as precipitation intensity. Lafon *et al.* (2013) applied four bias-correction techniques (linear scaling, nonlinear scaling, gamma distribution-based quantile mapping and empirical distribution-based quantile mapping) to reduce the bias in daily precipitation simulated by the RCM over the UK. They commented that all bias-correction techniques were able to correct the average and the standard deviation of daily precipitation with a good degree of accuracy. However, the accuracy of higher-order moments such as skewness and kurtosis of daily precipitation were sensitive to the bias-correction method and also to the period selected for the calibration of the bias-correction. Out of the four bias-correction techniques, the empirical distribution-based quantile mapping was identified as the best performing bias-correction. Gudmundsson *et al.* (2012) compared the performances of three variants of quantile mapping: distribution-derived, parametric and nonparametric (empirical distribution based quantile mapping) in correcting the bias in daily precipitation simulated by the RCM over Norway. They also concluded that nonparametric (empirical) quantile mapping is more effective in reducing the bias in precipitation. Themeßl *et al.* (2011) applied several bias-correction approaches to daily precipitation of the RCM over the Alps region in Europe. It was concluded that the empirical distribution-based quantile mapping technique displayed better performance than the other methods, particularly in correcting the extremes of precipitation.

Li *et al.* (2010) introduced a modified version of the quantile mapping technique called equidistant quantile mapping (EDQM). In equidistant quantile mapping, the difference between the CDF of the GCM output (to be corrected) and the CDF of the reference dataset (which can be field observations, reanalysis outputs, etc.), of the past climate, was subtracted from the CDF of the GCM output for future climate, for the bias-correction of future GCM outputs. In quantile mapping and equidistant quantile mapping, the CDFs of GCM outputs are corrected against the CDF of observations, therefore all statistical moments are explicitly corrected. On the other hand, NBC explicitly attempts to remove bias in the average, the standard deviation and the lag 1 autocorrelation of GCM outputs, and monthly bias-corrections reduces the bias in the average and the standard deviation only.

Ines and Hansen (2006) used the quantile mapping technique and the multiplicative shift method for bias-correction of daily mean precipitation output of a GCM. The multiplicative shift method involved the multiplication of daily precipitation output of the GCM by the ratio between the long-term observed and monthly precipitation output of the GCM. It was found that although this technique corrects the long-term observed monthly mean precipitation, it cannot correct any systematic error in the precipitation distribution. A regression-based bias-correction was employed by Kharin and Zwiers (2002) for the removal of bias from precipitation outputs of a

GCM. There a regression equation was built between the mean of the precipitation outputs of the GCM and observed precipitation, to correct the bias.

Above stated bias-correction techniques can be applied not only to GCM outputs, but also to the outputs of downscaling models, irrespective of whether the downscaling approach is dynamic or statistical. Ghosh and Mujumdar (2008) used the quantile mapping technique for the removal of bias in streamflows, which were statistically downscaled from GCM outputs. Teutschbein and Seibert (2012) used multiple bias-correction techniques (linear scaling, local intensity scaling, power transformation, variance scaling, quantile mapping and delta-change approach) on dynamically downscaled precipitation and temperature. The major advantage of applying the bias-correction techniques on the downscaled (either statistically or dynamically) hydroclimatic outputs is that, this process is computationally much cheaper than bias-correcting each GCM output individually, prior to downscaling. The advantage of applying a bias-correction to each GCM output separately (before introducing to the downscaling model) is that the bias in each variable is individually corrected. However, this procedure is useful only if the bias-correction was capable in adequately correcting the time series of each GCM output, rather than just their statistics.

The first article of this series of two articles which was entitled 'Statistical Downscaling of General Circulation Model Outputs to Precipitation. Part 1: Calibration and Validation' presented the calibration and validation of two statistical downscaling models, based on the MLR technique. In that study, the first model was developed with National Centers for Environmental Prediction/National Center for Atmospheric Research (NCEP/NCAR) reanalysis outputs and the second model was with Hadley Centre Coupled Model version 3 GCM (HadCM3) outputs. In both cases these outputs were used as the inputs to the downscaling models. According to the results of that study, it was seen that the model calibrated and validated with NCEP/NCAR reanalysis outputs was more capable in reproducing the observed precipitation, than its counterpart model which was built with HadCM3 20th century climate experiment outputs. Furthermore, a comparison of exceedance probability curves for the observed precipitation, precipitation reproduced by the downscaling models with NCEP/NCAR and HadCM3 outputs, and the raw precipitation output of HadCM3 model for 20th century climate experiment, over the period 1950–1999, revealed that there is large bias in the raw precipitation output of HadCM3 model. Therefore the need of a bias-correction was understood.

This article which is the second of the series of two articles, discusses the bias-correction and future precipitation projections of the statistical downscaling model developed in the first article, with NCEP/NCAR reanalysis outputs. This downscaling model was used in this study because of its better performances seen in the first article. The same MLR equations (with the same coefficients and constants) derived during the calibration phase of this downscaling model were used in this study. Here onwards in this article, this model is referred to as the 'downscaling model'. Initially, the downscaling model was used to downscale the 20th century climate experiment outputs of HadCM3, to monthly precipitation. Then these downscaled precipitation data were bias-corrected against the observed precipitation (reference dataset for the bias-correction). For this purpose, three bias-correction techniques, namely (1) EDQM, (2) MBC and (3) NBC were employed. As a demonstration, the above procedure was applied to a precipitation station in the Grampians water supply system in north-western Victoria, Australia. The same station was also used in the first article. A performance comparison of the above three bias-corrections, derived from the above demonstration, is presented in this article. Considering the performances of each of these three bias-corrections, only the EDQM technique was used for the bias-correction of monthly precipitation projections produced into future by the downscaling model with HadCM3 outputs pertaining to the future climate. In downscaling GCM outputs to monthly precipitation, characteristics of precipitation such as occurrences of wet and dry days, extreme precipitation events, precipitation intensity are not captured. Though such characteristics are important in certain hydrological exercises, monthly precipitation is more useful in water resources management operations such as determining the optimum water allocation to crops, recreational facilities, domestic and industrial needs and to the environment particularly in the planning stage of a water resources project.

Section 2 of this article provides a brief description of the study area and the data used in the study. Section 3 describes the generic methodology, and its application with the results is detailed in Section 4. In Section 5, a summary of this work is provided along with the conclusions derived from this study.

2. Study area and data

The precipitation station located at the Halls Gap post office (Lat. -37.14°, Lon. 142.52°, elevation from the mean sea level about 236 m) in the Grampians water supply system of north-western Victoria, Australia was used as the case study station. The Grampians system is a multi-reservoir system owned by the Grampians Wimmera Mallee Water Cooperation (www.gwmwater.org.au).

Observed daily precipitation data from 1950 to 1999 were obtained from the SILO database (http://www.longpaddock.qld.gov.au/silo/) of Queensland Climate Change Centre of Excellence and these data were added to monthly precipitation totals. These monthly observations were used for the evaluation of the downscaling model when it was run with HadCM3 20th century climate experiment outputs and NCEP/NCAR reanalysis outputs. Also the observed precipitation was used as the reference dataset for the bias-correction. Monthly outputs

produced by HadCM3 GCM for the 20th century climate experiment were obtained from the Programme for Climate Model Diagnosis and Inter-comparison (PCMDI) (https://esgcet.llnl.gov:8443/index.jsp) for the period 1950–1999, and for the same period NCEP/NCAR reanalysis outputs were obtained from http://www.esrl.noaa.gov/psd/, for providing the inputs to the downscaling model in reproducing the observed precipitation.

The HadCM3 outputs corresponding to the COMMIT GHG emission scenario were extracted from the PCMDI website (https://esgcet.llnl.gov:8443/index.jsp) for the period 2000–2099, to validate the performances of the bias-correction. The COMMIT GHG emission scenario assumed that the GHG concentrations at year 2000 are constant throughout the period 2000–2099. Therefore, it was assumed that the statistics of future precipitation (2000–2099) downscaled from the outputs of HadCM3 pertaining to COMMIT scenario will closely reflect the statistics of the past precipitation (1950–1999) simulated by HadCM3. For the future projections of precipitation at the station selected, monthly outputs of the HadCM3 GCM under the A2 and B1 scenarios (IPCC, 2000), defined in the Special Report on Emission Scenarios (SRES) of the Intergovernmental Panel on Climate Change (IPCC) were obtained from the PCMDI website (https://esgcet.llnl.gov:8443/index.jsp) for the period 2000–2099. A2 and B1 GHG emission scenarios described a world with rapid economic growth and a world with greater focus on environmental protection, respectively.

3. Generic methodology

The reproduction of observed precipitation at the station of interest using the downscaling model with the 20th century climate experiment outputs of the GCM is explained, in subsection 3.1. Also this subsection details the procedure followed in downscaling the future precipitation using the downscaling model. Subsection 3.2 describes the bias-correction of the past and future downscaled precipitation, against the observed precipitation.

3.1. Reproduction of past precipitation and projection of precipitation into future with GCM outputs

For each calendar month, GCM outputs of the 20th century climate experiment were standardized with the corresponding means and standard deviations of reanalysis outputs (used for the model development) relevant to the calibration period of the downscaling model. In the calibration of the downscaling model, the reanalysis outputs were standardized with their means and standard deviations pertaining to the calibration period. Hence, these means and standard deviations became fixed parts of the model. These standardized GCM outputs of the 20th century climate experiment were introduced to the downscaling model, for reproducing the past observed precipitation. In the same way, the standardized reanalysis outputs were introduced to the downscaling model for the reproduction of the past observed precipitation. The use of both GCM outputs of the 20th century climate experiment and reanalysis outputs enabled finding the capabilities of this model in reproducing past observations with these two sets of inputs obtained from two different sources. This was important as the downscaling model was developed with reanalysis outputs (refer to the first article of this series of articles) and it is used with GCM outputs in producing the projections into future.

The future GCM outputs for different GHG emission scenarios were standardized with the means and the standard deviations of reanalysis outputs (corresponding to calibration period of the downscaling model) for each calendar month and introduced to the downscaling model, for the projection of precipitation at the station of interest.

3.2. Bias-correction

The precipitation downscaled by the above model with GCM outputs was bias-corrected against the observed precipitation pertaining to the station of interest. The bias-correction was applied to the precipitation downscaled with GCM outputs as it was computationally efficient than bias-correcting each GCM output individually. Since the bias-correction techniques can be a source of uncertainty in statistical downscaling, Chen *et al.* (2011) investigated the use of several bias-correction techniques. Therefore, in this study the bias-correction was performed with three techniques: (1) EDQM, (2) MBC and (3) NBC. All these bias-correction techniques were applied separately on each calendar month and then for each technique the bias-corrected precipitation of each month was combined to produce the individual series. Bias-correction was performed for each calendar month in order to preserve the statistical attributes of precipitation in each calendar month. Considering the performances of these three bias-correction techniques, the best technique was identified. Thereafter the performances of the best bias-correction technique were validated. This was performed by comparing the statistics of the past observed precipitation with those of bias-corrected precipitation downscaled for a future GHG emission scenario (in this study the COMMIT scenario) which assumed that the GHG emission levels at the end of the 20th century remained constant throughout the 21st century. Owing to the above assumption it was assumed that this scenario which is pertaining to future could represent the statistics of the past climate simulated by the GCM closely. Following the validation, this bias-correction method was applied for the future precipitation projections produced by the downscaling model with GCM outputs.

3.2.1. Equidistant quantile mapping

EDQM (Li *et al.*, 2010) is a variant of the quantile mapping technique (Panofsky and Brier, 1968). In the EDQM technique, initially, the empirical CDFs were derived for the observed precipitation and precipitation downscaled with GCM outputs, for the past climate. Then the empirical CDF was developed for the precipitation

downscaled with GCM outputs, for the future climate under a GHG emission scenario. The periods which represented the past climate and the future climate were designated as period 1 and period 2, respectively.

The EDQM technique was applied in accordance with the following three steps (Salvi *et al.*, 2011). These three steps are graphically illustrated in Figure 1. In this figure, CDF1 and CDF2 correspond to the observed precipitation and precipitation reproduced by the downscaling model with GCM outputs respectively, for the past climate. CDF3 denotes the precipitation projected by the downscaling model with GCM outputs for a certain future GHG emission scenario. It should be noted that although this bias-correction technique corrects the CDF of the hydroclimatic variable, it does not explicitly correct the time series of the hydroclimatic variable.

3.2.1.1. Step 1: For a given precipitation value $a1$, the value $c1$ was found from CDF2 (see Step 1 in Figure 1). From CDF1, the precipitation value $a2$ that corresponded to $c1$ was determined (see Step 1 in Figure 1). $a2$ is the corrected precipitation value of $a1$. This corrective procedure was repeated for all precipitation values represented by CDF2. In other words, CDF2 was mapped onto CDF1. Once this mapping was performed, all the statistical properties of precipitation represented by CDF2 were automatically matched with those of CDF1. Hence, this step yielded the corrected CDF2 which exactly overlapped CDF1.

3.2.1.2. Step 2: Corresponding to a precipitation value $b1$, value $c2$ was found from CDF3 (see Step 2 in Figure 1). Pertaining to that CDF value $c2$, the difference of precipitation (d) between CDF3 (future climate) and CDF2 (past climate) was computed (the sign of d was also considered), as shown in Step 2 in Figure 2.

3.2.1.3. Step 3: The difference d (considering its sign) calculated in Step 2 pertaining to CDF value $c2$ was added to the corrected version of CDF2 (or CDF1) yielded in Step 1. This produced the bias-corrected precipitation value $b2$ corresponding to its original value of $b1$. Steps 2 and 3 were repeated until all the future precipitation values represented in CDF3 were corrected. The negative precipitation values yielded in the corrected CDF3 were set to zero. In order to obtain the same result described in Steps 2 and 3, alternatively, the difference between CDF2 and CDF1 could be subtracted from CDF3, in order to bias-correct CDF3 (Li *et al.*, 2010).

3.2.2. *Monthly bias-correction*

MBC is a relatively simple bias-correction method used by Johnson and Sharma (2012). In that study, it was used to correct the mean and the standard deviation of the precipitation output of a GCM with those of the observed precipitation. In this study, it was employed to correct the mean and the standard deviation of the precipitation downscaled with GCM outputs against those of observed precipitation.

Let monthly time series of precipitation downscaled with GCM outputs for a calendar month i be Y_i, for the past climate. As a first step, Y_i was standardized with its monthly mean ($\mu_{\mathrm{GCM},i}$) and standard deviation ($\sigma_{\mathrm{GCM},i}$) according to Equation (1). This yielded the standardized time series $Y_i{}'$ for each calendar month as follows:

$$Y_i{}' = \frac{Y_i - \mu_{\mathrm{GCM},i}}{\sigma_{\mathrm{GCM},i}} \tag{1}$$

Then this standardized precipitation time series for each calendar month i ($Y_i{}'$) was transformed back with Equation (2), using the monthly mean ($\mu_{\mathrm{Obs},i}$) and standard deviation ($\sigma_{\mathrm{Obs},i}$) of observed precipitation pertaining to the past climate. Equation (2) provided the monthly bias-corrected time series of precipitation downscaled with GCM outputs (Z_i). This bias-corrected time series of downscaled precipitation has the monthly mean and standard deviation of the observed precipitation.

$$Z_i = Y_i{}'.\sigma_{\mathrm{Obs},i} + \mu_{\mathrm{Obs},i} \tag{2}$$

For the correction of bias in future precipitation, the precipitation downscaled with GCM outputs for future were standardized with their means and standard deviations corresponding to the past climate following Equation (1), and transformed back with those of past observed precipitation according to Equation (2). In MBC, it is assumed that the bias in the mean and the standard deviation of the precipitation downscaled with GCM outputs for past climate (with respect to past observations) remains the same in the future. This assumption is also valid for the NBC detailed in the next subsection. In MBC, though the mean and the standard deviation of the precipitation downscaled with GCM outputs were explicitly corrected, the CDF of the precipitation was not corrected. Therefore, the CDF of precipitation downscaled with GCM outputs for the past, was different from that of observed precipitation. This fact was also valid for the NBC, explained in the following section.

3.2.3. *Nested bias-correction*

NBC, proposed by Johnson and Sharma (2012), is a more complex bias-correction technique than the monthly bias-correction. While the MBC corrects the mean and the standard deviation in each calendar month, NBC corrects the mean, the standard deviation and the lag 1 autocorrelations, simultaneously at both monthly and annual time scales.

Like in MBC, in NBC, first the time series of precipitation downscaled with GCM outputs (for past climate) for each calendar month (Y_i) was standardized according to Equation (1). Then the lag 1 auto correlations ($\Omega_{\mathrm{GCM},i}$) in the above standardized precipitation time series were replaced with the corresponding lag 1 auto correlations

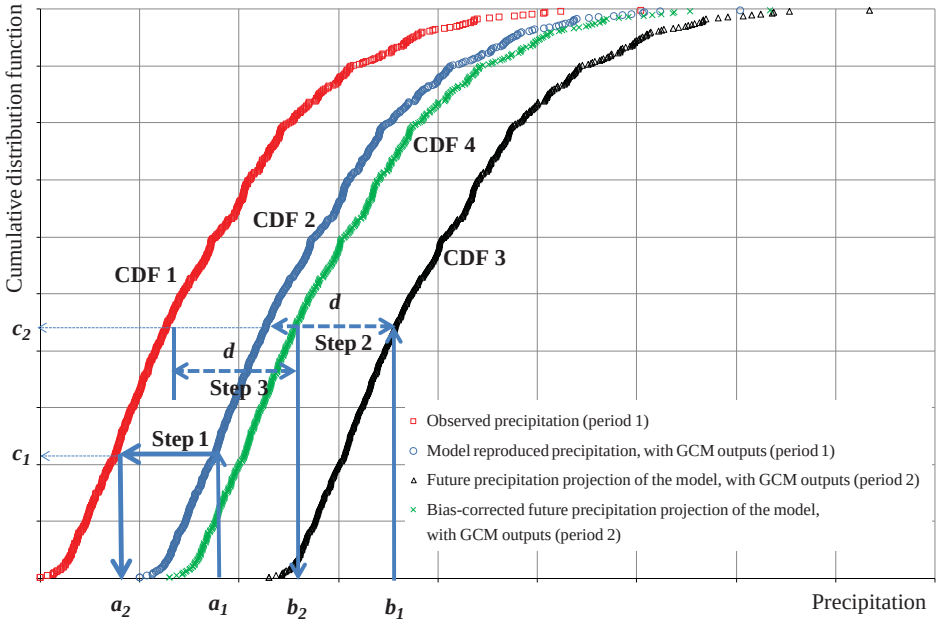

Figure 1. Equidistant quantile mapping.

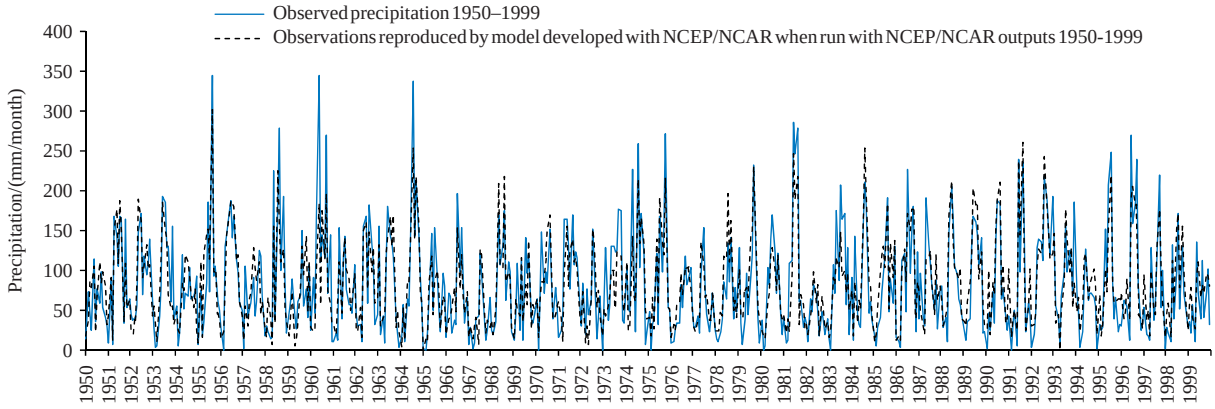

Figure 2. Time series plot for downscaling model run with NCEP/NCAR outputs as inputs (1950–1999).

in the observed precipitation ($\Omega_{\mathrm{Obs},i}$) to produce $Y_i{}''$ as shown in Equation (3). Lag 1 auto correlation for month i was calculated as the correlation between the monthly precipitation time series of month i and month $i-1$.

$$Y_i{}'' = \Omega_{\mathrm{Obs},i}\,.\,Y_{i-1}{}'' + \sqrt{1-\Omega^2_{\mathrm{Obs},i}}\cdot\left(\frac{Y_i{}' - \Omega_{\mathrm{GCM},i}\,Y_{i-1}{}'}{\sqrt{1-\Omega^2_{\mathrm{GCM},i}}}\right) \tag{3}$$

Then Y''_i was transformed back with the mean ($\mu_{\mathrm{Obs},i}$) and the standard deviation ($\sigma_{\mathrm{Obs},i}$) of observed precipitation for each calendar month, as shown in Equation (4).

$$Y'''_i = Y''_i.\sigma_{\mathrm{Obs},i} + \mu_{\mathrm{Obs},i} \tag{4}$$

The bias-corrected monthly time series of downscaled precipitation yielded in Equation (4) has the monthly lag 1 auto correlations, the mean and the standard deviation of the observed precipitation.

Next, these rescaled monthly precipitation time series (Y'''_i) in Equation (4) were summed to produce annual precipitation (Z_j) for each year j. This annual time series of precipitation was standardized with annual mean (μ_{GCM}) and standard deviation (σ_{GCM}) of the precipitation downscaled with GCM outputs, following Equation (5).

$$Z_j{}' = \frac{Z_j - \mu_{\mathrm{GCM}}}{\sigma_{\mathrm{GCM}}} \tag{5}$$

Thereafter, the annual lag 1 autocorrelations in Z'_j were replaced with those in the observed precipitation (Ω_{Obs}) to produce Z''_j as shown in Equation (6). The annual lag 1 autocorrelations were computed as the correlation between precipitation in a certain year and

the following year.

$$Z_j'' = \Omega_{\text{Obs}}.Z_{j-1}'' + \sqrt{1-\Omega_{\text{Obs}}^2}.\left(\frac{Z_j' - \Omega_{\text{GCM}}.Z_{j-1}'}{\sqrt{1-\Omega_{\text{GCM}}^2}}\right) \quad (6)$$

The annual time series modified in Equation (6) was rescaled with the annual mean (μ_{Obs}) and the annual standard deviation (σ_{Obs}) of observed precipitation time series, as given in Equation (7).

$$Z_j''' = Z_j''.\sigma_{\text{Obs}} + \mu_{\text{Obs}} \quad (7)$$

The bias-corrected annual time series of downscaled precipitation yielded in Equation (7) has the annual lag 1 auto correlations, the mean and the standard deviation of the observed precipitation.

Finally, the monthly time series of precipitation downscaled with GCM outputs were corrected using Equation (8).

$$Y_{i,j} = \frac{Z'''_j}{Z_j}.Y'''_{i,j} \quad (8)$$

The future precipitation projections downscaled with GCM outputs were nested bias-corrected with the statistics of observed precipitation and precipitation downscaled with GCM outputs for the past climate, following the procedure described in Equations (3) to (8).

3.2.4. Potential of bias-correcting GCM outputs against reanalysis outputs

In this study, the precipitation downscaled with GCM outputs were bias-corrected against the observed precipitation. However, the bias-correction of each GCM output prior to its use on the downscaling model may seem to be a better option, as it removes the bias in each input variable of the downscaling model, individually. Although this method is computationally more expensive than the correction of bias in the precipitation downscaled from GCM outputs, it was important to verify whether the individual bias-correction of each GCM output is beneficial than its counterpart technique. In the absence of any readily available observations corresponding to the GCM outputs, the reanalysis outputs can be used as the reference for the bias-correction.

Instead of bias-correcting each GCM output against the corresponding reanalysis output, in this study, the benefit of this approach (if any) was deduced indirectly. For this purpose, the scatter of the precipitation output of the GCM, was plotted against the precipitation output of reanalysis data, for all four seasons. It is noteworthy to state here that the precipitation output of the GCM was identified as the most dominant potential predictor on the monthly observed precipitation, in the first article of this series. It was assumed that, the magnitudes of the scatter of the other GCM outputs used in the downscaling model were similar to that of the precipitation output of GCM. Therefore, only the precipitation output of the GCM was considered in this analysis. Meanwhile, the scatter plots were also prepared for the precipitation downscaled with GCM outputs (before bias-correction) against the observed precipitation, for all seasons. Then the scatter of the precipitation downscaled with the outputs of the GCM (plotted against observed precipitation) was compared both visually and numerically with that of raw precipitation output of the GCM (plotted against reanalysis outputs). The numerical comparison of the magnitudes of the above described two scatter was performed considering the coefficient of determination (R^2).

Johnson and Sharma (2012) stated that, if the magnitude of the scatter of the variable to be bias-corrected is large (if large bias is present), then the bias-correction will not be effective. Therefore, it was understood that when the scatter of the raw outputs produced by the GCM is large, then the bias-correction of these GCM outputs prior to downscaling will not bring any additional advantage over the bias-correction of precipitation downscaled with the same GCM outputs.

4. Application

The generic methodology described in Section 3 was applied to the precipitation station at the Halls Gap post office in the operational area of GWMWater.

4.1. Reproduction of past precipitation and projection of precipitation into future with HadCM3 outputs

In this article, the downscaling model was run with both NCEP/NCAR reanalysis and HadCM3 20th century climate experiment data, for the reproduction of observed precipitation at the station of interest. The HadCM3 outputs were available at the spatial resolution of 2.75° latitude by 3.75° longitude. Owing to the mismatch of spatial resolutions between the NCEP/NCAR reanalysis outputs (2.5° latitude by 2.5° longitude) and HadCM3, the HadCM3 outputs were interpolated to the NCEP/NCAR grid (refer to Figure 1 in the first article of this series of articles) using the inverse distance weighted method (Ghosh and Mujumdar, 2008). The HadCM3 20th century climate experiment outputs for the period 1950–1999 were standardized with the means and the standard deviations of the corresponding NCEP/NCAR reanalysis outputs pertaining to the period 1950–1989 (calibration phase of this downscaling model) for each calendar month, before their application to the downscaling model. The means and the standard deviations of the NCEP/NCAR reanalysis output pertaining to the period 1950–1989 (calibration phase of the downscaling model) were treated as stationary components of the downscaling model. Figures 2 and 3 show the time series plots for the precipitation output of the downscaling model, with NCEP/NCAR and HadCM3 outputs respectively, over the period 1950–1999. The future precipitation projections were produced by introducing the HadCM3 outputs

corresponding to possible future climate, as inputs to the downscaling model, as described later in this article.

According to Figures 2 and 3, it was seen that, when the downscaling model developed with NCEP/NCAR outputs was run with HadCM3 outputs as inputs, it tended to overestimate the majority of precipitation compared to both observations and precipitation downscaled with NCEP/NCAR reanalysis outputs. This reflected the bias inherent in HadCM3 outputs with respect to that of NCEP/NCAR reanalysis outputs. The same finding was more clearly seen in scatter plot (b) of Figure 4. In scatter plot (a) of Figure 4, a good agreement between the precipitation downscaled with NCEP/NCAR outputs and the observations was seen (for more details refer to the first article). When the downscaling model was run with NCEP/NCAR outputs it displayed a Nash–Sutcliffe efficiency (NSE) (Nash and Sutcliffe, 1970) of 0.67 and a coefficient of determination (R^2) of 0.75. However, when the downscaling model was run with HadCM3 outputs those two statistics dropped to −0.62 and 0.12, respectively.

Table 1 shows the performances of the downscaling model when run with NCEP/NCAR and HadCM3 outputs as inputs, in reproducing the observed monthly precipitation over the period 1950–1999. It also shows the statistics of the raw precipitation output of HadCM3 at grid point {4,4} of the atmospheric domain. It is noteworthy to state that the NCEP/NCAR reanalysis outputs are quality controlled and corrected against observations (Kalnay *et al.*, 1996). Since this downscaling model was calibrated and validated with NCEP/NCAR outputs, it inherently had an advantage in reproducing the observed precipitation better with NCEP/NCAR outputs, than that with HadCM3 outputs. The model was able to reproduce the average, the standard deviation and the coefficient of variation of observed precipitation with good accuracy in the period 1950–1999, when it was run with NCEP/NCAR reanalysis outputs. Also it displayed a Seasonally Adjusted Nash–Sutcliffe efficiency (SANS) (Wang, 2006; Sachindra *et al.*, 2013) of 0.79, resembling its good capabilities in reproducing observed precipitation. When the same model was run with HadCM3 outputs, it largely overpredicted the average of the precipitation. The standard deviation in the observations was properly captured by the model, when it was run with HadCM3 outputs. However, the performances of this model were limited according to the NSE, SANS and R^2 as shown in Table 1.

In Table 1, it was seen that raw precipitation output of HadCM3 severely underestimated the average and the standard deviation of the observed precipitation over the period 1950–1999. Also the SANS and the R^2 of the raw precipitation output of HadCM3 were quite low in comparison to those of precipitation reproduced by the downscaling with the outputs of HadCM3. Hence it was realized that the precipitation reproduced by the downscaling model with the outputs of HadCM3 are in better agreement with observations with respect to that of raw precipitation simulated by HadCM3.

4.2. Bias-correction

In this section, the application of the three bias-correction techniques to the precipitation downscaled with HadCM3 20th century climate experiment outputs is detailed. The precipitation downscaled with HadCM3 outputs was bias-corrected against the observed precipitation. The potential of bias-correcting raw outputs of HadCM3 against the corresponding NCEP/NCAR outputs are discussed at the end of this section.

4.2.1. Bias-correction of precipitation downscaled with HadCM3 outputs

EDQM, MBC and NBC (described in Section 3.2) were applied to the precipitation downscaled with the HadCM3 outputs. All bias corrections were performed over the 50-year period from 1950 to 1999, against the observed precipitation (considered as the reference precipitation for bias-correction) at the station of interest. Table 2(a) and b shows the season-based statistics of the observed precipitation and that reproduced by the downscaling model with NCEP/NCAR and HadCM3 outputs, before and after the application of the three bias-correction techniques. Table 2(a) refers to summer (December–February) and autumn (March–May), while Table 2(b) refers to winter (June–August) and spring (September–November). According to Table 2(a) and (b), it was seen that all three bias-correction techniques were capable in correcting the average of the precipitation downscaled with HadCM3 outputs adequately, in all four seasons. EDQM and MBC near-perfectly corrected the standard deviation in the precipitation reproduced with HadCM3 outputs, in all seasons. The NBC properly corrected the standard deviation of precipitation in summer and autumn, but an over estimation of it was seen in winter and spring. In NBC, initially the monthly lag 1 autocorrelations, the means and the standard deviations were corrected. This was followed by the correction of the annual lag 1 autocorrelations, the means and the standard deviations. Owing to this monthly to annual nesting procedure employed in NBC, slight distortions of monthly mean and standard deviation of precipitation could occur in some seasons. The coefficient of variations in the precipitation downscaled with HadCM3 were corrected by all three bias-correction techniques successfully, despite the slight over-estimation seen in winter and spring by NBC, which was due to the over-estimation of standard deviation described earlier. Overall, all three bias-correction techniques adequately corrected the average, the standard deviation and the coefficient of variation in all four seasons. Skewness of precipitation was well corrected in all four seasons by the EDQM technique. This is because, in EDQM, the CDF to be corrected is mapped onto the reference CDF, allowing all statistical moments to be matched. As described in subsections 3.2.2 and 3.2.3, in MBC and NBC, no explicit measure was taken to correct the skewness in precipitation. All bias-correction techniques were capable in improving the NSE of the precipitation reproduced with HadCM3 outputs in summer, autumn and winter.

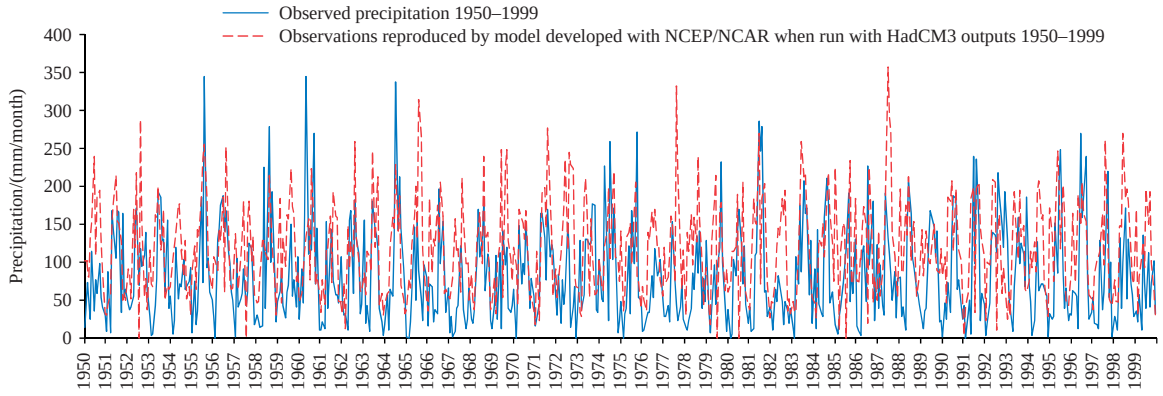

Figure 3. Time series plot for downscaling model run with HadCM3 outputs as inputs (1950–1999).

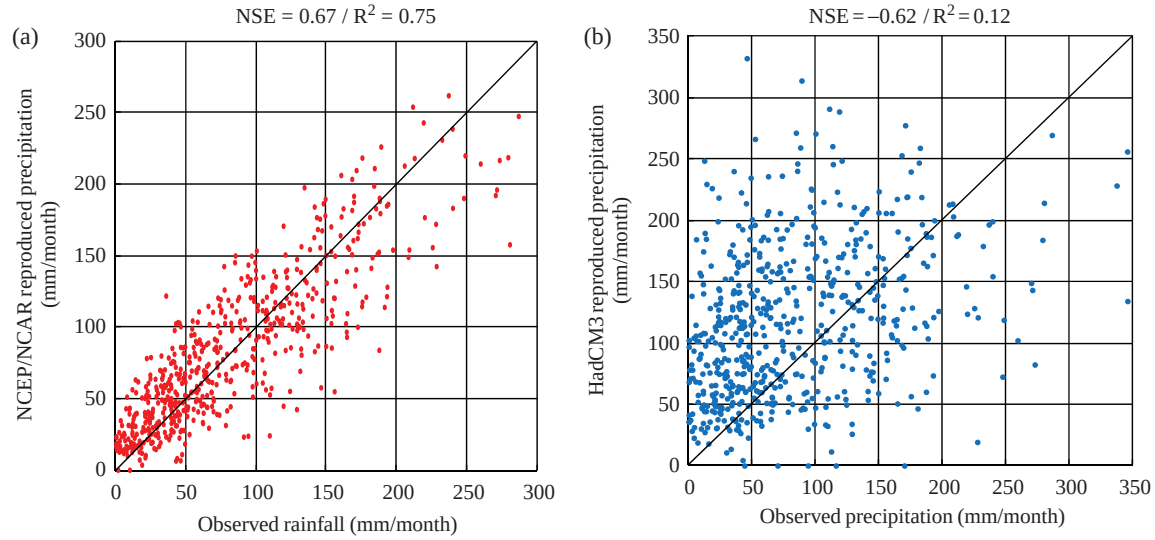

Figure 4. Scatter plots for downscaling model runs with (a) NCEP/NCAR and (b) HadCM3 outputs as inputs (1950–1999).

On the other hand, there was hardly any improvement to R^2 values of precipitation, after the bias-correction.

Figure 5 shows the seasonal scatter of the precipitation reproduced with HadCM3 outputs against the observed precipitation, before and after the application of three bias-correction methods. Before the application of the bias-corrections, during all four seasons, there was large scatter in precipitation, which mainly resembled an over-predicting trend. After each bias-correction, this large over-predicting trend reduced and it became a more balanced over and under-predicted scatter. In all four seasons, the scatter of precipitation after each bias-correction was visually similar to each other. However, the scatter which was seen prior to the bias-corrections did not shrink significantly after the application of any of the bias-correction techniques, in any of the four seasons. This is an indication that, these three bias-correction techniques hardly enhanced the accuracy of the time series of precipitation. Hence, it can be stated that when the scatter is very large as seen in Figure 5, the correction of the time series becomes difficult. However, all three bias-correction techniques were able to correct the statistics of precipitation downscaled with HadCM3 outputs. Therefore, it was argued that the bias-corrected precipitation should be interpreted as a probabilistic prediction/projection, rather than from the point of view of a time series. For this purpose, EDQM was identified as the most suitable bias-correction technique as it preserves all statistical moments of the reference precipitation (in this study the observed precipitation for the period 1950–1999) for the past climate. Therefore, in this study, the EDQM was used for the bias-correction of future precipitation downscaled with HadCM3 outputs.

4.2.2. Validation of performances of EDQM technique

It is important to validate the performance of the EDQM technique prior to its use in the bias-correction of future precipitation projections. For this purpose, the statistics of the observed precipitation for the period 1950–1999 were compared with those of bias-corrected future precipitation downscaled with HadCM3 COMMIT emission scenario outputs for the period 2000–2099. The COMMIT is an idealized GHG emission scenario which assumes the GHG concentrations in the atmosphere at year 2000

Table 1. Performances of downscaling model with NCEP/NCAR and HadCM3 outputs.

Statistic	Period (1950–1999)			
	Observations	With NCEP/ NCAR outputs	With HadCM3 outputs	Raw HadCM3 Precipitation at grid point {4,4}
Avg	**81.8**	83.1	117.4	46.2
SD	**62.2**	53.8	61.8	28.4
C_v	**0.76**	0.65	0.52	0.61
NSE		0.67	−0.62	−0.27
SANS		0.79	0.26	−0.71
R^2		0.75	0.12	0.08

Avg = average of monthly precipitation in mm; SD = standard deviation of monthly precipitation in mm; C_v = coefficient of variation; SANS = seasonally adjusted Nash Sutcliffe efficiency; NSE = Nash–Sutcliffe efficiency; R^2 = coefficient of determination. Bold values refer to statistics of observed precipitation.

(CO_2 concentration in the atmosphere $\approx$ 370 ppm) to be the same throughout the 21st century (Ojha *et al.*, 2010). Owing to the above attribute of the COMMIT emission scenario, it was assumed that it can closely characterize the climate simulated by HadCM3 in the latter half of the 20th century (1950–1999) during which the rise in the concentrations of GHGs was limited. In other words, a good agreement between the outputs of HadCM3 relevant to the 20th century climate experiment and for the COMMIT emission scenario was assumed. Furthermore, according to a study by Ojha *et al.* (2010), there is a close relation between the past observed precipitation and that statistically downscaled from the GCM outputs corresponding to the COMMIT scenario. Hence, in this study it was argued that if the statistics of the bias-corrected future precipitation downscaled from the HadCM3 COMMIT outputs were in close agreement with those of past observations, the EDQM technique has proven capabilities in bias-correcting future precipitation with adequate accuracy.

As a proof of the agreement between HadCM3 outputs of the 20th century climate experiment and those of COMMIT emission scenario, a comparison of the statistics of several potential predictors used in this study was performed. For this purpose, the HadCM3 simulated 1000 hPa specific humidity, 850 hPa relative humidity, 850 hPa zonal wind speed and precipitation corresponding to the 20th century climate experiment and the COMMIT emission scenario were interpolated to grid point {4,4} (refer to Figure 1 of the first article of this series of articles) using the inverse distance weighted method. Then the statistics of the above variables were computed for the 20th century climate experiment for the period 1950–1999 and also for the COMMIT emission scenario for the period 2000–2099. The comparison of these statistics of the potential predictors is shown in Table 3. In Table 3, it was seen that there is a very good agreement between the average, the standard deviation and the coefficient of variation of the potential variables simulated by HadCM3 under the 20th century climate experiment and the COMMIT emission scenario. It was assumed that, this is valid for all potential predictors used in this study.

For the validation of the performances of the EDQM technique, first the HadCM3 monthly outputs for the COMMIT emission scenario pertaining to the period 2000–2099 were standardized with the monthly means and the standard deviations of the corresponding NCEP/NCAR reanalysis outputs, relevant to the period 1950–1989 (model calibration period). Then these standardized HadCM3 outputs for the COMMIT scenario were introduced to the downscaling model for projecting the monthly precipitation at the station of interest. For bias-correcting, observed precipitation for the period 1950–1999 was considered as the reference set of data, which is denoted by CDF1 in Figure 1. The CDF2 in the same figure refers to the precipitation downscaled with HadCM3 20th century climate experiment outputs for the same period. The future precipitation downscaled with HadCM3 COMMIT outputs for the period 2000–2099 was depicted by CDF3 in Figure 1. Following the EDQM procedure detailed in subsection 3.2.1, the future precipitation downscaled with HadCM3 outputs for the COMMIT scenario was bias-corrected. The statistics of the monthly precipitation downscaled with HadCM3 outputs for the COMMIT emission scenario before and after the bias-correction, for the future period 2000–2099, were compared with those of observed precipitation pertaining to the period 1950–1999, in Table 4(a) and (b). Table 4(a) refers to summer (December–February) and autumn (March–May), while Table 4(b) refers to winter (June–August) and spring (September–November). In Table 4(a) and (b), COMMIT (Before) and COMMIT (After) refer to the precipitation downscaled with HadCM3 COMMIT outputs, before and after the bias-correction, respectively.

As shown in Table 4(a) and (b), prior to the bias-correction, it was seen that the averages of the precipitation downscaled from HadCM3 COMMIT outputs were quite larger than those of observed precipitation, for all seasons. After the bias-correction, it was seen that the precipitation downscaled from HadCM3 COMMIT outputs, were able to reproduce the average of observed precipitation with good accuracy, in winter and spring. Despite some over-estimation, following the bias-correction, the averages of precipitation downscaled from COMMIT outputs for summer and autumn adequately agreed with those of observations. Before the bias-correction, except in autumn, the standard deviation of the precipitation

Table 2. Statistics of precipitation before and after bias-correction for (a) summer and autumn and (b) winter and spring.

(a)	Summer (1950–1999)						Autumn (1950–1999)					
Statistic	Before bias-correction			After bias-correction			Before bias-correction			After bias-correction		
	Obs	With NCEP/NCAR outputs	With HadCM3 outputs	EDQM	MBC	NBC	Obs	With NCEP/ NCAR outputs	With HadCM3 outputs	EDQM	MBC	NBC
Avg	**41.4**	44.3	73.6	41.5	44.8	41.4	**70.4**	70.7	117.7	70.4	70.9	68.0
SD	**36.6**	28.6	39.9	36.8	36.1	36.9	**56.8**	44.7	45.5	56.8	55.9	55.6
C_v	**0.88**	0.65	0.54	0.89	0.86	0.89	**0.81**	0.63	0.39	0.80	0.79	0.82
Skewness	**1.62**	1.34	1.28	1.63	1.57	1.94	**1.36**	0.70	−0.20	1.36	0.91	1.04
NSE		0.62	−0.41	0.13	0.18	0.16		0.71	0.64	0.69	0.70	0.69
R^2		0.52	0.01	0.02	0.03	0.03		0.65	0.09	0.04	0.04	0.03

(b)	Winter (1950–1999)						Spring (1950–1999)					
Statistic	Before bias-correction			After bias-correction			Before bias-correction			After bias-correction		
	Obs	With NCEP/NCAR outputs	With HadCM3 outputs	EDQM	MBC	NBC	Obs	With NCEP/NCAR outputs	With HadCM3 outputs	EDQM	MBC	NBC
Avg	**127.3**	128.7	164.5	126.9	127.5	126.3	**88.1**	88.7	113.9	88.1	88.3	87.6
SD	**64.8**	55.7	68.2	65.2	64.4	75.2	**53.7**	43.7	53.4	53.7	53.4	60.4
C_v	**0.51**	0.43	0.41	0.51	0.50	0.59	**0.61**	0.49	0.47	0.61	0.60	0.69
Skewness	**0.76**	0.39	−0.20	0.73	0.55	0.87	**1.09**	0.99	0.65	1.09	0.82	1.11
NSE		0.85	0.11	0.32	0.34	0.23		0.80	−0.73	−0.85	−0.82	−1.15
R^2		0.72	0.00	0.01	0.01	0.01		0.69	0.03	0.00	0.00	0.00

Avg = average of monthly precipitation in mm; SD = standard deviation of monthly precipitation in mm; C_v = coefficient of variation; Skewness = (Avg − Mode)/SD; NSE = Nash–Sutcliffe efficiency; R^2 = coefficient of determination; Obs = observed monthly precipitation; EDQM = equidistant quantile mapping; MBC = monthly bias-correction; NBC = nested bias-correction. Bold values refer to statistics of observed precipitation.

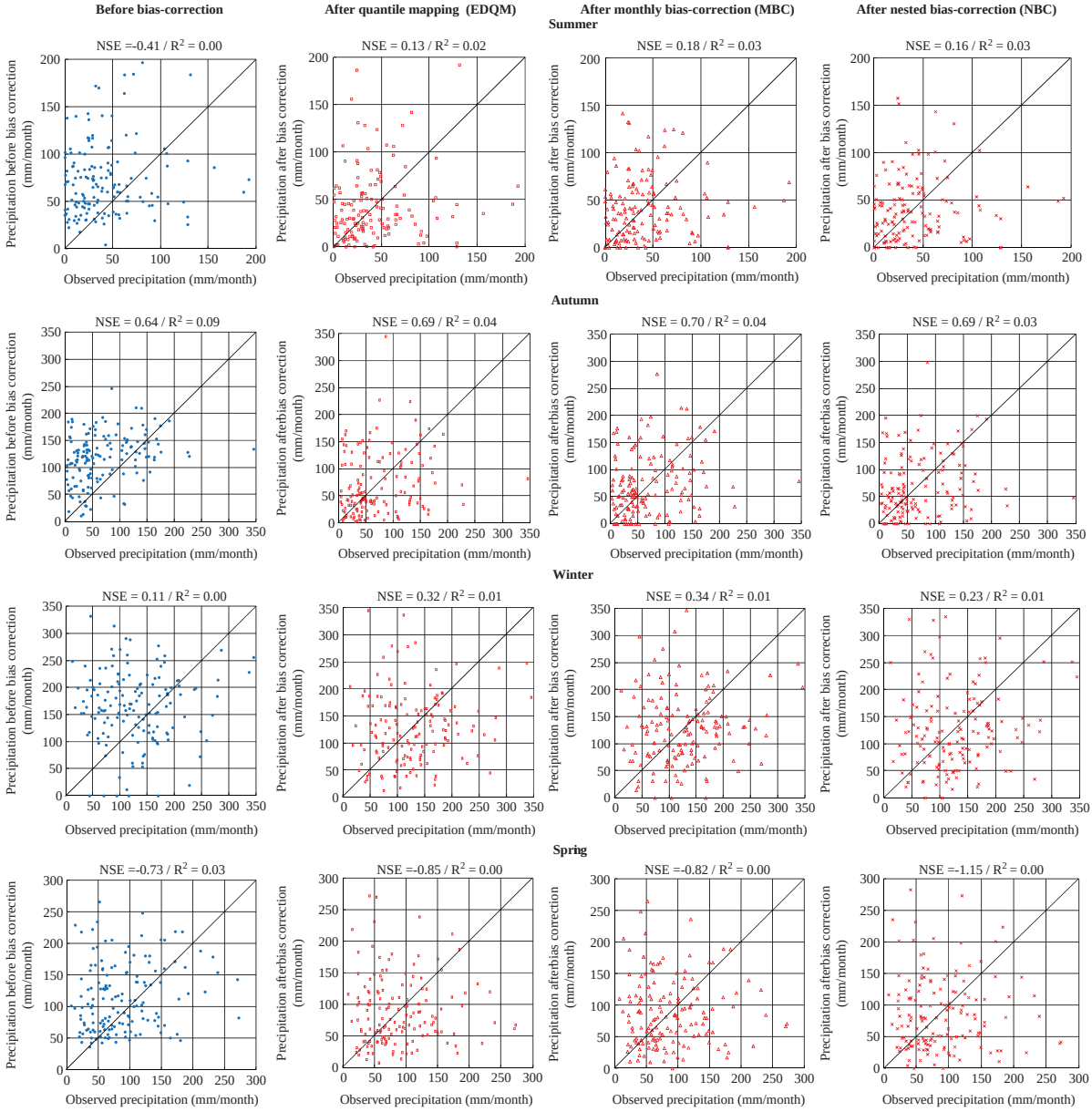

Figure 5. Seasonal scatter plots for precipitation downscaled with HadCM3 outputs, before and after bias-correction (1950–1999).

downscaled with HadCM3 COMMIT outputs displayed an over-predicting trend. Even after the bias-correction this trend was evident in all seasons.

In this study, empirical distribution functions of the observed precipitation and precipitation downscaled from HadCM3 outputs were used in applying the EDQM technique. This raised the need of frequent interpolation and extrapolation of the CDFs of observed precipitation and that downscaled with HadCM3 20th century climate experiment outputs. This procedure increases the severity of low and high extreme precipitation. The over-prediction of the maximum monthly precipitation was due to the extrapolation of the above CDFs and it can be minimized by fitting suitable theoretical distribution functions to the observed and downscaled precipitation time series, prior to the application of the EDQM technique (Li *et al.*, 2010). However, it should be noted that when a theoretical distribution function is fitted to a dataset, inevitably, there will be fitting errors as no theoretical distribution function can perfectly describe any precipitation dataset.

Before the bias-correction, the 10th, 25th, 50th, 75th and 90th percentiles of the downscaled precipitation for COMMIT scenario were largely over-estimated, in all seasons. After the bias-correction, in all seasons, the over-estimating characteristic of the above percentiles of precipitation downscaled with HadCM3 COMMIT outputs reduced. In all four seasons, the percentages of months with zero precipitation were over-estimated. However, this trend was minimal in summer. After the bias-correction, the percentages of months with above average

Table 3. Comparison of statistics of potential predictors between the 20th century climate experiment and the COMMIT scenario.

Statistic	Precipitation (mm)		1000 hPa Specific humidity (grams kg^{-1})		850 hPa Relative humidity (%)		850 hPa Zonal wind speed (m s^{-1})	
	20C3M 1950–1999	COMMIT 2000–2099	20C3M 1950–1999	COMMIT 2000–2099	20C3M 1950–1999	COMMIT 2000–2099	20C3M 1950–1999	COMMIT 2000–2099
Avg	47.9	45.2	7.2	7.7	63.7	63.8	4.2	4.2
SD	30.4	27.5	1.0	1.1	9.6	9.4	3.2	3.3
C_v	0.63	0.61	0.14	0.14	0.15	0.15	0.75	0.79

Avg = average; SD = standard deviation; C_v = coefficient of variation; 20C3M = 20th century climate experiment; COMMIT = COMMIT emission scenario.

precipitation under the COMMIT scenario matched with those of observations, in all seasons acceptably.

4.2.3. Potential of bias-correcting HadCM3 outputs against NCEP/NCAR outputs

Although the bias was prevalent in the HadCM3 outputs (as shown in the first article of this series of articles), in this study, the bias-correction was performed on the precipitation downscaled with the HadCM3 outputs. This method was employed as it was computationally much cheaper than bias-correcting each output of HadCM3 individually, prior to their use in downscaling. However, theoretically, the bias-correction of each GCM output individually, before introducing to a downscaling model seems to be a more effective approach than the correction of bias in the precipitation downscaled with raw GCM outputs. In the absence of any readily available observations corresponding to the GCM outputs used in the downscaling model, the bias-correction of these GCM outputs can be performed against the pertaining NCEP/NCAR or any other reanalysis outputs (e.g. Salvi *et al.*, 2011).

According to Figure 5, it was seen that if the scatter of the variable to be bias-corrected (e.g. precipitation downscaled with GCM outputs) was large, none of the bias-correction techniques used in this study was capable in adequately reducing this scatter. If the scatter was not adequately reduced, the time series of the variable is also not properly corrected. Based on this argument, it was decided to visualize the raw precipitation output of HadCM3 against that of NCEP/NCAR in scatter plots, pertaining to grid point {4,4} (refer to Figure 1 in the first article, for the location of this grid point), for each season. The grid point {4,4} referred to the point which was located closest to the precipitation station considered in this study. In the first article, precipitation output of HadCM3 at grid point {4,4} was identified as the most influential potential variable on the observed monthly precipitation.

Figure 6 shows the scatter plots of raw precipitation output of HadCM3 against that of NCEP/NCAR for the period 1950–1999, corresponding to grid point {4,4}. As shown in Figure 6, it is realized that there is large scatter in the raw precipitation outputs of HadCM3 in all four seasons. The very low R^2 values in all seasons numerically verified the presence of large scatter in precipitation outputs of HadCM3. It is also reasonable to assume that, such large scatter is prevalent in the other outputs of HadCM3 which were used in the downscaling model, since all these outputs were produced by the same GCM. Therefore, it was deduced that if the HadCM3 outputs were bias-corrected against the NCEP/NCAR reanalysis outputs with any of the bias-correction techniques used in this study, the improvement to their time series will be minimal. Without considerable improvement to the time series of HadCM3 outputs, it was difficult to expect any improvement to the precipitation downscaled with these individually bias-corrected HadCM3 outputs. Hence, the bias-correction of outputs of HadCM3, prior to downscaling, was identified as a procedure which brings no additional advantage.

4.3. Future precipitation projections

4.3.1. Greenhouse gas emission scenarios

For this study, two GHG emission scenarios namely; A2 and B1 were selected. A2 is a relatively high GHG emission scenario due to its economic focus. On the other hand, the B1 GHG emission scenario described a world with high level of concern on the environment and sustainable development. Therefore, it refers to relatively low level of GHG emissions. The A2 and B1 GHG emission scenarios referred to carbon dioxide concentrations of about 850 ppm and 550 ppm, respectively, by the end of the 21st century (IPCC, 2000). The downscaling model was used to project the future precipitation at the station of interest, up to year 2099. HadCM3 outputs for the A2 and B1 GHG emission scenarios of the IPCC were obtained from the PCMDI website (https://esgcet.llnl.gov:8443/index.jsp), for the period 2000–2099, and used as the inputs to the downscaling model used in this study.

4.3.2. Bias-corrected future precipitation projections

HadCM3 outputs for the A2 and B1 IPCC SRES GHG emission scenarios for the period 2000–2099 were standardized with the means and the standard deviations of the corresponding NCEP/NCAR reanalysis outputs, pertaining to the model calibration period which spanned over 1950–1989. Thereafter, these standardized HadCM3 outputs were introduced to the downscaling model. This allowed the monthly precipitation projections at the

Table 4. Seasonal statistics of observed and COMMIT precipitation for (a) summer and autumn and (b) winter and spring.

(a)	Summer			Autumn		
Statistic	1950–1999	2000–2099		1950–1999	2000–2099	
	Obs	COMMIT (Before)	COMMIT (After)	Obs	COMMIT (Before)	COMMIT (After)
Avg	**41.4**	*87.6*	55.6	**70.4**	*124.9*	78.7
SD	**36.6**	*57.4*	51.1	**56.8**	*51.0*	65
C_v	**0.88**	*0.65*	0.92	**0.81**	*0.41*	0.83
Minimum precipitation	**0.0**	*14.2*	0.0	**2.8**	*10.1*	0.0
Maximum precipitation	**192.3**	*347.0*	301	**345.4**	*271.0*	385
10th Percentile	**4.2**	*34.6*	5.3	**11.4**	*55.1*	13.6
25th Percentile	**16.4**	*46.7*	18.0	**30.1**	*82.7*	29.0
50th Percentile	**30.7**	*68.7*	45.1	**49.1**	*130.5*	61.4
75th Percentile	**54.9**	*112.6*	82.3	**108.6**	*161.1*	122.9
90th Percentile	**90.7**	*159.3*	114.9	**148.7**	*187.4*	168.1
Percentage of months with zero precipitation	**4**	*0*	6	**0**	*0*	6
Percentage of months with above average precipitation	**39**	*38*	37	**39**	*53*	41

(b)	Winter			Spring		
Statistic	1950–1999	2000–2099		1950–1999	2000–2099	
	Obs	COMMIT (Before)	COMMIT (After)	Obs	COMMIT (Before)	COMMIT (After)
Avg	**127.3**	*161.1*	124.3	**88.1**	*116.7*	91.5
SD	**64.8**	*72.9*	71.5	**53.7**	*67.3*	71.6
C_v	**0.51**	*0.45*	0.58	**0.61**	*0.58*	0.78
Minimum precipitation	**12.2**	*2.0*	0.0	**7.6**	*23.1*	0.0
Maximum precipitation	**345.2**	*387.5*	424.1	**272.4**	*321.6*	346.5
10th Percentile	**47.8**	*63.1*	41.4	**31.4**	*48.4*	17.4
25th Percentile	**77.4**	*109.0*	73.2	**48.7**	*63.2*	41.5
50th Percentile	**119.3**	*163.1*	118.2	**73**	*95.7*	67.9
75th Percentile	**167.6**	*208.5*	170.8	**118.8**	*156.8*	125.0
90th Percentile	**207.7**	*254.9*	202.5	**156.1**	*218.2*	198.6
Percentage of months with zero precipitation	**0**	*0*	5	**0**	*0*	3
Percentage of months with above average precipitation	**47**	*51*	47	**43**	*40*	41

Avg = average of monthly precipitation in mm; SD = standard deviation of monthly precipitation in mm; C_v = coefficient of variation; COMMIT (Before) = Precipitation downscaled for COMMIT scenario before bias-correction (italicized values); COMMIT (After) = Precipitation downscaled for COMMIT scenario after bias-correction. Bold values refer to statistics of observations.

station of interest up to year 2099. The precipitation projections under A2 and B1 emission scenarios by the downscaling model were bias-corrected using the EDQM technique, as detailed in subsection 3.2.1.

In Table 5, the statistics of the future precipitation projections for the period 2000–2099 are shown against those of observed precipitation for the period 1950–1999. The percentage changes in the statistics of the future precipitation projections with respect to the statistics of observed precipitation of the period 1950–1999 are also provided within parentheses in Table 5. According to Table 5, at the station of interest, in summer and spring, the average of monthly precipitation for the period 2000–2099 showed a decline under both A2 and B1 emission scenarios. On the other hand, in winter, both A2 and B1 emission scenarios indicated a rise in the average of monthly precipitation. During autumn, only A2 emission scenario showed a rise in the average of the monthly precipitation. The standard deviation of the precipitation under both A2 and B1 scenarios increased in all seasons in comparison to that of observations corresponding to the period 1950–1999. The two sample *t*-test revealed that the changes in the average of future precipitation in autumn and winter under both A2 and B1 scenarios are not significant at the 95% confidence level. However, it was found that the decrease in the average of precipitation projected into future in spring was significant at the 95% confidence level for both GHG emission scenarios. Furthermore, the two sample *F*-test revealed that the rise in the standard deviation of the precipitation

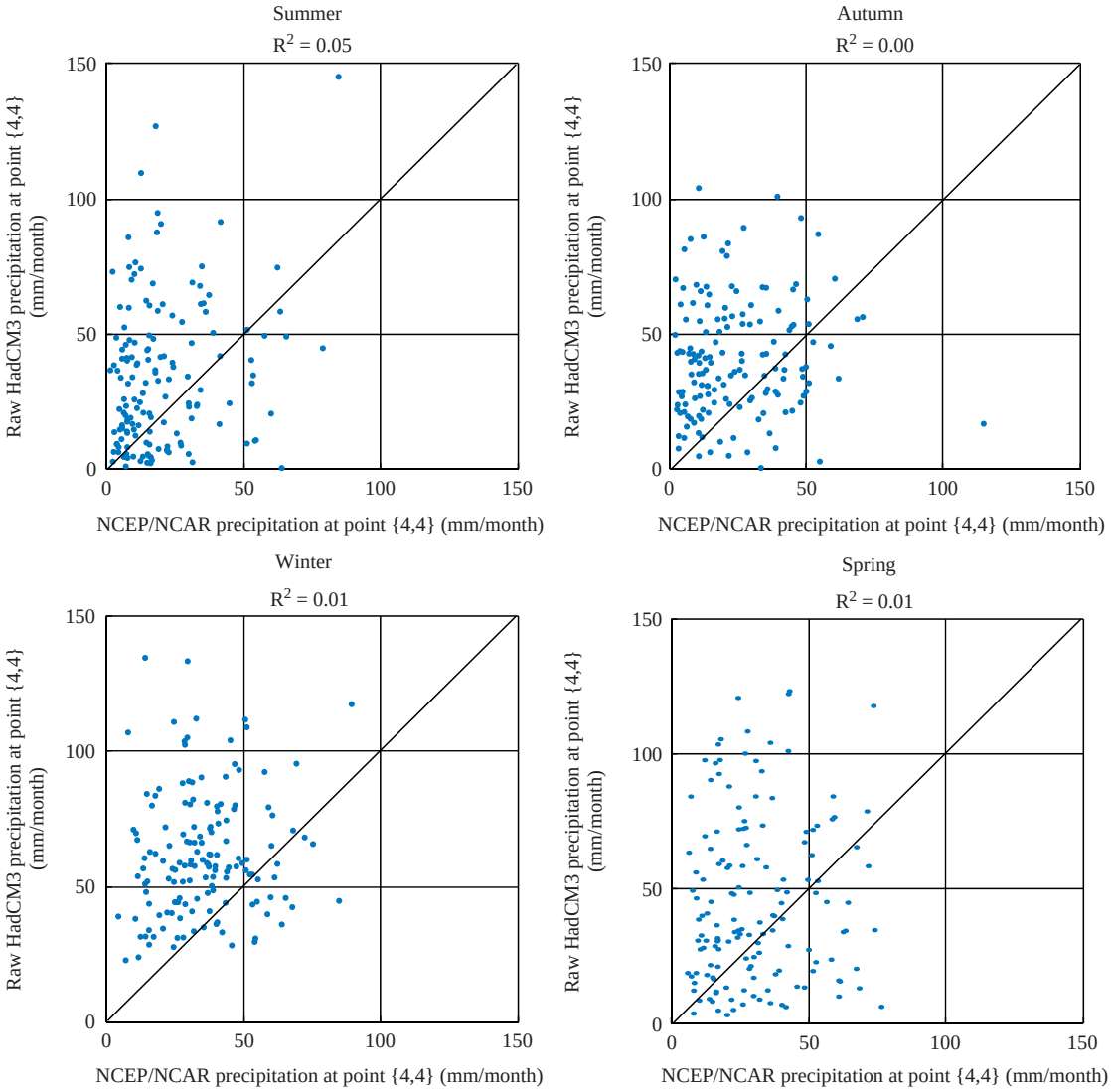

Figure 6. Seasonal scatter plots for raw precipitation output of HadCM3 at point {4,4} (1950–1999).

projected into future compared to that of observed precipitation of period 1950–1999 was statistically significant at the 95% confidence level for both A2 and B1 emission scenarios in all seasons except in winter.

In summer and winter, the precipitation in Victoria is influenced by the strength and the location of the sub-tropical ridge (http://www.climatekelpie.com.au/understand-climate/weather-and-climate-drivers/victoria#SubtropicalRidge). In summer, the sub-tropical ridge mainly lies over the southern part of the Australian continent (latitude 40°S – Timbal and Drosdowsky 2013). In winter, it is located over the north central region of Australia (latitude 29°S – Timbal and Drosdowsky 2013). The increase in the GHG emissions causes the atmospheric temperature to rise and this leads to strengthening (rise in pressure) and the southward movement of the sub-tropical ridge (Commonwealth Scientific and Industrial Research Organisation, 2010). This phenomenon can cause a decrease in precipitation in summer and winter as the pressure in the sub-tropical ridge is high. The relatively larger rise in the GHG emissions characterized by A2 scenario can intensify the sub-tropical ridge and cause relatively larger drop in the average of the precipitation in comparison to the same caused by B1 scenario which is associated with relatively low emissions in summer and winter, as shown in Table 5.

In all four seasons, both A2 and B1 scenarios depicted an increase in the maximum monthly precipitation, in comparison with that of past observations. This rise was particularly higher under A2 emission scenario which was associated with relatively higher levels of GHG emissions. This indicated that in future, with the rising GHG levels in the atmosphere, there will be months with large precipitation totals, at the station of interest. However, it should be noted that high monthly precipitations are prone to extrapolation errors of CDFs, as stated previously in the validation of the performances of the EDQM technique. The MLR technique used in developing the downscaling model employed in this study can only determine the linear component of the relationships

Table 5. Seasonal statistics of future A2 and B1 bias-corrected precipitation.

Statistic	Summer			Autumn			Winter			Spring		
	1950–1999	2000–2099		1950–1999	2000–2099		1950–1999	2000–2099			2000–2099	
	Obs	A2	B1	Obs	A2	B1	Obs	A2	B1	Obs	A2	B1
Avg	**41.4**	33.6 (**−19**%↓)*	35.3 (**−15**%↓)^	**70.4**	76.8 (+9%↑)^	67.6 (**−4**%↓)^	**127.3**	132.2 (+4%↑)^	135.6 (+7%↑)^	**88.1**	74.5 (**−15**%↓)*	71.0 (**−19**%↓)*
SD	**36.6**	44.0 (+20%↑)*	43.1 (+18%↑)*	**56.8**	65.5 (+15%↑)*	66.8 (+18%↑)*	**64.8**	72.0 (+11%↑)^	73.4 (+13%↑)*	**53.7**	69.2 (+29%↑)*	63.1 (+18%↑)*
Maximum precipitation	**192.3**	376.4 (+96%↑)	251.9 (+31%↑)	**345.4**	424.2 (+23%↑)	418.5 (+21%↑)	**345.2**	527.4 (+53%↑)	494.1 (+43%↑)	**272.4**	383.8 (+41%↑)	319.9 (+17%↑)
Percentage of months with zero precipitation	**4**	20 (+16%↑)	24 (+20%↑)	**0**	6 (+6%↑)	10 (+10%↑)	**0**	1 (+1%↑)	0 (*0%* =)	**0**	8 (+8%↑)	5 (+5%↑)
Percentage of months with above average precipitation	**39**	31 (**−8**%↓)	37 (**−2**%↓)	**39**	40 (+1%↑)	39 (*0%* =)	**47**	46 (**−1%↓**)	48 (+1%↑)	**43**	39 (**−4**%↓)	38 (**−5**%↓)

Avg = average of monthly precipitation in mm; SD = standard deviation of monthly precipitation in mm; C_v = coefficient of variation; A2 = high emission scenario; B1 = low emission scenario; ↑ = percentage increase in 2000–2099 with respect to observations of period 1950–1999; ↓ = percentage decrease in 2000–2099 with respect to observations of period 1950–1999 (in bold); Symbol = indicates change in percentage in 2000–2099 with respect to observations of period 1950–1999 (in italics); Symbol * indicates statistically significant change at 95% confidence level; Symbol ^ statistically insignificant change at 95% confidence level.

between the predictors and the precipitation. High values of precipitation usually display nonlinear relationships with predictors. Therefore the downscaling technique used in this study can be regarded as another source of uncertainty in the simulations of high precipitation values.

In all four seasons, the A2 scenario projected a rise in the percentage of months with zero precipitations, indicating that there will be greater number of dryer months in future, with increasing GHG emissions. A similar trend was seen in the projected precipitation pertaining to the B1 scenario, except in winter, when no months with zero precipitation was seen. It is noteworthy to state that the rise in the percentage of months with zero precipitation was highest in summer, for both A2 and B1 emission scenarios. In winter, the rise in the percentage of zero precipitation months was relatively low, in comparison with that of rest of the seasons, for the A2 emission scenario. In summer and spring both A2 and B1 emission scenarios indicated a slight decrease in the percentage of months with above average precipitation. In autumn and winter the changes in the percentage of months with above average precipitation was negligible for both emission scenarios.

A comparison conducted between the statistics of the raw precipitation outputs of HadCM3 corresponding to A2 and B1 GHG emission scenarios of the period 2000–2099, revealed that the differences between the averages and the standard deviations of precipitation at point {4,4} of the atmospheric domain were quite negligible in all seasons. However, the maximum of monthly precipitation simulated by HadCM3 under A2 scenario was clearly higher than that under B1 scenario in all seasons. This indicated that the relative changes in the GHG concentrations characterized by the A2 and B1 scenarios do not cause a significant difference in the long-term average and the standard deviation of precipitation simulated by HadCM3 over the study area, but the high emissions associated with A2 scenario causes HadCM3 to simulate peak precipitation values higher than those simulated with B1 scenario in all seasons. Similar characteristics are seen in the statistics of precipitation in Table 5 downscaled using the HadCM3 outputs pertaining to A2 and B1 scenarios. When the atmospheric GHG concentration rises, it causes an imbalance in radiative energy which increases the heat energy stored in the sea leading to an elevation in the sea surface temperatures (Trenberth *et al.*, 2007). The rise in the sea surface temperature increases the rate of evaporation, hence the water vapour content in the atmosphere. These phenomena lead to intensification of the hydrologic cycle causing a rise in the magnitude of the maximum precipitation (Kunkel *et al.*, 2013). Since the GHG emissions associated with the A2 scenario are higher in comparison to those of B1, the rise in the magnitude of the maximum precipitation is higher for A2 in all seasons as shown in Table 5.

Figure 7 depicts the exceedance curves for future A2 and B1 bias-corrected monthly precipitation for the period 2000–2099, along with the exceedance curves for the observed monthly precipitation pertaining to the period 1950–1999. According to Figure 7, it is evident that the precipitation in autumn and winter will increase with respect to the observations of the period 1950–1999, for the majority of exceedance probabilities. However, in spring there will be a drop in precipitation pertaining to the majority exceedance probabilities, and in summer a relatively small decrease in precipitation was indicated for most of the exceedance probabilities. These findings are also consistent with the numerical assessments provided in Table 5.

Smith and Chandler (2009) stated that, over the Murray Darling basin (MDB) in south east Australia, the raw precipitation output of HadCM3 under the A1B emission scenario (mid-level scenario which refers to an atmospheric CO_2 concentration of about 720 ppm at the end of the 21st century) shows a decrease in precipitation of about 15% for the period 2071–2099, with respect to the observed precipitation in the period 1971–2000. According to the findings of this study, at the Halls Gap post office which is located close to the southern boundary of the MDB (within it), the precipitation downscaled with HadCM3 outputs pertaining to A2 and B1 scenarios for the period 2071–2099, showed decrease of about 12% and 3.4%, respectively, with respect to the observed precipitation in the period 1971–2000. The Victorian Government Department of Sustainability and Environment (2008) stated that the median estimates obtained from the raw precipitation outputs of number of GCMs under B1 (low emissions), and A1F1 (high emissions) emission scenarios have indicated a drop in the average of precipitation in all four seasons by the year 2070 over the Wimmera region, which included the Halls Gap post office. Furthermore, it was stated that the greatest reduction in precipitation is likely to occur in spring, which is consistent with the findings of this study. Also it was stated that the intensity of extreme daily precipitation is likely to increase in the Wimmera region. However, it should be noted that there were no evidence in the literature of previous attempts on statistical downscaling of GCM outputs to precipitation at Halls Gap or its surrounding area. Future climate information for water resource planning purposes in the study area is currently based on the regional estimates derived from the raw outputs of GCMs (e.g. Commonwealth Scientific and Industrial Research Organisation, 2007) and does not provide the spatial resolution of detail that will be needed at the catchment scale.

The long-term statistics of monthly precipitation such as average, variance, extremes, and so on, extracted from the bias-corrected time series of monthly precipitation are useful for water resource planning purposes. The average of the future precipitation enables the understanding of the future water availability in a catchment, in meeting the future demand. The variance

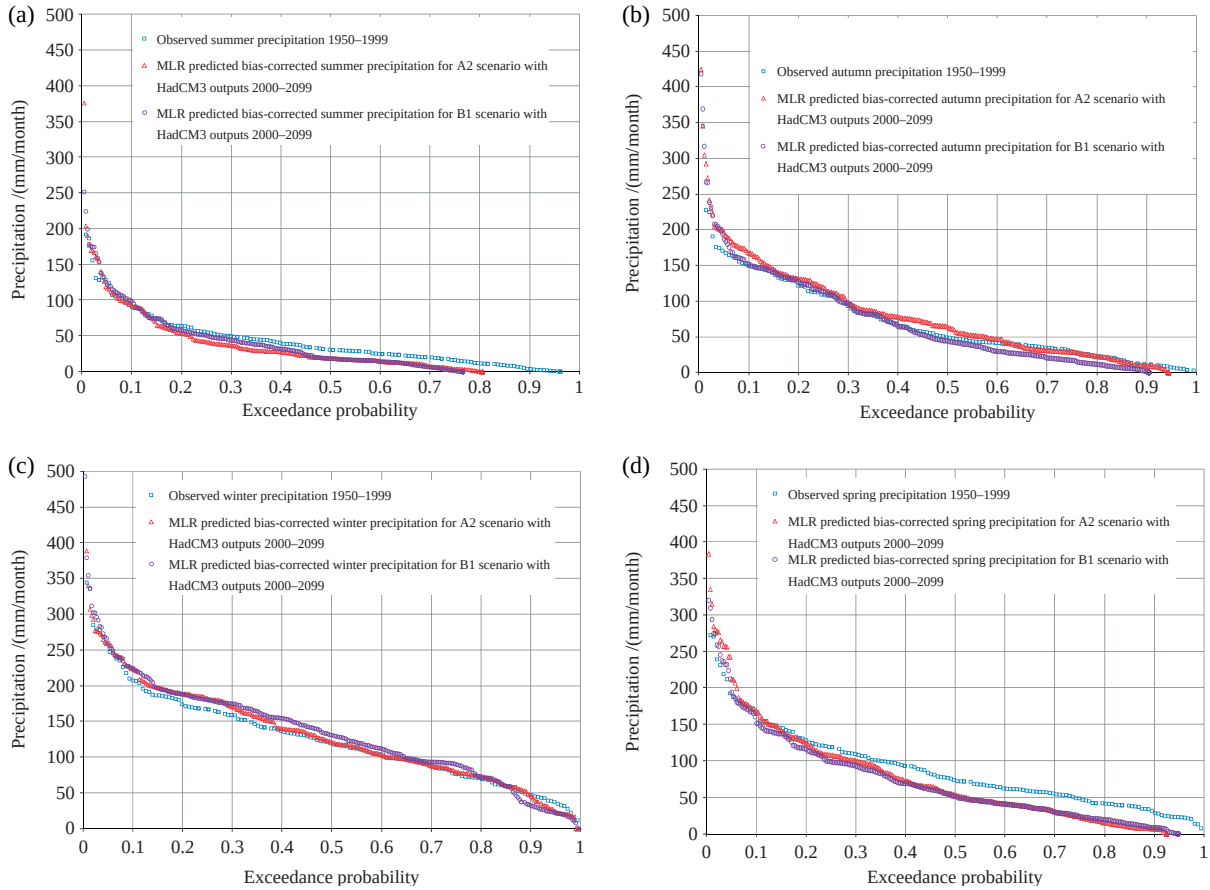

Figure 7. Seasonal exceedance curves for future bias-corrected precipitation under A2 and B1 emission scenarios (2000−2099). (a) Summer, (b) autumn, (c) winter and (d) spring.

of precipitation describes the amount of change in precipitation with respect to its average. A larger variance in future precipitation at the catchment scale shows unique challenges in managing water resources to withstand the larger fluctuations in precipitation. Greater variation in future precipitation will need to be considered in the planning and operation of water resources infrastructure, and will impact on the reliability of supply to customers. Modelling extreme low and high precipitation values are important in the management of droughts and floods, respectively.

Owing to the downscaling of GCM outputs followed by the bias-correction of downscaled precipitation, this research provides useful, area-specific information to the water resource planners (in the study area), than the currently available future climatic information derived from raw GCM outputs. In future, the methodology described in this article will be applied to a number of sites in the operational area of GWMWater (refer to Figure 1 of the first article) for producing the future precipitation projections with the outputs of multiple GCMs.

4.3.3. Caveats and uncertainties involved in the study

Statistical downscaling is a useful tool for the determination of catchment scale hydroclimatology using the GCM outputs. However, the projections produced using statistical downscaling techniques are subject to uncertainties arising from many sources such as GHG emission scenarios, GCMs, observations of predictands against which the downscaling models are calibrated and also from the downscaling techniques used (Hashmi *et al.*, 2009). The largest uncertainty in a downscaling study often arises from the GHG emission scenarios. This is because the actual levels of GHG emissions pertaining to the future climate are not known at the time the climate projections are produced. In this study, A2 which is a high emission scenario and B1 which is a low emission scenario were used for the projection of precipitation into future. Therefore, the statistics of precipitation derived from the outputs of the downscaling model refer to two plausible climate states conditioned by high and low GHG emission levels. Hence the precipitation projections produced in this study should not be treated as definite but as plausible.

Mainly owing to the different assumptions and approximations employed in the structure, different GCMs may tend to produce different projections of the future climate (Yu *et al.*, 2002) even under the same GHG emission scenario. This causes the downscaling models fed with the outputs of different GCMs to simulate future climate over the same study area differently. The above effect due to

the use of different GCMs is particularly evident when the predictors used as inputs to the downscaling models have a low degree of convergence among different GCMs. Johnson and Sharma (2009) found that GCMs show relatively high convergence for pressure and surface air temperature and comparably low convergence for precipitation, over Australia under both A2 and B1 GHG emission scenarios. This indicated that if the precipitation outputs of different GCMs are used as inputs to a downscaling model, it will probably tend to produce different projections of precipitation at the catchment scale. In this study, precipitation simulated by HadCM3 was used as an input to 11 of the 12 calendar month-based downscaling models, for the projection of precipitation into future. Therefore, the downscaling model used in this study will tend to produce a range of catchment scale projections of precipitation when run with the outputs of different GCMs. It should be noted that the statistics of the precipitation projected into future in this study correspond to the future climate simulated by HadCM3. By using the outputs of different GCMs and hence obtaining the ensemble average projection for precipitation can reduce the dependence on one specific GCM.

The uncertainties rising from the observations of precipitation also can cause the downscaling model to be less robust. In this study, the daily precipitation data were used to derive the monthly precipitation needed for the model calibration and validation and also for the correction of bias in the precipitation simulated by the downscaling model. The daily observed precipitation record at the Halls Gap post office contained 31% missing data over the period 1950–2010. These missing data have been filled by the Queensland Climate Change Centre of Excellence in the SILO database, using the spatial interpolation method described by Jeffrey *et al.* (2001). Since about one third of the daily precipitation observations were estimated, the record of observations at the Halls Gap post office may have introduced uncertainties to the downscaling model and also to the bias-correction.

Another possible source of uncertainty in a downscaling exercise is the downscaling technique used for deriving the relationship between the predictors and the predictand. In this study, MLR which is a linear regression technique was employed for the above purpose. Though MLR is a simple and convenient technique for developing a downscaling model, it cannot capture the nonlinear component of the relationships between the predictors and precipitation. Theoretically a complex nonlinear regression technique such as SVM or ANN could be able to better capture the relationships between the predictors and precipitation. However, the improvement to the simulations produced by such downscaling model built using a complex nonlinear regression technique over a downscaling model developed with a relatively simpler linear regression method may depend upon the degree of nonlinearity in the relationships between the predictors and the predictand.

5. Summary and conclusions

In the first article of this series of two articles, two models were developed using the MLR technique for downscaling NCEP/NCAR and HadCM3 outputs to monthly precipitation. In that study, it was realized that the model built with NCEP/NCAR outputs performed better than the model that was developed with HadCM3 outputs. The large mismatch seen between the raw precipitation output of HadCM3 and the observed precipitation in the first article, showed the need of a bias-correction. In this study the model built with NCEP/NCAR outputs (which is referred to as 'the downscaling model' throughout this article) was used for the future projections of monthly precipitation at the Halls Gap post office located in north western Victoria, Australia, with HadCM3 outputs corresponding to possible future climate as inputs. Also a bias-correction to the precipitation downscaled with HadCM3 outputs was performed.

The HadCM3 outputs for the 20th century climate experiment for the period 1950–1999 were standardized with the means and standard deviations of NCEP/NCAR reanalysis outputs corresponding to the period 1950–1989 (this was the calibration period of the downscaling model). Then these standardized HadCM3 outputs were introduced to the downscaling model for reproducing the observed monthly precipitation from 1950 to 1999, for the precipitation station at the Halls Gap post office. The precipitation downscaled with HadCM3 20th century climate experiment outputs were bias-corrected against the observed precipitation relevant to the period 1950–1999. The bias-correction of precipitation was performed using three different techniques: (1) EDQM, (2) MBC and (3) NBC. Each of these techniques were applied separately on the monthly precipitation downscaled with HadCM3 outputs on each calendar month. Based on the performances, the EDQM technique was identified as the most suitable method for correcting the bias in precipitation downscaled with HadCM3 outputs. The performances of the EDQM technique was validated by comparing the statistics of the precipitation downscaled with HadCM3 outputs pertaining to the COMMIT emission scenario for the period 2000–2099, with those of observed precipitation for the period 1950–1999.

HadCM3 outputs for the future climate were obtained under the A2 and B1 greenhouse emission scenarios for the projection of monthly precipitation into future. The A2 and B1 HadCM3 outputs for the period 2000–2099 were standardized with the means and standard deviations of NCEP/NCAR reanalysis outputs pertaining to the period 1950–1989. These standardized outputs of HadCM3 for the A2 and B1 emission scenarios were applied on the downscaling model for producing the future precipitation at the Halls Gap post office. The future precipitation downscaled from HadCM3 outputs corresponding to A2 and B1 emission scenarios were bias-corrected against the observed precipitation, using the EDQM technique.

The conclusions drawn from this study are:

1. When the downscaling model developed with NCEP/NCAR reanalysis data was run with HadCM3 20th century climate experiment outputs for the period 1950–1999, the model largely over-estimated the majority of monthly precipitation. There was large scatter in precipitation reproduced with HadCM3 outputs, during all four seasons.
2. After the application of EDQM, monthly bias-correction and NBC techniques for the period 1950–1999, the large over-predicting trend of precipitation reduced and turned into a more balanced over and under-predicted scatter. However, none of the bias-correction techniques could satisfactorily reduce the scatter of monthly precipitation.
3. Considering the scatter that was present in precipitation after the bias-correction, it was seen that all three bias-correction techniques hardly enhanced the accuracy of the time series of monthly precipitation.
4. In all seasons, during the period 1950–1999, EDQM, MBC and NBC techniques adequately corrected the average, the standard deviation and the coefficient of variation of monthly precipitation.
5. Following (3) and (4), it was argued that the bias-corrected precipitation should produce probability distributions of the projections more accurately than the time series.
6. For the bias-correction of monthly precipitation, EDQM was identified as the most suitable technique, employed in this study, as this method was the best in correcting the cumulative distribution (and hence the probability distribution) of the precipitation downscaled with GCM outputs. EDQM has a sound theory to model the CDF accurately.
7. If the scatter of the raw GCM outputs against NCEP/NCAR outputs was large, it was understood that the bias-correction of raw outputs of a GCM against NCEP/NCAR outputs prior to downscaling is not advantageous, than the bias-correction of the predictand (e.g. precipitation) downscaled from the same set of raw GCM outputs.
8. For the period 2000–2099, in spring, the precipitation downscaled using HadCM3 outputs pertaining to both A2 (relatively high emissions) and B1 (relatively low emissions) scenarios showed a statistically significant (at 95% confidence level) decrease in the average of monthly precipitation with respect to the average of observed precipitation of the period 1950–1999.

Acknowledgements

The authors acknowledge the financial assistance provided by the Australian Research Council Linkage Grant scheme and the Grampians Wimmera Mallee Water Corporation for this project. The authors also wish to thank the editor and the two anonymous reviewers for their useful comments, which have improved the quality of this article.

References

Arnell NW, Gosling SN. 2013. The impacts of climate change on river flow regimes at the global scale. *J. Hydrol.* **486**: 351–364, DOI: 10.1016/j.jhydrol.2013.02.010.

Charles A, Timbal B, Fernandez E, Hendon H. 2013. Analog downscaling of seasonal rainfall forecasts in the Murray darling basin. *Mon. Weather Rev.* **141**: 1099–1117, DOI: 10.1175/MWR-D-12-00098.1.

Chen C, Haerter JO, Hagemann S, Piani C. 2011. On the contribution of statistical bias correction to the uncertainty in the projected hydrological cycle. *Geophys. Res. Lett.* **38**: 1–6, DOI: 10.1029/2011GL049318.

Chen J, Brissette FP, Leconte R. 2012. Downscaling of weather generator parameters to quantify hydrological impacts of climate change. *Clim. Res.* **51**: 185–200, DOI: 10.3354/cr01062.

Chu JT, Xia J, Xu CY, Singh VP. 2010. Statistical downscaling of daily mean temperature, pan evaporation and precipitation for climate change scenarios in Haihe River, China. *Theor. Appl. Climatol.* **99**: 149–161, DOI: 10.1007/s00704-009-0129-6.

Commonwealth Scientific and Industrial Research Organisation. 2007. *Wimmera Region Fact Sheet: Murray-Darling Basin Sustainable Yields Project*. Retrieved October 28, 2012. http://www.csiro.au/Outcomes/Water/Water-for-the-environment/Wimmera-region-fact-sheet-Murray-Darling-Basin-Sustainable-Yields-Project.aspx

Commonwealth Scientific and Industrial Research Organisation. 2010. *Climate Variability and Change in South-Eastern Australia: A Synthesis of Findings from Phase 1 of the South Eastern Australian Climate Initiative (SEACI)*. Retrieved July 17, 2013. http://www.seaci.org/publications/documents/SEACI-1%20Reports/Phase1_SynthesisReport.pdf

Dessai S, Lu X, Hulme M. 2005. Limited sensitivity analysis of regional climate change probabilities for the 21st century. *J. Geophys. Res. D: Atmos.* **110**: 1–17, DOI: 10.1029/2005JD005919.

Earth System Research Laboratory. 2013. *Trends in Atmospheric Carbon Dioxide*. Retrieved June 20, 2013. http://www.esrl.noaa.gov/gmd/ccgg/trends/global.html

Fatichi S, Ivanov VY, Caporali E. 2011. Simulation of future climate scenarios with a weather generator. *Adv. Water Resour.* **34**: 448–467, DOI: 10.1016/j.advwatres.2010.12.013.

Fu G, Charles SP, Kirshner S. 2012. Daily rainfall projections from general circulation models with a downscaling nonhomogeneous hidden Markov model (NHMM) for south-eastern Australia. *Hydrol. Process.* **27**: 3663–3673, DOI: 10.1002/hyp.9483.

Ghosh S, Katkar S. 2012. Modeling uncertainty resulting from multiple downscaling methods in assessing hydrological impacts of climate change. *Water Resour. Manage.* **26**: 3559–3579, DOI: 10.1007/s11269-012-0090-5.

Ghosh S, Mujumdar PP. 2008. Statistical downscaling of GCM simulations to streamflow using relevance vector machine. *Adv. Water Resour.* **31**: 132–146, DOI: 10.1016/j.advwatres.2007.07.

Gudmundsson L, Bremnes JB, Haugen JE, Skaugen TE. 2012. Technical note: downscaling RCM precipitation to the station scale using quantile mapping – a comparison of methods. *Hydrol. Earth Syst. Sci. Discuss.* **9**: 6185–6201, DOI: 10.5194/hessd-9-6185-2012.

Hashmi MZ, Shamseldin AY, Melville BW. 2009. Statistical downscaling of precipitation: state-of-the-art and application of bayesian multi-model approach for uncertainty assessment. *Hydrol. Earth Syst. Sci.* **6**: 6535–6579, DOI: 10.5194/hessd-6-6535-2009.

Hughes L. 2003. Climate change and Australia: trends, projections and impacts. *Aust. Ecol.* **28**: 423–443, DOI: 10.1046/j.1442-9993.2003.01300.x.

Iizumi T, Nishimori M, Dairaku K, Adachi SA, Yokozawa M. 2011. Evaluation and intercomparison of downscaled daily precipitation indices over Japan in present-day climate: strengths and weaknesses of dynamical and bias correction-type statistical downscaling methods. *J. Geophys. Res. D: Atmos* **116**: 1–21, DOI: 10.1029/2010JD014513.

Ines AVM, Hansen JW. 2006. Bias correction of daily GCM rainfall for crop simulation studies. *Agr. Forest. Meteorol.* **138**: 44–53, DOI: 10.1016/j.agrformet.2006.03.009.

IPCC. 2000. *IPCC Special Report on Emissions Scenarios – Summary for Policymakers*. http://www.ipcc.ch/pdf/special-reports/spm/sres-en.pdf.

Jeffrey SJ, Carter JO, Moodie KB, Beswick AR. 2001. Using spatial interpolation to construct a comprehensive archive of Australian climate data. *Environ. Model. Softw.* **16**: 309–330, DOI: 10.1016/S1364-8152(01)00008-1.

Johnson F, Sharma A. 2009. Measurement of GCM skill in predicting variables relevant for hydroclimatological assessments. *J. Clim.* **22**: 4373–4382, DOI: 10.1175/2009JCLI2681.1.

Johnson F, Sharma A. 2012. A nesting model for bias correction of variability at multiple time scales in general circulation model precipitation simulations. *Water Resour. Res.* **48**: 1–16, DOI: 10.1029/2011WR010464.

Kalnay E, Kanamitsu M, Kistler R, Collins W, Deaven D, Gandin L, Iredell M, Saha S, White G, Woollen J, Zhu Y, Chelliah M, Ebisuzaki W, Higgins W, Janowiak J, Mo KC, Ropelewski C, Wang J, Leetmaa A, Reynolds R, Jenne R, Joseph D. 1996. The NCEP/NCAR reanalysis project. *Bull. Am. Meteorol. Soc.* **77**: 437–471, DOI: 10.1175/1520-0477(1996)077<0437:TNYRP>2.0.CO;2.

Kharin VV, Zwiers FW. 2002. Climate predictions with multimodel ensembles. *J. Clim.* **15**: 793–799, DOI: 10.1175/1520-0442(2002)015<0793:CPWME>2.0.CO;2.

Kunkel KE, Karl TR, Easterling DR, Redmond K, Young J, Yin X, Hennon P. 2013. Probable maximum precipitation and climate change. *Geophys. Res. Lett.* **40**: 1402–1408, DOI: 10.1002/grl.50334.

Lafon T, Dadson S, Buys G, Prudhomme C. 2013. Bias correction of daily precipitation simulated by a regional climate model: a comparison of methods. *Int. J. Climatol.* **33**: 1367–1381, DOI: 10.1002/joc.3518.

Li H, Sheffield J, Wood EF. 2010. Bias correction of monthly precipitation and temperature fields from Intergovernmental Panel on Climate Change AR4 models using equidistant quantile matching. *J. Geophys. Res D: Atmos* **115**: 1–20, DOI: 10.1029/2009JD012882.

Maraun D, Wetterhall F, Ireson AM, Chandler RE, Kendon EJ, Widmann M, Brienen S, Rust HW, Sauter T, Themel M, Venema VKC, Chun KP, Goodess CM, Jones RG, Onof C, Vrac M, Thiele-Eich I. 2010. Precipitation downscaling under climate change: recent developments to bridge the gap between dynamical models and the end user. *Rev. Geophys.* **48**, DOI: 10.1029/2009RG000314.

Meenu R, Rehana S, Mujumdar PP. 2013. Assessment of hydrologic impacts of climate change in Tunga-Bhadra river basin, India with HEC-HMS and SDSM. *Hydrol. Process.* **27**: 1572–1589, DOI: 10.1002/hyp.9220.

Murphy J. 1998. An evaluation of statistical and dynamical techniques for downscaling local climate. *J. Clim.* **12**: 2256–2284, DOI: 10.1175/1520-0442(1999)012<2256:AEOSAD>2.0.CO;2.

Nash JE, Sutcliffe JV. 1970. River flow forecasting through conceptual models, part 1 – a discussion of principles. *J. Hydrol.* **10**: 282–290, DOI: 10.1016/0022-1694(70)90255-6.

Nasseri M, Tavakol-Davani H, Zahraie B. 2013. Performance assessment of different data mining methods in statistical downscaling of daily precipitation. *J. Hydrol.* **492**: 1–14, DOI: 10.1016/j.jhydrol.2013.04.017.

Ojha CSP, Goyal MK, Adeloye AJ. 2010. Downscaling of precipitation for lake catchment in arid region in India using linear multiple regression and neural networks. *Open Hydrol. J.* **4**: 122–136, DOI: 10.2174/1874378101004010122.

Ojha R, Kumar DN, Sharma A, Mehrotra R. 2012. Assessing severe drought and wet events over India in a future climate using a nested bias correction approach. *J. Hydrol. Eng.* **18**: 760–772, DOI: 10.1061/(ASCE)HE.1943-5584.0000585.

Panofsky HA, Brier GW. 1968. *Some Applications of Statistics to Meteorology*. PennState University: University Park, PA.

Piani C, Haerter JO, Coppola E. 2010. Statistical bias correction for daily precipitation in regional climate models over Europe. *Theor. Appl. Climatol.* **99**: 187–192, DOI: 10.1007/s00704-009-0134-9.

Prudhomme C, Crooks S, Kay AL, Reynard N. 2013. Climate change and river flooding: Part 1 classifying the sensitivity of British catchments. *Clim. Change.* **119**: 933–948, DOI: 10.1007/s10584-013-0748-x.

Sachindra DA, Huang F, Barton AF, Perera BJC. 2013. Least square support vector and multi-linear regression for statistically downscaling general circulation model outputs to catchment streamflows. *Int. J. Climatol.* **33**: 1087–1106, DOI: 10.1002/joc.3493.

Salvi K, Kannan S, Ghosh S. 2011. Statistical downscaling and bias-correction for projections of Indian rainfall and temperature in climate change studies. In *4th International Conference on Environmental and Computer Science*, 16–18 September 2011, Singapore, 7–11.

Samadi S, Wilson CAME, Moradkhani H. 2013. Uncertainty analysis of statistical downscaling models using Hadley Centre Coupled Model. *Theor. Appl. Climatol.* **114**: 673–690, DOI: 10.1007/s00704-013-0844-x.

Schnur R, Lettenmaier DP. 1998. A case study of statistical downscaling in Australia using weather classification by recursive partitioning. *J. Hydrol.* **213**: 362–379, DOI: 10.1016/S0022-1694(98)00217-0.

Shao Q, Li M. 2013. An improved statistical analogue downscaling procedure for seasonal precipitation forecast. *Stochast. Environ. Res. Risk Assess.* **27**: 819–830, DOI: 10.1007/s00477-012-0610-0.

Smith I, Chandler E. 2009. Refining rainfall projections for the Murray Darling basin of south-east Australia-the effect of sampling model results based on performance. *J. Clim. Change* **102**: 377–393, DOI: 10.1007/s10584-009-9757-1.

Sun J, Chen H. 2012. A statistical downscaling scheme to improve global precipitation forecasting. *Meteorol. Atmos. Phys.* **117**: 87–102, DOI: 10.1007/s00703-012-0195-7.

Teutschbein C, Seibert J. 2012. Bias correction of regional climate model simulations for hydrological climate-change impact studies: review and evaluation of different methods. *J. Hydrol.* **456–457**: 12–29, DOI: 10.1016/j.jhydrol.2012.05.052.

Themeßl MJ, Gobiet A, Leuprecht A. 2011. Empirical-statistical downscaling and error correction of daily precipitation from regional climate models. *Int. J. Climatol.* **31**: 1530–1544, DOI: 10.1002/joc.2168.

Thomas P, Swaminathan A, Lucas RM. 2012. Climate change and health with an emphasis on interactions with ultraviolet radiation: a review. *Glob. Chang. Biol.* **18**: 2392–2405, DOI: 10.1111/j.1365-2486.2012.02706.x.

Timbal B, Drosdowsky W. 2013. The relationship between the decline of Southeastern Australian rainfall and the strengthening of the subtropical ridge. *Int. J. Climatol.* **33**: 1021–1034, DOI: 10.1002/joc.3492.

Timbal B, Fernandez E, Li Z. 2009. Generalization of a statistical downscaling model to provide local climate change projections for Australia. *Environ. Model. Software* **24**: 341–358, DOI: 10.1016/j.envsoft.2008.07.007.

Trenberth KE, Jones PD, Ambenje P, Bojariu R, Easterling D, Tank AK, Parker D, Rahimzadeh F, Renwick JA, Rusticucci M, Soden B, Zhai P. 2007. Observations: surface and atmospheric climate change. In *Climate Change 2007: The Physical Science Basis. Contribution of Working Group I to the Fourth Assessment Report of the Intergovernmental Panel on Climate Change*, Solomon S, Qin D, Manning M, Chen Z, Marquis M, Averyt KB, Tignor M, Miller HL (eds). Cambridge University Press: Cambridge, UK.

Tripati AK, Roberts CD, Eagle RA. 2009. Coupling of CO_2 and ice sheet stability over major climate transitions of the last 20 million years. *Science* **326**: 1394–1397, DOI: 10.1126/science.1178296.

Victorian Government Department of Sustainability and Environment. 2008. *Climate change in the Wimmera*. Retrieved October 28, 2012. http://www.climatechange.vic.gov.au/regional-projections/wimmera.

Wang W. 2006. *Stochasticity, Nonlinearity and Forecasting of Streamflow Processes*. Deft University Press: Amsterdam, the Netherlands.

Wilby RL, Charles SP, Zorita E, Timbal B, Whetton P, Mearns LO. 2004. Guidelines for use of climate scenarios developed from statistical downscaling methods, supporting material to the IPCC. http://www.ipcc-data.org/.

Wood AW, Leung LR, Sridhar V, Lettenmaier DP. 2004. Hydrologic implications of dynamical and statistical approaches to downscaling climate model outputs. *Clim. Change* **62**: 189–216, DOI: 10.1023/B:CLIM.0000013685.99609.9e.

Yu PS, Yang TC, Wu CK. 2002. Impact of climate change on water resources in southern Taiwan. *J. Hydrol.* **260**: 161–175, DOI: 10.1016/S0022-1694(01)00614-X.

Ziska LH, Bunce JA, Shimono H, Gealy DR, Baker JT, Newton PC, Reynolds MP, Jagadish KS, Zhu C, Howden M, Wilson LT. 2012. Food security and climate change: on the potential to adapt global crop production by active selection to rising atmospheric carbon dioxide. *Proc. R. Soc. Biol. Sci.* **279**: 4097–4105, DOI: 10.1098/rspb.2012.1005.

CHAPTER 4

STATISTICAL DOWNSCALING USING A MULTI-MODEL ENSEMBLE APPROACH

4.1 Introduction

In a statistical downscaling study, projections of a predictand (e.g. precipitation) produced into future can vary based on the GCM used in providing the inputs to the downscaling model. As a solution to this issue, ensemble techniques which can combine multiple projections into one single projection are used in statistical downscaling. Ensemble techniques are used in either combining the different outputs produced by the same climate model when run with different initial conditions into one single prediction or combining the outputs of different climate models into one single prediction. In this chapter, details of a statistical downscaling model developed using the multi-model ensemble outputs derived from three different GCMs; HadCM3, ECHAM5 and GFDL2.0 are presented. For this investigation, the above three GCM were selected owing to their good ability in simulating the precipitation over Australia and credible simulation of El Niño-Southern Oscillation (ENSO) (Smith and Chandler, 2010).

The 20th century climate experiment outputs of the above three GCMs were linked to the corresponding NCEP/NCAR reanalysis outputs using multi-linear regression equations. The outputs of these multi-linear regression equations called the multi-model ensemble outputs were used as inputs to the downscaling model in its calibration and

validation phases. It should be noted that, since reanalysis outputs are quality controlled and corrected against observations they are more accurate than the corresponding 20th century climate experiment outputs of GCMs. When the 20th century climate experiment outputs of GCMs are regressed against the reanalysis outputs, the outputs of those regressions relationships (multi-model ensemble inputs to the downscaling model) undergo a bias-correction. Therefore, the multi-model ensemble inputs to the downscaling model generated by combining the outputs of three GCMs are able to provide more reliable estimates of the global-scale climate predictors.

As described in Chapter 6 in the journal paper entitled "Least square support vector and multi-linear regression for statistically downscaling general circulation model outputs to catchment streamflows", the multi-linear regression technique was able to perform quite comparably with a complex non-linear regression technique called the least-square support vector machine regression. Therefore, in the study detailed in this chapter, for the generation of multi-model ensemble inputs to the downscaling model and for its development, multi-linear regression technique was employed.

The performances of this downscaling model developed with multi-model ensemble outputs were compared with those of a downscaling model developed using the NCEP/NCAR reanalysis outputs, as an assessment. The multi-linear regression equations developed between the GCM outputs and the NCEP/NCAR reanalysis outputs for the past climate were used with GCM outputs pertaining to future in generating the multi-model ensemble outputs for the future climate. In this manner, this downscaling model was calibrated, validated and projections into future were produced using a homogeneous set of inputs derived from the same set of GCMs. Furthermore, this multi-model ensemble approach aided in combining the outputs of several different GCMs into one single output for the prediction of precipitation at a station in the study area using statistical downscaling.

This chapter contains the following journal paper;

1. **Sachindra DA**, Huang F, Barton AF, Perera BJC. 2013b. Multi-model ensemble approach for statistically downscaling general circulation model outputs to precipitation. *Quarterly Journal of the Royal Meteorological Society*, (Article in Press), DOI: 10.1002/qj.2205. (SCImago journal rank indicator = Q1; ERA Rank = A; Impact Factor = 3.327).

VICTORIA UNIVERSITY
MELBOURNE AUSTRALIA

4.2
PART B:

DECLARATION OF CO-AUTHORSHIP AND CO-CONTRIBUTION: PAPERS INCORPORATED IN THESIS BY PUBLICATION

This declaration is to be completed for each conjointly authored publication and placed at the beginning of the thesis chapter in which the publication appears.

Declaration by [candidate name]: Signature: Date: 08/07/2014

Sachindra Dhanapala Arachchige

Paper Title:
Multi-model ensemble approach for statistically downscaling general circulation model outputs to precipitation

In the case of the above publication, the following authors contributed to the work as follows:

Name	Contribution %	Nature of Contribution
Sachindra Dhanapala Arachchige	85	Conceptual ideas, analysis, paper writing
Fuchun Huang	5	Critical comments, help with statistics
Andrew Barton	5	Critical comments, industry inputs
Chris Perera	5	Critical comments, discussion of conceptual ideas

VICTORIA UNIVERSITY
MELBOURNE AUSTRALIA

DECLARATION BY CO-AUTHORS

The undersigned certify that:

1. They meet criteria for authorship in that they have participated in the conception, execution or interpretation of at least that part of the publication in their field of expertise;
2. They take public responsibility for their part of the publication, except for the responsible author who accepts overall responsibility for the publication;
3. There are no other authors of the publication according to these criteria;
4. Potential conflicts of interest have been disclosed to **a)** granting bodies, **b)** the editor or publisher of journals or other publications, and **c)** the head of the responsible academic unit; and
5. The original data is stored at the following location(s):

Location(s):
College of Engineering and Science,Victoria University,Melbourne,Australia

and will be held for at least five years from the date indicated below:

		Date
Signature 1	[redacted]	29/07/2013
Signature 2	[redacted]	29/07/2013
Signature 3	[redacted]	16/8/2013
Signature 4	[redacted]	26/07/13

CHAPTER 5

MULTI-STATION AND MULTI-STATION MULTIVARIATE DOWNSCALING

5.1 Introduction

In the majority of the studies, statistical downscaling is performed at individual stations without attempting to preserve the spatial coherence seen in the observations at the stations in a study area. This causes the projections of a predictand produced by downscaling models at different stations in the study area to show limited agreement over space. In other words for the predictand of interest, the spatial correlation structure among the stations is violated. This affects the plausible representation of spatial variations of the climatic variables over the study area. Therefore in a study which involves statistical downscaling at multiple locations, the preservation of the cross-correlation structure among the stations in the study area for a certain predictand is an important task. For this purpose, multi-station downscaling techniques capable of downscaling at multiple stations concurrently are used. However, the majority of the currently used multi-station downscaling techniques are complex. In this chapter, a relatively simple yet effective multi-station downscaling technique based on a key-station approach is presented.

The use of this key-station approach was demonstrated in this chapter by its application to monthly precipitation, evaporation, minimum temperature and maximum temperature

at 17 stations in the study area considering one predictand at a time. The precipitation received by a catchment determines the availability of its water resources. Evaporation is regarded as a process which causes loss of water from the catchment. Temperature is highly influential on the rate of evaporation. Therefore in this investigation above climatic variables were considered. However, this key-station approach can only be used with one single predictand at a time. Therefore the key-station approach was extended to key-predictand and key-station approach for the multi-station multivariate statistical downscaling of GCM outputs to evaporation, minimum temperature and maximum temperature at 17 stations in the study area. In other words, the key-predictand and key-station approach detailed in this chapter is capable of downscaling GCM outputs to multiple predictands at multiple stations concurrently. This procedure enables the preservation of cross-correlation structures among the stations for each individual predictand while maintaining the cross-correlation structures between different climatic variables at individual stations.

This chapter contains the following two journal papers. The first paper discusses the application of the key-station approach for downscaling GCM outputs to precipitation, evaporation, minimum temperature and maximum temperature at multiple stations (one predictand at a time). The second paper details the application of the key-predictand and key-station approach for downscaling GCM outputs to evaporation, minimum temperature and maximum temperature at multiple stations concurrently.

1. **Sachindra DA**, Huang F, Barton AF, Perera BJC. 2013d. Statistical downscaling of general circulation model outputs to precipitation, evaporation and temperature using a key-station approach. *Global and Planetary Change*. (Under review). (SCImago journal rank indicator = Q1; ERA Rank = A; Impact Factor = 3.155).

2. **Sachindra DA**, Huang F, Barton AF, Perera BJC. 2013e. Statistical downscaling of general circulation model outputs to evaporation, minimum temperature and maximum temperature using a key-predictand and key-station

approach. *Journal of Water and Climate Change*. (Under review). (SCImago journal rank indicator = Q2; Impact Factor = 1.000).

VICTORIA UNIVERSITY
MELBOURNE AUSTRALIA

5.2

PART B:

DECLARATION OF CO-AUTHORSHIP AND CO-CONTRIBUTION: PAPERS INCORPORATED IN THESIS BY PUBLICATION

This declaration is to be completed for each conjointly authored publication and placed at the beginning of the thesis chapter in which the publication appears.

Declaration by [candidate name]: Sachindra Dhanapala Arachchige

Signature:

Date: 08/07/2014

Paper Title:
Statistical downscaling of general circulation model outputs to precipitation, evaporation and temperature using a key-station approach.

In the case of the above publication, the following authors contributed to the work as follows:

Name	Contribution %	Nature of Contribution
Sachindra Dhanapala Arachchige	85	Conceptual ideas, analysis, paper writing
Fuchun Huang	5	Critical comments, help with statistics
Andrew Barton	5	Critical comments, industry inputs
Chris Perera	5	Critical comments, discussion of conceptual ideas

VICTORIA UNIVERSITY
MELBOURNE AUSTRALIA

DECLARATION BY CO-AUTHORS

The undersigned certify that:

1. They meet criteria for authorship in that they have participated in the conception, execution or interpretation of at least that part of the publication in their field of expertise;
2. They take public responsibility for their part of the publication, except for the responsible author who accepts overall responsibility for the publication;
3. There are no other authors of the publication according to these criteria;
4. Potential conflicts of interest have been disclosed to **a)** granting bodies, **b)** the editor or publisher of journals or other publications, and **c)** the head of the responsible academic unit; and
5. The original data is stored at the following location(s):

Location(s):
College of Engineering and Science,Victoria University,Melbourne,Australia

and will be held for at least five years from the date indicated below:

		Date
Signature 1	[redacted]	29/07/2013
Signature 2	[redacted]	29/07/2013
Signature 3	[redacted]	16/8/2013
Signature 4	[redacted]	26/07/13

VICTORIA UNIVERSITY
MELBOURNE AUSTRALIA

PART B:

DECLARATION OF CO-AUTHORSHIP AND CO-CONTRIBUTION: PAPERS INCORPORATED IN THESIS BY PUBLICATION

This declaration is to be completed for each conjointly authored publication and placed at the beginning of the thesis chapter in which the publication appears.

Declaration by [candidate name]: Sachindra Dhanapala Arachchige

Signature:

Date: 08/07/2014

Paper Title:
Statistical downscaling of general circulation model outputs to evaporation, minimum temperature and maximum temperature using a key-predictand and key-station approach.

In the case of the above publication, the following authors contributed to the work as follows:

Name	Contribution %	Nature of Contribution
Sachindra Dhanapala Arachchige	85	Conceptual ideas, analysis, paper writing
Fuchun Huang	5	Critical comments, help with statistics
Andrew Barton	5	Critical comments, industry inputs
Chris Perera	5	Critical comments, discussion of conceptual ideas

VICTORIA UNIVERSITY
MELBOURNE AUSTRALIA

DECLARATION BY CO-AUTHORS

The undersigned certify that:

1. They meet criteria for authorship in that they have participated in the conception, execution or interpretation of at least that part of the publication in their field of expertise;
2. They take public responsibility for their part of the publication, except for the responsible author who accepts overall responsibility for the publication;
3. There are no other authors of the publication according to these criteria;
4. Potential conflicts of interest have been disclosed to **a)** granting bodies, **b)** the editor or publisher of journals or other publications, and **c)** the head of the responsible academic unit; and
5. The original data is stored at the following location(s):

Location(s):
College of Engineering and Science,Victoria University,Melbourne,Australia

and will be held for at least five years from the date indicated below:

		Date
Signature 1	[redacted]	29/07/2013
Signature 2	[redacted]	29/07/2013
Signature 3	[redacted]	16/8/2013
Signature 4	[redacted]	26/07/13

Manuscript Submitted to Global and Planetary Change

5.3 Statistical Downscaling of General Circulation Model Outputs to Precipitation, Evaporation and Temperature Using a Key-Station Approach

D.A. Sachindra[a]*, F. Huang[a], A. Barton[a,b], and B.J.C. Perera[a]

[a]*Victoria University, P.O. Box 14428, Melbourne, Victoria 8001, Australia.*

[b]*Federation University, PO Box 663, Ballarat, Victoria 3353, Australia.*

*Correspondence to: D. A. Sachindra, College of Engineering and Science, Footscray Park Campus, Victoria University, P.O. Box 14428, Melbourne, Victoria 8001, Australia. E-mail: sachindra.dhanapalaarachchige@live.vu.edu.au. Telephone: +61 03 9919 4907.

Published as: Dhanapala Arachchige, Sachindra , Huang, Fuchun, Barton, A and Perera, Bodiyabaduge (2015) Statistical downscaling of general circulation model outputs to evaporation, minimum temperature and maximum temperature using a key-predictand and key-station approach. Journal of Water and Climate Change, 6 (2). 241 - 262.

Available from: https://doi.org/10.2166/wcc.2014.145

Abstract

In this study, using a key-station approach, statistical downscaling of monthly GCM outputs to monthly precipitation, evaporation, minimum temperature and maximum temperature at 17 observation stations located in north western Victoria, Australia was performed. Using the observations of each predictand, over the period 1950-2010, correlations among all stations were computed. For each predictand, the station which showed the highest number of correlations above 0.80 ($p \leq 0.05$) with other stations was selected as the first key-station. The stations that were highly correlated with that key-station were considered as the member stations of the first cluster. By employing this same procedure on the remaining stations, the next key-station was found. This procedure was performed until all stations were segregated into clusters. Thereafter using the observations of each predictand, linear regression equations (inter-station regression relationships) were developed between the key-stations and the member stations for each calendar month separately. The downscaling models at the key-stations were developed using the NCEP/NCAR reanalysis data as inputs to them. The outputs of HadCM3 pertaining to the A2 greenhouse gas emission scenario were introduced to these downscaling models to produce projections of the predictands over the period 2000-2099. Then the outputs of these downscaling models were introduced to the inter-station regression relationships to produce the projections of the predictands into future, at all member stations. It was found that, the key-station approach employed in this study was effective and proved beneficial in maintaining the cross correlation structure among the stations, for the predictand of interest.

Keywords: *Statistical downscaling; Key station; General circulation model; Multi-linear regression*

1. INTRODUCTION

Climate change due to rising concentrations of atmospheric greenhouse gases (Wilks, 2010) is a major issue in the present world. It is believed that the spatio-temporal changes in precipitation pattern, increase in the intensity and frequency of extreme precipitation events, rise in the global temperature, and heat waves are some of the consequences of the increasing concentrations of greenhouse gases (GHG) in the atmosphere (Nicholls, 2008). It is believed that the climate of earth will continue to change in future (Hundecha and Bardossy, 2008). The study of the impact of changing climate on water resources is of great importance, particularly at the catchment scale, as water is essential for the existence of life.

General Circulation Models (GCMs) are the most widely used tools for projection of global climate into future (King et al., 2012), considering the GHG concentrations in the atmosphere. GCMs are based on the physics of the atmosphere, and they employ various assumptions and approximations to simplify the naturally complex atmosphere in modelling (Sachindra et al., 2013). However, due to the coarse spatial resolution of the GCM outputs, they cannot be used directly in catchment scale studies which need climatic data at finer spatial resolutions (Jeong et al., 2012). As a solution to the issue of coarse spatial resolution of GCM outputs, downscaling techniques have been developed. They link the coarse resolution GCM outputs with fine resolution hydroclimatic variables at the catchment scale. There are two broad classes of downscaling methods in use: (1) dynamic downscaling and (2) statistical downscaling (Wilby and Dawson, 2007; Liu et al., 2013).

Dynamic downscaling involves the introduction of boundary and initial conditions obtained from a GCM to a regional climate model (RCM) (Murphy, 1998). RCMs are also atmospheric physics based models capable of producing their outputs at spatial resolutions finer than the outputs of GCMs. Dynamic downscaling techniques produce spatially continuous projections of climatic variables, while maintaining their correlations over space (Maurer and Hidalgo, 2008). The major issue with dynamic

downscaling techniques is the high computational costs and the long simulation time involved in their implementation.

In statistical downscaling, mathematical relationships are first developed between the GCM outputs and the catchment scale hydroclimatic variable of interest using the data of past climate. Then these relationships are used in downscaling GCM outputs pertaining to future climate. Therefore, all statistical downscaling techniques assume that the relationships developed between the GCM outputs and catchment scale hydroclimatic variable using the data of past climate, will remain the same in future. Furthermore, statistical downscaling techniques can only produce point scale projections of climate, while the dynamic downscaling techniques produce spatially continuous fields of outputs. Nevertheless, statistical downscaling methods are computationally cheaper compared to dynamic downscaling techniques and also faster in producing their outputs. Unlike dynamic downscaling, statistical downscaling methods can produce data of predictands such as streamflows, leaf wetness etc which are not simulated by the GCMs.

Statistical downscaling techniques are further subdivided into three groups; (1) regression methods, (2) weather classification and (3) weather generation (Wilby et al., 2004). In regression downscaling methods, either linear or non-linear relationships between the GCM outputs and the catchment scale hydroclimatic variables are constructed (Chen et al., 2010). Weather classification involves the determination of the values of catchment scale hydroclimatic variables by matching the current state of large scale weather with past similar conditions in the record (Wilby et al., 2004). Weather generators produce synthetic sequences of the climatic variable, which capture the statistics of the observations (Kou et al., 2007).

Statistical downscaling studies are conducted at individual stations without explicitly preserving the observed cross-correlation structures between stations (e.g. Tripathi et al. (2006), Anandhi et al. (2008), Sachindra et al. (2013)), and also at multiple stations attempting to maintain the observed cross-correlation structures (or spatial covariance

structure) between the stations (e.g. Jeong et al. (2012)). In a statistical downscaling study which involves downscaling at a large number of stations over a study area, the preservation of the cross-correlation structure among stations is an important objective, as it enables the plausible representation of spatial variations of the climatic variables over the study area. However, under changing climate in future, the cross-correlation structures among stations may also tend to change. Jeong et al. (2012) used the multivariate multi-linear regression (MMLR) technique for downscaling NCEP/NCAR reanalysis outputs to daily precipitation, simultaneously at 9 observation stations in Canada. Wilks (1999) used a weather generation technique to generate daily precipitation, minimum temperature, maximum temperature and solar radiation, simultaneously at 62 stations in the western part of the USA. The same weather generation technique was used by Qian et al. (2002) for generating the daily precipitation, minimum temperature and maximum temperature at six observation stations in Portugal. Wilby et al. (2003) used the conditional resampling method to downscale GCM outputs to daily precipitation at multiple stations in the UK. However the multi-site downscaling methods employed in the past were of high degree of complexity and also involved high computational cost.

Gupta (2008) stated that a short streamflow data set at a station can be lengthened by using a linear regression equation fitted between the data of that station and data of another station, which has a long record of data and also displays a high correlation with the former station. Anandhi et al. (2008) successfully used this regression technique to estimate missing data of minimum and maximum temperature at a station. The same idea can be extended to a statistical downscaling exercise in which a number of stations are involved.

In such a case, initially a station at which the observed data of the predictand (e.g. precipitation) are highly correlated with those at some other stations in the study area is identified. This station is referred to as the key station. Thereafter, regression relationships are developed between the key station and the other stations which are correlated with the key station, using observed data. A statistical downscaling model is

then developed for the key station. The outputs of this downscaling model are used in the regression relationships developed between the key station and the other stations, to produce the values of the predictand at the other stations. In this study, the aforementioned key station approach was employed in order to determine the values of monthly precipitation, evaporation, minimum and maximum temperature at multiple stations in an area, using the outputs of the downscaling models developed at few key stations. Precipitation is the predominant factor which determines the amount of water available in a catchment, while evaporation is a key process which governs the loss of water from a catchment. Temperature is directly influential on the rate of evaporation. Therefore precipitation, evaporation and temperature are three climatic variables which largely influence the water resources in a catchment. Hence, the study of the variations of these three climatic variables under changing climate in future is immensely helpful in determining the availability of surface water resources in a catchment. The operational area of Grampians Wimmera Mallee Water Cooperation in the north western region of Victoria, Australia was selected as the study area to demonstrate the key station approach employed in this study. This area is sensitive to severe droughts (Barton et al., 2011), therefore reliable information on the likely future water availability is quite important.

The major advantage of the key station approach is that, the observed cross-correlation structure among the stations in the past climate for a certain climatic variable is also preserved in the climatic projections produced into future. However, for the successful implementation of the key station approach, the correlations between the observations of the predictand of interest at the key station and the corresponding observations at the other stations in the study area should be high. If these correlations are low, the relationships between the key station and the other stations become weaker. Furthermore, in the key station approach, downscaling models are only developed at the key stations. Hence, it avoids the need of having downscaling models at all stations in the study area.

Section 2 of this paper provides the details of the study area and the data used in this research. The generic methodology is explained in Section 3 of the paper. The application of the generic methodology to the study area is detailed in Section 4, together with the results of the application. Section 5 provides the broad conclusions derived from this study.

2. STUDY AREA AND DATA

For the case study, monthly precipitation, evaporation, minimum temperature and maximum temperature measured at 17 stations were used. These stations were located within the operational area of Grampians Wimmera Mallee Water Cooperation (GWMWater) (www.gwmwater.org.au) in north-western Victoria, Australia. The operational area of GWMWater is shown in Figure 1 and is about 62,000 km^2 in extent. The elevation of the study area varies from about 25 m to 1200 m (above mean sea level) from north to south. The northern part of the study area is relatively flatter and its climate is persistently dry and warm (Bureau of Meteorology, 2013). On the other hand, the southern region of the study area is mountainous and has a less pronounced dry season (Bureau of Meteorology, 2013).

Figure 1 Study area

Table 1 shows the 17 stations considered in this study with their latitudes and longitudes.

Table 1 Stations considered in this study

Name of the	Station ID	Latitude	Longitude
Eversley	79014	-37.18	143.15
Ouyen post office	76047	-35.07	142.32
Birchip post office	77007	-35.98	142.92
Swan Hill post office	77042	-35.34	143.55
Rainbow	77083	-35.90	141.99
Great Western	79019	-37.18	142.86
Polkemmet	79023	-36.66	142.07
Lake Lonsdale	79026	-37.03	142.58
Longerenong	79028	-36.67	142.30
Moyston post office	79034	-37.30	142.77
Wartook reservoir	79046	-37.09	142.43
Hamilton airport	90173	-37.65	142.06
Halls Gap post office	79074	-37.14	142.52
Tottington	79079	-36.79	143.12
Stawell	79080	-37.07	142.79
Balmoral post office	89003	-37.25	141.84
Ararat prison	89085	-37.28	142.98

Station ID is as defined by the Bureau of Meteorology Australia at http://www.bom.gov.au/climate/data/stations/

Monthly observed precipitation, evaporation, maximum temperature and minimum temperature for the 17 stations shown in Table 1 were obtained from the SILO database of Queensland Climate Change Centre of Excellence at http://www.longpaddock.qld.gov.au/silo/, for the period 1950-2010. These data were used for identification of key stations and also for calibration and validation of the downscaling models. The observed records of precipitation, evaporation, maximum temperature and minimum temperature were also used in the bias-correction of the outputs of the downscaling models, as the reference data set. For providing inputs to the downscaling models in calibration and validation, monthly National Centers for Environmental Prediction/ National Center for Atmospheric Research (NCEP/NCAR) reanalysis outputs were extracted from the physical sciences division of the National Oceanic and Atmospheric Administration / Earth System Research Laboratory (NOAA/ESRL) at http://www.esrl.noaa.gov/psd/.

For reproducing the past observed precipitation, evaporation, maximum temperature and minimum temperature using the downscaling models, monthly outputs of HadCM3 for the 20th century climate experiment (20C3M) were downloaded from the Programme for Climate Model Diagnosis and Inter-comparison (PCMDI) (https://esgcet.llnl.gov:8443/index.jsp) for the period 1950-1999. For producing the projections of catchment scale precipitation, evaporation, maximum temperature and minimum temperature into future, using the downscaling models, monthly outputs of HadCM3 pertaining to the A2 GHG emission scenario were also downloaded from https://esgcet.llnl.gov:8443/index.jsp.

Smith and Chandler (2009) stated that HadCM3 is among the few GCMs which are capable in properly simulating the precipitation over Australia and produce credible predictions of El Niño Southern Oscillation (ENSO). In that study, they argued that any GCM capable in simulating precipitation with good degree of accuracy should also simulate other climatic variables plausibly. Therefore HadCM3 was selected for the present study. The distinct link between ENSO and precipitation in Australia is

discussed in detailed by Chiew et al. (1998). The use of the A2 GHG emission scenario in the current study enables the projection of the worst plausible impacts of the rising GHG concentrations on the climate over the study area, as this scenario refers to high levels of emissions of GHGs, owing to the rapid economic growth of the future world. The A2 GHG emission scenario provides similarities to the severe drought experienced by the study region from 1997 to 2009 (Barton et al. 2011) which now provides the basis for many government planning efforts (for example refer to Victorian Government Department of Sustainability and Environment, 2011).

3. GENERIC METHODOLOGY

The procedure for application of the key station approach used in this study is shown in brief in the flow chart provided in Figure 2. The steps shown in Figure 2 are described in detail later.

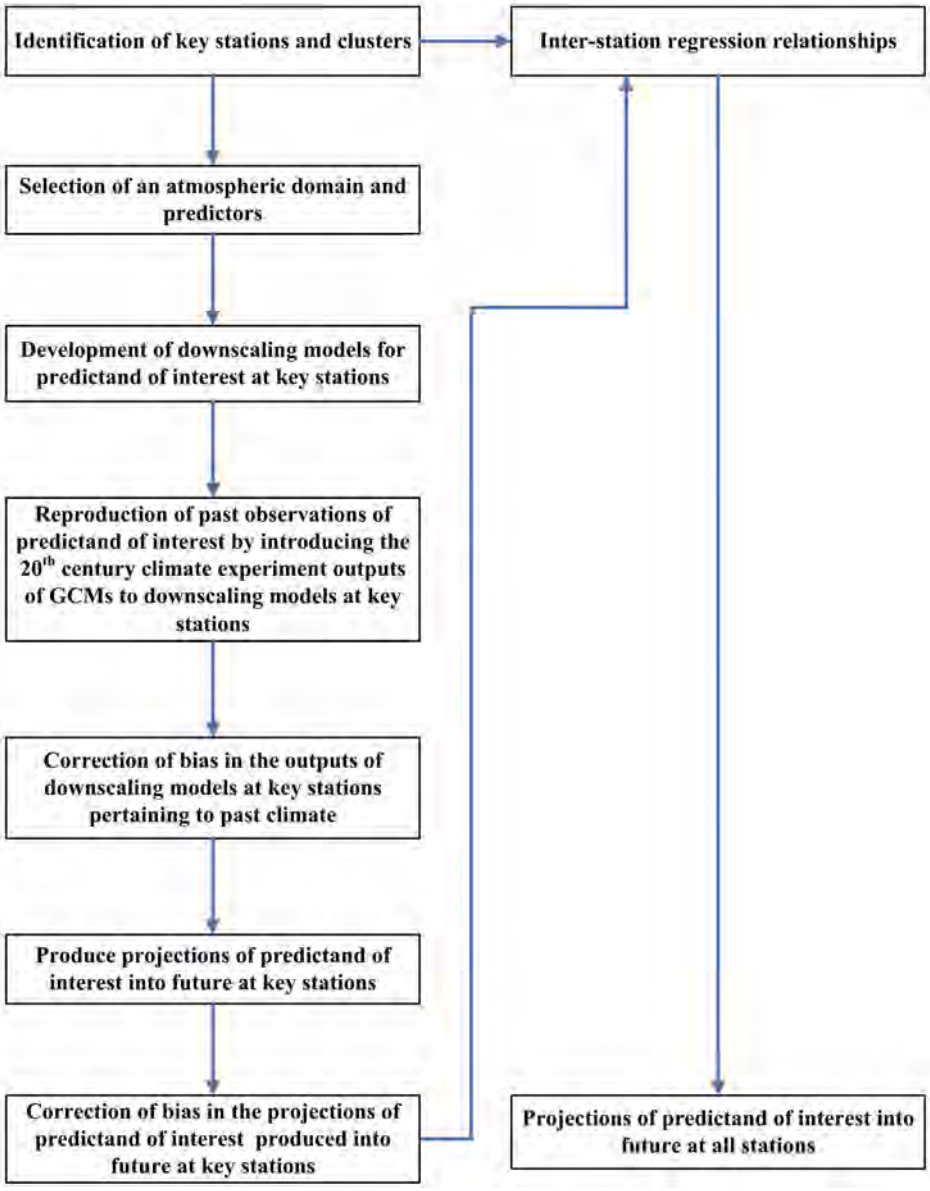

Figure 2 Steps involved in application of the key station approach

3.1. Identification of key stations and clusters

In this paper, a key station is defined as an observation station whose data for a specific climatic variable (e.g. monthly precipitation) are highly correlated with those of a set of other observation stations in the same study area. The key station and the other observation stations (member stations) which are highly correlated with it are called a cluster. A study area can have several clusters; each cluster contains a key station, and a cluster can have any number of member stations.

For identification of key stations and clusters for each climatic variable, initially the Pearson correlation coefficients (Pearson, 1895) between each station and the rest of the stations were computed for the past climate, considering all calendar months together. This yielded a matrix of correlation coefficients among all stations in the study area. Once the correlation matrix was computed, by examining it, a station at which the data of the considered climatic variable are highly correlated (magnitude of 0.80 or above preferred) with those at other stations in the study area was identified. This station was the key station and the other stations which were highly correlated with it were the member stations of the cluster, for the climatic variable considered.

If one such key station for the whole study area cannot be found, then multiple key stations for the study area were identified. In such case, first, a threshold value of 0.80 was imposed on the correlation matrix of a climatic variable of interest. Note that the threshold value of 0.80 refers only to the magnitude of the correlation. Once the threshold value was imposed on the correlation matrix, the station which has the highest number of correlations above the threshold with other stations was selected as the first key station, and the stations which showed high correlation with this station were considered as the members of the first cluster. When multiple stations showed the same number of stations with which they have correlations above 0.80, any such station was selected as the first key station. Thereafter, the same procedure which was used in identifying the first key station was applied on the correlation matrix which included only the stations which were not included in the first cluster. In this manner, the second key station and the member stations of the second cluster were identified. This

procedure was repeated until all stations are assigned to clusters. Also the different clusters should be less correlated with each other as much as possible. Clusters and key stations were identified for each variable considered in this study separately. If there is any station which does not display a correlation above the threshold with any other station, that station should be treated as a solitary key station (no any member stations in the cluster).

The magnitude of the correlation threshold can be changed based on the correlations in the matrix. However, if the correlations among the stations for a certain predictand were relatively low, the advantage of application of the key station approach becomes limited. This is because low correlations refer to poor linear associations between a predictand at the key station and that at the member stations in the cluster. These poor linear associations will cause the regression relationships built between a predictand at a key station and that at member stations to be less effective.

3.2. Relationships between key stations and member stations in clusters

Once the key stations were identified, using the observations simple linear regression relationships were developed for each predictand between the key station and the member stations, in each cluster, for each calendar month separately. In this paper, these relationships are referred to as inter-station regression relationships. The first two thirds of the observations at the key and the member stations were used to calibrate these linear regression relationships. Then, these linear regression relationships were validated using the remaining observations.

3.3. Atmospheric domain and predictor selection

After the development of the inter-station regression relationships, an atmospheric domain over the study area was defined. The atmospheric domain allows the inclusion of influences of the large scale atmospheric circulations on the catchment scale climate in the downscaling models. This atmospheric domain was used for the development of downscaling models for all predictands at all key stations.

For this study, probable predictors which are the likely variables to influence a predictand at the catchment scale were selected based on a review of past literature and hydrological principles. Probable predictors can vary from predictand to predictand and also geographically. The potential predictors are a subset of probable predictors and they are the most influential predictors on the predictand considered. Potential predictors also vary from predictand to predictand and also spatiotemporally.

The potential predictors for each calendar month at each key station were selected from the set of probable predictors, based on their correlations with the observations of the predictand. The selection of potential predictors for each calendar month enables the consideration of seasonal variations of the atmosphere, and hence it allows better modelling of the predictand (Sachindra et al., 2013). The data corresponding to the probable predictors were obtained from a reanalysis database. These reanalysis data and observations of the predictand (pertaining to a key station) were chronologically separated into 20 year time slices. Then the Pearson correlation coefficients between the observations and the reanalysis data were computed for each time slice and for the whole time period of the study. This was performed at each grid point in the atmospheric domain, for each calendar month separately. The probable predictors which displayed the best correlations (statistical significance: $p \leq 0.05$) consistently over the 20 year time slices and the whole period of the study were selected as the potential predictors for each calendar month.

3.4. Development of downscaling models at key stations

Downscaling models were developed (calibrated and validated) for the key stations using the potential predictors identified in Section 3.3. The first two thirds of the observations of predictands and the reanalysis data corresponding to the potential predictors were used for the calibration of the downscaling models and the remaining data were used for the validation. The reanalysis data for potential predictors for both calibration and validation were standardised using the means and the standard deviations of the reanalysis data corresponding to the calibration phase of the downscaling model. This was done as the means and the standard deviations of the

reanalysis data become a fixed component of the downscaling model throughout its development (calibration and validation) and projection phases (Sachindra et al., 2014). For the calibration of the downscaling model, initially the potential predictor which displayed the best correlation with the predictand over the whole period of the study at the station of interest was introduced to the downscaling model. By minimising the sum of squared errors between the observations and the outputs of the downscaling model, the optimum values for the coefficient and constant in the multi-linear regression (MLR) equation (in this case a simple linear regression equation, as there is only one independent variable) were computed. Following this, the downscaling model was validated as an independent simulation. The model performance in calibration and validation was measured using the Nash-Sutcliffe efficiency (NSE) (Nash and Sutcliffe, 1970) by comparing the model outputs with the corresponding observations. Then, one at a time, the next best potential predictors were introduced to the downscaling model, and it was calibrated and validated. This stepwise introduction of predictors was continued until the performance of the downscaling model attains a maximum in validation, in terms of the NSE. The stepwise model development allowed the identification of the best set of predictors and the development of the best downscaling model for each calendar month. Following the same procedure, downscaling models were developed for all calendar months at each key station for each predictand, separately. The performances of the downscaling models during the calibration and validation phases were assessed by comparing the statistics of the model outputs with those of observations. Graphical comparisons (scatter plots) of outputs of downscaling models and observations were also performed.

3.5. Reproduction of past climate at key stations and bias-correction

After the development of downscaling models at the key stations, the 20C3M outputs of the GCM pertaining to the calibration and validation phases of the downscaling models were standardised with the means and the standard deviations of the reanalysis outputs corresponding to the calibration phase of the downscaling models. Then, by introducing these standardised 20C3M outputs of the GCM to the downscaling models, the observations of the predictands (e.g. precipitation) were reproduced for the past climate.

This was performed to analyse the performances of the downscaling models in reproducing the past observations when these were run with the GCM outputs pertaining to the past climate. It was an important investigation as the downscaling models have been developed with better quality reanalysis data for the past climate, and for the projection of climate into future they will be used with GCM outputs which are associated with greater uncertainties. If any bias was seen in the outputs of the downscaling models when run with the 20C3M outputs of the GCM, a correction to bias was applied.

In this study, the monthly bias-correction (Johnson and Sharma, 2012) was applied on the outputs of the downscaling models (e.g. precipitation) produced with the 20C3M outputs of the GCM. The monthly bias-correction is based on the assumption that the bias in the mean and the standard deviation of the outputs of the downscaling models (with respect to past observations) for the past climate will remain the same in future (Johnson and Sharma, 2012). The procedure for the application of the monthly bias-correction is described below.

This bias-correction was applied to the calibration period of the downscaling model, by replacing the means and the standard deviations of the outputs of the downscaling models produced with the 20C3M outputs of the GCM, with those of observations relevant to the calibration period of the downscaling models. For the validation of the bias-correction, outputs of the downscaling models produced with the 20C3M outputs of the GCM pertaining to the validation period of the downscaling models were standardised with the means and the standard deviations of the outputs of the downscaling models pertaining to the calibration period. Then those standardised outputs were transformed back with the means and the standard deviations of the observations relevant to the calibration period of the downscaling models. The bias-correction was applied to each predictand in each calendar month separately.

3.6. Development of a downscaling model at a member station

It was important to compare the statistics of the outputs (e.g. monthly precipitation) produced by the inter-station regression relationships against those of outputs of a downscaling model developed at a member station, for the past climate. Since this enables the determination of how well the key station approach can replace the need of having individual downscaling models at member stations. For this purpose, for a predictand, a downscaling model was developed at a member station. In the development of the downscaling model at this member station, the same procedure which was adopted in building downscaling models at the key stations was employed. The outputs of the inter-station regression relationships and the corresponding outputs of the downscaling model built at the member station were compared both numerically and graphically with each other.

3.7. Projections into future

In order to produce catchment scale projections of the predictands into future, GCM outputs pertaining to the future climate were obtained. Then these were standardised with the means and the standard deviations of the reanalysis data corresponding to the calibration phase of the downscaling models. These standardised GCM outputs were introduced to the downscaling models developed at key stations for producing the projections of predictands into future. In the same way as the bias-correction was validated (refer to Section 3.5), it was applied to the projections produced into future by the downscaling models developed at the key stations. Using the inter-station regression relationships, the projections produced into future at key stations were extended to the member stations.

4. APPLICATION

The generic methodology described in Section 3 was applied to downscale monthly GCM outputs to precipitation, evaporation, minimum temperature and maximum temperature at 17 stations (see Table 1) located in the operational area of GWMWater (see Figure 1).

4.1. Identification of key stations and clusters

4.1.1 Key stations and clusters for precipitation

For identification of key stations, first the correlations of monthly precipitation among the stations were computed for the period 1950-2010, considering all calendar months together. Then the correlations above 0.80 ($p \leq 0.05$) in the matrix were identified. This correlation matrix is shown in Table 2. The correlations above 0.80 were highlighted in bold text. For monthly precipitation, the stations 79023 (Polkemmet) and 79046 (Wartook reservoir) showed the highest number of correlations above 0.80 with the rest of the stations in the study area. Therefore, one of these stations, in this case station 79046 was selected as the first key station for monthly precipitation. The stations which displayed correlations above 0.80 with station 79046 (first key station) were identified as the member stations of the first cluster. These member stations were 79014, 79019, 79023, 79026, 79028, 79034, 90173, 79074, 79079, 79080, 89003 and 89085.

Table 2 Correlations among the 17 stations for monthly observed precipitation over the period 1950-2010.

Station ID	79014	76047	77007	77042	77083	79019	79023	79026	79028	79034	79046	90173	79074	79079	79080	89003	89085
79014	**1.00**	0.62	0.75	0.62	0.71	**0.91**	**0.83**	**0.85**	**0.84**	**0.88**	**0.84**	0.76	**0.82**	**0.87**	**0.89**	0.78	**0.93**
76047	0.62	**1.00**	0.79	**0.81**	0.77	0.63	0.68	0.63	0.69	0.64	0.56	0.49	0.55	0.68	0.68	0.53	0.63
77007	0.75	0.79	**1.00**	0.79	**0.82**	0.74	0.77	0.73	0.79	0.74	0.66	0.57	0.65	**0.83**	0.79	0.63	0.75
77042	0.62	**0.81**	0.79	**1.00**	0.71	0.62	0.64	0.61	0.66	0.61	0.53	0.45	0.53	0.67	0.66	0.50	0.61
77083	0.71	0.77	**0.82**	0.71	**1.00**	0.72	**0.80**	0.75	**0.82**	0.74	0.67	0.59	0.67	0.79	0.78	0.65	0.71
79019	**0.91**	0.63	0.74	0.62	0.72	**1.00**	**0.85**	**0.89**	**0.85**	**0.91**	**0.85**	0.76	**0.84**	**0.86**	**0.93**	**0.81**	**0.94**
79023	**0.83**	0.68	0.77	0.64	**0.80**	**0.85**	**1.00**	**0.89**	**0.94**	**0.83**	**0.85**	0.75	**0.83**	**0.85**	**0.89**	**0.83**	**0.83**
79026	**0.85**	0.63	0.73	0.61	0.75	**0.89**	**0.89**	**1.00**	**0.88**	**0.87**	**0.91**	0.79	**0.92**	**0.88**	**0.95**	**0.86**	**0.87**
79028	**0.84**	0.69	0.79	0.66	**0.82**	**0.85**	**0.94**	**0.88**	**1.00**	**0.83**	**0.81**	0.71	0.79	**0.86**	**0.89**	0.78	**0.84**
79034	**0.88**	0.64	0.74	0.61	0.74	**0.91**	**0.83**	**0.87**	**0.83**	**1.00**	**0.84**	0.78	**0.83**	**0.85**	**0.90**	**0.81**	**0.93**
79046	**0.84**	0.56	0.66	0.53	0.67	**0.85**	**0.85**	**0.91**	**0.81**	**0.84**	**1.00**	**0.84**	**0.95**	**0.82**	**0.86**	**0.90**	**0.85**
90173	0.76	0.49	0.57	0.45	0.59	0.76	0.75	0.79	0.71	0.78	**0.84**	**1.00**	**0.82**	0.72	0.75	**0.88**	0.79
79074	**0.82**	0.55	0.65	0.53	0.67	**0.84**	**0.83**	**0.92**	0.79	**0.83**	**0.95**	**0.82**	**1.00**	**0.81**	**0.85**	**0.89**	**0.84**
79079	**0.87**	0.68	**0.83**	0.67	0.79	**0.86**	**0.85**	**0.88**	**0.86**	**0.85**	**0.82**	0.72	**0.81**	**1.00**	**0.91**	0.76	**0.85**
79080	**0.89**	0.68	0.79	0.66	0.78	**0.93**	**0.89**	**0.95**	**0.89**	**0.90**	**0.86**	0.75	**0.85**	**0.91**	**1.00**	**0.81**	**0.91**
89003	0.78	0.53	0.63	0.50	0.65	**0.81**	**0.83**	**0.86**	0.78	**0.81**	**0.90**	**0.88**	**0.89**	0.76	**0.81**	**1.00**	**0.81**
89085	**0.93**	0.63	0.75	0.61	0.71	**0.94**	**0.83**	**0.87**	**0.84**	**0.93**	**0.85**	0.79	**0.84**	**0.85**	**0.91**	**0.81**	**1.00**

Bold shaded correlations are above the correlation threshold 0.80

After the delineation of the first cluster, the rest of the stations (76047, 77007, 77042 and 77083) in the study area were considered for the identification of the next key stations. The correlations among these stations for monthly precipitation were highlighted in the box shown in Table 2. Similar to the selection of the first key station, a threshold of 0.80 was imposed on the correlation matrix in this box. Since each station highlighted in the box in Table 2 (76047, 77007, 77042 and 77083) had only one correlation above 0.80 with other stations, one of these stations, in this case station 76047 (Ouyen post office) was selected as the second key station. Due to the high correlation displayed by the precipitation data at station 77042 (Swan Hill post office) with those at station 76047 (Ouyen post office), station 76042 was identified as the only member of the second cluster. Then again a correlation threshold of 0.80 was imposed on the last two stations left (77007 and 77083). Since these two stations were highly correlated with each other for precipitation, station 77007 (Birchip post office) was defined as the third and the last key station, and station 77083 (Rainbow) was identified as the only member station of the third cluster. It was understood that the key station approach was able to segregate the precipitation observation stations in the study area into number of clusters, depending on the spatial correlation structures seen in the past precipitation observations. The stations in different cluster were least correlated with each other. This allowed the maintenance of adequate independence between the stations in different clusters. Figure 3 shows the key stations, member stations and the clusters delineated over the study area for monthly precipitation.

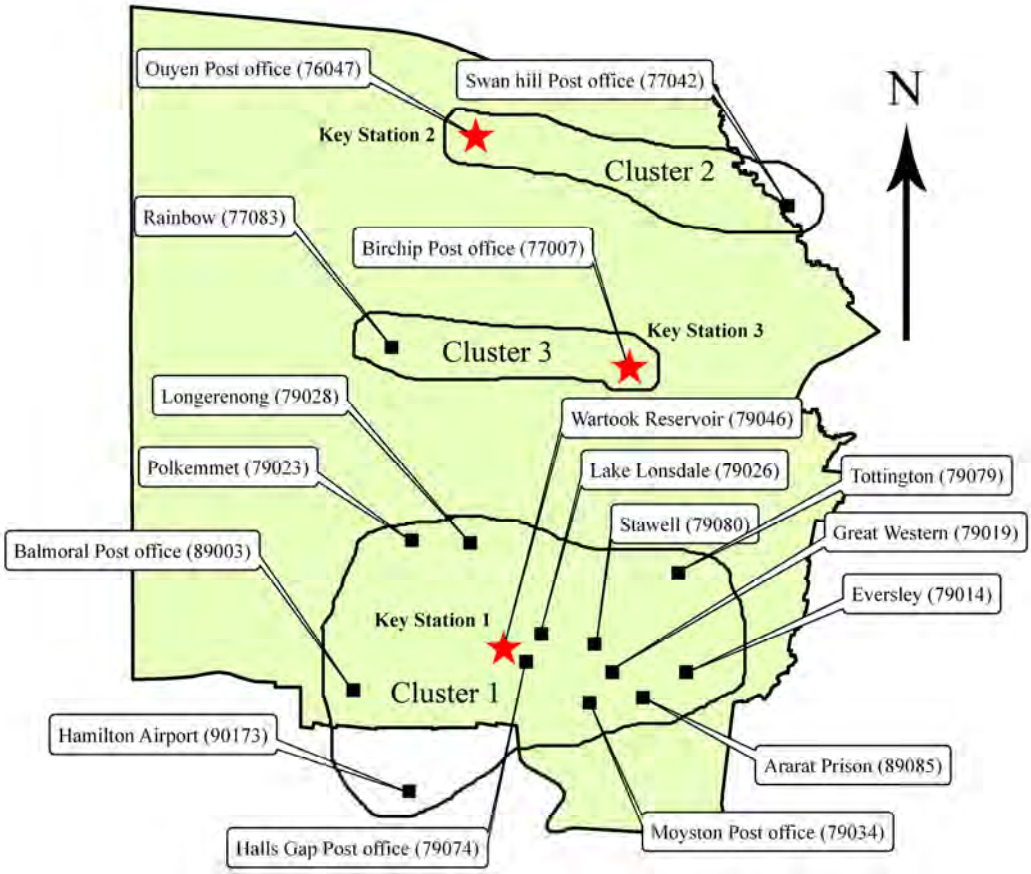

Figure 3 Clusters of stations for precipitation

4.1.2 Key stations and clusters for evaporation, minimum temperature and maximum temperature

In the same manner as for monthly precipitation, correlation matrices for the monthly observed evaporation, minimum temperature and maximum temperature were also calculated for the period 1950-2010 (not shown in the paper). It was seen that the correlations among stations for monthly evaporation, minimum and maximum temperature were much higher than those for monthly precipitation. The minimum correlation among the 17 stations for evaporation which was about 0.94 was seen between stations 90173 and 76047, as these two stations are located in two different climatic zones and separated by a large distance. The lowest correlations for both minimum temperature and maximum temperature were seen between the stations 90173 and 77042, which were 0.96 and 0.98 respectively. These two stations are located far

apart from each other (see Figure 4) in two distinctly different climatic zones (refer to Section 2).

Considering the very high correlations (higher than the correlation threshold of magnitude of 0.80) seen between the stations for evaporation, minimum temperature and maximum temperature, it was realised that any station in the study area can be regarded as a key station, for those climatic variables. Therefore, for evaporation, minimum temperature and maximum temperature, station 79046 (Wartook reservoir) was selected as the sole key station. The rest of the stations were considered as the member stations of the cluster. Figure 4 shows the key station and the cluster for evaporation, minimum temperature and maximum temperature over the study area.

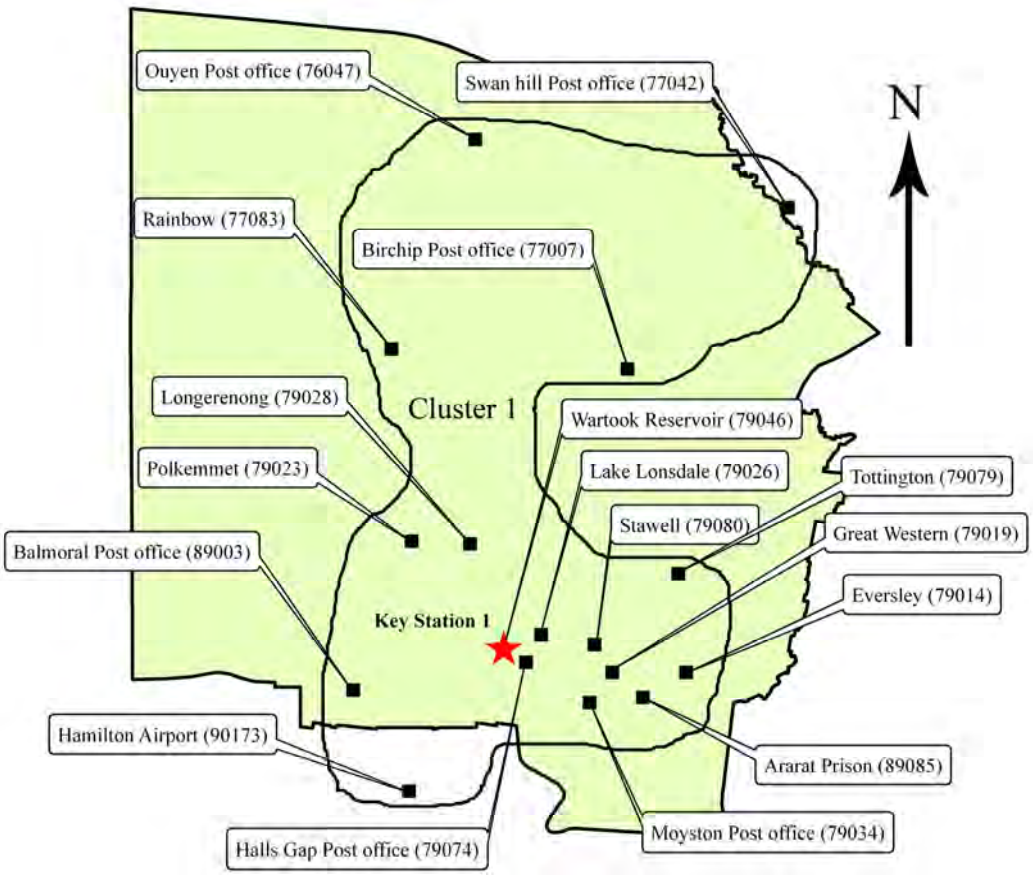

Figure 4 Cluster of stations for evaporation, minimum temperature and maximum temperature

4.2. Relationships between key stations and member stations in clusters

As described in Section 3.2, simple linear regression relationships were developed (calibrated and validated) between the key stations and the member stations of each cluster, for each predictand and for each calendar month separately. The constants and coefficients of the MLR equations in the inter-station regression relationships determined for the past climate were assumed to be valid for future, under changing climate.

4.2.1 Relationships between key stations and member stations for precipitation

Table 3 shows the statistics of the calibration (1950-1989) and validation (1990-2010) phases of inter-station regression relationships for precipitation. In all four seasons in all clusters, and at all member stations during the calibration phase of the inter-station regression relationships, the average of the monthly precipitation was near-perfectly reproduced. However, during the calibration period, the standard deviation of the precipitation was under-estimated at all member stations, in all clusters and in all seasons. In cluster 1 in the calibration period, the NSEs ranged between; 0.57 to 0.83 (summer), 0.68 to 0.90 (autumn), 0.68 to 0.84 (winter) and 0.68 to 0.90 (spring).

In the calibration phase of the inter-station regression relationships, the highest NSEs in all clusters, in all four seasons, were seen at station 79074 (Halls Gap post office). This was due to the very high correlation (0.95 in Table 2) which prevailed between the observed precipitation at the key station of cluster 1 (79046) and that at station 79074. Also these stations were located geographically close to each other (see Figure 3). In cluster 1, during the calibration phase, the lowest NSEs in summer, autumn and winter were seen at station 79079. In the calibration period in clusters 2 and 3, NSEs were relatively low in summer, and the highest NSEs in those clusters were seen in winter.

In the validation phase of the inter-station regression relationships for precipitation, despite some under-predictions in all four seasons, in all clusters the average of precipitation was well reproduced at all member stations. During the same period, the

standard deviation of the precipitation was well reproduced at the majority of member stations in cluster 1, in all seasons, despite some under and over-predictions. Under-prediction of the standard deviation of precipitation was evident at all member stations in clusters 2 and 3 in all seasons. In cluster 1 during validation, NSEs for precipitation at member stations varied between; 0.34 to 0.82 (summer), 0.51 to 0.89 (autumn), 0.55 to 0.88 (winter) and 0.58 to 0.85 (spring). In summer and autumn, station 79074 showed the highest NSEs in all clusters during the validation phase. In winter and spring, station 79026 displayed the highest NSEs in all clusters.

Considering the performances of the outputs of inter-station regression relationships seen in their calibration and validation phases, it was realised that they are robust enough for satisfactory modelling of precipitation at the member stations.

Table 3 Statistics for calibration and validation of inter-station regression relationships for precipitation

Season	Key Station	Cluster	Member Station	Period 1950-1989 (Calibration)					Period 1990-2010 (Validation)				
				Average		Std		NSE	Average		Std		NSE
				Obs	Inter	Obs	Inter		Obs	Inter	Obs	Inter	
Summer	79046	1	79014	33.5	33.7	33.1	28.1	0.73	36.5	32.5	28.0	25.5	0.61
			79019	32.7	32.9	33.5	28.7	0.75	28.2	31.5	22.7	25.6	0.49
			79023	25.2	25.2	23.6	19.5	0.68	24.3	24.4	18.6	17.1	0.34
			79026	30.5	30.5	26.7	22.9	0.73	30.4	29.7	26.0	21.2	0.80
			79028	25.0	25.2	26.7	21.3	0.66	24.1	24.2	20.9	18.3	0.39
			79034	33.4	33.4	32.3	26.7	0.68	31.0	32.4	27.4	26.0	0.70
			90173	36.1	36.1	26.9	20.3	0.57	33.2	35.7	25.3	22.2	0.37
			79074	40.7	40.7	33.7	30.8	0.83	42.9	40.0	41.0	31.9	0.82
			79079	29.6	29.6	28.5	21.4	0.57	28.7	29.2	25.8	21.0	0.50
			79080	30.3	30.3	28.6	24.2	0.72	31.3	29.5	26.5	21.9	0.67
			89003	28.5	28.5	23.8	18.2	0.59	28.4	27.9	20.4	18.6	0.41
			89085	34.8	34.9	34.3	29.5	0.75	36.2	33.5	28.2	26.8	0.64
	76047	2	77042	24.3	24.3	27.0	20.3	0.56	24.1	24.1	22.1	18.8	0.60
	77007	3	77083	23.1	23.1	25.2	19.9	0.62	25.5	21.1	32.6	12.9	0.39
Autumn	79046	1	79014	46.8	46.8	33.1	28.2	0.73	36.0	36.8	25.3	21.7	0.71
			79019	47.1	47.1	34.0	28.1	0.69	32.2	37.0	24.9	22.0	0.71
			79023	36.6	36.6	28.2	24.7	0.77	24.9	27.9	19.5	18.9	0.72
			79026	49.2	49.3	40.1	35.0	0.77	32.8	36.9	26.3	26.8	0.86
			79028	35.6	35.7	30.2	25.2	0.70	22.4	26.6	19.3	19.5	0.66
			79034	48.8	48.8	34.9	29.2	0.70	32.4	38.4	25.6	23.5	0.62
			90173	53.2	53.2	32.8	28.2	0.74	39.8	43.6	24.0	22.9	0.51
			79074	73.7	73.7	58.8	55.7	0.90	54.1	53.8	43.1	41.5	0.89
			79079	46.2	46.2	35.5	29.3	0.68	30.3	35.7	26.9	22.5	0.74
			79080	46.5	46.5	36.6	31.2	0.73	30.5	35.1	23.6	24.4	0.74
			89003	47.9	47.9	34.1	30.4	0.80	31.9	37.6	21.7	23.6	0.73
			89085	50.7	50.7	32.8	27.8	0.72	33.5	40.9	23.1	22.0	0.70
	76047	2	77042	32.8	32.8	27.9	22.8	0.67	21.1	24.0	20.7	19.0	0.63
	77007	3	77083	31.1	31.1	27.5	23.3	0.72	21.1	20.7	21.6	15.8	0.76
Winter	79046	1	79014	62.7	62.7	29.0	25.4	0.77	63.8	60.6	29.4	24.0	0.71
			79019	63.0	63.0	32.1	28.3	0.78	60.9	60.4	30.4	26.5	0.72
			79023	48.3	48.3	24.9	21.1	0.72	49.2	47.4	27.0	20.9	0.77
			79026	72.4	72.4	38.6	33.7	0.76	72.9	70.3	39.3	32.9	0.88
			79028	44.2	44.2	23.3	19.8	0.73	43.1	43.1	26.1	19.5	0.73
			79034	63.0	63.0	32.3	28.0	0.75	60.3	60.6	28.6	26.3	0.75
			90173	73.6	73.6	29.2	25.2	0.74	70.6	72.2	28.7	24.4	0.55
			79074	125.1	125.1	64.5	59.2	0.84	119.4	120.3	61.2	56.6	0.86
			79079	58.9	58.9	28.2	23.3	0.68	55.0	57.7	32.7	22.8	0.67
			79080	60.1	60.1	31.0	26.4	0.73	61.0	58.4	32.8	25.9	0.81
			89003	73.6	73.6	33.4	29.7	0.79	66.5	71.1	31.3	28.1	0.78
			89085	64.3	64.3	29.3	26.5	0.82	60.9	62.3	27.0	25.1	0.74
	76047	2	77042	35.9	35.9	23.0	19.5	0.72	30.8	32.9	18.7	16.2	0.55
	77007	3	77083	36.8	36.8	20.4	17.3	0.72	37.1	33.1	21.5	15.9	0.66
Spring	79046	1	79014	55.7	55.7	32.8	27.9	0.72	51.7	49.7	29.6	23.9	0.66
			79019	53.0	53.0	32.2	28.2	0.77	49.0	46.9	28.9	23.7	0.58
			79023	42.6	42.6	27.2	23.1	0.73	40.9	37.0	26.2	18.7	0.72
			79026	53.2	53.2	33.9	30.2	0.80	50.2	46.6	30.7	25.0	0.84
			79028	40.5	40.5	28.1	23.2	0.68	35.8	34.9	23.3	18.3	0.73
			79034	56.3	56.3	33.9	29.1	0.74	48.5	49.4	25.3	24.4	0.72
			90173	63.5	63.5	29.1	25.2	0.75	59.8	58.4	26.8	21.5	0.70
			79074	87.7	87.7	53.5	50.8	0.90	78.3	78.5	48.4	45.8	0.83
			79079	50.4	50.4	32.8	27.2	0.69	44.1	44.5	30.8	22.4	0.64
			79080	50.5	50.5	32.1	27.7	0.74	47.1	44.5	29.2	22.9	0.74
			89003	57.2	57.2	31.4	27.9	0.79	48.9	51.4	27.5	23.8	0.85
			89085	58.7	58.7	34.0	30.4	0.80	49.9	51.6	23.9	25.5	0.65
	76047	2	77042	34.0	34.0	23.7	20.1	0.72	34.0	31.3	29.6	18.1	0.72
	77007	3	77083	36.0	36.0	26.2	21.9	0.70	31.6	31.6	24.8	17.7	0.65

Average = average of monthly precipitation in mm, Std = standard deviation of monthly precipitation in mm, Inter = Inter-station regression relationships, NSE = Nash Sutcliffe efficiency

4.2.2 Relationships between key stations and member stations for evaporation and temperature

At the majority of member stations, the NSEs for the calibration (1950-1989) and validation (1990-2010) phases of the inter-station regression relationships for evaporation, minimum temperature and maximum temperature were quite high in all four seasons (results not shown in the paper). It was realised that these high NSEs were due to the high correlations seen between the key station and member stations (Section 4.1.2) for evaporation, minimum temperature and maximum temperature. Furthermore, it was seen that NSEs for the inter-station regression relationships developed for evaporation, minimum temperature and maximum temperature were relatively higher than those for precipitation. Also, in the calibration phase the inter-station regression relationships near-perfectly reproduced the averages of evaporation, minimum temperature and maximum temperature, at all member stations, in all seasons. Also at the majority of stations the standard deviations of evaporation, minimum temperature and maximum temperature were near-perfectly reproduced by the inter-station regression relationships during the calibration period. In the validation phase, despite slight over and under-predictions, the inter-station regression relationships built for evaporation, minimum temperature and maximum temperature were able to capture the average and the standard deviations of these variables well in all seasons, at all member stations. It was realised that the inter-station regression relationships developed between the key station and member stations for evaporation, minimum temperature and maximum temperature are quite robust.

4.3. Atmospheric domain and predictor selection

As shown in Figure 5, an atmospheric domain with 7 points in the longitudinal direction and 6 points in the latitudinal direction was demarcated over the study area for the current study. This atmospheric domain had a spatial resolution of 2.5˚ in both longitudinal and latitudinal directions.

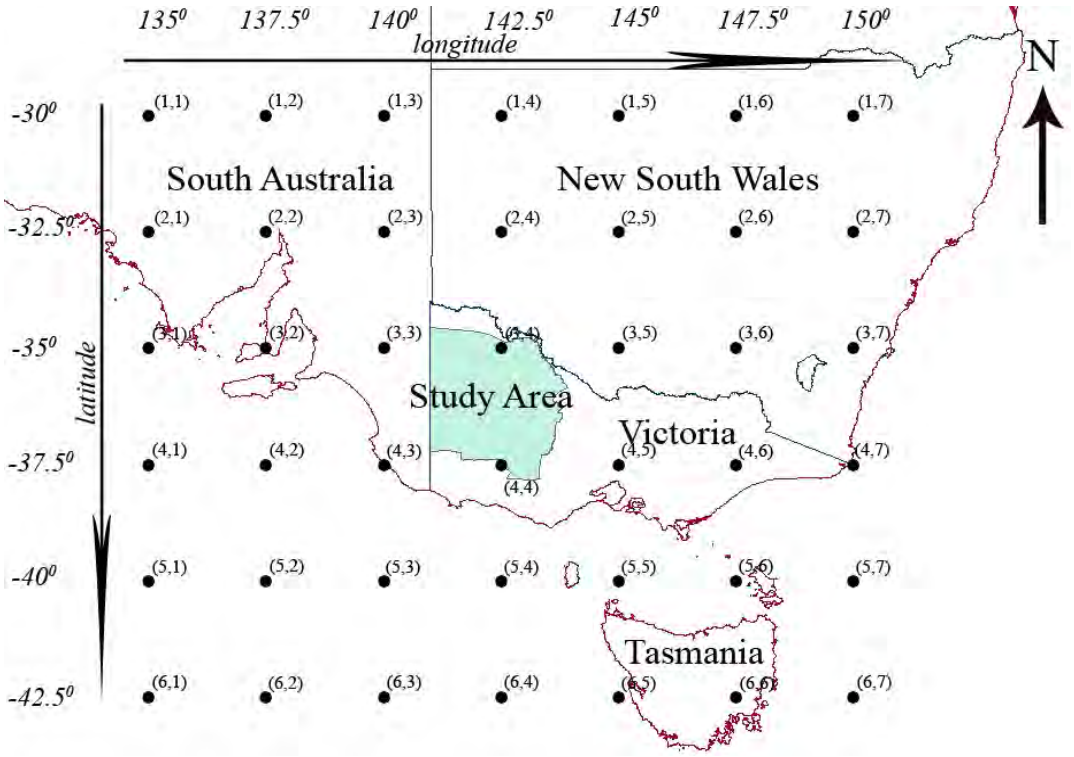

Figure 5 Atmospheric domain for downscaling

The probable predictors for the current study were selected mainly based on the study by Timbal et al. (2009). Timbal et al. (2009) used the method of meteorological analogues to statistically downscale GCM outputs to daily precipitation, pan evaporation, minimum temperature, maximum temperature, and dew point temperature over six regions in the southern half of Australia. In that study they identified the best predictors for each predictand for each season over the six regions. Since the current study area is also located in south eastern Australia, the predictors used in the study by Timbal et al. (2009) were included in the probable predictor pool of the current study. Some of the predictors used by Anandhi et al. (2008, 2009) in downscaling GCM outputs to monthly precipitation, minimum temperature and maximum temperature were also included in the pool of probable predictors used in the current study. The probable predictors which were selected for the present study based on past literature and hydrology are shown in Table 4.

Table 4 Probable predictors for precipitation, evaporation and temperature

Probable predictor	**Level**	**Precipitation**	**Evaporation**	**$T_{min/max}$**
Geopotential height	200hPa	✓	✓	✓
	500 hPa	✓	✓	✓
	700 hPa	✓	✓	✓
	850 hPa	✓	✓	✓
	1000 hPa	✓	✓	✓
Relative humidity	500 hPa	✓	✓	✓
	700 hPa	✓	✓	✓
	850 hPa	✓	✓	✓
	925 hPa		✓	✓
	1000 hPa	✓	✓	✓
Specific humidity	2m height	✓	✓	✓
	500 hPa	✓	✓	✓
	850 hPa	✓	✓	✓
	1000 hPa	✓	✓	✓
Air temperature	2m height	✓	✓	✓
	500 hPa	✓	✓	✓
	850 hPa	✓	✓	✓
	1000 hPa	✓	✓	✓
Skin temperature	surface	✓	✓	✓
Pressure	surface	✓	✓	✓
	mean sea level	✓	✓	✓
Precipitation rate	surface	✓	✓	
Precipitable water	N/A		✓	
Zonal wind speed	850 hPa	✓	✓	✓
Meridional wind speed	850 hPa	✓	✓	✓

✓= included in the pool of probable predictors, N/A = not applicable, hPa = Atmospheric pressure in hectopascal, $T_{min/max}$ = minimum temperature and maximum temperature

Following the procedure described in Section 3.3, potential predictors from the pool of probable predictors were extracted for each predictand at each key station for each calendar month.

4.4. Development of downscaling models at key stations

Using the procedure described in Section 3.4, downscaling models were developed at the key stations for precipitation, evaporation, minimum temperature and maximum temperature. These models were calibrated and validated over the periods 1950-1989 and 1990-2010 respectively. Sections 4.4.1, 4.4.2 and 4.4.3 detail the performances of

the downscaling models developed at the key stations for precipitation, evaporation, minimum temperature and maximum temperature respectively. All downscaling models in this study were developed using the MLR option available in the statistics toolbox of MATLAB (Version - R2008b) software.

4.4.1 Downscaling models developed at key stations for precipitation

As stated in Section 4.1.1, three key stations were identified for precipitation. Tables 5 shows the statistics of the precipitation reproduced by the downscaling model developed at the key station 79046 of cluster 1. The statistics of the precipitation reproduced by the downscaling models developed at key stations 76047 (cluster 2) and 77007 (cluster 3) are not shown in tabular form. During the calibration phase of the downscaling models at key stations 79046, 76047 and 77007, the average of the precipitation was near-perfectly reproduced in all seasons. In validation at all three key stations, the average of precipitation was successfully reproduced, in all seasons, despite some under and over-predictions. In the majority of seasons, the standard deviation of precipitation was under-estimated by the downscaling models at all three key stations, during both the calibration and validation periods. During calibration at all three key stations, the maximum of precipitation was under-predicted in all seasons. In validation, the maximum of precipitation was under-predicted in all seasons at station 79046 (key station 1). At the other two key stations, this pattern was evident in the majority of seasons. The R^2 values and NSEs of the precipitation reproduced by the downscaling models at the three key stations were also comparable with each other in the calibration and validation periods.

Table 5 Statistics of precipitation reproduced by downscaling model developed at station 79046 (Key station 1)

Model	Statistic	Calibration (1950-1989)				*Validation (1990-2010)*			
		Season				*Season*			
		Summer	**Autumn**	**Winter**	**Spring**	***Summer***	***Autumn***	***Winter***	***Spring***
Observed	Avg	40.9	67.9	108.5	80.8	*39.3*	*50.2*	*106.3*	*72.3*
Model output		40.9	67.9	108.5	80.8	*47.8*	*56.5*	*110.9*	*76.9*
Observed	Std	32.2	49.6	50.2	43.2	*31.6*	*36.7*	*49.1*	*37.9*
Model output		20.4	39.8	41.6	32.2	*24.3*	*28.3*	*40.1*	*30.2*
Observed	Min	2.3	3.1	14.5	10.4	*0.0*	*4.0*	*25.2*	*9.0*
Model output		8.5	0.0	11.1	23.8	*15.8*	*0.0*	*21.4*	*18.3*
Observed	Max	163.4	246.7	273.7	246.2	*155.0*	*137.8*	*234.2*	*189.6*
Model output		123.7	182.1	240.4	166.6	*112.7*	*117.5*	*221.6*	*164.4*
Model output	NSE	0.40	0.65	0.69	0.56	*0.41*	*0.56*	*0.74*	*0.73*
Model output	R^2	0.40	0.65	0.69	0.56	*0.49*	*0.59*	*0.75*	*0.75*

Avg = average of monthly precipitation in mm, Std = standard deviation of monthly precipitation in mm, Min = minimum of monthly precipitation in mm, Max = maximum of monthly precipitation in mm, NSE = Nash Sutcliffe efficiency, R^2 = coefficient of determination

Figure 6 shows the scatter plots for the precipitation reproduced by the downscaling models developed at the key stations 79046, 76047 and 77007, for the calibration and validation phases. The best model performance in terms of the NSE (0.75) was seen at the key station 79046 in its validation. Similarly, a good NSE of 0.70 was also seen in its calibration phase. The other two key stations showed low NSEs in both calibration and validation, relative to those of key station 79046. At all three key stations, the scatter of precipitation reproduced by the downscaling models in their calibration and validation periods was comparable with each other. According to the six scatter plots in Figure 6, it was seen that the high precipitation values were under-predicted by the downscaling models at all key stations, during both the calibration and validation periods. Also all three downscaling models in general displayed an over-predicting pattern for the low precipitation values in the calibration and validation periods.

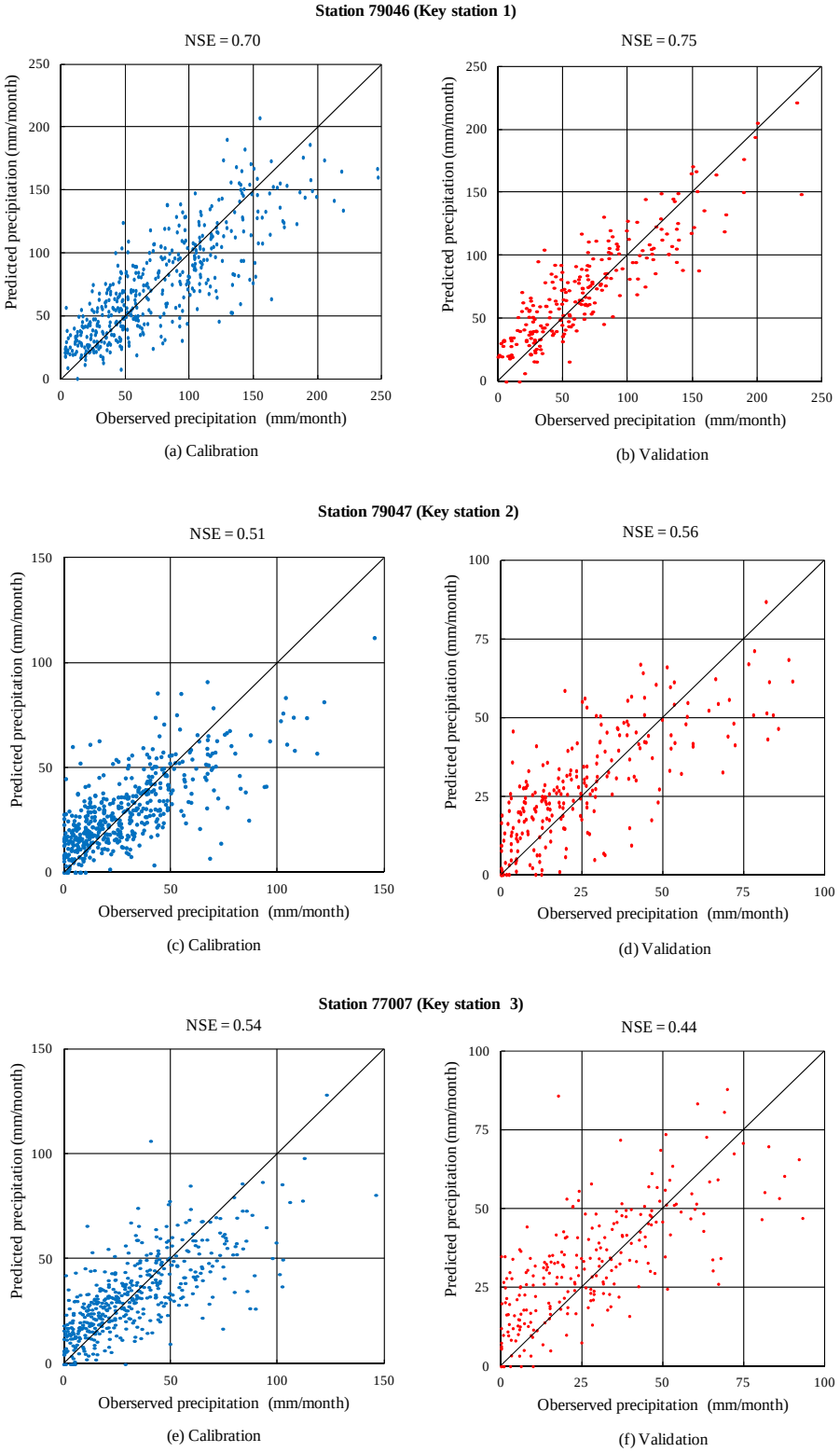

Figure 6 Scatter plots for precipitation reproduced by downscaling models developed at key stations 79046, 76047 and 77007

4.4.2 Downscaling models developed at key stations for evaporation and temperature

As stated in Section 4.1.2, for the entire study area one single key station was identified for evaporation, minimum temperature and maximum temperature. The statistics of the monthly evaporation, minimum temperature and maximum temperature reproduced by the downscaling models developed at the key station 79046 were compared with the statistics of corresponding observations (results not shown).

During the calibration phase, the average of evaporation was perfectly reproduced by the downscaling model at key station 79046, in all seasons. Despite negligible over and under-predictions seen during the validation period of this downscaling model, in all seasons, the average of evaporation was well reproduced. The standard deviation of evaporation was reproduced with good accuracy in both calibration and validation, in all seasons, despite slight over and under-predictions. For evaporation, relatively high NSE and R^2 values were seen in the calibration and validation phases of the downscaling model, in all seasons. According to the statistics of the monthly evaporation reproduced by the downscaling model developed at key station 79046, it was realised that this model is quite capable in reproducing the statistics of observations of evaporation.

In all seasons, the averages of the minimum temperature and maximum temperature were near-perfectly reproduced by the downscaling models which were developed for the key station 79046, in both the calibration and validation periods. Despite slight under and over-estimations, the standard deviation of the minimum temperature was well reproduced in the calibration and the validation phases of the downscaling model, in all seasons. However, both in calibration and validation, the standard deviation of the maximum temperature was slightly under-estimated by the downscaling model in all four seasons. In all seasons, an over-prediction of the minimum of the minimum temperature was seen in both calibration and validation. The minimum of the minimum temperature was important as it referred to extreme minimum temperature. In both the calibration and validation periods, despite slight over and under-predictions, the maximum of the maximum temperature were reproduced with good accuracy by the

downscaling model, in all seasons. The maximum of the maximum temperature was important as it referred to extreme maximum temperature.

Figure 7 show the scatter plots for evaporation, minimum temperature and maximum temperature reproduced by the downscaling models developed at key station 79046. It was evident that, for evaporation, minimum temperature and maximum temperature, the scatter was small and quite comparable in both the calibration and validation periods. However, the scatter of evaporation (see Figures 7a and 7b) and maximum temperature (see Figures 7e and 7f) in both the calibration and validation periods was relatively smaller for lower values and larger for higher values. On the other hand, the scatter of the minimum temperature was almost even along the 45˚ line in both the calibration and validation periods (see Figures 7c and 7d).

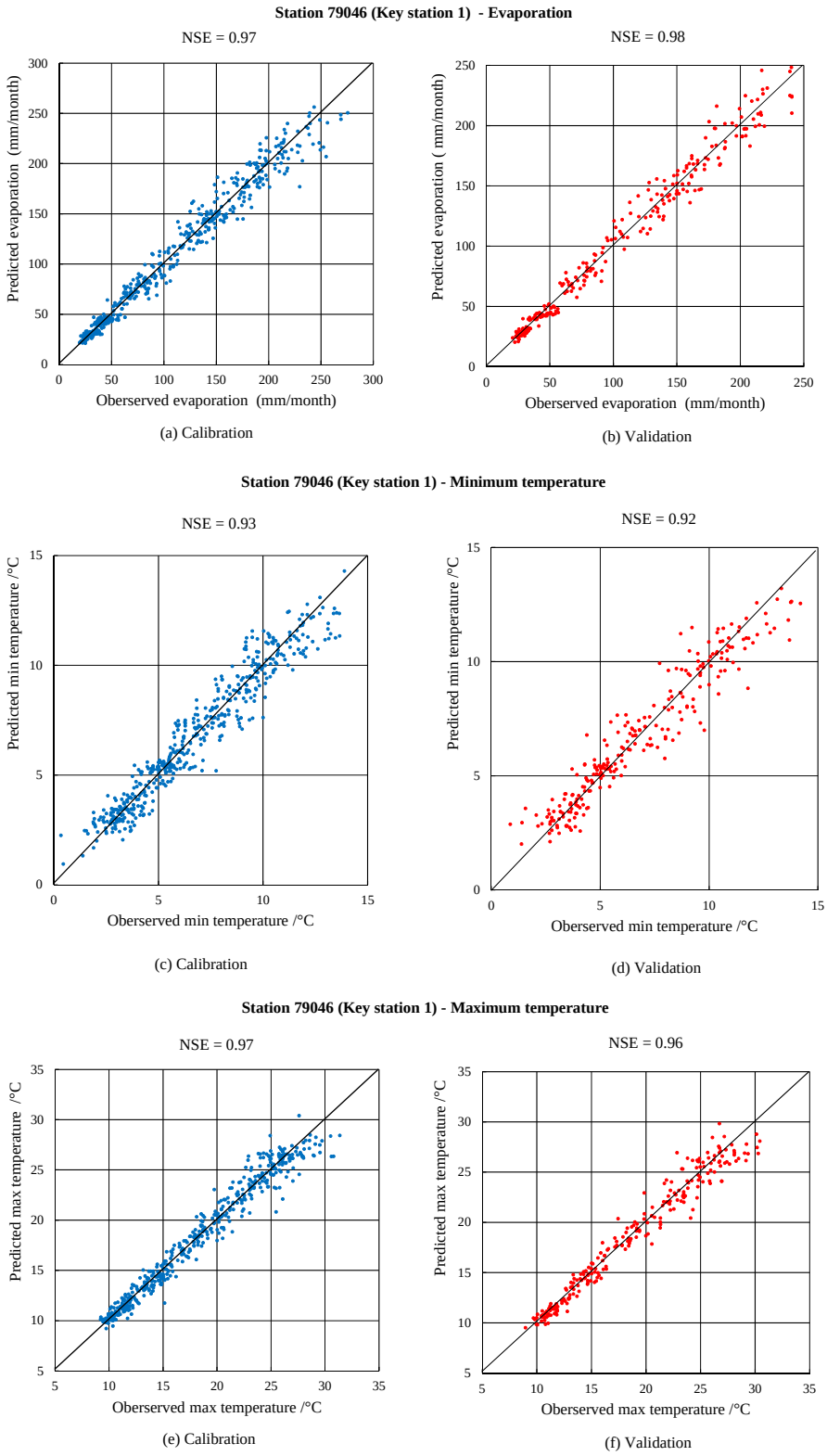

Figure 7 Scatter plots for evaporation, minimum temperature and maximum temperature reproduced by downscaling model developed at key station 79046

4.4.3 Bias-correction of the outputs produced by downscaling models with 20C3M outputs of HadCM3 at key stations

Following the procedure detailed in Section 3.5, the monthly bias-correction (Johnson and Sharma, 2012) was applied over the period 1950-1989 and it was validated for the period 1990-2010. Table 6 shows the statistics of precipitation reproduced by the downscaling model developed at key station 79046 when it was run with the 20C3M outputs of HadCM3, before and after the application of the monthly bias-correction. Note that the statistics of evaporation, minimum temperature and maximum temperature reproduced by the downscaling model developed at key station 79046 before and after the monthly bias-correction were not shown in tabular form.

As shown in Table 6, the downscaling model at the key station 79046, when it was run with the 20C3M outputs of HadCM3, tended to over-estimate the average of precipitation in the application and validation periods of the bias-correction, in all seasons, before the bias-correction. After the application of the monthly bias-correction the average of precipitation reproduced by the downscaling model was corrected with good accuracy, in all seasons in the application period. During the validation period of the bias-correction in summer and spring, the average of precipitation was successfully corrected. The correction to the standard deviation of precipitation reproduced by the downscaling model was successful in the majority of seasons in the application and validation phases of the bias-correction. In both the application and validation periods of the bias-correction, the minimum of precipitation was well corrected in all seasons except spring. However, the correction to the maximum of precipitation was limited in the majority of seasons, in both application and validation periods.

In the application and validation periods, before the implementation of the bias-correction, the NSEs were quite low during all seasons for precipitation. This indicated that there is large mismatch in the precipitation reproduced by the downscaling model when it was run with the 20C3M outputs of HadCM3 (i.e. considerable bias) and the observed precipitation. After the application of the bias-correction, the NSEs in all

seasons in the application period and also in summer and winter in the validation period showed some increase. This hinted some improvement to the time series of the variable following the application of monthly bias-correction.

Table 6 Statistics of precipitation reproduced by downscaling model at key station 79046, with 20C3M outputs of HadCM3, before and after bias-correction

Model	Statistic	Application (1950-1989)				*Validation (1990-1999)*			
		Season				*Season*			
		Summer	**Autumn**	**Winter**	**Spring**	***Summer***	***Autumn***	***Winter***	***Spring***
Observed	Avg	40.9	67.9	108.5	80.8	*42.3*	*53.1*	*119.0*	*77.8*
Before B-C		66.3	102.2	156.5	83.4	*69.9*	*106.1*	*137.0*	*82.6*
After B-C		41.1	68.1	108.5	80.8	*44.5*	*75.4*	*101.8*	*81.1*
Observed	Std	32.2	49.6	50.2	43.2	*37.2*	*42.9*	*57.8*	*41.8*
Before B-C		32.1	34.4	137.0	47.6	*35.1*	*39.4*	*93.6*	*52.5*
After B-C		31.9	49.2	50.2	43.2	*35.0*	*70.7*	*37.1*	*47.5*
Observed	Min	2.3	3.1	14.5	10.4	*0.0*	*4.0*	*29.8*	*21.8*
Before B-C		17.7	18.4	0.0	0.0	*21.3*	*46.3*	*0.0*	*0.0*
After B-C		0.0	0.0	2.4	17.0	*0.0*	*9.0*	*3.5*	*20.6*
Observed	Max	163.4	246.7	273.7	246.2	*155.0*	*137.8*	*234.2*	*189.6*
Before B-C		183.7	189.6	1091.1	187.9	*145.4*	*212.7*	*420.7*	*163.7*
After B-C		144.0	245.4	323.6	193.5	*126.2*	*298.1*	*209.3*	*236.8*
Before B-C	NSE	-1.17	-0.40	-9.29	-1.00	*-1.30*	*-1.91*	*-2.70*	*-0.87*
After B-C		-0.54	-0.27	-1.03	-0.90	*-0.64*	*-2.46*	*-0.48*	*-1.22*

Avg = average of monthly precipitation in mm, Std = standard deviation of monthly precipitation in mm, Min = minimum of monthly precipitation in mm, Max = maximum of monthly precipitation in mm, NSE = Nash Sutcliffe efficiency, Before B-C = before bias-correction, After B-C = after bias-correction

For evaporation in general, the over and under-predictions in the statistics were quite small in comparison with those for precipitation. During the application period of the bias-correction, the bias in the average of evaporation was perfectly corrected in all seasons. In the validation phase of the bias-correction, the bias in the average of evaporation reproduced by the downscaling model increased in the majority of seasons. The standard deviation of the evaporation reproduced by the downscaling model was well corrected in the application phase of the bias-correction. In the validation phase, the bias in the standard deviation of the evaporation decreased in winter and spring. The maximum of the evaporation reproduced by the downscaling model was well corrected by the bias-correction in summer during both the application and validation periods. The NSEs for the evaporation reproduced by the downscaling model when it was run

with the 20C3M outputs of HadCM3 were relatively higher than those for precipitation, in both the application and validation periods.

The bias in the average of the minimum temperature and the maximum temperature reproduced by the downscaling model at key station 79046, when it was run with the 20C3M outputs of HadCM3 was quite small in all seasons even before the bias-correction. The over-prediction of the standard deviation of the minimum temperature that was seen in summer and spring in the application and validation periods of the bias-correction was successfully corrected. Also the under and over-predictions in the standard deviation of the maximum temperature in the application and validation periods of the bias-correction were successfully corrected in all seasons.

4.5. Development of a downscaling model at a member station

Using the same procedure used in developing downscaling models at key stations (Section 4.4), a downscaling model was built for precipitation at member station 89003. This was performed to compare the performances of the inter-site regression relationship (between the key station 79046 and the member station 89003) against the performances of the downscaling model developed at this member station in reproducing the observed precipitation. Table 7 shows the statistics of precipitation reproduced by the downscaling models at station 89003, and also the statistics of precipitation reproduced at station 89003 by applying the precipitation outputs of the downscaling model developed at key station 79046 on the inter-site regression relationship.

As shown in Table 7, in all seasons the average of precipitation was near-perfectly reproduced by the downscaling model at station 89003 and the inter-station regression relationship, in the calibration period. In the validation period the average of precipitation was over-estimated in all seasons by both the downscaling model at station 89003 and the inter-station regression relationship. However, still these results were quite comparable with each other. In both calibration and validation, the standard deviation of precipitation was under-predicted, in all seasons by the downscaling model

at station 89003 and the inter-station regression relationship. Nevertheless, in all seasons, the standard deviation of precipitation reproduced by the downscaling model at station 89003 and the inter-station regression relationship were comparable with each other. Also the maximum of precipitation reproduced by the downscaling model at station 89003 and that by inter-station regression relationship was comparable in all seasons. In both the calibration and validation periods, in the majority of seasons, the NSEs of the downscaling model at station 89003 and the inter-station regression relationship were quite comparable with each other.

In summary, it was seen that the statistics of the precipitation reproduced by the downscaling model developed for station 89003 and the inter-station regression relationship between the key station 79046 and station 89003 are comparable with each other in the majority of instances. It was then assumed that the inter-station regression relationships can reproduce precipitation, evaporation and minimum temperature and maximum temperature quite well at all stations, in comparison with the individual downscaling models developed for them.

Table 7 Statistics of precipitation reproduced at station 89003 by downscaling models and inter-site regression relationship

Model	Statistic	Calibration (1950-1989)				*Validation (1990-2010)*			
		Season				*Season*			
		Summer	**Autumn**	**Winter**	**Spring**	***Summer***	***Autumn***	***Winter***	***Spring***
Observed	Avg	28.5	47.9	73.6	57.2	*28.4*	*31.9*	*66.5*	*48.9*
Model output		28.5	48.0	73.6	57.2	*33.3*	*37.9*	*73.1*	*54.8*
Inter-station Reg		28.5	47.9	73.6	57.2	*32.3*	*41.3*	*74.7*	*54.7*
Observed	Std	23.8	34.1	33.4	31.4	*20.4*	*21.7*	*31.3*	*27.5*
Model output		14.1	27.3	28.2	23.3	*17.3*	*19.6*	*27.0*	*23.3*
Inter-station Reg		12.2	24.3	24.7	20.4	*14.3*	*18.5*	*23.8*	*19.4*
Observed	Min	0.0	0.0	5.7	4.4	*0.0*	*0.0*	*10.0*	*3.2*
Model output		12.0	0.0	1.7	18.8	*13.3*	*0.0*	*17.8*	*0.0*
Inter-station Reg		8.9	2.5	18.3	18.2	*14.9*	*2.5*	*23.9*	*14.6*
Observed	Max	143.7	136.8	182.9	184.0	*85.8*	*90.7*	*147.7*	*125.2*
Model output		88.6	114.8	161.7	148.5	*81.6*	*88.0*	*143.1*	*111.1*
Inter-station Reg		79.8	111.3	158.4	112.3	*73.4*	*76.9*	*136.3*	*109.4*
Model output	NSE	0.35	0.65	0.72	0.55	*0.44*	*0.45*	*0.66*	*0.60*
Inter-station Reg		0.36	0.50	0.65	0.46	*0.46*	*0.31*	*0.66*	*0.64*

Avg = average of monthly precipitation in mm, Std = standard deviation of monthly precipitation in mm, Min = minimum of monthly precipitation in mm, Max = maximum of monthly precipitation in mm, NSE = Nash Sutcliffe efficiency, Inter-station Reg = inter-station regression relationship

4.6. Projections into future

The A2 GHG emission scenario of the Intergovernmental Panel on Climate Change (IPCC) defined in the Special Report on Emission Scenarios (SRES) (IPCC, 2000) was used for the projection of precipitation, evaporation, minimum temperature and maximum temperature into future, at the 17 stations considered in this study. The monthly outputs of HadCM3 for the period 2000-2099 pertaining to the A2 GHG emission scenario were used for producing inputs to the downscaling models developed at the key stations. Following the procedure detailed in Section 3.7 projections of precipitation, evaporation, minimum temperature and maximum temperature were produced into future, at the 17 stations.

The percentage changes in the statistics of monthly precipitation, evaporation, minimum temperature and maximum temperature, for each season, over the period 2000-2099, were compared with the statistics of the observations of those predictands of the period

1950-1989. In Table 8 the comparison of average of monthly precipitation, evaporation, minimum temperature and maximum temperature, for each season, over the period 2000-2099 with that of observations of the period 1950-1989 were shown.

As seen in Table 8, the average of the monthly precipitation showed a decline in summer and spring at the majority of stations in the period 2000-2099, in comparison with the average of the observed precipitation 1950-1989. In autumn and winter, the average of precipitation displayed a rise at the majority of stations. It was realised that, with respect to the past climate of the period 1950-1989, summer and spring in the period 2000-2099 will be dryer and autumn and winter tend to be wetter, over the study area. In all seasons except autumn, the standard deviation of the monthly precipitation over the period 2000-2099, indicated a drop, at most of the stations. The maximum of the monthly precipitation indicated a rise in magnitude at the majority of stations in summer, autumn and winter during the period 2000-2099.

Table 8 Percentage changes in the average of precipitation, evaporation, minimum temperature and maximum temperature over the period 2000-2099

Predictand	Season	79014	76047	77007	77042	77083	79019	79023	79026	79028	79034	79046	90173	79074	79079	79080	89003	89085
Precipitation	Summer	**-9↓**	**-10↓**	+28↑	**-9↓**	21↑	**-10↓**	**-10↓**	**-10↓**	**-9↓**	**-9↓**	**-10↓**	**-6↓**	**-9↓**	**-8↓**	**-9↓**	**-7↓**	**-10↓**
	Autumn	+4↑	+36↑	+40↑	+23↑	+35↑	+6↑	+7↑	+9↑	+9↑	+8↑	+4↑	+7↑	+5↑	+5↑	+8↑	+6↑	+6↑
	Winter	+14↑	+23↑	**-1↓**	21↑	**-1↓**	+15↑	+15↑	+16↑	+15↑	+15↑	+16↑	+11↑	+17↑	+13↑	+15↑	+14↑	+14↑
	Spring	**-26↓**	**-18↓**	**-15↓**	**-14↓**	**-11↓**	**-27↓**	**-29↓**	**-30↓**	**-30↓**	**-27↓**	**-27↓**	**-19↓**	**-28↓**	**-28↓**	**-28↓**	**-24↓**	**-27↓**
Evaporation	Summer	+7↑	+8↑	+9↑	+8↑	+9↑	+13↑	+11↑	+12↑	+11↑	+13↑	+13↑	+7↑	+13↑	+12↑	+12↑	+12↑	+13↑
	Autumn	+6↑	+11↑	+9↑	+8↑	+9↑	+11↑	+10↑	+11↑	+10↑	+11↑	+12↑	+6↑	+11↑	+11↑	+11↑	+10↑	+11↑
	Winter	+2↑	+4↑	+3↑	+3↑	+3↑	+4↑	+4↑	+5↑	+4↑	+5↑	+5↑	+2↑	+5↑	+5↑	+5↑	+4↑	+4↑
	Spring	+13↑	+19↑	+18↑	+16↑	+18↑	+21↑	+20↑	+22↑	+19↑	+22↑	+23↑	+11↑	+22↑	+24↑	+21↑	+18↑	+21↑
Min Temp	Summer	+1↑	+1↑	+0↑	+0↑	+1↑	+1↑	+1↑	+1↑	+1↑	+1↑	+1↑	+1↑	+1↑	+1↑	+1↑	+1↑	+1↑
	Autumn	+22↑	+21↑	+22↑	+20↑	+23↑	+22↑	+22↑	+22↑	+24↑	+23↑	+25↑	+21↑	+24↑	+22↑	+21↑	+22↑	+23↑
	Winter	+40↑	+31↑	+36↑	+28↑	+36↑	+41↑	+39↑	+37↑	+41↑	+41↑	+49↑	+32↑	+44↑	+38↑	+34↑	+37↑	+46↑
	Spring	+29↑	+21↑	+26↑	+21↑	+26↑	+30↑	+26↑	+27↑	+29↑	+31↑	+34↑	+28↑	+32↑	+27↑	+26↑	+29↑	+33↑
Max Temp	Summer	+2↑	+2↑	+2↑	+1↑	+2↑	+2↑	+2↑	+2↑	+2↑	+2↑	+2↑	+2↑	+2↑	+2↑	+2↑	+2↑	+2↑
	Autumn	+5↑	+4↑	+5↑	+4↑	+5↑	+6↑	+5↑	+5↑	+5↑	+6↑	+6↑	+5↑	+6↑	+5↑	+5↑	+5↑	+6↑
	Winter	+24↑	+21↑	+23↑	+22↑	+22↑	+25↑	+23↑	+24↑	+23↑	+25↑	+28↑	+21↑	+26↑	+24↑	+24↑	+22↑	+24↑
	Spring	+21↑	+16↑	+18↑	+16↑	+18↑	+22↑	+20↑	+21↑	+20↑	+23↑	+24↑	+20↑	+23↑	+20↑	+21↑	+20↑	+23↑

Min Temp = minimum temperature, Max Temp = maximum temperature

According to Table 8, the average of the monthly evaporation displayed a rise in all seasons, at all stations, over the period 2000-2099, in comparison with that of observations of the period 1950-1989. This implies that in future, throughout the study area, the loss of water into the atmosphere due to evaporation will tend to increase. In the period 2000-2099, the standard deviation of the monthly evaporation showed a rise in summer, autumn and spring at the majority of stations. In all four seasons, the maximum of the monthly evaporation indicated an increase at the majority of stations, in the period 2000-2099.

At all stations, the average (see Table 8) and the standard deviation of the monthly minimum temperature displayed a rise over the period 2000-2099, with respect to those statistics of the observations of the minimum temperature of the period 1950-1989. However, the increase in the average of the monthly minimum temperature in summer was negligible at all stations. Except in summer, the minimum of the monthly minimum temperature also indicated a rise at the majority of stations.

According to Table 8, at all stations, the average of the monthly maximum temperature showed an increase in all four seasons over the period 2000-2099, in comparison with that of observations of the period 1950-1989. This rise in the average of the monthly maximum temperature was relatively higher in winter and spring, at all stations. Only in summer, at all stations, the standard deviation of the monthly maximum temperature indicated a decline in the period 2000-2099. The maximum of the monthly maximum temperature showed a rise in all seasons, at all stations, in the period 2000-2099.

The Victorian Government Department of Sustainability and Environment (2008 a, b) stated that according to the median estimates obtained from the raw outputs of number of GCMs under B1 (low emissions), A1B (medium emissions) and A1F1 (high emissions) emission scenarios, the average temperature and evaporation are likely to increase in all seasons, across the Wimmera and Mallee regions which include the present study area. These findings of the Victorian Government Department of Sustainability and Environment further reinforced the findings of the present study.

5. CONCLUSIONS

Following broad conclusions were drawn from this study:

1. The key station approach was proven to be a simple and yet effective methodology for downscaling GCM outputs to a predictand of interest at multiple stations concurrently. It allows maintaining the cross-correlation structure among the observations of a predictand of interest, across number of observation stations in a study area. Therefore, plausible representation of spatial variations of the predictand of interest among observation stations can be maintained in the projections produced by the downscaling models into future. Also the key station approach is able to segregate the stations in a study area into separate clusters according to the spatial variations of the predictand of interest seen in the past observations. This allows the maintenance of independence among stations in different clusters while preserving dependence structure among the station in individual clusters.

2. Nevertheless, for the effective application of the key station approach the presence of high correlations (preferably magnitudes above 0.80 at $p \leq 0.05$) among the observation stations (in a cluster) for the predictand of interest is a prerequisite. However, when the correlations between the stations for a predictand of interest are less strong (limited linear association), a non-linear regression technique can be used for developing effective inter-station regression relationships.

3. In the application of the key station approach, downscaling models are developed for the predictand of interest only at the key stations. Therefore, unlike downscaling at each individual station separately, in this approach the selection of potential predictors and the correction of bias have to be performed only at several stations.

4. When the bias is limited, the monthly bias-correction was found to be very effective in correcting the bias in the monthly mean and the standard deviation of a climatic variable (e.g. output of a GCM or downscaling model). In monthly bias-correction, though no explicit measure is employed to correct the bias in the minimum and the maximum of a climatic variable, yet it is capable in effectively reducing the bias in the minimum and the maximum of the variable when the bias is limited. Therefore, monthly bias-correction is recommended for variables which show little bias in their statistics.

ACKNOWLEDGEMENTS

The authors acknowledge the financial assistance provided by the Australian Research Council Linkage Grant scheme and the Grampians Wimmera Mallee Water Corporation for this project.

REFERENCES

Anandhi, A., Srinivas, V.V., Nanjundiah, R.S., Kumar, D.N., 2008. Downscaling precipitation to river basin in India for IPCC SRES scenarios using support vector machine. Int. J. Climatol. 28, 401-420.

Anandhi, A., Srinivas, V.V., Nanjundiah, R.S., Kumar, D.N., 2009. Role of predictors in downscaling surface temperature to river basin in India for IPCC SRES scenarios using support vector machine. Int. J. Climatol. 29, 583-603.

Barton, A.F., Briggs, S., Prior, D., McRae-Williams, P., 2011. Coping with severe drought: stories from the front line. Aust. J. Water Resour. 15, 21-32.

Bureau of Meteorology., 2013. Climate classification of Australia. http://www.bom.gov.au/climate/environ/other/kpn.jpg. (Accessed on 20th February 2013).

Chen, T.S., Yu, P.S., Tang, Y.H., 2010. Statistical downscaling of daily precipitation using support vector machines and multivariate analysis. J. Hydrol. 385, 13-22.

Chiew, F.H.S., Piechota, T.C., Dracup, J.A., McMahon, T.A., 1998. El Nino/Southern Oscillation and Australian rainfall, streamflow and drought: Links and potential for forecasting. J. Hydrol. 204, 138-149.

Gupta, R.S., 2008. Hydrology and hydraulic systems, third ed. Waveland Press, Illinois.

Hundecha, Y., Bárdossy, A., 2008. Statistical downscaling of extremes of daily precipitation and temperature and construction of their future scenarios. Int. J. Climatol. 28, 589-610.

IPCC., 2000. IPCC special report on emissions scenarios - Summary for policymakers. http://www.ipcc.ch/pdf/special-reports/spm/sres-en.pdf. (Accessed on 5th January 2013).

Jeong, D.I., St-Hilaire, A., Ouarda, T.B.M.J., Gachon, P., 2012. Multisite statistical downscaling model for daily precipitation combined by multivariate multiple linear regression and stochastic weather generator. Climatic Change 114, 567-591.

Johnson, F., Sharma, A., 2012. A nesting model for bias correction of variability at multiple time scales in general circulation model precipitation simulations. Water Resour. Res. 48, 1-16.

King, L.M., Irwin, S., Sarwar, R., McLeod, A.I., Simonovic, S.P., 2012. Can. Water Res. J. 37, 253-274.

Kou, X., Ge, J., Wang, Y., Zhang, C., 2007. Validation of the weather generator CLIGEN with daily precipitation data from the Loess Plateau, China. J. Hydrol. 347, 347-357.

Liu, W., Fu, G., Liu, C., Charles, S.P., 2013. A comparison of three multi-site statistical downscaling models for daily rainfall in the North China Plain. Theor. Appl. Climatol. 111, 585-600.

Maurer, E.P., Hidalgo, H.G., 2008. Utility of daily vs. monthly large-scale climate data: an intercomparison of two statistical downscaling methods. Hydrol. Earth Syst. Sci. 12, 551-563.

Murphy, J., 1998. An evaluation of statistical and dynamical techniques for downscaling local climate. J. Climate 12, 2256-2284.

Nash, J.E., Sutcliffe, J.V., 1970. River flow forecasting through conceptual models, part 1 - A discussion of principles. J. Hydrol. 10, 282-290.

Nicholls, N., 2008. Australian climate and weather extremes: past, present and future, A report for the department of climate change, Australia. http://www.climatechange.gov.au/~/media/publications/science/weather-extremes.pdf. (Accessed on 15th January 2013)

Pearson, K., 1895. Mathematical contributions to the theory of evolution. iii. regression heredity and panmixia. Philos. T. Roy. Soc. A 187, 253-318.

Qian, B., Corte-Real, J., Xu, H., 2002. Multisite stochastic weather models for impact studies. Int. J. Climatol. 22, 1377-1397.

Sachindra, D.A., Huang, F., Barton, A.F., Perera, B.J.C., 2014. Statistical downscaling of general circulation model outputs to precipitation Part 2: bias-correction and future projections. Int. J. Climatol. Article in press. DOI: 10.1002/joc.3915.

Sachindra, D.A., Huang, F., Barton, A.F., Perera, B.J.C., 2013. Least square support vector and multi-linear regression for statistically downscaling general circulation model outputs to catchment streamflows. Int. J. Climatol. 33, 1087-1106.

Smith, I., Chandler, E., 2009. Refining rainfall projections for the Murray Darling basin of south-east Australia-the effect of sampling model results based on performance. Climatic Change 102, 377-393.

Timbal, B., Fernandez, E., Li, Z., 2009. Generalization of a statistical downscaling model to provide local climate change projections for Australia. Environ. Modell. Softw. 24, 341-358.

Tripathi, S., Srinivas, V.V., Nanjundiah, R.S., 2006. Downscaling of precipitation for climate change scenarios: a support vector machine approach. J. Hydrol. 330, 621-640.

Victorian Government Department of Sustainability and Environment., 2008a. Climate change in the Wimmera. Available at http://www.climatechange.vic.gov.au/regional-projections/wimmera. (Accessed on 28th October 2012). 3-8.

Victorian Government Department of Sustainability and Environment., 2008b. Climate change in the Mallee. Available at http://www.climatechange.vic.gov.au/regional-projections/mallee. (Accessed on 28th October 2012). 4-7.

Victorian Government Department of Sustainability and Environment., 2011. Western region sustainable water strategy. Available at http://www.water.vic.gov.au/initiatives/sws/western (Accessed on 03rd April 2013).

Wilby, R.L., Charles, S.P., Zorita, E., Timbal, B., Whetton, P., Mearns, L.O., 2004. Guidelines for use of climate scenarios developed from statistical downscaling methods. http://unfccc.int/resource/cd_roms/na1/v_and_a/Resoursce_materials/Climate/StatisticalDownscalingGuidance.pdf. (Accessed on 18th February 2013).

Wilby, R.L., Tomlinson, O.J., Dawson, C.W., 2003. Multi-site simulation of precipitation by conditional resampling. Climate Res. 23, 183-194.

Wilby, R.L., Dawson, C.W., 2007. SDSM 4.2 - A decision support tool for the assessment of regional climate change impacts, Version 4.2 User Manual. http://co-public.lboro.ac.uk/cocwd/SDSM/SDSMManual.pdf. (Accessed on 24th February 2013).

Wilks, D.S., 1999. Simultaneous stochastic simulation of daily precipitation, temperature and solar radiation at multiple sites in complex terrain. Agr. Forest Meteorol. 96, 85-101.

Wilks, D.S., 2010. Use of stochastic weather generators for precipitation downscaling. Wiley Interdisciplinary Reviews. Climate Change 1, 898-907.

Manuscript Submitted to Journal of Water and Climate Change

5.4 Statistical Downscaling of General Circulation Model Outputs to Evaporation, Minimum Temperature and Maximum Temperature Using a Key-Predictand and Key-Station Approach

D.A. Sachindra[a]*, F. Huang[a], A. Barton[a,b], and B.J.C. Perera[a]

[a]*Victoria University, P.O. Box 14428, Melbourne, Victoria 8001, Australia.*

[b]*Federation University, PO Box 663, Ballarat, Victoria 3353, Australia.*

*Correspondence to: D. A. Sachindra, College of Engineering and Science, Footscray Park Campus, Victoria University, P.O. Box 14428, Melbourne, Victoria 8001, Australia. E-mail: sachindra.dhanapalaarachchige@live.vu.edu.au. Telephone: +61 03 9919 4907.

Published as: Dhanapala Arachchige, Sachindra, Huang, Fuchun, Barton, A and Perera, Bodiyabaduge (2016) Statistical downscaling of general circulation model outputs to precipitation, evaporation and temperature using a key station approach. Journal of Water and Climate Change, 7 (4). 683 - 707.

Available from: https://doi.org/10.2166/wcc.2016.021

Abstract

A key-predictand and key-station approach was employed in downscaling general circulation model outputs to monthly evaporation, minimum temperature (T_{min}) and maximum temperature (T_{max}) at 5 observation stations concurrently. T_{max} was highly correlated (magnitudes above 0.80 at $p \leq 0.05$) with evaporation and T_{min} at each individual station, hence T_{max} was identified as the key-predictand. One station was selected as the key-station, as T_{max} at that station showed high correlations with evaporation, T_{min} and T_{max} at all stations. Linear regression relationships were developed between the key-predictand at the key-station and evaporation, T_{min} and T_{max} at all stations using observations. A downscaling model was developed at the key-station for T_{max}. Then, outputs of this downscaling model at the key-station were introduced to the linear regression relationships to produce projections of monthly evaporation, T_{min} and T_{max} at all stations. This key-predictand and key-station approach was proven to be effective as the statistics of the predictands simulated by this approach were in close agreement with those of observations. This simple multi-station multivariate downscaling approach enabled the preservation of the cross-correlation structures of each individual predictand among the stations and also the cross-correlation structures between different predictands at individual stations.

Keywords: *Downscaling, Key predictand, Key station, General circulation model*

INTRODUCTION

General Circulation Models (GCMs) are considered as the most reliable tools available for the projection of global climate into future (Anandhi et al. 2008). These GCMs are based on the physics of the atmosphere and they project the climate hundreds of years into future considering the greenhouse gas (GHG) concentrations in the atmosphere. The resolution of the outputs of modern GCMs is still in the order of few hundred kilometres (Tripathi et al. 2006). This coarse spatial resolution of GCM outputs hinders their direct application at the catchment scale. This is because the climate information needed by most of the catchment scale studies is much finer in spatial resolution than that of GCM outputs. As a solution to this resolution mismatch, downscaling techniques have been developed. They relate the coarse resolution GCM outputs to the catchment scale hydroclimatic variables.

There are two classes of downscaling techniques in use; (1) dynamic downscaling and (2) statistical downscaling. In dynamic downscaling, a finer resolution regional climate model (RCM) is nested in a coarse resolution GCM (Murphy 1998). Since RCMs are atmospheric physics based models, they can more realistically model the relationships between the large scale climate simulated by GCMs and the climate in the catchment. The other advantage of dynamic downscaling is that, it can produce spatially continuous fields of climatic variables while reliably maintaining the correlations over space (Maurer et al. 2008). However, the high computational cost and the long run time needed for the completion of a simulation are regarded as the major issues associated with dynamic downscaling.

On the other hand, in statistical downscaling, empirical relationships between the GCM outputs and the catchment scale hydroclimatic variables are determined (Hay and Clark 2003). Statistical downscaling methods are computationally cheaper and they are faster in producing their outputs. Hence, they can easily be used with different GCMs and different GHG emission scenarios for the development of series of climate change scenarios (Khalili et al. 2013). Statistical downscaling methods produce there outputs at a point scale (e.g. at observation stations) which is a finer spatial scale than

the spatial scale at which most of the dynamic downscaling methods produce their outputs (Willems et al. 2012). Also unlike dynamic downscaling, statistical downscaling methods can produce data of predictands such as streamflows, leaf wetness etc which are not simulated by the GCMs. However, for the proper calibration and validation of a statistical downscaling model, a long time series of observations is needed (Heyen et al. 1996). All statistical downscaling methods are dependent on the assumption that the relationships developed between GCM outputs and catchment scale hydroclimatic variables (e.g. precipitation) for the past climate is also valid for the climate in future (von Storch et al. 2000). Statistical downscaling methods are classified into three main categories; regression methods, weather classification methods and weather generators (Wilby et al. 2004). In regression based downscaling methods, linear or non-linear relationships between the large scale atmospheric variables (e.g. reanalysis or GCM outputs) and the observations of catchment scale hydroclimatic variables are developed. Then these relationships are used with the outputs of GCMs pertaining to future climate for the determination of the catchment scale climate relevant to future. In weather classification, the current state of the large scale weather (e.g. characterised by GCM outputs) is matched with that of past weather in record. Then corresponding to the large scale weather in the past, the present catchment scale weather is determined. Weather generators are used to produce weather sequences which contain the statistical properties of observations of weather (Kou et al. 2007). For the generation of catchment scale weather sequences corresponding to future, the parameters in the weather generators are scaled up or down corresponding to the changes in the GCM outputs pertaining to future.

Statistical downscaling exercises are performed at individual stations (e.g. Tripathi et al. (2006)) and also at multiple stations simultaneously (e.g. Jeong et al. (2013a, b)). When downscaling is performed at individual stations, a separate downscaling model is developed at each station. In such case, no explicit attempt is made in maintaining the spatial correlations (cross-correlations) seen among the observations of stations, in the outputs of the downscaling models. When downscaling is performed at multiple stations simultaneously, explicit measures are made to preserve the spatial correlation structure

among the stations. This enables the realistic representation of spatial variations of the climatic variable of interest, over the study area. Khalili et al. (2011) found that neglecting the spatial correlation structure among precipitation and temperature data generated at multiple stations may result in large under-predictions of high streamflows estimated using a hydrologic model fed with those precipitation and temperature data. Cannon (2008) stated that maintaining the correlations among the outputs of downscaling models developed at precipitation stations in a certain study area is critical as spatial variations of precipitation can significantly influence the streamflow. Furthermore, Jeong et al. (2013a) commented that projections of precipitation produced at multiple stations considering the spatial coherence is quite important in the management of water resources. However, it should be noted that, under changing climate the observed spatial correlation structure can still change in future. According to Khalili et al. (2013), the majority of downscaling exercises have been performed at individual stations owing to the complexity of simultaneously downscaling at multiple stations which involves correctly maintaining both temporal persistence at individual stations and also spatial correlation structures between the stations. Also when downscaling is performed at multiple stations concurrently, the accuracy at each individual station may tend to decrease as spatial correlations among number of stations have to be maintained in parallel.

A weather generation technique was used by Wilks (1999) to generate daily precipitation, minimum temperature, maximum temperature and solar radiation simultaneously at 62 stations over the western USA. The conditional resampling method was employed by Wilby et al. (2003) in order to downscale daily precipitation from GCM outputs to multiple locations in the UK. Mehrotra et al. (2006) used parametric (Hidden Markov Model) and non-parametric (k-nearest neighbour) weather generation techniques for the generation of precipitation occurrences at multiple stations simultaneously. It was concluded that the parametric multi-station weather generation techniques are associated with large number of parameters in comparison to non-parametric weather generators. The concept of spatial autocorrelation (degree of dependence of observations over space) was used in a weather generator by Khalili et

al. (2007) for the generation of daily precipitation at multiple stations. The same concept was employed in the generation of daily maximum temperature, minimum temperature and solar radiation at multiple stations concurrently by Khalili et al. (2009). Again Khalili et al. (2011) used the concept of spatial autocorrelation for the generation of daily precipitation and temperature at multiple stations concurrently (considering each predictand separately) over a catchment in Canada, which were then used in a hydrologic model to simulate streamflow in the catchment. Khalili et al. (2013) used a linear regression technique for linking the GCM outputs to catchment scale maximum temperature and minimum temperature and then the spatial dependence structure among the stations for the two predictands were determined using a stochastic technique. It was found that this multi-station multivariate downscaling methodology was able to reproduce the spatial and temporal characteristics of maximum temperature and minimum temperature with good accuracy. Jeong et al. (2012b) applied MMLR technique for downscaling GCM outputs to daily maximum temperature and daily minimum temperature concurrently at 9 stations in Canada. In that study it was found that, the addition of spatially correlated random noise (randomization process) between the predictands and the stations to the deterministic time series of the predictands produced by the MMLR technique can aid in correctly reproducing the cross-correlation structures of predictands between the stations and the cross-correlation structures between the two predictands at individual stations. The multivariate multi-linear regression (MMLR) technique combined with a stochastic weather generation technique was used by Jeong et al. (2013b) for downscaling reanalysis outputs to daily precipitation, simultaneously at 9 observation stations in Canada. In that study, it was found that the use of the stochastic weather generation technique (along with the regression technique) enhanced the capabilities of the downscaling model in capturing the spatial and temporal characteristics of precipitation. More applications of multi-stations weather generation techniques are found in the studies by Qian et al. (2002), Kottegoda et al. (2003), Apipattanavis et al. (2007) and Bardossy & Pegram (2009).

The majority of the existing multi-station and multi-station multivariate downscaling techniques are quite complex in nature. Hence there is a need for simple yet effective

multi-station and multi-station multivariate downscaling techniques (e.g. Maraun et al. (2010)). Unlike the complex multi-station downscaling techniques used in the previous studies, in the present study a relatively simple yet effective multi-station multivariate downscaling methodology was investigated. In the present study, a key predictand and key station approach was used for simultaneously downscaling GCM outputs to monthly evaporation, minimum temperature and maximum temperature at several observation stations. Using this key predictand and key station approach the cross-correlation structures for each predictand among the stations and also the cross-correlation structures among different predictands at individual stations can be preserved. Hence the key predictand and key station approach allows the plausible representation of the spatial variations of each predictand and also aids in maintaining realistic representation of the relationships among different predictands considered in a downscaling exercise. Furthermore, since downscaling models are developed only at the key stations for the key predictands, the predictor selection, calibration and validation of the downscaling models and the bias-correction have to be performed only for limited number of predictands at limited number of stations.

However, it should be noted that for the effective implementation of the key predictand and key station approach, the predictands of interest should be highly correlated (preferably magnitudes above 0.80 at $p \leq 0.05$) with each other over space. If these spatial correlations are low, the overall effectiveness of this approach becomes limited. Details of the key predictand and key station approach employed in this study are provided later in the paper.

Evaporation is one of the many processes responsible for the loss of water from a catchment. Temperature variations are directly influential on the changes in the evaporation, snow melt etc (King et al. 2012). Therefore, evaporation, minimum temperature and maximum temperature were considered as the catchment scale predictands in this study. For the demonstration of the methodology, 5 observation stations located in the operational area of the Grampians Wimmera Mallee Water Corporation in north western Victoria, Australia were considered in this study. This

region contains several large water supply reservoirs which supply water to large number of domestic and industrial users. Also this area is quite sensitive to severe droughts (Barton et al. 2011). Hence, the determination of dependable point scale climatic information pertaining to likely future climate over the study area was identified an important task.

STUDY AREA AND DATA

The study area is located in the southern region of the operational area of Grampians Wimmera Mallee Water Corporation (GWMWater) (www.gwmwater.org.au). The operational area (62, 000 km^2) of GWMWater is located in the north western part of Victoria, Australia and is shown in Figure 1. The study area is mountainous and does not have a clear dry season (Bureau of Meteorology 2013) in comparison with the northern region of the operational area of the GWMWater, which is relatively flatter and persistently dry. This study area contains some important water supply reservoirs such as Lake Taylor, Lake Lonsdale, Lake Bellfield and Rockland Reservoir, several rivers such as Wimmera River and Glenelg River, and some agricultural production areas. Hence the study of impact of climate change over this area was identified as a timely need.

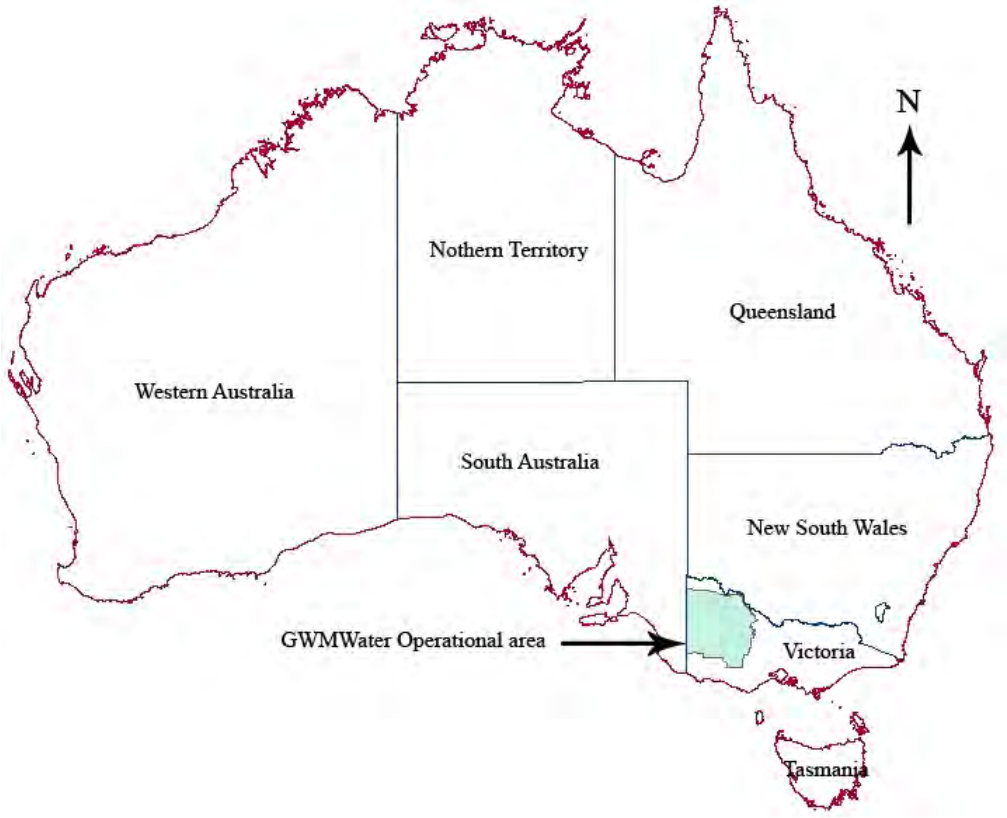

Figure 1 Operational area of Grampians Wimmera Mallee Water Corporation

For the demonstration of the methodology five observation stations were considered in this study and they are shown with their latitudes and longitudes in Table 1. Over the period 1950-2010, the observations of monthly evaporation, maximum temperature and minimum temperature at the five stations considered in this study displayed high positive correlations with those at other stations (Ouyen post office, Longerenong, Halls Gap post office, Birchip post office, Great Western, Swan hill post office, Rainbow, Wartook Reservoir, Hamilton Airport, Stawell, Eversley, Ararat prison) located across the operational area of GWMWater. Therefore it was assumed that the likely changes in the future climate at the other stations located in the operational area of GWMWater will be consistent with those at the five stations considered in this study.

Observations of daily evaporation, maximum temperature and minimum temperature for the 5 observation stations, were obtained from the SILO database of Queensland

Climate Change Centre of Excellence at http://www.longpaddock.qld.gov.au/silo/ for the period 1950-2010. These daily observations were added to derive the corresponding monthly observations at each station. Monthly observations were used for the computation of correlations between the predictands at stations in identifying key predictands and key stations. Also these observations were used in calibration and validation of the downscaling models developed at the key stations. Furthermore, the observations were used as the reference data set for the correction of bias in the outputs of the downscaling models.

Table 1 Stations considered in this study

Name of the station	Station ID	Latitude	Longitude
Polkemmet	79023	-36.66	142.07
Lake Lonsdale	79026	-37.03	142.58
Moyston Post Office	79034	-37.30	142.77
Tottington	79079	-36.79	143.12
Balmoral Post Office	89003	-37.25	141.84

Station ID is as defined by the Bureau of Meteorology Australia at http://www.bom.gov.au/climate/data/stations/

National Centers for Environmental Prediction / National Center for Atmospheric Research (NCEP/NCAR) reanalysis outputs were obtained from the physical sciences division of the National Oceanic and Atmospheric Administration / Earth System Research Laboratory (NOAA/ESRL) at http://www.esrl.noaa.gov/psd/, for providing inputs to the downscaling models in their calibration and validation phases. To reproduce the past observations of key predictands using the downscaling models, the 20th century climate experiment (20C3M) outputs of ECHAM5 were extracted from the Programme for Climate Model Diagnosis and Inter-comparison (PCMDI) at https://esgcet.llnl.gov:8443/index.jsp over the period 1950-1999. Also ECHAM5 outputs pertaining to the A2 GHG emission scenario were obtained for the period 2000-2099, from the https://esgcet.llnl.gov:8443/index.jsp, for the projection of catchment scale climate into future.

Smith and Chandler (2009) stated that a few GCMs including ECHAM5 are capable in correctly simulating the precipitation over Australia and also able to produce credible predictions of El Niño Southern Oscillation (ENSO). They also argued that a GCM

which can correctly simulate precipitation should be able to simulate other climatic variables with a good degree of accuracy. Therefore, for the present study, the outputs of ECHAM5 were used. The A2 GHG emission scenario of Intergovernmental Panel on Climate Change (IPCC) was used in this study as it refers to relatively higher amounts GHGs in the atmosphere in future. Therefore, the projections produced based on the A2 GHG emission scenario will refer to high levels of impact on the environment.

GENERIC METHODOLOGY

The procedure for application of the key predictand and key station approach is shown in brief in the flow chart displayed in Figure 2. The steps shown in Figure 2 are described in detail later.

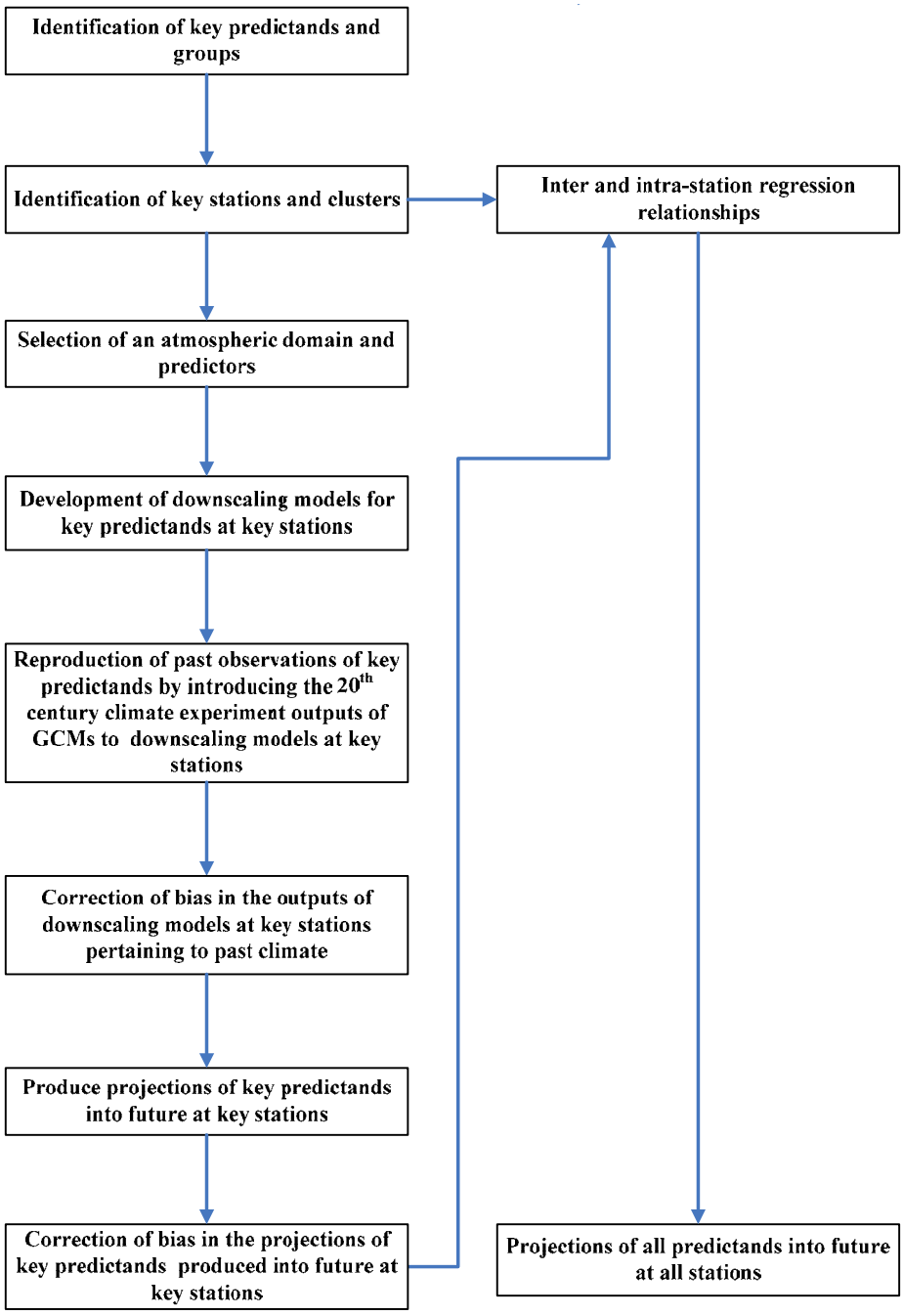

Figure 2 Steps involved in application of the key predictand and key station approach

Identification of key predictands and groups

In this paper, a key predictand refers to a climatic variable (e.g. evaporation, temperature) which is highly correlated (magnitude above 0.80 at $p \leq 0.05$) with other climatic variables of interest at each individual observation station, in a group of

observation stations, located in a certain study area. If the study area contains only one observation station, a predictand which is highly correlated with other predictands at that station becomes the key predictand.

As a simple example consider the 3 predictands P_1, P_2 and P_3 at the 5 observation stations St_1, St_2, St_3, St_4 and St_5 located in a certain study area. For the identification of key predictands, initially, the Pearson correlations (Pearson, 1895) among the observations of different predictands were computed for each individual observation station (intra-station correlations), considering all calendar months together. Then at each observation station, the predictand combinations (e.g. P_1 against P_2; referred later in this paragraph as P_1 - P_2) which showed high correlations (magnitude above 0.80 at $p \leq 0.05$) were identified as shown in Figure 3. Note that in Figure 3, high correlations were denoted with a ✓ and relatively low correlations were indicated with a ×. Thereafter, groups of stations were identified based on the highly correlated combinations of predictands common to the stations. For example, as shown in Figure 3, at stations St_1, St_2 and St_5 predictand combinations P_1 - P_2 and P_2 - P_3 showed high correlations. Therefore St_1, St_2 and St_5 were considered under group 1. At these stations predictand P_2 was common to both predictand combinations which showed high correlations. Hence predictand P_2 was identified as the key predictand for group 1. At stations St_3 and St_4 predictand combinations P_1 - P_3 and P_2 - P_3 showed high correlations. Therefore stations St_3 and St_4 were considered as group 2 (see Figure 3). Since predictand P_3 was common to both the combinations P_1 - P_3 and P_2 - P_3, it was identified as the key predictand for group 2. In the same manner, this procedure can be extended to n ($\subseteq \mathbb{Z}^+$) number of stations and m ($\subseteq \mathbb{Z}^+$) number of predictands for the identification of key predictands and groups of observation stations.

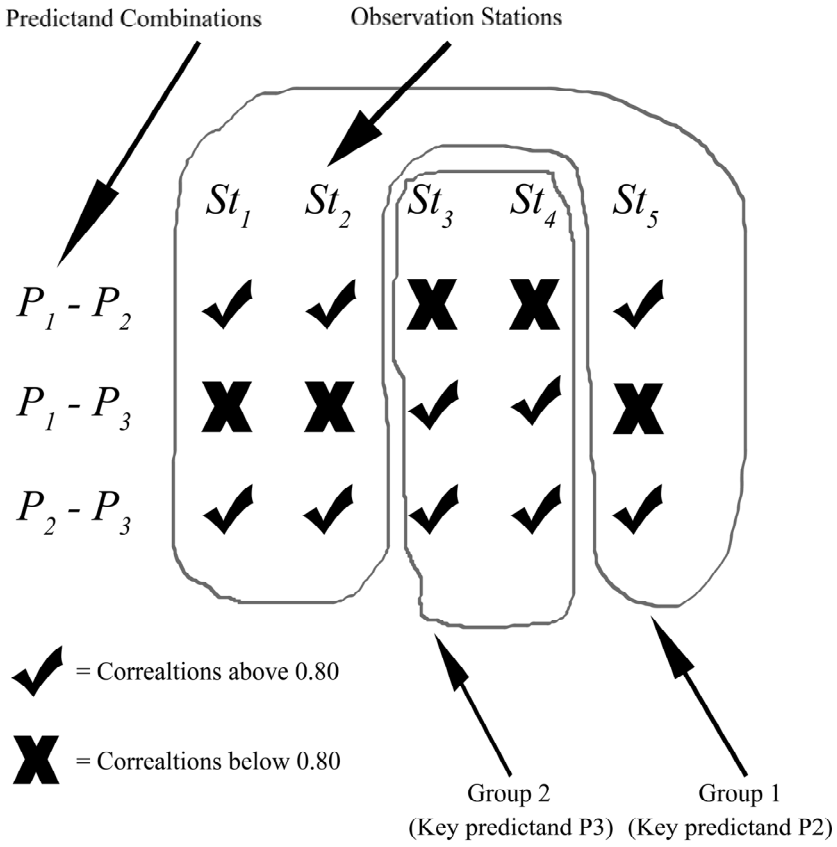

Figure 3 Groups of stations and key predictands

Note that, at times, there can be one single key predictand over the entire study area, as this predictand shows high correlations with all other predictands, at all stations. Also the maximum number of key predictands is always equal to the total number of predictands considered in the study. The maximum number of groups is also equal to the total number of predictands, as each group is governed by a key predictand.

Identification of key stations and clusters

Once the key predictands were identified, as the next step, key stations were determined over the study area. In this paper, a key station is an observation station where a key predictand (refer to previous section) is highly correlated (magnitude above 0.80 at $p \leq 0.05$) with all predictands (this also includes the key predictand) in a cluster of observation stations located within a group of observation stations governed by that key

predictand. The key station and the other stations which showed high correlations between the key predictand and all predictands were defined as a cluster of stations. These other stations in a cluster were referred to as the member stations. Note that a group of stations can have one or more clusters and each cluster is governed by a key station.

In order to determine the key stations, the correlations between the key predictands and all predictands of interest were computed at all stations in each group of stations, identified in previous section. For this purpose, at each station, data of each predictand for all calendar months together were considered. The above procedure yielded correlation matrices between each key predictand and all predictands of interest in each group. In other words, one correlation matrix for each key predictand and each of the predictands of interest was computed. Then for each of these correlation matrices, a threshold with a magnitude of 0.80 was imposed. In a group, a certain station in which the key predictand showed the highest number of high correlations with all predictands of interest was identified as the first key station. Note that, when a certain key predictand at several stations show the highest number of high correlations with all predictands of interest, any such station can be considered as a key station. The key station and the other stations which showed high correlations between the key predictand and all predictands were defined as a cluster of stations. Then the same procedure was repeated on the rest of the stations in the group. This procedure was continued until all stations in all groups were assigned to clusters.

As an example, in Figure 4 (same stations and predictands as in Figure 3), in group 1, if the key predictand P_2 at station St_1 showed high correlations with predictands P_1, P_2 and P_3 (all predictands of interest) at station St_2 and relatively low correlations with those predictands at station St_5, then station St_1 becomes the key station of cluster 1 and station St_2 becomes a member station of that cluster. In such case, station St_5 becomes the second key station in group 1 since it is the only remaining station in the group. Likewise, in group 2, if key predictand P_3 at station St_3 was highly correlated with

predictands P_1, P_2 and P_3 (all predictands of interest) at station St_4, then station St_3 becomes the key station and station St_4 becomes a member station of cluster 2.

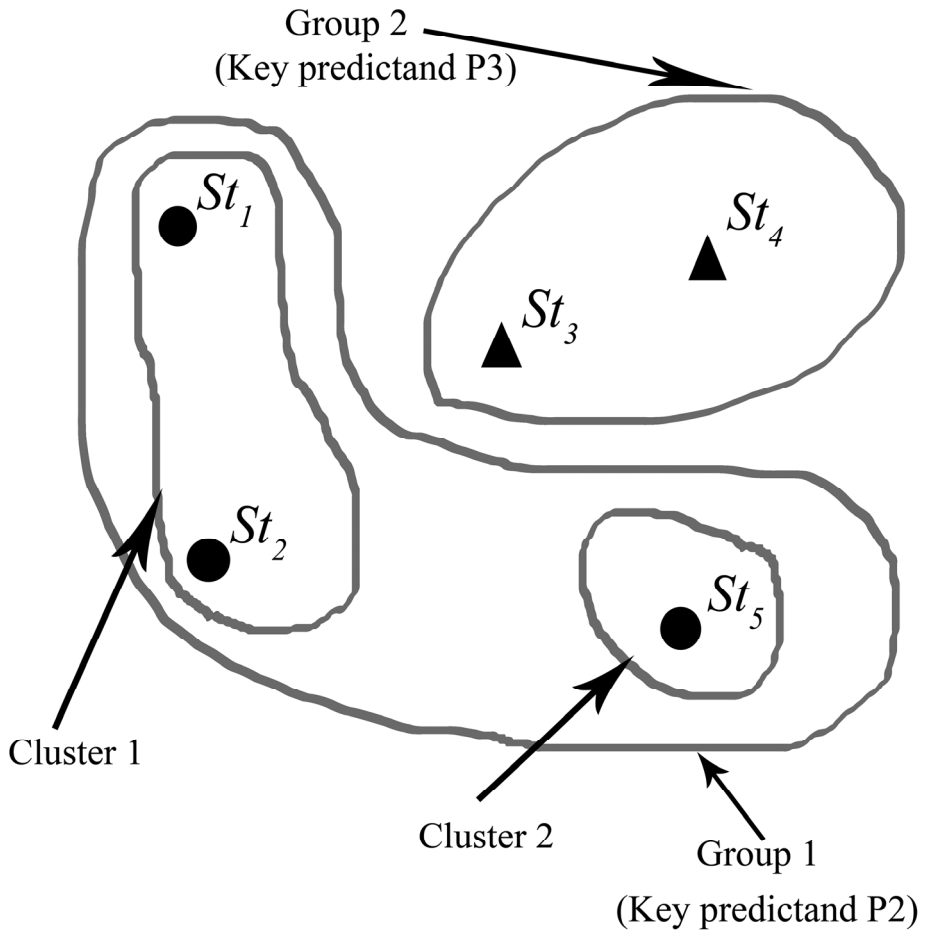

Figure 4 Clusters of stations and key stations

Intra and inter-station regression relationships in clusters

Once the key predictands and key stations were identified, simple linear regression equations were built between the key predictands at key stations and other predictands at the key stations in all clusters using observations. These regression equations are referred to as the intra-station regression relationships in this paper. Also simple linear regression equations were developed between the key predictands at key stations and all predictands at the member stations in all clusters using observations. In this paper, these regression equations are called the inter-station regression relationships.

All simple linear regression relationships (intra and inter-station) between the predictands were computed for each calendar month separately. This was done in order to better capture the seasonal variations in the relationships between the predictands. The first two thirds of the observations of predictands were used for the calibration of intra and inter-station regression relationships, while the rest of the observations were used for the validation of these relationships (derived in the calibration). In the calibration of the intra and inter-station regression relationships, the optimum values of the coefficients and the constants of the equations were determined by minimising the sum of squared errors between the observations and the outputs of these regression relationships.

Atmospheric domain and predictor selection

Once intra and inter-station regression relationships were determined in each cluster, an atmospheric domain was defined over the study area. The atmospheric domain enables the inclusion of the influences of the atmospheric circulations on the catchment scale climate which is modelled by the downscaling models. The same atmospheric domain was used for the development of downscaling models at all key stations for all key predictands.

The probable predictors for the study were selected for each key predictand separately, from the past literature and based on principles of hydrology. The probable predictors were the likely predictors to influence a certain key predictand at the catchment scale. The pool of probable predictors varies from one key predictand to another. The potential predictors are subsets of probable predictors which vary seasonally and also from one key station to another. These potential predictors are the most influential predictors on a certain key predictand at a key station.

In this study, the correlations between the reanalysis data (e.g. NCEP/NCAR) of probable predictors and the observations of the key predictands at the key stations were used as the basis for the extraction of potential predictors, from the pool of probable

predictors. The reanalysis data pertaining to the probable predictors, and the observations of the key predictands at key stations were split into 20 year time slices (in this study 1950-1969, 1970-1989, and 1990-2010), in the chronological order. Then, for each calendar month, the Pearson correlation coefficients between the probable predictors and the key predictand at each key station were computed for each time slice and the whole period of the study (in this study 1950-2010), at all grid points in the atmospheric domain. The probable predictors which showed the best correlations ($p \leq 0.05$) with a key predictand at a key station, consistently, in all time slices and the whole period of the study were extracted as the potential predictors for that key predictand at that key station. The extraction of potential predictors was practised for each calendar month separately as it can yield sets of potential predictors which can reflect the seasonal variations of the atmospheric conditions. Sachindra et al. (2013a, b) successfully used the above procedure, for the selection of potential predictors in the development of models used for statistically downscaling NCEP/NCAR reanalysis outputs to monthly streamflows and monthly precipitation.

Development of downscaling models for key predictands at key stations

For each key predictand at each key station, downscaling models were then developed (calibrated and validated). The first two thirds of the reanalysis data pertaining to the potential predictors and the observations of the key predictands at key stations were used for the calibration of the downscaling models. The rest of the data were used for the validation of these models. The reanalysis data pertaining to the calibration and validation phases of the downscaling models were standardised using the means and the standard deviations of those corresponding to the calibration phase, for each calendar month separately. The means and the standard deviations of the reanalysis data pertaining to the calibration period of the downscaling models were considered as fixed components of them.

In calibration of a downscaling model for a key predictand at a key station (in a cluster), first the standardised data of the potential predictor which displayed the best correlation with the observations of the key predictand of interest over the whole period of the

study was introduced to the downscaling model. Then by minimising the sum of squared errors between the model outputs and the observations, the optimum values of the constant and the coefficient of the linear regression equation were determined. The performances of the downscaling model in calibration were also monitored using the Nash-Sutcliffe efficiency (NSE) (Nash & Sutcliffe 1970). Thereafter the reanalysis data of that predictand pertaining to the validation period was introduced to the downscaling model while keeping the optimum values of the constant and the coefficient of the linear regression equation determined in calibration fixed. During the validation, the performance of the downscaling model was measured using the NSE. Then the next best potential predictors based on their correlations with the key predictand of interest over the whole period of the study were added to the downscaling model at the key station of interest, one at a time. The downscaling model was calibrated and validated, following the addition of each predictand. It produced multi-linear regression equations between the key predictand and the potential predictors introduced to the downscaling model. This procedure was performed until the model performance in validation reaches a maximum in each calendar month. This procedure yielded the best set of potential predictors and the optimum downscaling model for each calendar month. In this manner, downscaling models were developed for each key predictand at each key station in each cluster in each group. The performances of the downscaling models built for each key predictand at each key station were assessed numerically by comparing the statistics of the model outputs with those of observations. Also the model outputs were graphically compared with the observations using scatter plots.

Reproduction of past observations of key predictands and bias-correction

Once the downscaling models were developed for the key predictand at the key station in each cluster in each group, the 20C3M outputs of the GCM (in this study ECHAM5) were standardised with the means and the standard deviation of the reanalysis outputs corresponding to the calibration period. This procedure was practised for each calendar month separately. Then, the past observations of the key predictands at the key stations were simulated by introducing these standardised 20C3M outputs of the GCM, to the downscaling models developed in previous section. This analysis enabled the

assessment of the performances of the downscaling models (developed with reanalysis data) in reproducing the past climate with the 20C3M outputs of the GCM. This analysis was important as these downscaling models which were developed with better quality reanalysis outputs were meant to be used with GCM outputs which have higher degree of uncertainty, for the projection of catchment scale climate into future.

The bias contained in GCM outputs can cause downscaling models to produce erroneous projections into future. According to Salvi et al. (2011), bias is the mismatch between the GCM outputs and the observations. Ojha et al. (2012) emphasised the importance of bias correction in downscaling. Hence, it was realised that either the bias in the GCM outputs (which are used as inputs to downscaling model) or the bias in the outputs of the downscaling models run with the GCM outputs should be corrected prior to any use (Sachindra et al. 2014). In the current study, the monthly bias-correction (for theory refer to Johnson and Sharma (2012)) was used on the outputs of the downscaling models produced when they were run with the 20C3M outputs of the GCM. The monthly bias-correction assumes that the bias in the means and the standard deviations of the outputs of the downscaling models produced for the past will remain the same in future.

In the application of the monthly bias-correction, outputs of the downscaling models pertaining to the calibration period produced with the 20C3M outputs of the GCM were standardised with their means and standard deviations corresponding to the same period. Then these standardised outputs of the downscaling models were rescaled using the means and the standard deviations of the observations relevant to the calibration period of the downscaling model. In the validation of the monthly bias-correction, the outputs of the downscaling models produced over the validation period with the 20C3M outputs of the GCM were standardised with the means and the standard deviations of the outputs of the downscaling models produced over the calibration period with the 20C3M outputs of the GCM. Then these standardised outputs of the downscaling models were rescaled using the means and the standard deviations of the observations

pertaining to the calibration period of the downscaling model. The monthly bias-correction was applied and validated for each calendar month separately.

Development of downscaling models at a key station and a member station for a predictand not identified as a key predictand

A downscaling model was developed at a key station (of a cluster) for downscaling reanalysis outputs to a predictand which was not identified as a key predictand. This was performed to assess the quality of the outputs produced by the intra-station regression relationships against the outputs of the downscaling model developed at that key station for that predictand which was not identified as a key predictand. In order to assess the quality of the outputs produced by the inter-station regression relationships, a downscaling model was built at a member station (of a cluster) for downscaling reanalysis outputs to a predictand which was not identified as a key predictand. For the development of these two downscaling models, the same procedure that was practised in building downscaling models for key predictands at key stations was adopted. The calibration and validation of these downscaling models were performed over the same periods as those of the downscaling models developed for key predictands at key stations in each cluster. The outputs of the intra-station and inter-station regression relationships were compared with those of downscaling models, both numerically and graphically.

Projections into future

For producing projections of catchment scale climate into future, the outputs of a GCM (in this study ECHAM5) pertaining to the future climate were obtained. Then these GCM outputs were standardised using the means and the standard deviations of the reanalysis outputs relevant to the calibration period of the downscaling models, for each calendar month. Thereafter these standardised GCM outputs were introduced to the downscaling models which were developed at key stations for key predictands. This way, at the key stations, the projections of the key predictands were produced into future. The projections of the key predictands produced at key stations were then bias-corrected using the monthly bias-correction following the procedure employed in the

validation of the bias-correction which was detailed in Section entitled "Reproduction of past observations of key predictands and bias-correction". Then these bias-corrected projections were introduced to the intra and inter-station regression relationships for the projection of catchment scale climate into future at all stations in each cluster in each group.

APPLICATION

The generic methodology detailed previously was used to downscale monthly GCM outputs to monthly evaporation, minimum temperature and maximum temperature at the 5 observation stations (see Table 1) located in the southern region of the operational area of GWMWater, in north western Victoria, Australia (see Figure 1).

Identification of key predictands

For the identification of the key predictands, the correlations among the three predictands; evaporation, minimum temperature and maximum temperature were computed at each individual station using the monthly observations of these predictands of the period 1950-2010. Table 2 shows these correlations.

Table 2 Correlations among evaporation, minimum temperature and maximum temperature at each individual station

Predictand combination	**Station**				
	79023	**79026**	**79034**	**79079**	**89003**
Evaporation-T_{max}	0.953	0.951	0.952	0.951	0.949
Evaporation-T_{min}	0.876	0.878	0.864	0.879	0.861
T_{max}-T_{min}	0.929	0.949	0.944	0.955	0.939

T_{max} = monthly maximum temperature, T_{min} = monthly minimum temperature

According to Table 2, at all stations all predictand combinations (e.g. evaporation – maximum temperature) showed correlations above 0.80 ($p \leq 0.05$). Therefore it was realised that, there are strong linear relationships between evaporation, minimum temperature and maximum temperature at all stations. Then at each individual station, the predictand which showed high correlations with all other predictands was identified. It was seen that, at all stations, maximum temperature showed the highest correlations

with the other two predictands (evaporation, minimum temperature). Hence, the maximum temperature was identified as the only key predictand and all 5 stations were included in one group governed by this key predictand. Furthermore, evaporation displayed consistently higher correlations with maximum temperature than with minimum temperature. This indicated that maximum temperature is more influential than minimum temperature on evaporation.

Identification of key stations and clusters

Since maximum temperature was identified as the only key predictand, the correlations between the maximum temperature and all predictands (i.e. evaporation, minimum temperature and maximum temperature) over the period 1950-2010 were computed at all stations using observations. Table 3 shows the correlations between the maximum temperature and all predictands at all stations.

Table 3 Correlations between observations of key-predictand and all predictands

Key predictand	Other predictand	Station	79023	79026	79034	79079	89003
		79023	0.953	0.953	0.955	0.948	0.955
		79026	0.951	0.951	0.954	0.947	0.954
T_{max}	**Evaporation**	**79034**	0.948	0.948	0.952	0.943	0.952
		79079	0.955	0.954	0.958	0.951	0.957
		89003	0.942	0.943	0.947	0.937	0.949
		79023	0.929	0.945	0.936	0.954	0.928
		79026	0.930	0.949	0.940	0.957	0.932
T_{max}	**T_{min}**	**79034**	0.935	0.952	0.944	0.960	0.936
		79079	0.929	0.946	0.937	0.955	0.929
		89003	0.934	0.954	0.946	0.962	0.939
		79023	1.000	0.998	0.996	0.998	0.996
		79026	0.998	1.000	0.999	0.999	0.998
T_{max}	**T_{max}**	**79034**	0.996	0.999	1.000	0.998	0.998
		79079	0.998	0.999	0.998	1.000	0.996
		89003	0.996	0.998	0.998	0.996	1.000

T_{max} = monthly maximum temperature, T_{min} = monthly minimum temperature

According to Tables 3, it was seen that the observations of maximum temperature at all stations were highly correlated ($p \leq 0.05$) with those of evaporation, minimum temperature and maximum temperature at all stations over the period 1950-2010. Therefore any station was seen as a potential key station and also all 5 observation stations were considered in one cluster. In this study the observation station at Lake Lonsdale (79026) was selected as the only key station. Hence, stations at Polkemmet (79023), Moyston post office (79034), Tottington (79079) and Balmoral post office (89003) were identified as the member stations of the only cluster defined in this study. Note that in this study, both the group and the cluster referred to the same set of stations as there was only one cluster located within the only group identified. Figure 5 shows the locations of the key station and the member stations identified in this study along with some of the water resources (lakes and rivers) in the region.

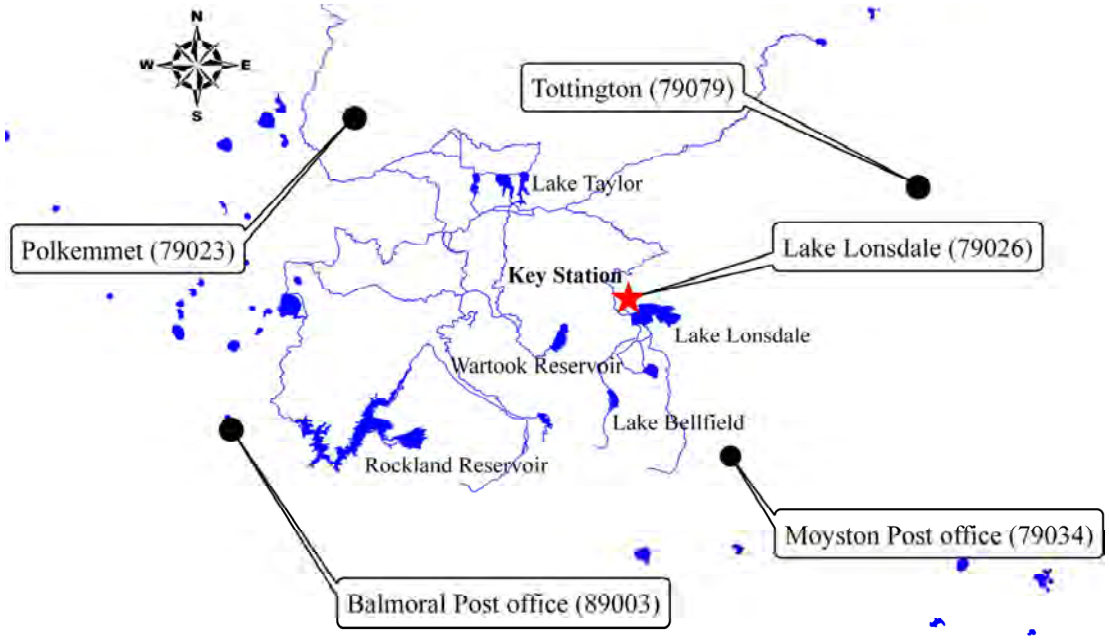

Figure 5 Locations of the key station and member stations

Intra and Inter-station regression relationships

Following the procedure stated in generic methodology, intra and inter-station regression relationships were developed (calibrated and validated). The calibration and

validation of the intra and inter-station regression relationships were performed over the periods 1950-1989 and 1990-2010 respectively. The constants and coefficients of the MLR equations in the inter/intra-station regression relationships determined for the past climate were assumed to be valid for the future, under changing climate.

The intra-station regression relationships were developed at the key station 79026, between the maximum temperature (key predictand) and evaporation, and also between the maximum temperature and the minimum temperature. The inter-station regression relationships were developed between the maximum temperature at the key station 79026 and evaporation, minimum temperature and maximum temperature at each member station of the cluster.

Table 4 shows the statistics of the monthly evaporation at all stations reproduced by the intra and inter-station regression relationships built between the maximum temperature and evaporation. According to Table 4, the intra and inter-station regression relationships were able to reproduce the average and the standard deviation of monthly evaporation with good accuracy in all seasons during the calibration period 1950-1989 and the validation period 1990-2010 at all stations. In all seasons, the intra and inter-station regression relationships were able to reproduce the maximum of monthly evaporation at the majority of stations in both calibration and validation periods with considerable accuracy despite some under and over-estimations. It was realised that these relationships built between the maximum temperature and evaporation were effective in translating maximum temperature to evaporation.

Table 4 Statistics of evaporation reproduced by intra and inter-station regression relationships of all stations between maximum temperature and evaporation.

Season	Station	Period 1950-1989 (Calibration)							Period 1990-2010 (Validation)						
		Average		Std		Max		NSE	Average		Std		Max		NSE
		Obs	Reg	Obs	Reg	Obs	Reg		Obs	Reg	Obs	Reg	Obs	Reg	
Summer	79023	232.9	232.9	29.7	26.9	307.8	301.0	0.82	223.9	238.7	30.0	28.0	288.2	296.5	0.51
	79026	211.0	211.0	29.5	26.2	287.2	278.9	0.79	209.7	216.5	29.2	27.1	280.2	274.5	0.70
	79034	198.7	198.7	28.2	25.4	272.3	262.5	0.81	194.6	204.4	28.4	26.2	262.2	258.3	0.63
	79079	216.3	216.3	30.4	25.9	293.0	279.6	0.73	222.8	221.9	36.1	26.8	309.6	275.5	0.58
	89003	205.2	205.2	28.0	25.6	276.8	269.0	0.84	195.4	211.2	27.2	26.6	250.8	264.7	0.44
Autumn	79023	107.9	107.9	49.1	48.4	208.8	188.4	0.97	106.0	111.1	47.9	48.8	193.2	200.9	0.95
	79026	97.5	97.5	45.5	44.4	194.2	169.1	0.96	99.2	100.1	45.1	44.8	181.8	179.1	0.97
	79034	90.9	90.9	42.9	42.2	179.4	161.4	0.97	91.0	93.8	42.5	42.6	171.0	172.8	0.96
	79079	96.6	96.6	46.6	45.6	196.8	174.8	0.96	101.3	99.6	49.8	46.4	191.2	188.4	0.93
	89003	96.5	96.5	43.6	43.0	187.0	168.2	0.97	93.4	99.6	43.0	43.3	175.8	179.7	0.94
Winter	79023	47.7	47.7	11.4	10.5	82.2	83.2	0.85	46.7	49.3	11.6	10.9	75.0	73.6	0.76
	79026	40.9	40.9	10.9	7.8	71.2	55.6	0.52	42.9	41.6	10.4	7.4	67.2	53.7	0.75
	79034	37.6	37.6	9.6	8.8	63.7	64.5	0.85	38.4	38.7	9.9	9.1	59.6	57.9	0.84
	79079	39.0	39.0	11.2	9.6	69.6	70.5	0.74	35.7	40.4	9.3	9.9	64.0	62.2	0.52
	89003	44.1	44.1	10.6	9.9	73.2	75.9	0.87	42.6	45.4	10.3	10.3	64.0	67.7	0.74
Spring	79023	131.2	131.2	39.3	38.0	257.8	235.3	0.94	132.6	137.5	40.3	42.8	208.0	250.4	0.91
	79026	115.3	115.3	36.2	33.5	230.2	201.9	0.85	122.0	120.4	37.8	37.3	198.4	213.9	0.94
	79034	108.9	108.9	32.8	31.3	234.0	196.6	0.91	112.3	114.2	34.9	35.5	185.6	209.6	0.93
	79079	118.7	118.7	40.1	37.4	278.8	220.1	0.87	122.4	124.8	46.5	42.1	231.4	234.9	0.90
	89003	114.7	114.7	32.2	31.4	229.4	203.6	0.95	115.5	120.1	32.9	35.7	184.8	216.9	0.90

Average = average of monthly evaporation in mm, Std = standard deviation of monthly evaporation in mm, Max = maximum of monthly evaporation in mm, Obs = observed, Reg = intra or inter-station regression relationships, NSE = Nash Sutcliffe efficiency

It was found that, the intra and inter-station regression relationships built between the maximum temperature at key station 79026 and minimum temperature at all stations are quite robust in all seasons in capturing the average of minimum temperature. However in winter, these relationships were relatively weaker at all stations and they under-estimated the standard deviation and the minimum of the minimum temperature was over-estimated.

It was proven that the inter-station regression relationships were able to reproduce the statistics of the maximum temperature at all member stations in all seasons with high degree of accuracy. Hence it was realised that, the inter-station regression relationships built between the maximum temperature at key station 79026 and that of member stations are quite reliable.

Atmospheric domain and predictor selection

An atmospheric domain consisting of 7 grid points in the longitudinal direction and 6 grid points in the latitudinal direction was defined over the study area. This atmospheric domain is shown in Figure 6. In this atmospheric domain, grid points were 2.5˚ apart from each other in both longitudinal and latitudinal directions. This grid resolution was maintained across the atmospheric domain in order to comply with the spatial resolution of the NCEP/ NCAR reanalysis outputs. All GCM outputs used in this study were interpolated to the grid shown in Figure 6, using the inverse distance weighted method.

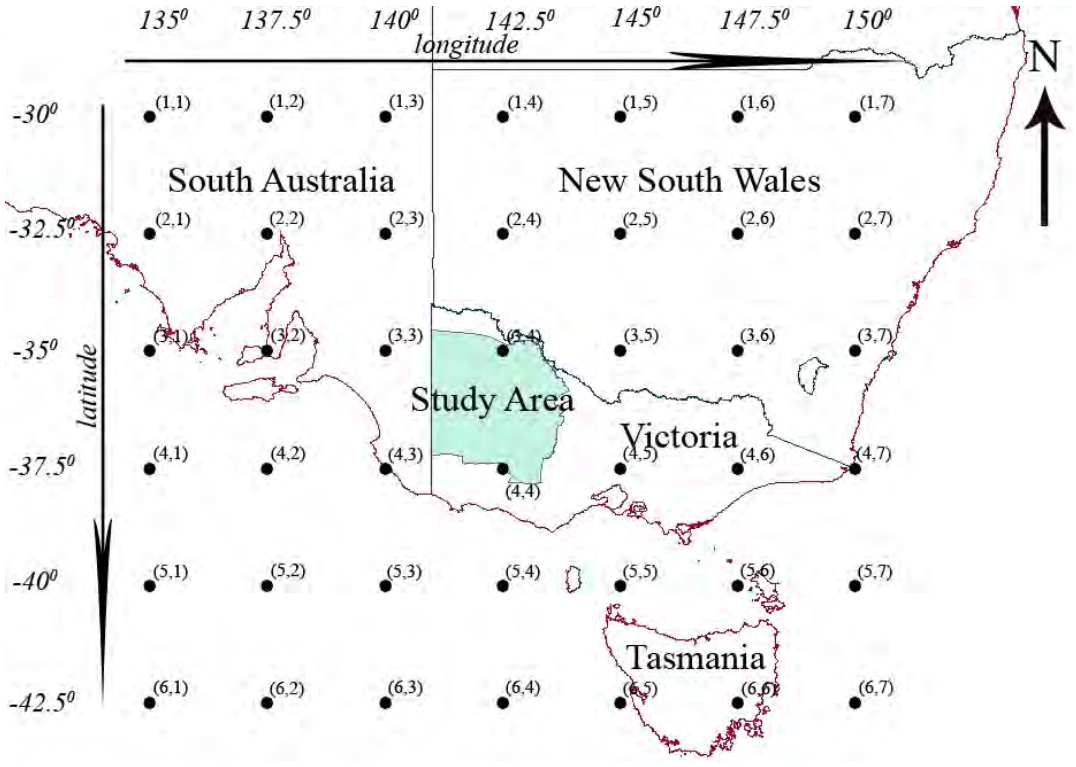

Figure 6 Atmospheric domain for downscaling

Timbal et al. (2009) used the method of meteorological analogues for downscaling NCEP/NCAR reanalysis data to daily precipitation, pan evaporation, minimum temperature, maximum temperature, and dew point temperature over six regions in the southern half of Australia. The present study area is located in the southern half of Australia. Hence the predictors used by Timbal et al. (2009) were included in the pool of probable predictors used in the present study. The pool of probable predictors used in this study included the geopotential heights at 200, 500, 700, 850 and 1000 hPa pressure levels, relative humidity at 700, 850, 925 and 1000 hPa pressure levels, specific humidity at 500, 850 and 1000 hPa pressure levels, air temperature at 500, 850 and 1000 hPa pressure levels, surface air temperature, surface skin temperature, surface air pressure, mean sea level pressure and, zonal and meridional wind speeds at 850 hPa pressure level. Following the procedure detailed in generic methodology, potential predictors for maximum temperature at key station 79026 were extracted for each calendar month from the pool of probable predictors.

Development of a downscaling model for monthly maximum temperature at key station 79026

For the development of the downscaling model for monthly maximum temperature at the key station 79026, the observations of monthly maximum temperature and the NCEP/NCAR reanalysis outputs pertaining to the potential predictors were split into two chronological groups; 1950-1989 and 1990-2010. The first group of data was used in the calibration of the downscaling model and the second group was used in the validation. Following the procedure detailed in generic methodology, downscaling models were developed for each calendar month. Hence, the final sets of potential predictors and the best downscaling models for each calendar month were identified. When the key predictand and key station approach is employed in a downscaling exercise the downscaling models are developed only for the key predictands at the key stations. Therefore the selection of probable predictors and the correction of bias have to be performed only for a few predictands at a few stations.

Table 5 displays the final sets of potential predictors used in the development of the downscaling model for monthly maximum temperature at the key station 79026. According to Table 5, it was seen that in the majority of calendar months, air temperature at earth surface and also air temperature at various pressure levels in the atmosphere are among the potential predictors. This indicated the high degree of influence of air temperature fields on the monthly maximum temperature at the catchment scale. Other than air temperature, relative and specific humidity fields were also seen among the final sets of potential predictors used in the development of the downscaling model for monthly maximum temperature at the key station 79026.

Table 5 Final sets of potential predictors for each calendar month

Month	Potential variables used for downscaling model with grid locations
January	1000hPa air temperature{(5,1)} 700hPa relative humidity {(3,6),(3,7)} 1000hPa specific humidity {(5,1),(6,2)}
February	850hPa zonal wind {(1,1),(2,1),(2,2)} 500hPa relative humidity {(4,7),(5,6),(5,7)} 500hPa specific humidity {(1,3)}
March	Surface air temperature{(2,2)}
April	850hPa air temperature {(1,4),(1,5)} 850hPa relative humidity {(5,2),(5,3),(5,4),(6,4),(6,5)} 700hPa relative humidity {(6,5)} 850hPa specific humidity {(5,1),(6,2),(6,3)}
May	1000hPa relative humidity {(2,1),(3,1)} 925hPa relative humidity {(1,1),(2,1),(2,2),(3,1),(3,2)} 500hPa relative humidity {(5,6)}
June	Surface air temperature{(6,2)}
July	Surface air temperature{(4,7), (5,6)}
August	Surface air temperature{(3,3),(4,3)}
September	Surface air temperature{(3,5),(4,3)} 850hPa air temperature {(4,5)}
October	Surface air temperature{(5,1),(5,2),(5,3),(5,4),(6,1),(6,2)}
November	850hPa relative humidity {(6,5)} 500hPa specific humidity {(6,1),(6,2)}
December	Surface air temperature{(2,1),(3,1),(4,2),(4,3),(4,4)} 500hPa relative humidity {(4,1),(4,2)} 500hPa specific humidity {(3,1),(3,2)}

hPa = Atmospheric pressure in hectopascal; and the locations are given within brackets (see Figure 6)

Table 6 shows the statistics of the observed monthly maximum temperature and those of model reproduced monthly maximum temperature for the calibration and validation periods of the downscaling model at key station 79026. As seen in Table 6, the average, the standard deviation and the maximum of the monthly maximum temperature were reproduced by the downscaling model during both calibration and validation periods in all seasons with good degree of accuracy. Hence, it was realised that, this downscaling model is capable in properly reproducing the statistics of observed monthly maximum temperature with the NCEP/NCAR reanalysis outputs.

Table 6 Statistics of monthly maximum temperature reproduced by downscaling model developed at key station 79026

Model	Statistic	Calibration (1950-1989)				*Validation (1990-2010)*			
		Season				*Season*			
		Summer	Autumn	Winter	Spring	*Summer*	*Autumn*	*Winter*	*Spring*
Observed	Avg	27.4	20.5	13.1	19.3	*27.9*	*21.0*	*13.5*	*19.9*
Model output		27.4	20.5	13.1	19.3	*27.7*	*20.7*	*13.2*	*19.6*
Observed	Std	2.2	4.0	1.1	3.0	*2.3*	*3.9*	*1.1*	*3.4*
Model output		1.7	3.9	0.9	2.8	*1.5*	*3.6*	*0.9*	*3.1*
Observed	Max	32.6	27.3	17.5	27.8	*32.1*	*28.9*	*15.9*	*29.1*
Model output		33.6	27.0	16.1	24.6	*31.5*	*27.6*	*15.3*	*25.4*
Model output	NSE	0.59	0.97	0.67	0.88	*0.49*	*0.94*	*0.71*	*0.87*
Model output	R^2	0.59	0.97	0.67	0.88	*0.51*	*0.95*	*0.77*	*0.87*

Avg = average of monthly maximum temperature in ˚C, Std = standard deviation of maximum temperature in ˚C, Max = maximum of maximum monthly temperature in ˚C, NSE = Nash Sutcliffe efficiency, R^2 = coefficient of determination

Figure 7 shows the scatter plots for the calibration (1950-1989) and validation (1990-2010) periods of the downscaling model developed at the key station 79026 for monthly maximum temperature. Owing to the limited scatter seen in Figure 7, it was realised that there is a very good agreement between the observations of monthly maximum temperature and the monthly maximum temperature reproduced by the downscaling model, in both calibration (NSE = 0.97) and validation (NSE = 0.96) periods. However, the scatter of the monthly maximum temperature tended to increase slightly with the increase in its magnitude during both calibration and validation periods. This indicated that the accuracy of relatively high values of monthly maximum temperature are less accurate compared to relatively low and the medium values of monthly maximum temperature simulated by the downscaling model.

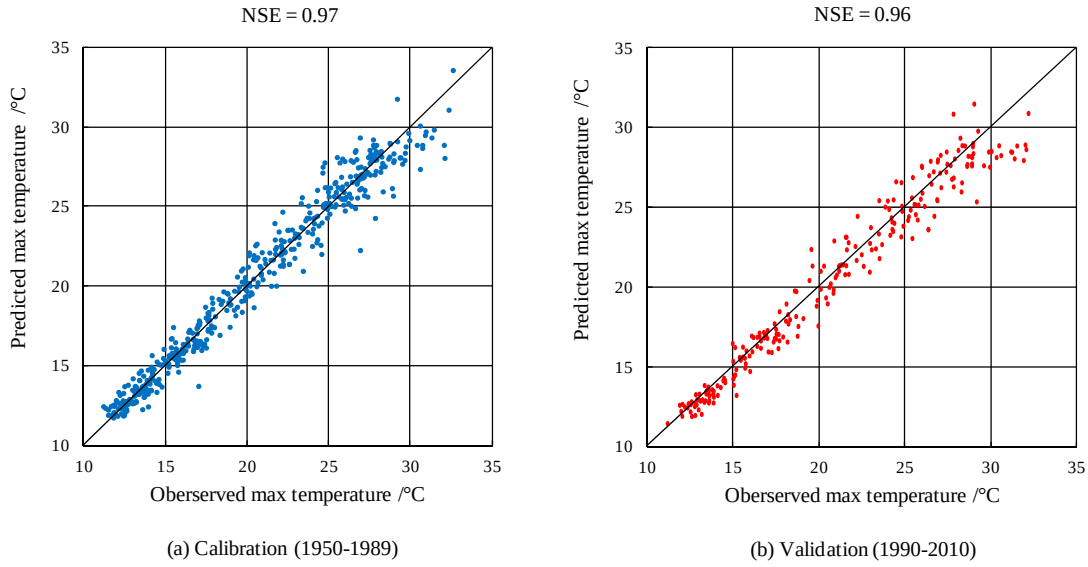

Figure 7 Scatter plots for the calibration and validation periods of the downscaling model for monthly maximum temperature at key station 79026

Reproduction of past observations of maximum temperature and bias-correction

Following the procedure detailed in generic methodology, the monthly bias-correction (Johnson and Sharma, 2012) was applied over the period 1950-1989 and it was validated for the period 1990-1999. The statistics of the monthly maximum precipitation reproduced by the downscaling model with the 20C3M outputs of ECHAM5, before and after bias-correction for both application and validation periods are shown in Table 7.

Table 7 Statistics of maximum temperature reproduced by downscaling model at key station 79026, with 20C3M outputs of ECHAM5, before and after bias-correction

Model	Statistic	Application (1950-1989)				*Validation (1990-1999)*			
		Season				*Season*			
		Summer	Autumn	Winter	Spring	*Summer*	*Autumn*	*Winter*	*Spring*
Observed	Avg	27.4	20.5	13.1	19.3	*27.4*	*20.5*	*13.3*	*19.2*
Before B-C		30.9	18.3	12.8	17.0	*31.7*	*18.5*	*12.7*	*17.0*
After B-C		27.4	20.5	13.1	19.3	*28.1*	*20.8*	*13.0*	*19.3*
Observed	Std	2.2	4.0	1.1	3.0	*2.1*	*3.8*	*1.0*	*2.8*
Before B-C		6.1	2.5	0.8	4.3	*6.6*	*2.6*	*0.8*	*4.5*
After B-C		2.2	4.0	1.1	3.0	*2.3*	*4.1*	*1.1*	*3.2*
Observed	Max	32.6	27.3	17.5	27.8	*32.0*	*26.7*	*15.7*	*24.3*
Before B-C		46.2	24.7	15.3	24.8	*43.2*	*24.8*	*14.0*	*24.4*
After B-C		31.9	27.5	16.8	26.7	*33.9*	*28.5*	*15.7*	*25.9*
Before B-C	NSE	-13.71	-0.07	-0.63	-0.82	*-16.77*	*-0.07*	*-1.07*	*-1.16*
After B-C		-0.37	0.79	-0.30	0.54	*-0.77*	*0.79*	*-0.61*	*0.69*

Avg = average of monthly maximum temperature in ˚C, Std = standard deviation of monthly maximum temperature in ˚C, Max = maximum of monthly maximum temperature in ˚C, NSE = Nash Sutcliffe efficiency, Before B-C = before bias-correction, After B-C = after bias-correction

According to Table 7, it was seen that the mismatches between the average, the standard deviation and the maximum of observed monthly maximum temperature and those reproduced by the downscaling model at key station 79026 when it was run with the 20C3M outputs of ECHAM5 were successfully corrected by the monthly bias-correction in both application and validation periods. Following the bias-correction, the NSEs in all seasons in both the calibration and validation periods showed an increase. This indicated that, the scatter of the maximum monthly temperature reproduced by the downscaling model reduced after the bias-correction in all seasons in both calibration and validation periods. Figure 8 shows the scatter plots for the monthly maximum temperature reproduced by the downscaling model with the 20C3M outputs of ECHAM5, before and after the application of the monthly bias-correction. It was observed that the scatter of the monthly maximum temperature reproduced by the downscaling model reduced after the bias-correction.

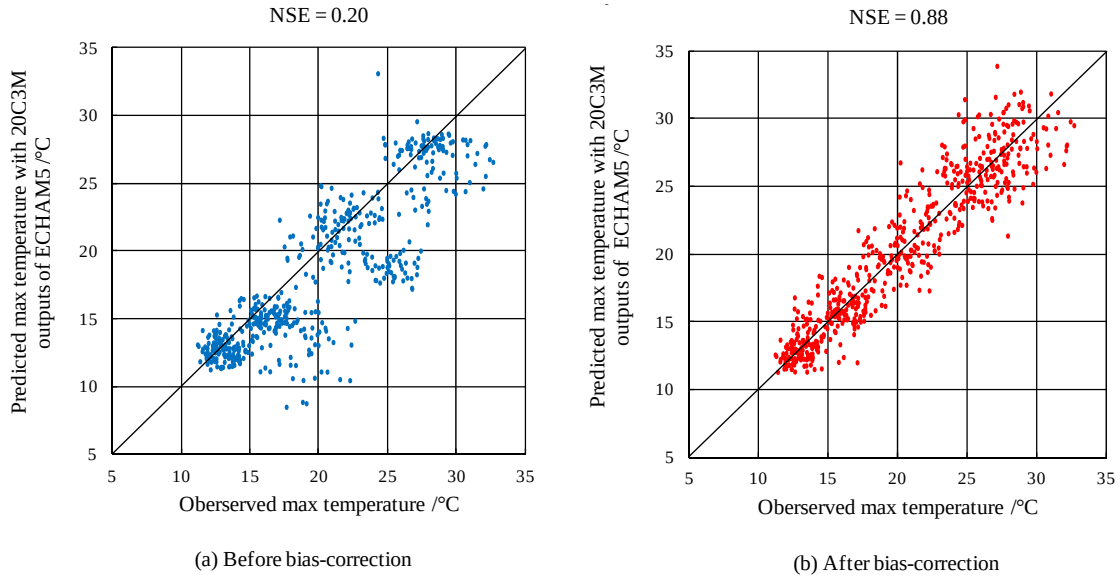

Figure 8 Scatter of the monthly maximum temperature reproduced by the downscaling model at key station 79026 with the 20C3M outputs of ECHAM5, before and after the application of the monthly bias-correction.

In the application of the monthly bias-correction explicit measures are taken only for the correction of the monthly mean and the monthly standard deviation of the variable of interest. However, it was realised that when the scatter of the variable prior to the application of the monthly bias-correction is limited (refer to Figure 8(a)), the monthly bias-correction can reduce the scatter (refer to Figure 8(b)) and improve the time series of the variable. Sachindra et al. (2014) found that when the scatter of the variable prior to the application of the monthly bias-correction is very large the monthly bias-correction fails to reduce the scatter of the variable.

Development of downscaling models at key station 79026 and member station 79023 for evaporation

For the purpose of comparing the quality of the outputs of an intra-station regression relationship with the outputs of the downscaling model at the key station, a downscaling model was built at the key station 79026 for evaporation which was not selected as a key predictand. This downscaling model was calibrated and validated over the periods

1950-1989 and 1990-2010 respectively, following the same procedure used in the development of a downscaling model for a key-predictand.

It was found that the average, the standard deviation and the maximum of monthly evaporation reproduced by the above downscaling model at the key station 79026 were in close agreement with those of observations and those produced by the intra-station regression relationship at this station. It was assumed that, the other intra-station regression relationship between the maximum temperature and the minimum temperature at key station 79026 also can properly capture the statistics of observations of minimum temperature. Furthermore it was realised that when the correlations between the observations of the key predictand and other predictands at a key station (in a cluster) are high, instead of developing downscaling models for each of the other predictands (at that key station) the intra-station regression relationships can be used effectively for the determination of the values of the other predictands.

Figure 9 shows the scatter plots for the monthly evaporation simulated by the intra-station regression relationship against the monthly evaporation simulated by the downscaling model developed at key station 79026. According to the small scatter seen in Figure 9, it was further realised that the time series of monthly evaporation reproduced by the intra-station regression relationship and that reproduced by the downscaling model developed at key station 79026 are in good agreement with each other.

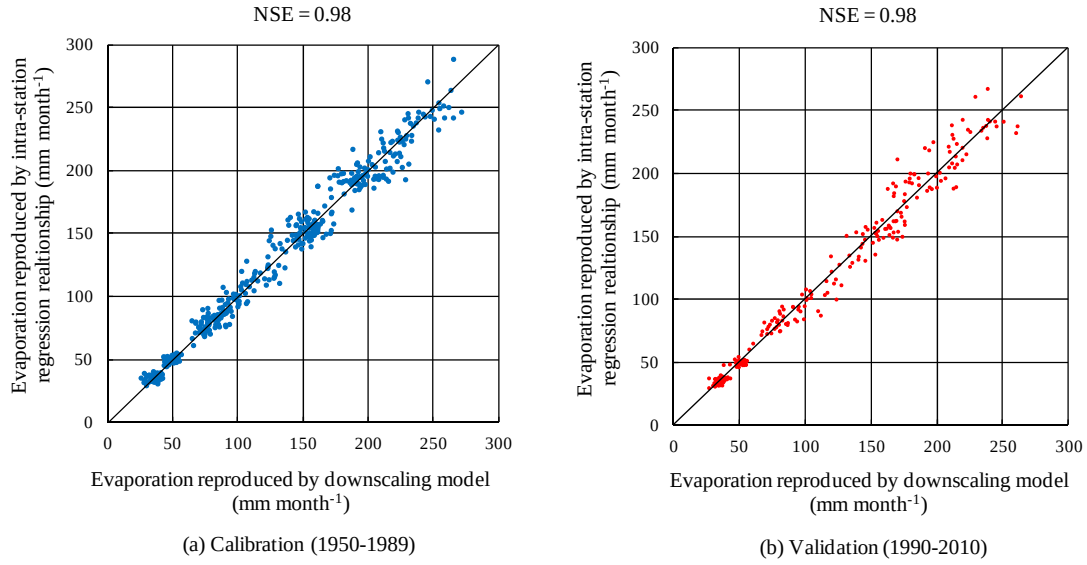

Figure 9 Evaporation reproduced by intra-station regression relationship against evaporation reproduced by downscaling model developed at station 79026

In order to compare the quality of the outputs of an inter-station regression relationship against the outputs of a downscaling model, a downscaling model was built at member station 79023 (Polkemmet) for evaporation which was not selected as a key predictand. This downscaling model was also calibrated and validated over the periods 1950-1989 and 1990-2010 respectively, following the same procedure used in the development of a downscaling model for a key predictand.

It was found that the average, the standard deviation and the maximum of the monthly evaporation at station 79023 estimated by the above downscaling model were in close agreement with those of observations and those produced by the inter-station regression relationships. The scatter of the evaporation simulated by the inter-station regression relationship between the maximum temperature at key station 79026 and evaporation at member station 79023 against the evaporation simulated by the downscaling model developed at station 79023 was also quite limited (not shown).

Following the above findings, it was assumed that the statistics and the time series of the outputs of all inter-station regression relationships developed in this study can

closely represent those of the outputs of downscaling models. It was realised that when the correlations between the observations of a key predictand at a key station and all predictands at member stations (in a cluster) are high, instead of developing separate downscaling models for each predictand at each station, inter-station regression relationships can be used effectively for the determination of the values of all predictands at member stations.

Projections of evaporation, minimum temperature and maximum temperature into future

Following the procedure detailed in generic methodology, projections of monthly evaporation, minimum temperature and maximum temperature were produced into future using the outputs of ECHAM5 pertaining to A2 GHG emission scenario for the period 2000-2099. Table 8 shows the percentage changes in the statistics of monthly evaporation, minimum temperature and maximum temperature in the period 2000-2099 at all stations with respect to the observations of the period 1950-1989.

Table 8 Percentage changes in the statistics of evaporation, and minimum and maximum temperature over the period 2000-2099

Variable	Season	79023			79026			79034			79079			89003		
		Avg	**Std**	**M**	**Avg**	**Std**	**M**	**Avg**	**Std**	**M**	**Avg**	**Std**	**M**	**Avg**	**Std**	**M**
E_v	**Summer**	+9↑	+27↑	+17↑	+10↑	+21↑	+17↑	+10↑	+21↑	+16↑	+9↑	+15↑	+13↑	+11↑	+24↑	+17↑
	Autumn	+11↑	+19↑	+17↑	+10↑	+16↑	+10↑	+12↑	+20↑	+19↑	+13↑	+23↑	+20↑	+12↑	+20↑	+18↑
	Winter	+20↑	+14↑	+17↑	+12↑	-37↓	-18↓	+17↑	+9↑	+15↑	+21↑	+5↑	+17↑	+18↑	+14↑	+19↑
	Spring	+10↑	+10↑	+33↑	+9↑	+4↑	+25↑	+10↑	+9↑	+23↑	+11↑	+5↑	+16↑	+10↑	+12↑	+30↑
T_{max}	**Summer**	+9↑	+27↑	+17↑	+10↑	+21↑	+17↑	+10↑	+21↑	+16↑	+9↑	+15↑	+13↑	+11↑	+24↑	+17↑
	Autumn	+11↑	+19↑	+17↑	+10↑	+16↑	+10↑	+12↑	+20↑	+19↑	+13↑	+23↑	+20↑	+12↑	+20↑	+18↑
	Winter	+20↑	+14↑	+17↑	+12↑	-37↓	-18↓	+17↑	+9↑	+15↑	+21↑	+5↑	+17↑	+18↑	+14↑	+19↑
	Spring	+10↑	+10↑	+33↑	+9↑	+4↑	+25↑	+10↑	+9↑	+23↑	+11↑	+5↑	+16↑	+10↑	+12↑	+30↑
T_{min}	**Summer**	+10↑	+4↑	*+21↑*	+10↑	+4↑	*+17↑*	+10↑	+3↑	*+22↑*	+10↑	+5↑	*+15↑*	+10↑	NC	*+21↑*
	Autumn	+10↑	+36↑	*+57↑*	+10↑	+37↑	*+34↑*	+10↑	+38↑	*+37↑*	+10↑	+36↑	*+35↑*	+10↑	+34↑	*+27↑*
	Winter	+7↑	-63↓	*+406*	+10↑	-48↓	*+165*	+11↑	-46↓	*+296*	+12↑	-47↓	*+170*	+12↑	-47↓	*+218*
	Spring	-3↓	+23↑	*+35↑*	-1↓	+24↑	*+9↑*	NC	+23↑	*+18↑*	-1↓	+26↑	*+9↑*	NC	+18↑	*+24↑*

E_v = monthly evaporation, T_{max} = monthly maximum temperature, T_{min} = monthly minimum temperature, Avg = average of climatic variable, Std = standard deviation of climatic variable, M = maximum of evaporation, maximum of maximum temperature, minimum of minimum temperature (*in italics*), ↑ = percentage increase in 2000-2099 with respect to observations of period 1950-1989, ↓ = percentage decrease in 2000-2099 with respect to observations of period 1950-1989 (in bold), NC = No change in percentage in 2000-2099 with respect to observations of period 1950-1989

According to Table 8, it was seen that at each station in all seasons the changes in the average, the standard deviation and the maximum of monthly evaporation are equal to those of the monthly maximum temperature. This showed the uniform relationship between the maximum temperature and evaporation. However, the changes in the statistics of monthly minimum temperature did not display clear uniform association with either monthly evaporation or monthly maximum temperature. As shown in Table 8, in all seasons at all stations the averages of monthly evaporation and monthly maximum temperature in the period 2000-2099 indicated a rise in comparison with observations of the period 1950-1989. This indicated that in future, the loss of water into atmosphere due to evaporation will tend to increase with the rising GHG concentrations in the atmosphere over the study area. Except in winter, at all stations the standard deviations of evaporation and maximum temperature showed an increase in the period 2000-2099. This hinted that, in future there will be more fluctuations in the regimes of evaporation and maximum temperature across the present study area. The maximum of monthly evaporation and the maximum of monthly maximum temperature also displayed a rise at all stations in summer, autumn, and spring during the period 2000-2099.

The average of the minimum temperature showed a rise at all stations except in spring. Except in winter, at the majority of stations the standard deviation of the minimum temperature also showed an increase indicating more fluctuations in the minimum temperature in future. The minimum of minimum temperature indicated an increase in all seasons in the period 2000-2099, however these predictions are less reliable as intra and inter-station regression relationships consistently over-estimated the minimum of minimum temperature during their calibration and validation phases.

It was concluded that, in future the evaporation, minimum and the maximum temperature will tend to increase across the study area and hence the future climate in the study area will be dryer and warmer. Furthermore the fluctuations in these predictands are also likely to increase with the rising GHGs.

According to median estimates obtained from the raw outputs of number of GCMs, the Victorian Government Department of Sustainability and Environment (2008) found that the average of temperature and evaporation over the present study area are likely to increase under B1 (low emissions), A1B (medium emissions) and A1F1 (high emissions) emission scenarios, in all seasons. It was realised that the findings of the present research are in close agreement with those of the Victorian Government Department of Sustainability and Environment (2008).

However, unlike that previous study which directly used the raw outputs of GCMs for the determination of future climate in this study area, in this study using a statistical downscaling methodology the raw outputs of a GCM were translated to point specific climatic information pertaining to future. This was performed while maintaining the spatial correlation structures of each individual predictand among the stations and also the correlation structures between different predictands at individual stations. The observations of monthly evaporation, maximum temperature and minimum temperature at all observation stations (including the stations not considered in this study) located in the operational area of GWMWater showed high positive correlations with each other. Hence it can be assumed that the patterns of changes in evaporation, maximum temperature and minimum temperature determined for the 5 observations station considered in this study are also valid for those at the other stations in the operational area of GWMWater.

Furthermore it was realised that the key predictand and key station approach can also be applied to an area of any extent with any number of stations and any number of predictands effectively, provided that there are high correlations among stations (in a cluster) for each individual predictand and high correlations among different predictands at each individual station in the clusters.

SUMMARY AND CONCLUSIONS

Statistical downscaling of GCM outputs to monthly evaporation, minimum temperature and maximum temperature was performed using a key predictand and key station

approach at 5 observation stations located in north western Victoria, Australia. For the effective application of the key predictand and key station approach high correlations (magnitudes above 0.80 at $p \leq 0.05$) should prevail between the observations of each individual predictand among the stations and also among different predictands at each individual station. In this study, high correlations between monthly evaporation, minimum temperature and maximum temperature were seen over the period 1950-2010 at each individual station and among the 5 stations for each individual predictand. Hence the key predictand and key station approach was effectively employed. Due to the good agreement seen between the outputs of intra and inter-station regression relationship and those of downscaling models developed at a key station and a member station respectively, the effectiveness of the key predictand and key station approach was realised.

Following conclusions were drawn from this study:

1. The correlations between the evaporation and the maximum temperature were consistently higher than those between the evaporation and the minimum temperature at each individual station. Therefore it was realised that the maximum temperature is more influential than the minimum temperature on evaporation.

2. The key predictand and key station approach was proven to be a simple and effective methodology for downscaling GCM outputs to multiple predictands at multiple stations simultaneously. It not only aids in maintaining the cross-correlation structures among the observation stations for each individual predictand but also enables the preservation of the cross-correlation structures among different predictands at each individual observation station. Therefore the plausible representation of spatial variations of individual predictands among observation stations and also the realistic relationships between different predictands can be maintained in the projections produced by the downscaling models into future.

3. However, for the effective implementation of the key predictand and key station approach the presence of high correlations (magnitudes above 0.80 at $p \leq 0.05$) among the observation stations (in a cluster) for each individual predictand and high correlations among different predictands at each individual observation station are prerequisites.

4. In the application of the key predictand and key station approach, downscaling models are only developed for the key predictands at key stations. Therefore unlike downscaling at each individual station separately, in this approach the selection of potential predictors and the correction of bias have to be performed only at several stations for several predictands.

5. Although the monthly bias-correction employs explicit measures to correct only the monthly mean and the standard deviation of a climatic variable (e.g. output of a GCM or downscaling model), when the bias is limited, monthly bias-correction is also capable of improving the time series of the climatic variable.

ACKNOWLEDGEMENTS

The authors acknowledge the financial assistance provided by the Australian Research Council Linkage Grant scheme and the Grampians Wimmera Mallee Water Corporation for this project.

REFERENCES

Anandhi A, Srinivas VV, Nanjundiah RS, Kumar DN. 2008. Downscaling precipitation to river basin in India for IPCC SRES scenarios using support vector machine. *Int. J. Climatol.* **28:** 401-420. DOI: 10.1002/joc.1529.

Apipattanavis S, Podestá G, Rajagopalan B, Katz RW. 2007. A semiparametric multivariate and multisite weather generator. *Water Resour. Res.* **43:** 1-19. DOI: 10.1029/2006WR005714.

Barton AF, Briggs S, Prior D, McRae-Williams P. 2011. Coping with severe drought: stories from the front line. *Aust. J. Water Resour.* **15:** 21-32.

Bárdossy A, Pegram GGS. 2009. Copula based multisite model for daily precipitation simulation. *Hydrol. Earth Syst. Sci.* **13:** 2299-2314. DOI: 10.5194/hess-13-2299-2009.

Bureau of Meteorology. 2013. Climate classification of Australia. Available online at http://www.bom.gov.au/climate/environ/other/kpn.jpg. (Accessed 20th February 2013)

Cannon AJ. 2008. Probabilistic multisite precipitation downscaling by an expanded Bernoulli–Gamma density network. *J. Hydrometeor.* **9:** 1284-1300. DOI: 10.1175/2008JHM960.1.

Hay LE, Clark MP. 2003. Use of statistically and dynamically downscaled atmospheric model output for hydrologic simulations in three mountainous basins in the western United States. *J. Hydrol.* **282:** 56-75. DOI: 10.1016/S0022-1694(03)00252-X.

Heyen H, Zorita E, von Storch H. 1996. Statistical downscaling of monthly mean North Atlantic air-pressure to sea level anomalies in the Baltic Sea. *Tellus.* **48:** 312-323. DOI: 10.1034/j.1600-0870.1996.t01-1-00008.x.

Jeong DI, St-Hilaire A, Ouarda TBMJ, Gachon P. 2012a. Multisite statistical downscaling model for daily precipitation combined by multivariate multiple linear regression and stochastic weather generator. *Climatic Change.* **114:** 567-591. DOI: 10.1007/s10584-012-0451-3.

Jeong DI, St-Hilaire A, Ouarda TBMJ, Gachon P. 2012b. A multivariate multi-site statistical downscaling model for daily maximum and minimum temperatures. *Clim. Res.* **54:** 129-148. DOI: 10.3354/cr01106.

Jeong DI, St-Hilaire A, Ouarda TBMJ, Gachon P. 2013a. Projection of future daily precipitation series and extreme events by using a multi-site statistical downscaling model over the great Montréal area, Québec, Canada. *Hydrol. Res.* **44:** 147-168. DOI: 10.2166/nh.2012.183.

Jeong DI, St-Hilaire A, Ouarda TBMJ, Gachon P. 2013b. A multi-site statistical downscaling model for daily precipitation using global scale GCM precipitation outputs. *Int. J. Climatol.* **33:** 2431–2447. DOI: 10.1002/joc.3598.

Johnson F, Sharma A. 2012. A nesting model for bias correction of variability at multiple time scales in general circulation model precipitation simulations. *Water Resour. Res.* **48:** 1-16. DOI: 10.1029/2011WR010464.

Khalili M, Brissette F, Leconte R. 2007. Stochastic multi-site generation of daily precipitation data using spatial autocorrelation. *J. Hydrometeor.* **8:** 396-412. DOI: 10.1175/JHM588.1.

Khalili M, Brissette F, Leconte R. 2009. Stochastic multi-site generation of daily weather data. *Stoch. Environ. Res. Risk Assess.* **23:** 837-849. DOI: 10.1007/s00477-008-0275-x.

Khalili M, Brissette F, Leconte R. 2011. Effectiveness of multi-site weather generator for hydrological modelling. *J. Am. Water Resour. As.* **47:** 303-314. DOI: 10.1111/j.1752-1688.2010.00514.x.

Khalili M, Nguyen VTV, Gachon P. 2013. A statistical approach to multi-site multivariate downscaling of daily extreme temperature series. *Int. J. Climatol.* **33:** 15-32. DOI: 10.1002/joc.3402.

King LM, McLeod AI, Simonovic SP. 2012. Simulation of historical temperatures using a multi-site, multivariate block resampling algorithm with perturbation. *Hydrol. Process.* Article in press. DOI: 10.1002/hyp.9596.

Kottegoda NT, Natale L, Raiteri E. 2003. A parsimonious approach to stochastic multisite modelling and disaggregation of daily rainfall. *J. Hydrol.* **274:** 47-61. DOI: 10.1016/S0022-1694(02)00356-6.

Kou X, Ge J, Wang Y, Zhang C. 2007. Validation of the weather generator CLIGEN with daily precipitation data from the Loess Plateau, China. *J. Hydrol.* **347:** 347-357. DOI: 10.1016/j.jhydrol.2007.09.051.

Maurer EP, Hidalgo HG. 2008. Utility of daily vs. monthly large-scale climate data: an intercomparison of two statistical downscaling methods. *Hydrol. Earth Syst. Sci.* **12:** 551-563. DOI: 10.5194/hess-12-551-2008.

Maraun D, Wetterhall F, Ireson, AM, Chandler RE, Kendon EJ, Widmann M, Brienen S, Rust HW, Sauter T, Themel M, Venema VKC, Chun KP, Goodess CM, Jones RG, Onof C, Vrac M, Thiele-Eich I. 2010. Precipitation downscaling under climate change: Recent developments to bridge the gap between dynamical models and the end user. *Rev. Geophys.* **48:** DOI:10.1029/2009RG000314.

Mehrotra R, Srikanthan R, Sharma A. 2006. A comparison of three stochastic multi-site precipitation occurrence generators. *J. Hydrol.* **331:** 280-292. DOI: 10.1016/j.jhydrol.2006.05.016.

Murphy J. 1998. An evaluation of statistical and dynamical techniques for downscaling local climate. *J. Climate.* **12:** 2256-2284. DOI: 10.1175/1520-0442(1999)012<2256:AEOSAD>2.0.CO;2.

Nash JE, Sutcliffe JV. 1970. River flow forecasting through conceptual models, part 1 - A discussion of principles. *J. Hydrol.* **10:** 282-290. DOI: 10.1016/0022-1694(70)90255-6.

Ojha R, Kumar DN, Sharma A, Mehrotra R. 2012. Assessing severe drought and wet events over India in a future climate using a nested bias correction approach. *J. Hydrologic Eng.* Article in press. DOI: 10.1061/(ASCE)HE.1943-5584.0000585.

Pearson K. 1895. Mathematical contributions to the theory of evolution. iii. regression heredity and panmixia. *Philos. T. Roy. Soc. A.* **187:** 253-318. DOI: 10.1098/rsta.1896.0007.

Qian B, Corte-Real J, Xu H. 2002. Multisite stochastic weather models for impact studies. *Int. J. Climatol.* **22:** 1377–1397.DOI: 10.1002/joc.808.

Sachindra DA, Huang F, Barton AF, Perera BJC. 2013a. Least square support vector and multi-linear regression for statistically downscaling general circulation model outputs to catchment streamflows. *Int. J. Climatol.* **33:** 1087-1106. DOI: 10.1002/joc.3493.

Sachindra DA, Huang F, Barton AF, Perera BJC. 2013b. Multi-model ensemble approach for statistically downscaling general circulation model outputs to precipitation. *Q. J. Roy. Meteor. Soc.* Article in Press. DOI**:** 10.1002/qj.2205.

Sachindra DA, Huang F, Barton AF, Perera BJC. 2014. Statistical downscaling of general circulation model outputs to precipitation part 2: Bias-correction and future projections. *Int. J. Climatol.* Article in Press. DOI**:** 10.1002/joc.3915

Salvi K, Kannan S, Ghosh S. 2011. Statistical downscaling and bias-correction for projections of Indian rainfall and temperature in climate change studies. *In proceeding of the 4th International Conference on Environmental and Computer Science, Singapore, 16 Sep - 18 Sep 2011.*

Smith I, Chandler E. 2009. Refining rainfall projections for the Murray Darling basin of south-east Australia-the effect of sampling model results based on performance. *J. Climate Change.* **102:** 377-393. DOI: 10.1007/s10584-009-9757-1.

Timbal B, Fernandez E, Li Z. 2009. Generalization of a statistical downscaling model to provide local climate change projections for Australia. *Environ. Modell. Softw.* **24:** 341-358. DOI: 10.1016/j.envsoft.2008.07.007.

Tripathi S, Srinivas VV, Nanjundiah RS. 2006. Downscaling of precipitation for climate change scenarios: a support vector machine approach. *J. Hydrol.* **330:** 621-640. DOI: 10.1016/j.jhydrol.2006.04.030.

Victorian Government Department of Sustainability and Environment. 2008. *Climate change in the Wimmera.* Available online at http://www.climatechange.vic.gov.au/regional-projections/wimmera. (Accessed on 28th October 2012). 3-8.

von Storch H, Hewitson B, Mearns L. 2000. Review of empirical downscaling techniques. *Proceedings of RegClim spring meeting, 8 - 9 May 2000, Jevnaker, Norway*. Available online at http://regclim.met.no/rapport_4/Default.htm. (Accessed on 1st October 2012).

Wilby RL, Tomlinson OJ, Dawson CW. 2003. Multi-site simulation of precipitation by conditional resampling. *Clim. Res.* **23:** 183-194. DOI: 10.3354/cr023183.

Wilby RL, Charles SP, Zorita E, Timbal B, Whetton P, Mearns LO. 2004. *Guidelines for use of climate scenarios developed from statistical downscaling methods, supporting material to the IPCC*. Available online at http://www.ipcc-data.org/. 3-21. (Accessed on 28th January 2012).

Wilks DS. 1999. Simultaneous stochastic simulation of daily precipitation, temperature and solar radiation at multiple sites in complex terrain. *Agr. Forest. Meteorol.* **96:** 85-101. DOI: 10.1016/S0168-1923(99)00037-4.

Willems P, Olsson J, Arnbjerg-Nielsen K, Beecham S, Pathirana A, Bülow Gregersen I, Madsen H, Nguyen VTV. 2012. *Impacts of climate change on rainfall extremes and urban drainage systems*. IWA publishing: London; pp 47-110.

CHAPTER 6

STATISTICAL DOWNSCALING OF GCM OUTPUTS TO STREAMFLOWS

6.1 Introduction

In the literature, studies on statistical downscaling of GCM outputs to catchment scale precipitation, temperature and evaporation are abundantly found. However, the direct downscaling of GCM outputs to catchment streamflows is rarely documented. In this chapter, the development of two statistical models for downscaling NCEP/NCAR reanalysis outputs to monthly streamflows is detailed. In this investigation, the first downscaling model was developed using the least square support vector machine regression (non-linear regression technique) and the second downscaling was established using the multi-linear regression (linear regression technique). This chapter provides a comparison between the performances of the downscaling models developed using the above two techniques. Also in this chapter the issues associated with the use of principal component analysis (PCA) in preparing inputs to statistical downscaling models are investigated. Furthermore, this was the first study conducted in Australia on direct downscaling of catchment streamflows from large scale atmospheric variables.

This chapter contains the following journal paper;

1. **Sachindra DA**, Huang F, Barton AF, Perera BJC. 2013a. Least square support vector and multi-linear regression for statistically downscaling general circulation model outputs to catchment streamflows. *International Journal of Climatology* **33:** 1087-1106. DOI: 10.1002/joc.3493. (SCImago journal rank indicator = Q2; ERA Rank = A; Impact Factor = 2.886)

VICTORIA UNIVERSITY
MELBOURNE AUSTRALIA

6.2

PART B:

DECLARATION OF CO-AUTHORSHIP AND CO-CONTRIBUTION: PAPERS INCORPORATED IN THESIS BY PUBLICATION

This declaration is to be completed for each conjointly authored publication and placed at the beginning of the thesis chapter in which the publication appears.

Declaration by [candidate name]: Signature: Date: 08/07/2014

Sachindra Dhanapala Arachchige

Paper Title:

Least square support vector and multi-linear regression for statistically downscaling general circulation model outputs to catchment streamflows

In the case of the above publication, the following authors contributed to the work as follows:

Name	Contribution %	Nature of Contribution
Sachindra Dhanapala Arachchige	85	Conceptual ideas, analysis, paper writing
Fuchun Huang	5	Critical comments, help with statistics
Andrew Barton	5	Critical comments, industry inputs
Chris Perera	5	Critical comments, discussion of conceptual ideas

VICTORIA UNIVERSITY
MELBOURNE AUSTRALIA

DECLARATION BY CO-AUTHORS

The undersigned certify that:

1. They meet criteria for authorship in that they have participated in the conception, execution or interpretation of at least that part of the publication in their field of expertise;
2. They take public responsibility for their part of the publication, except for the responsible author who accepts overall responsibility for the publication;
3. There are no other authors of the publication according to these criteria;
4. Potential conflicts of interest have been disclosed to **a)** granting bodies, **b)** the editor or publisher of journals or other publications, and **c)** the head of the responsible academic unit; and
5. The original data is stored at the following location(s):

Location(s):
College of Engineering and Science,Victoria University,Melbourne,Australia

and will be held for at least five years from the date indicated below:

		Date
Signature 1	[redacted]	29/07/2013
Signature 2	[redacted]	29/07/2013
Signature 3	[redacted]	16/8/2013
Signature 4	[redacted]	26/07/13

CHAPTER 7

SUMMARY, CONCLUSIONS AND RECOMMENDATIONS FOR FUTURE WORK

7.1 Summary

The greenhouse gases (GHGs) such as carbon dioxide, methane and water vapour in the earth's atmosphere absorb some of the solar energy which is reflected by the earth's surface. Then these GHGs radiate the absorbed energy back into the atmosphere causing a rise in the atmospheric temperature. The elevation of the atmospheric temperature due the emission of thermal energy back to the earth by GHGs is called the greenhouse effect. The rising GHG concentrations in the atmosphere owing to human activities such as burning of fossil fuels, agricultural and other practices, intensify the greenhouse effect causing an imbalance in the earth's radiative energy budget, which alters the global climate. Climate change influences droughts, floods, extreme temperatures and, sea level changes, and has shed its adverse impacts on agriculture, energy generation, human health, biodiversity, water resources and land resources.

General Circulation Models (GCMs) are used for the projection of global climate into future. They consider the GHG concentrations in the atmosphere for the simulation of global climate. Though GCMs are capable of providing credible simulations of climate at the global and continental scales, their coarse spatial resolution does not permit the

proper simulation of climate at the catchment scale. Hence the direct use of the coarse resolution GCM outputs in catchment scale studies is not feasible. Therefore in order to determine the catchment scale climate using the GCM outputs, either dynamic or statistical downscaling techniques are used.

This study focused on investigating and providing potential solutions to the following issues associated with statistical downscaling; (1) non-homogeneity in inputs used in the development (calibration and validation) and future projection phases of statistical downscaling models (SDMs), (2) propagation of bias in GCM outputs to the outputs of SDMs, (3) varying nature of climate projections produced by SDMs depending on the GCM used for providing inputs, (4) complexity of multi-station and multivariate SDMs, and (5) use of linear regression and non-linear regression techniques in SDMs.

The above aims of this study were demonstrated through a case study in the operational area of the Grampians Wimmera Mallee Water Corporation (GWMWater) in north-western Victoria, Australia. This study area contains a large scale multi-reservoir water supply system which supplies water to domestic, industrial, agricultural and environmental purposes. Hence the analysis of the impacts of changing climate on the water resources in this study area was identified as a timely need. In this study, 17 weather observation stations located within the operational area of GWMWater were considered. All SDMs detailed in this study were developed at monthly time steps. The monthly hydroclimatic data are helpful from the agricultural and water management point of view, especially in relation to water resources planning activities.

Conventionally SDMs are developed using some form of reanalysis outputs as inputs, and then the outputs from GCMs are used for the projection of catchment scale climate into future. Since reanalysis outputs and GCM outputs are derived from two different sources with different degrees of accuracy, inputs to the SDM in the development and projection phases are not homogeneous. As a potential solution to the above issue of non-homogeneity in inputs, a SDM was developed (calibrated and validated) in this study for monthly precipitation at an observation station (in the study area) using the

20th century climate experiment outputs of HadCM3 GCM. It was developed in view of using the outputs of HadCM3 pertaining to the future for producing catchment scale precipitation projections into the future. The performances of this downscaling model in its development phase were compared with those of a downscaling model developed in the conventional manner using NCEP/NCAR reanalysis outputs. Despite the advantage of using homogeneous sets of inputs for both development and future projections, the downscaling model developed with HadCM3 outputs displayed limited performances in the development phase in comparison to its counterpart model developed with reanalysis outputs. However, it was found that the precipitation output of the downscaling model developed with HadCM3 outputs were in better agreement with observations in comparison to the agreement between the raw precipitation output of HadCM3 and observations. The poor agreement between the raw precipitation output of HadCM3 and observations indicated the presence of large bias in GCM outputs. Hence the need of a correction to GCM bias was realised.

Due to assumptions and approximations used in GCMs, their outputs contain bias, and this bias propagates into the outputs of SDMs. In order to address the GCM bias, various bias-correction techniques have been used in the past. In this study, three different bias-correction techniques; (1) equidistant quantile mapping, (2) nested bias-correction, and (3) monthly bias-correction were applied to the monthly precipitation outputs of a SDM. For the analysis of the performances of the above three bias-correction techniques, the SDM which was developed in the previous study with NCEP/NCAR reanalysis outputs was run with the 20th century climate experiment outputs of HadCM3, for the reproduction of past observed precipitation at the station of interest. Then each of the above bias-correction techniques was applied to the precipitation reproduced by that SDM, considering the observed precipitation as the reference. Following a comparison of performances between the above three bias-correction techniques, it was found that equidistant quantile mapping outperformed the other two techniques.

Owing to differences in the internal structures, even for the same GHG emission scenario different GCMs tend to simulate future climate differently. Therefore when projections of different GCM are used in a SDM, it also tends to produce projections of catchment scale climate which vary with the GCM. As the catchment scale climate projections produced by the SDM into future varies with the GCM, decision making in the management of water resources becomes difficult. Therefore there is a need for deriving a single climate projection at the catchment scale from the different climate projections produced by a set of GCMs. As a potential solution to the issue of having multiple climate projections at the catchment scale, a SDM for monthly precipitation was developed in this study with a set of outputs derived from the outputs of different GCMs. The set of outputs derived from the outputs of different GCMs is called the multi-model ensemble (MME) outputs. These MME outputs for the past and future climate were derived from the outputs of three GCMs; HadCM3, ECHAM5 and GFDL2.0. The above three GCMs were selected for this investigation as in the past literature, it was stated that they are capable of simulating the precipitation over Australia and El Niño-Southern Oscillation (ENSO) with a good degree of accuracy. As the first step, the regression relationships between the NCEP/NCAR reanalysis outputs and the 20^{th} century climate experiment outputs of HadCM3, ECHAM5 and GFDL2.0 for each calendar month were determined using the multi-linear regression (MLR) technique. These MME outputs (values generated from the above MLR relationships) pertaining to the past climate were used for the calibration and the validation of the SDM. Then the outputs of HadCM3, ECHAM5 and GFDL2.0 corresponding to the future climate were introduced to the MLR relationships. This process yielded a set of MME outputs pertaining to the future climate. These MME outputs for future were used on the SDM for the projection of monthly precipitation into future at the station of interest. Furthermore, since the inputs to this SDM were derived from the same three GCMs throughout its development and future projection phases, this MME approach allowed the use of homogeneous inputs to the SDM.

When a statistical downscaling exercise is performed for a certain predictand over number of stations in a study area, it is important to preserve the cross-correlation

structure among the stations. The preservation of the cross-correlation structure among the stations (for a predictand) enables the plausible representation of spatial variation of the predictand of interest. However, the majority of the currently used multi-station downscaling techniques capable of preserving the cross-correlation structure among the stations for a predictand of interest are complex. In this study, a relatively simple yet effective multi-station downscaling methodology was developed. As the first step, cross-correlation coefficients between the 17 stations located in the study area were computed for monthly precipitation, evaporation, minimum temperature and maximum temperature using the observations, considering each predictand at a time. Then for each predictand, the station which displayed the highest number of high correlations (magnitude above 0.80 at $p \leq 0.05$) with the other stations was selected as the first key station. The stations which showed high correlations with the first key station were considered as the member stations of the first cluster. The same procedure was repeated until all stations were classified into clusters (each governed by a key station). Then using the observations, for each predictand, linear regression relationships between the key station and the member stations of each cluster were determined for each calendar month. Thereafter, for each key station, SDMs were developed for each predictand. Then by using the outputs of these SDMs on the above linear regression relationships, the values of each predictand at all member stations were determined for the past and the future climate. This multi-station downscaling methodology was able to downscale GCM outputs to monthly precipitation, evaporation, minimum temperature and maximum temperature at multiple stations effectively while preserving the cross-correlation structures among the stations for each individual predictand. However this methodology could only be applied to one predictand at a time. Hence this multi-station downscaling methodology was upgraded to a multi-station multivariate downscaling approach which can downscale GCM outputs to multiple predictands at multiple stations concurrently.

In this multi-station multivariate downscaling approach, the predictands which are highly correlated (magnitude above 0.80 at $p \leq 0.05$) with other predictands of interest at each individual observation station in a group observation stations was determined.

These predictands were called the key predictands. In this investigation, three predictands; monthly evaporation, minimum temperature and maximum temperature at 5 of the 17 observation stations were considered for the demonstration of the methodology. It was found that, the maximum temperature was highly correlated with evaporation and minimum temperature at each individual station. Hence the maximum temperature was identified as the only key predictand. One station at which the maximum temperature showed high correlations with all three predictands at all observation stations was identified as the only key station. Then using the observations, linear regression relationships between the key predictand at the key station and evaporation, minimum temperature and maximum temperature at all stations were determined. A SDM for maximum temperature at the key station was developed and by introducing the outputs of a GCM (pertaining to future) to this SDM, projections of the maximum temperature were produced into future. Then by introducing the outputs of the SDM to the above linear regression relationships the projections of evaporation, minimum temperature and maximum temperature at all stations were determined. In this multi-station multivariate downscaling approach, the cross-correlation structures between the stations for each individual predictand and also the cross-correlation structures among different predictands at each individual station were preserved. It was found that the multi-station multivariate downscaling approach developed in this study was effective in downscaling GCM outputs to multiple predictands at multiple stations concurrently.

Both linear and non-linear regression techniques are widely used in statistical downscaling studies. In this study, two statistical downscaling models were developed using the MLR (a linear regression technique) and the least square support vector machine regression (LS-SVM - a non-linear regression technique) for downscaling NCEP/NCAR reanalysis outputs to monthly streamflows. In the comparison of performances, it was found that LS-SVM is marginally better than MLR in downscaling reanalysis outputs to streamflows.

7.2 Conclusions

The following conclusions were drawn from this study;

1. In a statistical downscaling exercise, consideration of the statistical significance and the consistency of the correlations between the predictors and the predictand of interest over time is a potential way to select a robust set of predictors for a downscaling model. In other words, the predictors which show correlations with fluctuations in the signs (positive to negative or vice versa) or largely varying magnitudes over time (one time slice to another) can be omitted, as these are indications of inconsistent relationships with the predictand.

2. In statistical downscaling, principal component (PC) analysis is used for extracting the variance present in a large set of predictors to a limited number of PCs (linear combinations of predictors). Then these PCs are used as inputs to statistical downscaling models. In such an exercise, the coefficients of the PCs extracted from the predictor data pertaining to the model calibration phase are used for the generation of PCs in the validation and future projection phases. When this is done some of the PCs in the validation or future projection phases can become markedly correlated with each other, leading to poor performances in the validation and future projection phases. Hence PC analysis in statistical downscaling studies should be performed cautiously.

3. There is a large quality mismatch (bias) between the 20^{th} century climate experiment outputs of GCMs and NCEP/NCAR reanalysis outputs. Hence, it was understood that a correction to GCM bias is necessary.

4. When the bias in the GCM outputs are large, the bias-correction of each individual GCM output against the corresponding reanalysis outputs and using them in a statistical downscaling model is not better than using the same set of GCM outputs (without bias correction) on a downscaling model and applying the bias-correction to the output of that downscaling model against observations.

The application of a bias-correction to the output of a downscaling model is computationally much cheaper than the application of the same bias-correction to each individual GCM output used for the development of a downscaling model.

5. When the bias in the outputs of a statistical downscaling model is large, equidistant quantile mapping, monthly bias-correction and nested bias-correction techniques cannot reduce the scatter of the predictand. In other words, following the bias-correction the improvement to the time series of the predictand was minimal.

6. The equidistant quantile mapping technique was identified as the most suitable bias-correction technique, employed in this study, as this method was capable of correcting the cumulative distribution of the predictand downscaled using GCM outputs.

7. A downscaling model developed with multi-model ensemble outputs derived from the 20th century climate experiment outputs of a set of GCMs, showed limited performances in comparison a downscaling model developed using the NCEP/NCAR reanalysis outputs. Nevertheless, the multi-model ensemble approach used in the former downscaling model enabled the use of homogeneous sets of inputs to the downscaling model in its development and future projection phases and also provided a potential way for combining the outputs of different GCMs into single prediction.

8. In the development phases, downscaling models for monthly evaporation, minimum temperature and maximum temperature showed very limited scatter compared to that of monthly precipitation. It was realised that downscaling GCM outputs to precipitation is associated with limited accuracy in comparison to that of evaporation, minimum temperature and maximum temperature.

9. The key station approach (multi-station downscaling methodology) and the key predictand and key station approach (multi-station multi-predictand downscaling methodology) developed in this study were effective and capable of reducing computational costs associated with downscaling multiple predictands at multiple stations. Also the former downscaling approach is capable of preserving the cross-correlation structures among the observation stations for a predictand of interest and the latter downscaling approach is capable of preserving the cross-correlation structures among the observation stations for each predictand of interest also between the predictands at individual stations.

7.3 Recommendations for Future Work

1. Study of potential improvements to the model developed in this study for directly downscaling reanalysis outputs to monthly streamflows is considered as a useful investigation in future. Since precipitation and evaporation are highly influential on the streamflows, inclusion of them as predictors in the streamflow downscaling model is seen as a way for improving the streamflow predictions.

2. The key station approach detailed in this thesis was demonstrated only for precipitation, evaporation and temperature considering each predictand at a time. This multi-station downscaling approach can also be applied to the network of streamflow stations located within this study area. The application of key station approach to streamflow stations aids the preservation of cross-correlations among the streamflow stations and also it can reduce the computational cost.

3. The simulation of streamflows using the precipitation, evaporation and temperature produced by the downscaling models developed in this study is also seen as another useful piece of future work. For this purpose, regression relationships between precipitation, evaporation and temperature with

streamflows can be determined. Then the projections of precipitation, evaporation and temperature produced by the downscaling models into future can be used in those regression relationships for the determination of streamflows pertaining to future climate.

4. Also the use of a simple water balance model for the determination of streamflows using precipitation and evaporation produced by the downscaling models is seen as another potential investigation in future.

REFERENCES

Note that following are the references cited within the body text of this thesis in Chapters 1 and 2. References cited within the journal papers included in this thesis are found at the end of each journal paper.

Anandhi A, Srinivas VV, Nanjundiah RS, Kumar DN. 2008. Downscaling precipitation to river basin in India for IPCC SRES scenarios using support vector machine. *International Journal of Climatology* **28:** 401-420. DOI: 10.1002/joc.1529.

Baigorria GA, Jones JW. 2010. GiST: A stochastic model for generating spatially and temporally correlated daily rainfall data. *Journal of Climate* **23:** 5990-6008. DOI: 10.1175/2010JCLI3537.1.

Bates BC, Kundzewicz ZW, Wu S, Palutikof JP. 2008. Climate change and water. Technical paper VI of the Intergovernmental Panel on Climate Change, IPCC Secretariat, Geneva, Switzerland.

Bjerknes V. 1904. Das Problem der Wettervorhersage, betrachtet vom Standpunkte der Mechanik und der Physik (The problem of weather prediction, considered from the viewpoints of mechanics and physics) – *Meteorolgische Zeitschrift* **21:** 1-7. (Translated and edited in 2009 by Volken E, Bronnimann in *Meteorolgische Zeitschrift* **18:** 663-667. DOI: 10.1127/0941-2948/2009/416).

Bureau of Meteorology. 2010. Australian climate influences. Available online at http://www.bom.gov.au/watl/about-weather-and-climate/australian-climate-influences.shtml. (Accessed 25th September 2012).

Bureau of Meteorology. 2013. Climate classification of Australia. Available online at http://www.bom.gov.au/climate/environ/other/kpn.jpg. (Accessed 20th February 2013)

Cai W, Cowan T. 2008. Evidence of impacts from rising temperature on inflows to the Murray-Darling Basin. *Geophysical Research Letters* **35:** L07701, DOI: 10.1029/2008GL033390.

Cannon AJ, Whitfield PH, Lord ER. 2002. Synoptic map-pattern classification using recursive partitioning and principal component analysis. *Monthly Weather Review* **130:** 1187–1206. DOI: 10.1175/1520-0493(2002)130<1187:SMPCUR>2.0.CO;2.

Cassano EN, Lynch AH, Cassano JJ, Koslow MR. 2006. Classification of synoptic patterns in the western Arctic associated with extreme events at Barrow, Alaska, USA. *Climate Researchearch* **30:** 83–97. DOI: 10.3354/cr030083.

Charles SP, Bates BC, Smith IN, Hughes JP. 2004. Statistical downscaling of daily precipitation from observed and modelled atmospheric fields. *Hydrological Processes* **18:** 1373–1394. DOI: 10.1002/hyp.1418.

Chen TS, Yu PS, Tang YH. 2010. Statistical downscaling of daily precipitation using support vector machines and multivariate analysis. *Journal of Hydrology* **385**: 13–22. DOI: 10.1016/j.jhydrol.2010.01.021

Cheng CS, Li G, Li Q, Auld H. 2011. A synoptic weather-typing approach to project future daily rainfall and extremes at local scale in Ontario, Canada. *Journal of Climate* **24:** 3667-3685. DOI: 10.1175/2011JCLI3764.1.

Chiew FHS, Young WJ, Cai W, Teng J. 2010. Current drought and future hydroclimate projections in southeast Australia and implications for water resources management.

Stochastic Environmental Research and Risk Assessment **25:** 602-612. DOI:10.1007/s00477-010-0424-x.

Chiew FHS. 2007. Estimation of rainfall elasticity of streamflow in Australia. *Hydrological Sciences Journal* **51:** 613–625. DOI: 10.1623/hysj.51.4.613.

Commonwealth Scientific and Industrial Research Organisation (CSIRO). 2007. *Climate change in Australia: Technical report 2007*. Commonwealth Scientific and Industrial Research Organisation, Canberra; Australia.

Crowley TJ. 2000. Causes of climate change over the past 1000 years. *Science* **289:** 270-277. DOI: 10.1126/science.289.5477.270.

Denis B, Laprise R, Cay D, Côté J. 2002. Downscaling ability of one-way nested regional climate models: The Big-Brother experiment. *Climate Dynamics* **18:** 627-646. DOI: 10.1007/s00382-001-0201-0.

Department of Environment and Primary Industries. 2013a. *Victorian resources online – Mallee.* Available online at http://vro.dpi.vic.gov.au/dpi/vro/malregn.nsf/pages/mallee_soil_index. (Accessed 26th July 2013).

Department of Environment and Primary Industries. 2013b. *Victorian resources online – Wimmera*. Available online at http://vro.dpi.vic.gov.au/dpi/vro/wimregn.nsf/pages/natres_soilwimm. (Accessed 26th July 2013).

Department of Planning and Community Development. 2012. *The Wimmera plains*. Available online at http://www.dpcd.vic.gov.au/__data/assets/pdf_file/0007/113587/05-Wimmera-Plains-DRAFT120810.pdf. (Accessed 08th August 2013).

D'onofrio A, Boulanger JP, Segura EC. 2010. CHAC: A weather pattern classification system for regional climate downscaling of daily precipitation. *Climatic Change* **98:** 405-427. DOI: 10.1007/s10584-009-9738-4.

Earth System Research Laboratory. 2013. Trends in atmospheric Carbon Dioxide. Available online at http://www.esrl.noaa.gov/gmd/ccgg/trends/global.html (Accessed 20th June 2013).

Ferreira C. 2006. *Gene expression programming: Mathematical modelling by an artificial intelligence*. 2nd edition, Springer-Verlag, Germany. 480pp

Fowler HJ, Blenkinsop S, Tebaldi C. 2007. Linking climate change modelling to impacts studies: recent advances in downscaling techniques for hydrological modelling. *International Journal of Climatology* **27**: 1547–1578. DOI: 10.1002/joc.1556.

Frakes B. Yarnal B. 1997. A procedure for blending manual and correlation-based synoptic classifications. *International Journal of Climatology* **17:** 1381–1396. DOI: 10.1002/(SICI)1097-0088(19971115)17:13<1381::AID-JOC204>3.0.CO;2-Q.

Ghosh S, Katkar S. 2012. Modeling uncertainty resulting from multiple downscaling methods in assessing hydrological impacts of climate change. *Water Resources Management* **26:** 3559-3579. DOI: 10.1007/s11269-012-0090-5.

Goyal MK, Ojha CSP. 2012.Downscaling of surface temperature for lake catchment in an arid region in India using linear multiple regression and neural networks. *International Journal of Climatology* **32:** 552-566. DOI: 10.1002/joc.2286.

Grampians Wimmera Mallee Water Corporation (GWMWater). 2011a. *GWMWater sustainability report 2010 – 2011*. Available online at http://www.gwmwater.org.au/information/publications/reports-and-

policies/doc_download/1415-sustainability-report-201011. (Accessed 10th August 2013).

Grampians Wimmera Mallee Water Corporation (GWMWater). 2011b. *Storage management rules for the Wimmera-Mallee system headworks*. Available online at http://www.gwmwater.org.au/information/publications/ground-and-surface-water/west-wimmera-gma/cat_view/163-reservoir-operating-rules. (Accessed 10th August 2013).

Haas R, Pinto JG. 2012. A combined statistical and dynamical approach for downscaling large-scale footprints of European windstorms. *Geophysical Research Letters* **39:** L23804. DOI: 10.1029/2012GL054014.

Haylock MR, Hofstra N, Klein Tank AMG, Klok EJ, Jones PD, New M. 2008. A European daily high-resolution gridded dataset of surface temperature and precipitation. *Journal of Geophysical Research* **113:** D20119. DOI: 10.1029/2008JD10201.

Hess P, Brezowsky H. 1977. Katalog der GroBwetterlagen Europas (1881-1976) (Catalogue of European circulation patterns (1881-1976), in German).

Hessami M, Gachon P, Ouarda TBMJ, St-Hilaire A. 2008. Automated regression-based statistical downscaling tool. *Environmental Modelling and Software* **23:** 813-834. DOI: 10.1016/j.envsoft.2007.10.004.

Hughes JP, Guttorp P. 1994. A class of stochastic models for relating synoptic atmospheric patterns to regional hydrologic phenomena. *Water Resources Research* **30:** 1535–1546. DOI: 10.1029/93WR02983.

Hughes L. 2003. Climate change and Australia: trends, projections and impacts. *Austral Ecology* **28:** 423-443. DOI: 10.1046/j.1442-9993.2003.01300.x.

Huth R, Beck C, Philipp A, Demuzere M, Ustrnul Z, Cahynová M, Kyselý J, Tveito OE. 2008. Classifications of atmospheric circulation patterns. *Annals of the New York Academy of Sciences* **1146:** 105–152. DOI: 10.1196/annals.1446.019.

Isbell RF. 2002. *The Australian soil classification*. Australian soil and land survey handbooks series 4, Revised edition, CSIRO Publishing, Australia. 152 pp.

James PM. 2007. An objective classification method for Hess and Brezowsky Grosswetterlagen over Europe. *Theoretical and Applied Climatology* **88:** 17–42. DOI: 10.1007/s00704-006-0239-3.

Jeong DI, St-Hilaire A, Ouarda TBMJ, Gachon P. 2013. A multi-site statistical downscaling model for daily precipitation using global scale GCM precipitation outputs. *International Journal of Climatology* **33:** 2431–2447. DOI: 10.1002/joc.3598.

Jones RG, Murphy JM, Noguer M. 1995. Simulation of climate-change over Europe using a nested regional-climate model 1: Assessment of control climate, including sensitivity to location of lateral boundaries. *Quarterly Journal of the Royal Meteorological Society* **121:** 1413–1449. DOI: 10.1002/qj.49712152610.

Joshi D, St-Hilaire A, Daigle A, Ouarda TBMJ. 2013. Databased comparison of Sparse Bayesian Learning and Multiple Linear Regression for statistical downscaling of low flow indices. *Journal of Hydrology*. Article in press. DOI: 10.1016/j.jhydrol.2013.02.040.

Kalkstein LS, Nichols MC, Barthel CD, Greene JS. 1996. A new spatial synoptic classification: application to air-mass analysis. *International Journal of Climatology* **16:** 983–1004. DOI: 10.1002/(SICI)1097-0088(199609)16:9<983::AID-JOC61>3.0.CO;2-N.

Kalkstein LS, Tan G, Skindlov JA. 1987. An evaluation of three clustering procedures for use in synoptic climatological classification. *Journal of Applied Meteorology* **26:** 717–730. DOI: 10.1175/1520-0450(1987)026<0717:AEOTCP>2.0.CO;2.

Khalili M, Brissette F, Leconte R. 2007. Stochastic multi-site generation of daily precipitation data using spatial autocorrelation. *Journal of Hydrometeorology* **8:** 396-412. DOI: 10.1175/JHM588.1.

Kou X, Ge J, Wang Y, Zhang C. 2007. Validation of the weather generator CLIGEN with daily precipitation data from the Loess Plateau, China. *Journal of Hydrology* **347:** 347-357. DOI: 10.1016/j.jhydrol.2007.09.051.

Kreienkamp F, Spekat A, Enke W. 2013. The weather generator used in the empirical statistical downscaling method, WETTREG. *Atmosphere* **4:** 169-197. DOI: 10.3390/atmos4020169.

Kundzewicz ZW, Mata LJ, Arnell NW, Döll P, Jimenez B, Miller K, Oki T, Sen Z, Shiklomanov I. 2008. The implications of projected climate change for freshwater resources and their management. *Hydrological Sciences Journal* **53:** 3-10. DOI: 10.1623/hysj.53.1.3.

Kunkel KE, Karl TR, Easterling DR, Redmond K, Young J, Yin X, Hennon P. 2013. Probable maximum precipitation and climate change. *Geophysical Research Letters* **40:** 1402-1408. DOI:10.1002/grl.50334.

Lamb HH. 1972. *British Isles weather types and a register of daily sequence of circulation patterns, 1861-1971*. Her Majesty's stationery office, London, UK. 85pp.

Lund IA. 1963. Map-pattern classification by statistical methods. *Journal of Applied Meteorology* **2:** 56–65. DOI: 10.1175/1520-0450(1963)002<0056:MPCBSM>2.0.CO;2.

Lynch P. 2008. The origins of computer weather prediction and climate modeling. *Journal of Computational Physics* **227:** 3431–3444. DOI: 10.1016/j.jcp.2007.02.034.

Mala-Jetmarova H, Barton A, Briggs S. 2013. Securing water supply in western Victoria through the implementation of regional pipeline systems. In: Graymore M, McRae-Williams P, Barton A, Lehmann L. (Eds), *Pipes, ponds and people: Adaptive water management in drylands*. VURRN Press, Mt Helen, Victoria, 43-76.

Malby AR, Whyatt JD, Timmis RJ, Wilby RL, Orr HG. 2007. Long-term variations in orographic rainfall: analysis and implications for upland catchments. *Hydrological Sciences Journal* **52:** 276–291. DOI: 10.1623/hysj.52.2.276.

Mallee Catchment Management Authority. 2012. *Annual report 2011 – 2012*. Available online at http://www.malleecma.vic.gov.au/resources/corporate-documents/ar-2011-12-final.pdf/at_download/file (Accessed 8th August 2013).

Maraun D, Wetterhall F, Ireson, AM, Chandler RE, Kendon EJ, Widmann M, Brienen S, Rust HW, Sauter T, Themel M, Venema VKC, Chun KP, Goodess CM, Jones RG, Onof C, Vrac M, Thiele-Eich I. 2010. Precipitation downscaling under climate change: Recent developments to bridge the gap between dynamical models and the end user. *Reviews of Geophysics* **48:** DOI: 10.1029/2009RG000314.

McRobert J, Larsen C. 2011. Climate variability and land management practices. Available online at http://www.malleecma.vic.gov.au/resources/reports/final-report-mcma.pdf/at_download/file. (Accessed 18th August 2013).

Mearns LO, Giorgi F, Whetton P, Pabon D, Hulme M, Lal M. 2003. Guidelines for use of climate scenarios developed from Regional Climate Model experiments. Available online at http://www.ipcc-data.org/guidelines/dgm_no1_v1_10-2003.pdf. (Accessed 5th August 2013).

Meenu R, Rehana S, Mujumdar PP. 2013. Assessment of hydrologic impacts of climate change in Tunga-Bhadra river basin, India with HEC-HMS and SDSM. *Hydrological Processes* **27:** 1572-1589. DOI: 10.1002/hyp.9220.

Mehrotra R, Srikanthan R, Sharma A. 2006. A comparison of three stochastic multi-site precipitation occurrence generators. *Journal of Hydrology* **331:** 280-292. DOI: 10.1016/j.jhydrol.2006.05.016.

Murphy J. 1998. An evaluation of statistical and dynamical techniques for downscaling local climate. *Journal of Climate* **12:** 2256-2284. DOI: 10.1175/1520-0442(1999)012<2256:AEOSAD>2.0.CO;2.

Murray-Darling Basin Authority. 2010. *Guide to the proposed basin plan: Technical background Part II*. Available online at http://www.mdba.gov.au/sites/default/files/archived/Wimmera-Avoca-region.pdf. (Accessed 5th August 2013).

Nasseri M, Tavakol-Davani H, Zahraie B. 2013. Performance assessment of different data mining methods in statistical downscaling of daily precipitation. *Journal of Hydrology* **492:** 1-14. DOI: 10.1016/j.jhydrol.2013.04.017.

Nicholls N, Collins D. 2006. Observed climate change in Australia over the past century. *Energy and Environment* **17:** 1-12. DOI: 10.1260/095830506776318804.

Panitz HJ, Fosser G, Sasse R, Sehlinger A, Feldmann H, Schädler G. 2013. Modelling near future regional climate change for Germany and Africa. In: Nagel WE, Kröner DH, Resch MM. (Eds.), *High performance computing in science and engineering '12*. Springer Berlin Heidelberg, 390 pp.

Phillips NA. 1956. The general circulation of the atmosphere: a numerical experiment. *Quarterly Journal of the Royal Meteorological Society* **82:** 123–164. DOI: 10.1002/qj.49708235202.

Piani C, Haerter JO, Coppola E. 2010. Statistical bias correction for daily precipitation in regional climate models over Europe. *Theoretical and Applied Climatology* **99:** 187-192. DOI: 10.1007/s00704-009-0134-9.

Qian JH, Zubair L. 2010. The effect of grid spacing and domain size on the quality of ensemble regional climate downscaling over South Asia during the north-easterly monsoon. *Monthly Weather Review* **138:** 2780-2802. DOI: 10.1175/2010MWR3191.1.

Richardson CW. 1981. Stochastic simulation of daily precipitation, temperature, and solar radiation. *Water Resources Research* **17:** 182-190. DOI: 10.1029/WR017i001p00182.

Richardson LF. 1922. *Weather prediction by numerical process*. Cambridge University Press, Cambridge, UK. 236 pp.

Rojas M. 2006. Multiply nested regional climate simulation for Southern America: Sensitivity to model resolution. *Monthly Weather Review* **134:** 2208–2223. DOI: 10.1175/MWR3167.1.

Rowan JN, Downes RG. 1963. *A study of the land in North-Western Victoria*. Soil Conservation Authority, Technical Communication No. 2, Victoria.

Rummukainen M. 2010. State-of-the-art with regional climate models. Wiley Interdisciplinary Reviews: *Climate Change* **1:** 82–96. DOI: 10.1002/wcc.8.

Sachindra DA, Huang F, Barton AF, Perera BJC. 2013a. Least square support vector and multi-linear regression for statistically downscaling general circulation model

outputs to catchment streamflows. *International Journal of Climatology* **33:** 1087-1106. DOI: 10.1002/joc.3493.

Sachindra DA, Huang F, Barton AF, Perera BJC. 2014a. Statistical downscaling of general circulation model outputs to precipitation Part 1: Calibration and validation. *International Journal of Climatology*. (Article in press). DOI**:** 10.1002/joc.3914.

Sheridan SC. 2002. The redevelopment of a weather-type classification scheme for North America. *International Journal of Climatology* 22: 51-68. DOI: 10.1002/joc.709.

Smith IN, McIntosh P, Ansell TJ, Reason CJC, McInnes K. 2000. Southwest Western Australian winter rainfall and its association with Indian Ocean climate variability. *International Journal of Climatology* **20:** 1913-1930.DOI:10.1002/1097-0088(200012)20:15<1913::AID-JOC594>3.0.CO;2-J.

Srikanthan R, Pegram GGS. 2009. A nested multisite daily rainfall stochastic generation model. *Journal of Hydrology* **371:** 142-153. DOI: 10.1016/j.jhydrol.2009.03.025.

Tabachnick BG, Fidell LS. 2007. *Using multivariate statistics*. Pearson Publishers, Boston. pp980.

Timbal B. 2009. *The continuing decline in South-East Australian rainfall - Update to May 2009*. Available online at http://www.cawcr.gov.au/publications/researchletters.php. (Accessed 15th August 2013).

Tisseuil C, Vrac M, Lek S, Wade AJ. 2010. Statistical downscaling of river flows. *Journal of Hydrology* **385**: 279–291. DOI: 10.1016/j.jhydrol.2010.02.030.

Trenberth KE, Fasullo JT, Kiehl J. 2009. Earth's global energy budget. *Bulletin of the American Meteorological Society* **90:** 311–323. DOI: 10.1175/2008BAMS2634.1.

Tribbia JJ, Anthes RA. 1987. Scientific basis of modern weather prediction. *Science* **237:** 493-499. DOI: 10.1126/science.237.4814.493.

Tripathi S, Srinivas VV, Nanjundiah RS. 2006. Downscaling of precipitation for climate change scenarios: a support vector machine approach. *Journal of Hydrology* **330:** 621-640. DOI:10.1016/j.jhydrol.2006.04.030.

Tripati AK, Roberts CD, Eagle RA. 2009. Coupling of CO_2 and ice sheet stability over major climate transitions of the last 20 million years. *Science* **326:** 1394-1397. DOI: 10.1126/science.1178296.

Vasiliades L, Loukas A, Patsonas G. 2009. Evaluation of a statistical downscaling procedure for the estimation of climate change impacts on droughts. *Natural Hazards and Earth System Sciences* **9:** 879-894. DOI: 10.5194/nhess-9-879-2009.

Victorian Government Department of Sustainability and Environment. 2008. *Climate Change in Victoria Summary Report*. Available online at http://www.climatechange.vic.gov.au/publications. (Accessed on 28th July 2013).

von Storch H, Hewitson B, Mearns L. 2000. Review of empirical downscaling techniques. *Proceedings of RegClim spring meeting, 8 - 9 May 2000, Jevnaker, Norway*. Available online at http://regclim.met.no/rapport_4/Default.htm. (Accessed 1st October 2012).

Vorosmarty CJ, McIntyre PB, Gessner MO, Dudgeon D, Prusevich A, Green P, Glidden S, Bunn SE, Sullivan CA, Liermann CR, Davies PM. 2010. Global threats to human water security and river biodiversity. *Nature* **467:** 555–561. DOI: 10.1038/nature09440.

Wallis P, Birrell R, Griggs D, Healy E, Langford J, Stanley J. 2009. *Melbourne's water situation: the opportunity for diverse solutions*. Monash Sustainability Institute Report 09/2, Melbourne.

Water in Drylands Collaborative Research Program. 2009. *Driving water futures: The use of an interactive visualisation tool for community water allocation engagement*. WIDCORP Report 03/09, Horsham.

White M, Oates A, Barlow T, Pelikan M, Brown J, Rosengren N, Cheal D, Sinclair S, Sutter G. 2003. *The vegetation of north-west Victoria A report to the Wimmera, North Central and Mallee Catchment Management Authorities*. 460 pp

Wilby RL, Charles SP, Zorita E, Timbal B, Whetton P, Mearns LO. 2004. *Guidelines for use of climate scenarios developed from statistical downscaling methods, supporting material to the IPCC*. Available online at http://www.ipcc-data.org/. 3-21. (Accessed 28th January 2012).

Wilby RL, Dawson CW. 2012. The Statistical DownScaling Model: insights from one decade of application. *International Journal of Climatology*. Article in press. DOI: 10.1002/joc.3544.

Wilby RL, Fowler HJ. 2011. Regional climate modelling in modelling the impact of climate change on water resources. In: Fung F, Lopez A, New M. (Eds.), *Modelling the impact of climate change on water resources*. Wiley-Blackwell, Chichester, UK. 209 pp.

Wilby RL, Wigley TML. 1997. Downscaling general circulation model output: a review of methods and limitations. *Progress in Physical Geography* **21:** 530-548. DOI: 10.1177/030913339702100403.

Wilby RL, Wigley TML. 2000 Precipitation predictors for downscaling: observed and general circulation model relationships. *International Journal of Climatology* **20:** 641–661. DOI: 10.1002/(SICI)1097-0088(200005)20:6<641::AID-JOC501>3.3.CO;2-T.

Wilks DS, Wilby RL. 1999. The weather generation game: A review of stochastic weather models. *Progress in Physical Geography* **23:** 329-357. DOI: 10.1177/030913339902300302.

Wilks DS. 1992. Adapting stochastic weather generation algorithms for climate change studies. *Climatic Change* **22:** 67-84. DOI: 10.1007/BF00143.

Wilks DS. 1992. Multisite generalization of a daily stochastic precipitation generation model. *Journal of Hydrology* **210:** 178-191. DOI: 10.1016/S0022-1694(98)00186-3.

Wilks DS. 1998. Multisite generalizations of a daily stochastic precipitation generation model. *Journal of Hydrology* **210:** 178–91.DOI: 10.1016/S0022-1694(98)00186-3.

Wilks DS. 1999. Simultaneous stochastic simulation of daily precipitation, temperature and solar radiation at multiple sites in complex terrain. *Agricultural and Forest Meteorology* **96:** 85-101. DOI: 10.1016/S0168-1923(99)00037-4.

Wilks DS. 2010. Use of stochastic weather generators for precipitation downscaling. Wiley Interdisciplinary Reviews. *Climate Change* **1:** 898-907. DOI: 10.1002/wcc.85.

Willems P, Vrac M. 2011. Statistical precipitation downscaling for small-scale hydrological impact investigations of climate change. *Journal of Hydrology* **402:** 193-205. DOI: 10.1016/j.jhydrol.2011.02.030.

Yang T, Li H, Wang W, Xu CY, Yu Z. 2012. Statistical downscaling of extreme daily precipitation, evaporation, and temperature and construction of future scenarios. *Hydrological Processes* **26:** 3510–3523. DOI: 10.1002/hyp.8427.

Yarnal B. 1993. *Synoptic climatology in environmental analysis*. Belhaven Press, London, UK. 192 pp.

Yhang YB, Hong SY. 2008. Improved physical processes in a regional climate model and their impact on the simulated summer monsoon circulations over East Asia. *Journal of Climate* **21:** 963-979. DOI: 10.1175/2007JCLI1694.1.